UNIVERSITY OF SOUTHAMPTON

FACULTY OF MEDICINE

Pro-Inflammatory Actions of Human Mast Cell Tryptase: Immunopharmacological Studies into the Role of Protease Activated Receptor 2

By

Mogib El-Rahman Mohamed Shokry Khedr

Thesis for the degree of Doctor of Philosophy

August 2012

UNIVERSITY OF SOUTHAMPTON

ABSTRACT

SCHOOL OF MEDICINE

DOCTOR OF PHILOSOPHY

PRO-INFLAMMATORY ACTIONS OF HUMAN MAST CELL TRYPTASE: IMMUNOPHARMACOLOGICAL STUDIES INTO THE ROLE OF PROTEASE ACTIVATED RECEPTOR 2

By Mogib El-Rahman Mohamed Shokry Khedr

Tryptase, the most abundant protease of the human mast cell, has been implicated as a key mediator of allergic disease. The precise mechanisms involved are unclear, though a role for protease activated receptor 2 has long been proposed. We have investigated the contribution of PAR-2 in inflammatory reactions induced by tryptase in mouse *in vivo* and in human *in vitro* models. The injection of tryptase induced a significant increase in neutrophil numbers and in microvascular leakage in the peritoneum of mice, but there were no significant differences between wild-type and PAR-2 knockout animals. Tryptase also stimulated release of increased quantities of matrix metalloproteinases 9 and 2 (MMP9 and MMP2) in the peritoneum of both mice strains, with neutrophils identified as the main cellular source of MMP9. Microarray analysis of tryptase-treated human umbilical vein endothelial cells indicated an apparent upregulation of mRNA for cytokines including IL-2, IL-3, IL-6 and CXCL10, for adhesion molecules ICAM-1, VCAM-1, EpCAM and ITGAL, as well as for the cell signalling molecules TNFAIP3, TLL1 and SMAD2. Microarray data was confirmed by separate qPCR experiments, immunocytochemistry and by the measurement of cytokines in cell supernatants. In all cases, the actions of tryptase were dependent on an intact catalytic site. Tryptase, like the peptide agonist of PAR-2 SLIGKV-NH_2 was able to induce intracellular calcium in the endothelial cells (albeit a small one), but in most cases SLIGKV-NH_2 failed to replicate the actions of tryptase either *in vivo* or *in vitro*. A cleavage product of PAR-2 generated on receptor activation was found to have a distinct profile of pro-inflammatory actions, but being readily degraded it proved unsuitable as a biomarker. Tryptase can act as a potent mediator of inflammation in allergic disease and though PAR-2 can play a role, the underlying processes may be largely independent of the activation of PAR-2.

Table of Contents

List of Figures

List of Tables

Declaration of Authorship

I, **Mogib El-Rahman Mohamed Shokry Khedr**, declare that this thesis and the work presented in it are my own and has been generated by me as the result of my own original research.

'Pro-Inflammatory Actions of Mast Cell Tryptase: Immunopharmacological Studies into the Role of Protease Activated Receptor 2'

I confirm that:

1. This work was done wholly or mainly while in candidature for a research degree at this University;
2. Where any part of this thesis has previously been submitted for a degree or any other qualification at this University or any other institution, this has been clearly stated;
3. Where I have consulted the published work of others, this is always clearly attributed;
4. Where I have quoted from the work of others, the source is always given. With the exception of such quotations, this thesis is entirely my own work;
5. I have acknowledged all main sources of help;
6. Where the thesis is based on work done by myself jointly with others, I have made clear exactly what was done by others and what I have contributed myself.
7. Either none of this work has been published before submission, or Parts of this work have been published as: [please list references below]:

Signed:

.....

Date:

.....

Glossary

Arg	Arginine
Asp	Aspartic acid
BAL	Broncho-alveolar lavage
BApNA	N-α-benzoyl-DL-arginine *p*-nitroanilide hydrochloride
BCA	Bicinchoninic acid
BSA	Bovine serum albumin
C (3a, 4a, 5a)	Activated complement component fragment (3a, 4a, 5a)
CCL	Chemokine (C-C motif) ligand
CD (4, 8, …)	Cluster of differentiation (4, 8, …)
cDNA	Complementary deoxyribonucleic acid
CGRP	Calcitonin gene-related peptide
COX-2	Cyclooxygenase 2
cRNA	complementary RNA,
CXCL	Chemokine (C-X-C motif) ligand
DAG	1,2 diacylglycerol
dH_2O	Distilled water
DMEM	Dulbecco's modified eagle medium
DMSO	dimethyl sulphoxide
DNA	Deoxyribonucleic acid
dscDNA	double stranded complementary DNA
EDTA	Ethylenediaminetetraacetic acid
EGFR	Epidermal growth factor receptor
EpCAM	Epithelial cell adhesion molecule
ERK	Extracellular signal regulated kinase
FBS	Foetal bovine serum
FCS	Foetal calf serum

FITC	Fluorescein isothiocyanate
FVIIa	Activated clotting factor VII
FXa	Activated clotting factor X
Gly	Glycine
GM-CSF	Granulocyte-macrophage colony-stimulating factor
GPCRs	G protein coupled receptors
G-proteins	GTP-binding proteins
HEPES	4-(2-hydroxyethyl)-1-piperazineethanesulphonic acid)
HMC-1	Mast cell-like cell line
HPLC	High- pressure liquid chromatography
HRP	Horseradish peroxidase
HUVEC	Human umbilical vein cells
ICAM-1	Intracellular adhesion molecule-1
Ig	Immunoglobulin
IL	Interleukin
INFγ	Interferon γ
IP3	Inositol 1,4,5-triphosphate
ITGAL	Integrin alpha L chain
Jab-1	Jun activation domain-binding protein 1
JNK	c-Jun N-terminal kinase
kDa	Kilo Dalton
KOH	Potassium hydroxide
LDH	Lactic dehydrogenase
LT	Leukotriene
Lys	Lysine
MAPK	Mitogen-activated protein kinase
MEM	Minimal essential medium
MES	2-(N-morpholino) ethanesulphonic acid

MHC (I and II)	Major histocompatibility complex class I and II
MMP	Matrix metalloproteinase
MW	Molecular weight
NF-κB	Nuclear factor kappa B
NGF	Nerve growth factor
NO	Nitric oxide
PAR-2	Protease activated receptor 2
PAR-2 RP	Protease activated receptor released peptide
PBS	Phosphate buffered saline
PBST	Phosphate buffered saline and Tween
PCR	Polymerase chain reaction
PG (D_2, E_2, …)	Prostaglandin (D_2, E_2, …)
PI	Propidium iodide
PKC	Protein kinase C
PLC	Phospholipase C
PSG	penicillin-streptomycin-glutamine
RFU	Relative fluorescence units
RNA	Ribonucleic acid
RNase	Ribonuclease
RPMI	Roswell park memorial institute
SCF	Stem cell factor
SDS-PAGE	Sodium dodecyl sulphate polyacrylamide gel electrophoresis
Ser	Serine
SP	Substance P
TdPI	Tick-derived protease inhibitor
TGF-β	Transforming growth factor beta
Th1	T cell helper 1
Th2	T cell helper 2

TLR	Toll like receptor
TMB	Tetramethyl benzidine
TNF-α	Tumor necrosis factor α
Tris	Tris(hydroxymethyl)aminomethane
Val	Valine
VCAM-1	Vascular cell adhesion molecule 1
VEGF	Endothelial growth factor
VIP	Vasoactive intestinal peptide

Acknowledgments

My sincerest gratitude is always to ALLAH who has granted me the strength, ability and health to complete this thesis.

I wish to express great love and gratitude to my family for their patience and continuous support during course of my studies. I would particularly like to thank my Mother and Father, who have provided supportive assistance and guidance through my life. My gratefulness to my beloved wife, my forever best friend and my PhD companion: Dr. Naglaa Bahgat. It has been a hard time, and cannot imagine experiencing any of it with anyone else. My beloved children, while I love them dearly, I am proud of both of them for being tremendously wonderful and patient.

I owe a heartfelt debt of gratitude to my supervisors, Dr. Andrew F. Walls and Dr. Xiaoying Zhou, who have been a source of inspiration with their continuous encouragement and guidance over last years, and without whose support this thesis would not have been possible. With the oversight of Dr. Andrew F. Walls, editorial advice has been sought and no changes of intellectual content were made as a result of this advice.

My study in UK became possible through the award of a scholarship of the Cultural Affairs and Mission Sector in Egypt, which I gratefully acknowledge.

I would like also to thank all my colleagues for their support throughout my work and a big thanks to my colleague Dr. Ahmed Fawzy for his continuous help and support throughout my study. Special thanks to my colleague Dr. Ahmed Abdelmotelb for his assistance in analysis the supernatant parameters in the mouse model and qPCR experiments. I am also indebted to Dr. Jurai Majtan and Dr. Pawan Kumar who guided first steps of my PhD. I would like to thank Dr. Claire Jackson and Dr. Jonathan Ward for their kind help. My special thanks to Dr. Salah Mansour who gave me support to conduct the flow cytometry experiment.

List of Publications

Khedr ME, Abdelmotelb AM, Lau L, Arno M, Zhou X, Walls AF. Mast Cell Tryptase as a Stimulus for Upregulation of Adhesion Molecule Expression and Cytokine Release from Endothelial Cells. Journal of Allergy and Clinical Immunology 2012; 129(2):AB122.

Khedr MER, Abdelmotelb A, Pender SLF, Zhou X, Walls AF. Human mast cell tryptase as a stimulus of inflammation in a mouse model: the role of protease activated receptor 2 (PAR-2). Clinical and Experimental Allergy 2009; 39(12):1938.

Abdelmotelb AM, **Khedr ME**, Pender SLF, Zhou X, Sommerhoff CP, Holloway JW et al. Alpha Tryptase: Potential Roles in Inflammation Distinct from those of beta-tryptase. Journal of Allergy and Clinical Immunology 2010; 125(2):AB178.

Zhou X, Whitworth HS, **Khedr M**, Brown TA, Goswami R, Eren E, et al. Mast Cell Chymase: A Useful Serum Marker in Anaphylaxis. Journal of Allergy and Clinical Immunology 2011;127 (2):AB143.

To My parents,

My wife

And my sons:

Hassan and Ali

Chapter 1.
Introduction

Chapter 1. Introduction

1.1 General introduction

The mast cell has a well-established role in hypersensitivity reactions and there is increasing evidence for its involvement in diverse other processes. The actions of mast cells are mediated through the release of a range of mediators upon activation. Tryptase is the most abundant mast cell product and potent pro-inflammatory actions have been reported when added to cells or transferred to animal models. However, the mechanisms of action of tryptase are still unclear.

Tryptase can cleave and activate protease activated receptor 2 (PAR-2) and this has been assumed to be the main way that tryptase exerts its effects. Determination of the role of PAR-2 in mediating the actions of tryptase will be important in understanding this protease as a target for therapeutic intervention in inflammatory and allergic conditions. The generation of mice deficient in PAR-2 provides an important means for studying the potential roles of PAR-2 in inflammation, while the development in microarray gene expression has to give potential to new insights into understanding mechanisms of cellular responses towards this protease.

1.2 Mast cells in inflammation

A key role of mast cells has been proposed in many forms of inflammation. In addition to their widely recognized contributions in hypersentivity reactions [1], mast cells have been implicated in other disorders with a presumed autoimmune aetiology such as arthritis, multiple sclerosis and bullous pemphigoid [2, 3]. Reports have described changes in mast cell number (with or without activation) in the affected tissues in fibrotic conditions, inflammatory bowel disease and neoplasia [4, 5]. The consistent finding of an increase in numbers of mast cells and augmented secretion is a prominent characteristic of the chronic inflammation that occurs in asthmatic bronchi [6, 7]. Application of gene array techniques to mast cells after IgE stimulation, has revealed upregulation of genes for cytokines including interleukin 1β (IL-1β) and IL-6, chemokines such as IL-8, genes involved in cell adhesion, and other genes involved in innate and adaptive immune-response (such as toll like receptor 2 (TLR2) and genes coding for tumour necrosis factor alpha (TNF-α)

signalling pathways [8]. Such inflammatory reactions are mediated through a group of mast cell-derived mediators that may be stored in mast cell secretory granules or generated on mast cell activation.

The presence of mast cells at sites in contact with the external environment gives them the ability to be an initiator of allergic reactions. Features of immediate allergic reactions including vasodilatation, increased vascular permeability and leukocyte accumulation can be mediated by the release of histamine, prostaglandin D_2 (PGD_2), leukotriene C_4 (LTC_4), platelet activating factor (PAF) and other mediators from mast cells [4, 9]. Moreover, histamine and PAF release is associated with oedema involving exudation of plasma proteins and fluids into the extravascular compartment of the mucosa. Tryptase has been found to induce a prolonged increase in vascular permeability and stimulate eosinophil and neutrophil accumulation when injected in mouse and guinea pig models [10-13].

Mast cells can contribute to late phase inflammation by recruiting other inflammatory cells as well as participate in processes of chronic allergic disease themselves. During the acute phase of allergic inflammation, various cell types including macrophages, T cells, eosinophils, basophils, and perhaps invariant natural killer T cells can be recruited [14]. Chronic allergic inflammation is invariably associated with tissue eosinophilia, and a reciprocal interaction between mast cells and eosinophils has been observed [15]. Addition of a sonicate of rat peritoneal mast cells has been reported to stimulate growth of human peripheral blood eosinophils, their differentiation and survival, effects attributed to granulocyte-macrophage colony-stimulating factor (GM-CSF), IL-3, IL-5, IL-2 and TNF-α released from mast cells [16, 17]. In turn, mediators released from eosinophils such as stem cell factor (SCF), nerve growth factor (NGF), eotaxin and major basic protein (MBP) have been reported to regulate mast cell activation, differentiation, maturation and survival in various mast cell models *in vitro* [18-20]. In addition, physical interaction between mast cells and eosinophils has been observed. Other cells proposed to play roles in late phase reactions are neutrophils, macrophages, and $CD3^+$ and $CD4^+$ cells [4]. The accumulation of immuno-competent cells and mast cell migration itself is facilitated by increased expression of adhesion molecules on endothelial cells [21-23]. A role for mast cell derived TNF-α has

been proposed in increasing the expression and production of intracellular adhesion molecule 1 (ICAM-1), vascular cell adhesion molecule 1 (VCAM-1) and E-selectin in endothelial cells [24].

Mast cells can make an important contribution to body defense against microorganisms. These cells have been reported to decrease parasitic burden through production of IL-25, IL-33 and thymic stromal lymphopoietin (TSLP) in mouse models by both IgE-independent mechanisms [25] as well as IgE-dependent mechanisms [26, 27]. Mast cells may be involved in host defense towards bacteria and viruses (including HIV) that are recognized by mast cell TLRs [9, 28]. In adaptive immunity, mast cells can regulate T lymphocytes by phagocytizing bacteria and present their antigens via major histocompatibility complex class I and II (MHC I & II) to T lymphocytes. Mast cells can also migrate to the lymph node where they can release cytokines and chemokines including TNF-α and IL-6 which recruit and activate these cells [29].

Studies with mast cell deficient mice have provided useful insights into the roles of mast cells in processes of inflammation. Thirty years ago, mice with hereditary anaemia which had naturally occurring mutations at the Dominant Spotting (*W*) locus on chromosome 5 or at the Steel (*Sl*) locus on chromosome 10 were the subject of studies by Kitamura and colleagues [30, 31]. They reported that homozygous W/W^v and Sl/Sl^d mice lacked mature mast cells in all organs and anatomical sites examined including connective tissue type and mucosal-type mast cells. Mast cell deficiency could be corrected by bone marrow transplantation in W/W^v mice, while injection of SCF was able to repair mast cell deficiency in Sl/Sl^d mice. Although mast cells are almost wholly deficient in these mice, they have normal leukocyte and platelet counts and express peripheral T and B lymphocytes with normal function *in vivo* and *in vitro* [32]. It has been reported that injection of IgE into the ears of W/W^v mice is not associated with the tissue swelling and neutrophil recruitment that may be observed when IgE is injected into wild type-mice [33]. Reconstitution of mice by intradermal injection of cultured mast cells derived from congenic normal mice was able to restore susceptibility to inflammation in the ear on subsequent injection. Neutrophil accumulation has been reported to be mediated through the release of mast cell mediators in mast cell dependent IgE cutaneous allergic reactions as well as in host defence against Gram negative

bacterial infection [33-35]. The *W/W^v* mice have been reported to be 20-fold less efficient in bacterial clearance from peritoneum as compared to control or mast-cell-reconstituted (*W/W^v*+MC) mice [34]. The lack of mast cell-derived TNF-α has been demonstrated to result in an impairment of neutrophil accumulation and defective bacterial clearance. The study of mast cell mediators represents an important way in which to understand the contributions of these cells in inflammatory processes. A focus of the present studies has been to determine the actions of tryptase as the most abundant product of the mast cell.

1.3 Human mast cells

1.3.1 Development

Mast cells were first described by von Recklinghausen in 1863 [36] in unstained specimens from frog mesentery; these were characterized as cells with coarse granules located mostly along the blood vessels. However, these cells were first identified by staining by Paul Ehrlich in 1878. Staining with a metachromatic dye (triphenylmethane and thiazine dyes of the aniline family), the cells were noted to have unique large granules [37]. The mast cell we thought to be an 'overfed' connective tissue cell, and the name "Mastzellen" (from the German: Mast, "fattening" as of animals) was miss-applied.

Mast cells develop from Kit$^+$, CD34$^+$ pluripotent stem cells in bone marrow [38] and their precursors migrate into the circulation. Once in the tissue, the precursors mature into mast cells in a process influenced by the local environment. Maturation of mast cells is dependent on the presence of SCF (c-kit ligand) and other cytokines [38-40]. Of these, IL-4 has been found to potentiate IL-3 induced clonal differentiation of isolated mouse peritoneal mast cells to cells of the connective tissue type [41] but effects of IL-4 on SCF-mediated differentiation of human mast cells can be variable [40]. IL-5 has been found to enhance the proliferative effect of SCF on cord blood derived mast cells [42] while IFN-γ has been reported to be responsible for increased surface expression of FcγRI receptors in human mast cells derived from peripheral blood CD34$^+$ progenitors [43]. Mast cells are particularly abundant in connective tissue matrices and near epithelial cell surfaces [4], where they can be effective initiators of inflammation [44].

1.3.2 Mast cell activation

The best understood immunological trigger of the mast cell involves the binding of allergen to cell-bound IgE. Exposure to allergen can stimulate production of allergen-specific IgE which binds to high-affinity IgE receptors (FcεRI) on mast cells [45]. On subsequent exposure to the same multivalent allergen, cross-linking of IgE molecules results in receptor aggregation and initiation of downstream intracellular signalling. A huge number of non-FcεRI receptor dependent stimuli of mast cell activation has been described, including neuropeptides e.g. substance P (SP) through neurokinin 1 receptor (NK1R), proteases through protease activated receptors (PAR-1-4), bacterial and viral products through toll-like receptors, NGF through tyrosine kinase receptor (TrKA), IgG through FcγRI and complement components C5a and C3a through C3aR and C5aR (CD88) [1, 46-50]. Mast cells can be also activated upon exposure to physical injury e.g. excessive heat, mechanical trauma, ultra-violet light, X-rays or chemical substances e.g. toxins, venoms-insects, bees, wasps, snakes proteases, dextran and cationic protein released from neutrophils.

1.3.3 Release of Mast cell mediators

Following activation, a range of preformed mediators can be released from mast cells (Figure 1.1) these include histamine, neutral proteinases and proteoglycan [51]. The neutral proteinases may be subdivided into three major groups; tryptases, chymases and carboxypeptidase. Tryptases are the predominant proteases of human mast cells, forming about 25 % of the total protein content of the mast cell, though in the rat, chymases are the most abundant proteases in mast cell granules [52].

The high levels of tryptase detected in many biological fluids make it a useful clinical marker for assessing the activation of mast cells in diseases like asthma, anaphylaxis, interstitial lung disease and arthritis [53]. Mast cells upon activation also begin *de novo* synthesis and release of mediators derived from arachidonic acid, including PGD_2 and LTC_4 [1].

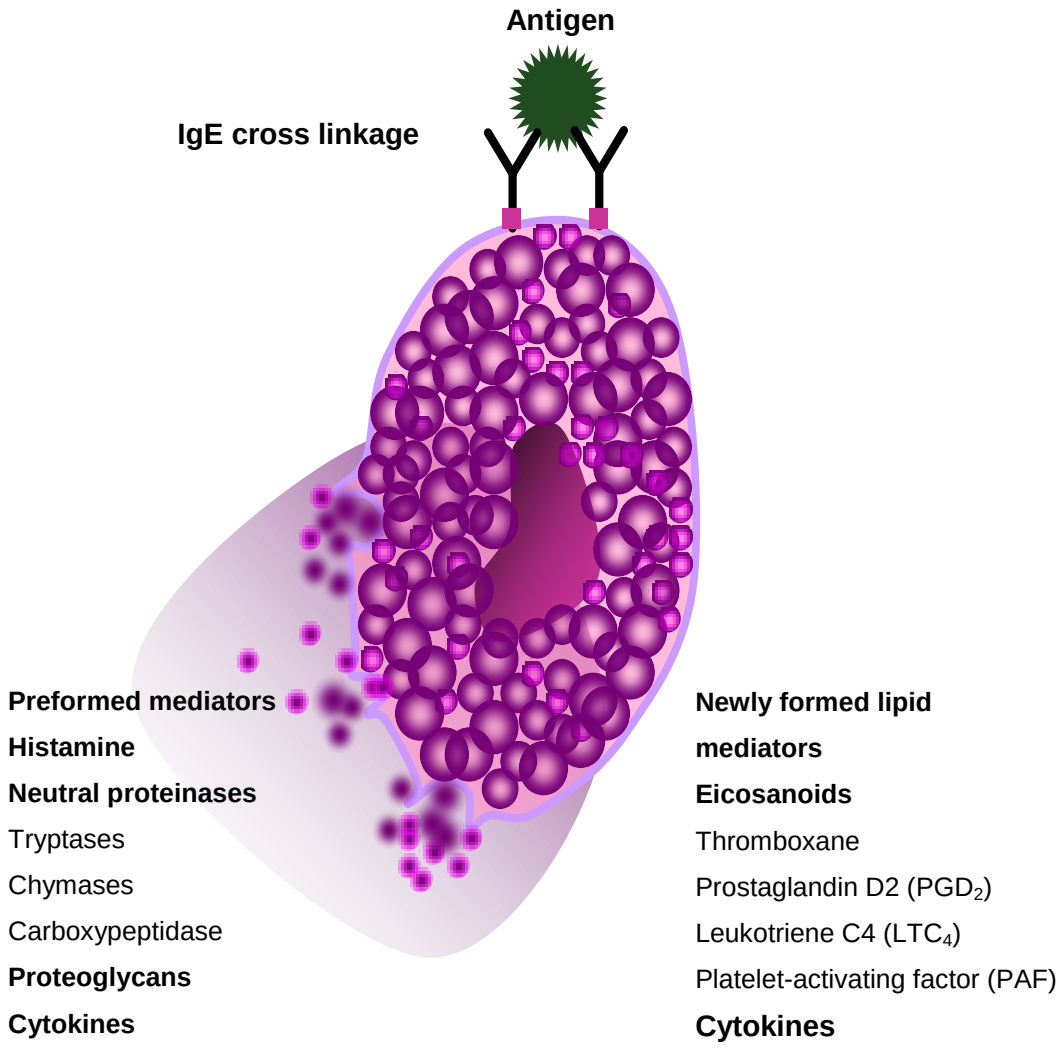

Figure 1.1 Products of IgE-dependent mast cell activation.

Mast cells are an important source of a range of inflammatory cytokines including TNF-α, IL-5, IL-6, GM-CSF and SCF which may be both stored in the cell granules or generated following degranulation. The activation of mast cells does not always involve complete degranulation. There have been reports that a selective release of mast cell mediators may occur. Thus for instance release of *de novo* synthesized IL-6 from human cord blood mast cells has been described following stimulation with IL-1 in the absence of tryptase release [54]. IL-6 has been found to be stored in separate vesicles from mast cell secretory granules. Similarly, release of vascular endothelial growth factor (VEGF) from corticotropin-releasing hormone stimulated human cord blood mast cells has been reported without tryptase, histamine, IL-6, IL-8, or TNF-α release [55]. The underlying mechanisms of selective IL-6 or VEGF may involve calcium-independent secretion of contents from certain granules rather than others (selective degranulation) [56, 57]. In addition, release of certain granular contents (piecemeal degranulation) has been described. T cell activation of cutaneous mast cells has been found to induce preferential release of serotonin without release of histamine, but evidence of mild degranulation of mast cells has been observed morphologically [58].

As well as, cytokines such as IL-6, IFN-γ, TNF, IL-1 and GM-CSF may be released following stimulation of mouse peritoneal mast cell TLR2 receptors with lipoteichoic acid (LTA) without β-hexosaminidase or serotonin release [59]. Monoclonal anti-CD30L antibody stimulated umbilical cord blood mast cells have been reported to induce IL-8, macrophage inflammatory protein-1α (MIP-1α) and MIP-1β without release of histamine or tryptase or leukotrienes [60].

1.4 Human mast cell tryptases

Tryptases are a family of serine proteases that like pancreatic trypsin can cleave peptides preferentially at the C-terminal side of Arg and Lys residues. Tryptases have been identified in many animal species, other than humans, including sheep, cow, dog, mouse, rat and gerbil. Human tryptases are a product of three or more non-allelic genes grouped on chromosome 16p13.3 [61].

1.4.1 Tryptase family

Human tryptase (EC 3.4.21.59) was first isolated by Schwartz et al. from partially purified mast cells of human lung tissue in 1981 [52] and later direct isolation of tryptase was performed with tissues of the lung, pituitary and skin [62–65]. Sequencing of tryptase cDNA from lung, skin and other tissues, and gene expression analysis has revealed several major variants of human tryptase and the family now composes α–, β–, γ–, δ–, ϵ–tryptase and the enzyme marapsin (Table 1.1).

There are several polymorphic variants of α and β tryptase that are expressed at the same gene locus. Beta tryptase is the most abundant form expressed in human lung and skin mast cells. The mature form of β–tryptase has been detected in the serum of patients with systemic anaphylaxis but it is not normally released in high levels into the circulation [66]. Amino acid differences between β–tryptase variants are quite small (≤ 5 amino acids). The βI and βIII tryptases differ from βII tryptase at amino acid 142 with Asn replacing Lys in the latter, and this is a putative glycosylation site of the βI and βIII tryptases. The single amino acid difference between βI and βII appears to lead to differences in enzymatic activity of both β–tryptase forms. The βIII form differs from βI and βII forms at position 60–63, where Arg–Asp–Arg replaces His–Gly–Pro [67] .

Alpha tryptase shows 93 % amino acid sequence homology with β–tryptase. The αI and αII variants are very similar and their recombinant forms have low activity compared to β–tryptase. Recombinant α–tryptase expressed without the pro–peptide is less efficient at cleaving the substrates H–D–HHT–Ala–Arg–*p*NA and tosyl–Gly–Pro–Arg–*p*NA than trypsin and βII–tryptase respectively [68]. A lack of enzymatic activity for α–tryptase may be explained by the presence of Asp215 (chymotrypsin numbering; corresponding to site 255) in the second of the seven loops forming the substrate–binding cleft instead of Gly in β–tryptase. A mutant α–tryptase (D215G) produced by substitution of Gly instead of Asp has been found to have enzymatic activity and can cleave fibrinogen and other substrates of β–tryptase [68]. Crystal structure analysis of the α–tryptase tetramer has shown kinking of the substrate binding site (Ser253–Gly257) which may be the cause of the decreased activity of α–tryptase. The presence of Arg at position –3 renders the pro–form of β–tryptase susceptible

to activation by dipeptidyl peptidase I (cathepsin C) whereas the Gln of α-tryptase prevents its activation.

Beta tryptase is a major constituent of the secretory granules of the mast cell [66]. In contrast to β-tryptase, α-tryptase has been proposed to be constitutively secreted into the circulation even in the absence of mast cell degranulation [66]. Schwartz et al. (2003) [69] employing monoclonal antibodies in ELISA that differentiate between pro- and mature forms of tryptase found that precursors of α and β-tryptase are secreted spontaneously. The mature forms appear to be stored in the cell and released upon activation of mast cells.

Gamma tryptases (γI and γII) are expressed in cells of the HMC-1 cell line (a cell line derived from a patient with mast cell leukemia) and in airway mast cells [70]. These tryptases have a characteristic C-terminal hydrophobic domain and a cytoplasmic tail.

The γ-tryptases are transmembrane tryptases which anchor to cytoplasmic or granular membranes. A transmembrane tryptase (TMT) has been identified which is identical to γ-I tryptase [71]. Substrate and inhibitor library screening of γ-tryptases has indicated substrate preference and inhibitor patterns different from those of β-tryptase[72]. Instillation of recombinant transmembrane tryptase into the mouse trachea has been reported to produce airway hyper-responsiveness and increased expression of IL-13 in lung tissue [73]. Delta tryptases (δI and δII) are very similar tryptases with a single amino acid difference (Val in δII and Met in δI) and this form has been reported to be expressed in colon, lung and heart tissues, and also in HMC-1 cells. Although there is a premature stop codon which is responsible for mature δ-tryptases being made shorter peptide than the older tryptase, the catalytic triad appears to be preserved and they have the characteristic trypsin-like cleavage specificity [74].

Table 1.1 Members of the human tryptase family

Type	Distribution		Pattern of release
α	Mast cells	[66, 75]	Constitutive
β	Mast cells	[52, 66]	Anaphylactic degranulation
γ	Mast cells, HMC-1 cells Many tissues	[70]	Trans-membrane
δ	HMC-1 cells and may be specific to mast cells Colon, lung and heart and synovial tissue	[74]	?
ϵ	Epithelial cells of airways (including trachea), oesophagus and foetal lung. Scarce in adult lung. Expressed at low levels in placenta, pancreas, prostate and thyroid gland	[76]	Constitutive
Marapsin	Stratified squamous epithelium; human oesophagus, tonsil, cervix, larynx and cornea	[77]	Constitutive

Marapsin is a serine protease which is encoded by the tryptase gene cluster at chromosome 16p13.3. Marapsin expression is limited to tissues containing stratified squamous epithelia and absent or weakly expressed in other tissues. Marapsin has been found to be constitutively expressed in non-keratinizing stratified squamous epithelia of human oesophagus, tonsil, cervix, larynx, and cornea [77]. In the keratinizing stratified squamous epidermis of skin, however, its expression is induced only during epidermal hyper-proliferation, such as in psoriasis and in murine wound healing. Its limited expression may give it a role in terminal differentiation of keratinocytes in hyper-proliferating squamous epithelia.

Human tryptase ε has been reported to be constitutively secreted in the airways and oesophagus [76]. The amino acid sequence is 38-44 % identical to human tryptase α, tryptase βI, tryptase βII, tryptase βIII, trans-membrane tryptase/tryptase γ and marapsin. Tryptase ε has a substrate preference distinct from that of other members of the tryptase family.

In the present study the focus has been on β-tryptase as this the form for which roles in allergic disease have been proposed. This has been the most extensively studied form of tryptases and it has been found to induce profound pro-inflammatory actions in animal models as well as *in vitro* models.

1.4.2 Structure and activity of tryptase

Following mast cell activation, tryptase is secreted along with heparin and histamine into the extracellular space [52, 78]. Upon release tryptase is enzymatically active in a non-covalently linked heparin-stabilized tetrameric form. Tryptase is resistant to most proteinaceous inhibitors and has an unusual substrate specificity in that has it has a preference for peptidergic rather than macromolecular substrates [79]. In the absence of heparin, tetramers of purified tryptase are converted to inactive monomers at neutral pH in physiological salt solutions. However, tryptase is stable in high salt solutions (>0.5 M NaCl) [79].

Derivation of the crystal structure has indicated that monomers are structurally similar (Figure 1.2) and each is formed of 245 amino acids. In the tetrameric form the molecular weight is approximately 135kDa. There are small

hydrophobic interfaces (A-B and C-D) which seem to be built-in shear points in the tryptase tetramer [80]. High salt concentrations strengthen the hydrophobic interaction and cause weak electrostatic repulsion of Arg/Arg in the interface [81].

Heparin which is an acidic proteoglycan, stabilizes the tetramer by its negative charge, and binds to a groove formed of a number of positively charged amino acid residues clustered on both sides of the interface (Figure 1.3). This could provide a means of regulating activity, as the tryptase tetramer breaks down rapidly into monomers [80] with conformational changes which are accompanied by the transformation of the active site into a zymogen-like structure [82]. Monomeric tryptase can be dimerized and reactivated completely at acidic pH [83].

The active site of each monomer faces into a central pore (Figure 1.2), which measures about 50 x 30Å. This tetrameric orientation restrict access of biological protease inhibitors to the active sites [84]. The tetrameric structure is likely to be responsible for the resistance of tryptase to inhibition and for restricted substrate specificity (rather than the structure of active site). The unique tetrameric structure makes tryptase different from most other serine proteases and it can be considered to be a self-compartmentalizing protease [85].

The geometry of the central pore of tryptase allows access to catalytic sites by peptidergic substrates such as neuropeptides, calcitonin gene-related peptide (CGRP), vasoactive intestinal peptide (VIP), peptide histidine-methionine (PHM) [86] and also vasopressin and kinetensin [62]. On the other hand most larger proteins appears to fail to gain access through the pore to active sites of the tryptase tetramer [87].

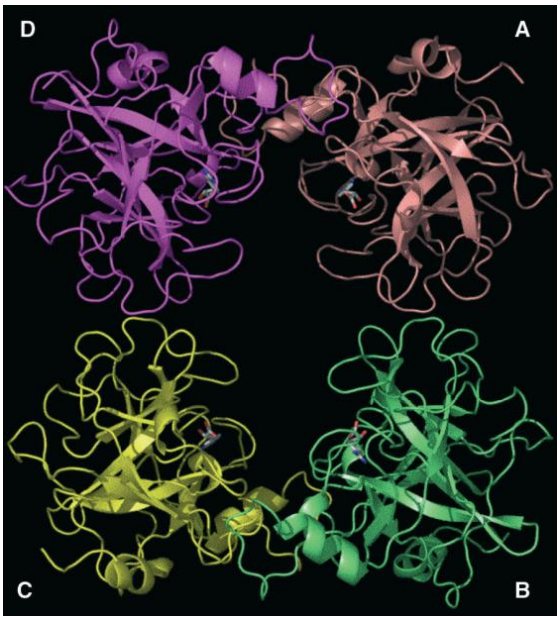

Figure 1.2 Structure of tetrameric human β-tryptase in a ribbon representation. The four monomers (A, B, C, D) are shown in different colours. The active-site inhibitor, APPA, is shown by a stick representation. Note the extensive contact areas between the subunits in the A–D and B–C interfaces, which contrast with the smaller contact areas in the A–B and C–D subunit interfaces, adapted from Pereira et al. (1998) [79].

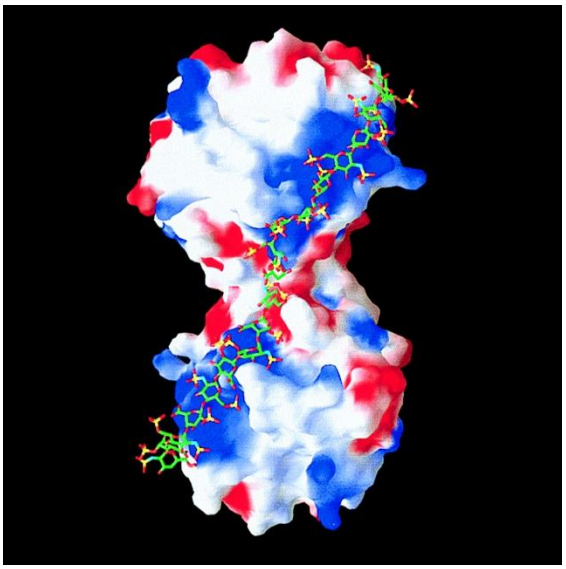

Figure 1.3 Model of the binding of a 20-mer heparin-like glycosaminoglycan chain along the A–B edge of the tryptase-tetramer. The solid-surface representation of tryptase indicates positive (blue) and negative (red) electrostatic potential contoured from −4 kT/e to 4 kT/e. The heparin chain (green/yellow/red stick model) is long enough to bind to clusters of positively charged residues on both sides of the monomer-monomer interface, thereby bridging and stabilizing the interface which is exclusively hydrophobic in nature (adapted from Sommerhoff et al. (1999) [86]).

A few molecules have been identified as substrates for tryptase (Table 1.2). Some large proteins such as prostromelysin (proMMP-3) and the zymogen of urinary type plasminogen can be activated by tryptase [88, 89]. This may be because these proteins are able to extend a cleavable surface loop (>20 Å) into the pore. This process of activation is facilitated by the negative electrostatic potential formed by negatively charged amino acid residues on the inner surface of the tryptase pore which promotes secondary interactions with basic substrates like histones.

In addition to soluble substrates, reports that tryptase can cleave membrane-bound protease activated receptor-2 (PAR-2) is of great interest. This receptor is a member of a family of G-protein coupled protease activated receptors. The PAR family is composed of a series of typically serpentine trans-membrane receptors with seven trans-membrane domains, with a $COOH^-$ terminal tail inside the cell and with N-terminal end in the extracellular environment [90]. This receptor will be considered in greater detail in Section 1.5.

Examining the activity of lung β-tryptase monomers using protease inhibitors and a tryptase specific monoclonal antibody (termed B12) which can facilitate conversion of tryptase from the tetrameric to the monomeric form, it has shown that heparin-activated monomers and B12-stabilized monomers have a broader spectrum and increased activity against protein substrates at acidic pH [84]. The tryptase monomers have also been postulated to contribute to the formation of anaphylatoxins C3a, C4a and C5a [46]. This may be of importance *in vivo* especially in tissues where to pH may be low, as has been reported in the airways of asthmatics [91] or areas of poor vascularity such as healing wounds, and in the periphery of solid tumours [92].

Table 1.2 Protein and peptide substrates of tryptase

Cleavage and inactivation of fibrinogen	[93]
Degradation of VIP, PHM, CGRP, vasopressin and kinetensin	[62, 86]
Activation of zymogen of urinary type plasminogen (pro-urokinase)	[89]
Activation of proMMP-3	[88]
Degradation of fibronectin	[94, 95]
Degradation of Type IV collagen	[96]
Cleavage of 72 kDa gelatinase	[94]
Generation of bradykinin from HMWK and LMWK	[12]
Activation of prekallikrein	[12]
Cleavge pro-atrial natriuretic factor	[97]
Cleavage of pro-nerve growth factor (pro-NGF)	[98]
Generation of complement component fragments C3a, C4a and C5a	[1, 46]
Activation of TGFβ	[99]
Degradation of high density lipoprotein $(HDL)_3$	[100]
Cleavage and activation of PAR-2	[101-103]

CGRP, Calcitonin gene-related peptide, HMWK, High molecular weight kininogen, LMWK, Low molecular weight kininogen, MMP, Matrix metalloproteinase, PAR, Proteinase-activated receptor, PHM, Peptide histidine methionine, Transforming growth factor beta (TGFβ), VIP, Vasoactive intestinal peptide.

1.4.3 Tryptase inhibitors

Tryptase inhibitors have been developed as potential therapeutic agents for asthma and other inflammatory conditions, and they are playing an important role as a means for exploring the actions of tryptase. There are a number of naturally occurring molecules that can inhibit the activity of tryptase, and there is a growing list of compounds that have been developed as potential drugs. These two categories will be considered separately.

1.4.3.1 Naturally occurring inhibitors

Few endogenous inhibitors of tryptase have been reported in man. There is some evidence that secretory leukocyte protease inhibitor (SLPI) can act as an inhibitor of tryptase, but the precise mechanism remains unclear [104]. Similarly, it has been reported that a tryptase-induced cleavage product of serpin-type proteinaceous inhibitor (SERPIN B6) (which is highly expressed in human mast cells and in HMC-1 cells) can inhibit tryptase activity by forming a covalent complex with the protease [105]. The unique tetrameric structure of tryptase is likely to restrict access to the catalytic sites. However, in the monomeric form, tryptase activity has been reported to be inhibited with various macromolecular inhibitors such as SERPIN B6, bovine pancreatic trypsin inhibitor, anti-thrombin and α_2-macroglobulin [67]. The lack of inhibitors of tetrameric tryptase has raised the possibility that other mechanisms may be involved in limiting tryptase activity in man.

It is possible that the activity of tryptase may be controlled by destabilization of the tetrameric form. Tryptase can be destabilized, rather than inhibited, by polycationic substances that compete with tryptase for binding to heparin. Anti-thrombin was the first heparin antagonist that was reported to inhibit tryptase activity [106], and subsequently several other heparin antagonists have been described in this context including lactoferrin, neutrophil myeloperoxidase (MPO) and protamine (as well as polybrene and certain synthetic polycationic peptides such as polyArg or polyLys) [67].

Leech-derived tryptase inhibitor (LDTI), an inhibitor originally isolated from the medicinal leech, can inhibit tryptase activity through active site-directed inhibition [107]. More recently, a tick-derived protease inhibitor (TdPI) has been reported to be an efficient inhibitor of tryptase. This tick protein was

identified in the saliva of this species and found to be structurally related to Kunitz-type protease inhibitors, such as those of the bovine pancreatic trypsin inhibitor (BPTI) family [108]. TdPI has been reported to be cleaved by tryptase resulting in generation of a potent inhibitor that may be able to inhibit three of the four catalytic sites of the tryptase tetramer. It has been suggested that one molecule of TdPI can block one of the catalytic sites in the tryptase tetramer which in turn can initiate cleavage of the TdPI molecule and generate an active C-terminal region. The active C-terminal region blocks a second tryptase catalytic site while another molecule of TdPI can still have access to the tryptase tetramer pore and block a third catalytic site. The therapeutic potential of this compound is attracting attention, and it has been evaluated in the present studies.

1.4.3.2 Synthetic inhibitors

The low molecular weight compound APC-366 was one of the first tryptase inhibitors to be developed as a therapeutic agent. It is a relatively non-selective and slow-acting tryptase peptide based inhibitor. APC-366 inhibits tryptase by forming a covalent bond with the active site [109]. In human and animal models, inhalation of APC-366 has been reported to prevent late phase bronchohyperresponsiveness on allergen challenge, and intradermal injection to block the cutaneous reaction to antigen [110-112]. In a clinical trial with sixteen mild asthmatic patients, pre-treatment with the synthetic tryptase inhibitor APC-366 caused a decrease in late phase asthmatic response after allergen challenge compared to placebo [111]. These findings provided early support for tryptase having a role in the induction of inflammation and airways hyper-reactivity. Other monovalent tryptase inhibitors that have been used in animal models of inflammation include BABIM and RWJ-56423 [113, 114]. Nafamostat mesilate, already used as an anticoagulant in humans, is a competitive inhibitor of tryptase [115]. This compound has been found at low doses to decrease trinitrobenzene sulphonic acid (TNBS) induced colitis in rats [116].

To enhance selectivity of inhibition, bivalent inhibitors of tryptase have been developed. They act through the bridging of two active sites in the tryptase tetramer [117]. The bivalent inhibitors AMG-126737 and MOL-6131 have been found to inhibit airway hyper-responsiveness and have anti-inflammatory

actions in sheep and mouse models of asthma respectively [118, 119]. Tryptase inhibition by intranasal or oral administration of selective tryptase MOL 6131 inhibitor has been observed to result in blocking of processes of inflammation in an ovalbumin-sensitized mouse model of asthma [119]. In treated animals, MOL 6131 was found to reduce goblet cell hyperplasia, mucus secretion and oedema, the numbers of eosinophils, endothelial cell VCAM-1 expression in pulmonary blood vessels, and the levels of IL-4, and IL-13 in broncho-alveolar lavage fluid of mice. In addition tryptase has been demonstrated to induce the proliferation of myocytes [101] and tracheal smooth muscle cells *in vitro* [120]. APC-2059, another bivalent inhibitor has been investigated in a small clinical pilot study in the treatment of mild to moderate ulcerative colitis [121], and reported to be safe and with some evidence of efficacy in the treatment of this condition.

The low molecular weight compound SAR160719A-5 though not bivalent, has been found to be a selective and reversible inhibitor of human β-tryptase, with a Ki of 38 nM, and it is undergoing pre-clinical evaluation as a drug [122]. SAR160719A-5 has been found to be efficacious in an animal model of dermatological allergic conditions, and in particular for atopic dermatitis. Co-injection of this inhibitor with *Ascaris suum* intradermally elicited a reduction of antigen-induced wheal formation when measured 15 minutes after injection. This compound may be useful as an inhibitor of β-tryptase in conditions associated with mast cell activation, and it has been employed in the present studies.

1.4.4 Pro-inflammatory actions of tryptase

Potential roles of tryptase in inflammatory processes have been studied in various *in vitro* and *in vivo* models. Some of the major findings (summarised in Figure 1.4) are consistent also with the findings reported above with administration of tryptase inhibitors in animal and human models.

In immediate allergic reactions, tryptase has been implicated as a stimulus for increased vascular permeability. The mechanism could involve the degranulation of mast cells by tryptase, as tryptase has been demonstrated to induce *in vitro* activation of mast cells from human lung, skin and tonsil tissue [10]. Degranulation of peripheral blood eosinophils from asthmatic patients

can also be induced in the presence of tryptase [123]. A role for tryptase has been proposed in the generation of kinins from both high and low molecular weight kininogens [124]. Tryptase can efficiently cleave the neuropeptides histidine-methionine, VIP and CGRP[86] and this protease could thus contribute to processes of neurogenic inflammation.

Potent pro-inflammatory actions of tryptase have been indicated by studies with animal models. Injection of human lung tryptase into the skin of guinea pigs or the peritoneum of mice has been found to result in the massive accumulation of neutrophils and eosinophils [10, 11]. Tracheal instillation of βI-tryptase in the mouse trachea has been reported to induce neutrophil accumulation in tissues [125]. Peritoneal injection of the mouse tryptase mMCP-6, has also been reported to induce intraperitoneal neutrophilia [126], while injection of another mouse tryptase mMCP-7, caused eosinophil accumulation in the peritoneal cavity [125].

Pretreatment of sheep with APC-366 or H-1 or H-2 antagonists has been found to decrease the size of cutaneous wheal induced by tryptase injected into the skin [127]. Tryptase can also induce the secretion of IL-8 and IL-1β from endothelial cells [128], up-regulate expression of ICAM-1 and stimulate IL-8 release from epithelial cell derived human cell line [129] which linked to tryptase-induced inflammation including accumulation of leukocytes.

Increased levels of tryptase have been found in the affected tissues of various chronic conditions, in addition to bronchial asthma, these include arthritis, psoriasis, renal interstitial fibrosis and atopic dermatitis [67]. Tryptase may contribute to processes of remodelling in such conditions. It can be a potent growth factor for epithelial cells and fibroblasts [129], activate stromelysin [88] and increase collagen production and release from fibroblasts [130]. The mitogenic actions of tryptase and the increase in collagen production stimulated by this protease [131] have been proposed as a mechanism for fibrosis in allergic conditions like asthma.

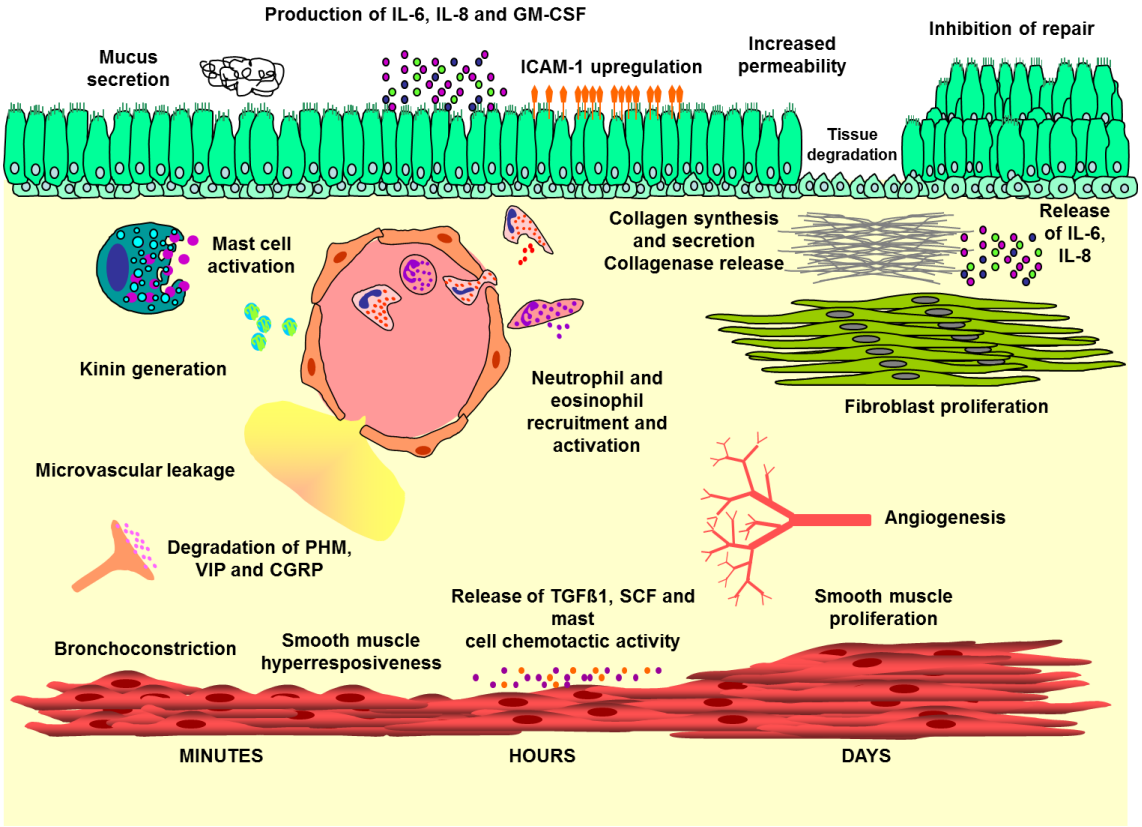

Figure 1.4 Diagrammatic representation of the potential pro-inflammatory actions of tryptase. Courtesy of Dr. Andrew F. Walls. ICAM-1, intercellular adhesion molecule 1; GM-CSF, granulocyte-macrophage colony-stimulating factor; IL, interleukin; TGFβ1, transforming growth factor beta 1; SCF, stem cell factor.

Addition of tryptase has been found to induce bronchial constriction and an increase in histamine levels in isolated human and guinea pig bronchi [6]. In sheep, inhalation of tryptase has been reported to result in a histamine-mediated airway hyper-responsiveness, which can be inhibited by the tryptase inhibitor APC-366 or by intravenous injection of the histamine-1 (H_1) receptor antagonist (chlorpheniramine) [132]. Similar findings have been reported when APC-366 has been administered by inhalation into pigs sensitized to the antigen *Ascaris suum* antigen [133]. The administration of APC-366 was found to protect pigs from an increase in airway resistance and an increase in urinary histamine levels after inhalation of allergen as compared to control pigs. Cleavage of bronchodilating peptides e.g. VIP and related peptides may provide another means whereby tryptase may cause brochoconstriction [86, 134]. Tryptase has been reported also to increase the sensitivity of isolated human bronchial tissue to bronchoconstrictive agonists e.g. histamine [135, 136].The induction of release of active transforming growth factor β (TGFβ) in airway smooth muscle (ASM) cells by tryptase may be an indirect way by which tryptase contributes in the remodelling processes [99, 137]. *In vitro* tryptase may have pro-angiogenic actions through increasing proliferation of endothelial cells which can play a role in wound healing in normal conditions or tumour progression [138]. Tryptase inhibitors show promise as new treatments for allergic and inflammatory conditions.

The roles of tryptase are not limited to the generation of mediators of inflammation or remodelling and this protease can contribute to the controlling of such processes by the cleavage of cytokines. Thus for example eotaxin and RANTES are both cleaved by tryptase *in vitro* [139], and this has been postulated to account for the small numbers of eosinophils in smooth muscle bundles of asthmatic airways. The enzymatic actions of tryptase may lead to cleavage of foreign peptides including allergens, as proposed for chymase with birch pollen profilin [140].

The actions of tryptase depend on the type of tryptase and animal species studied, and moreover tryptase inhibitors differ in their effectiveness and selectivity. The previously described tryptase actions were mostly reported with tryptase purified human lung and more studies are needed to explore the actions of recombinant tryptase. In addition the mechanism of action of

tryptase is remains unclear which needs further work. Caution should be employed when extrapolating findings with non-human tryptase to human disease, but the use of animal models may lead to useful insights.

1.5 Protease activated receptor 2 (PAR-2)

PARs have been characterized as G-protein coupled receptors with a unique means of activation. A range of proteases can cleave and activate PARs, including proteases from the coagulation cascade, inflammatory cells, and the digestive tract. PARs activation initiates various functions in many cell types ranging from haemostasis to pain transmission. Up to date four members of PAR family have been cloned including PAR-1, -2, -3 and -4, all of which activated by thrombin except PAR-2 that differentially activated by trypsin [141].

Cloning of human PAR-2 revealed a protein of 397 amino acids with a calculated molecular weight of 44,125 kDa and with seven hydrophobic trans-membrane domains with an N-terminal hydrophobic region [142, 143]. PAR-2 has been found to be highly expressed in human pancreas, kidney, colon, liver and small intestine, and in A549 lung and SW480 colon adenocarcinoma cells [144]. PAR-2 has characteristic putative signal peptides and an N-linked glycosylation site located in the N-terminus of human PAR-2, but their effects on the function of PAR-2 is not known. Although mouse PAR-2 is 83 % and human thrombin receptor is 35 % identical to the human PAR-2, the trypsin cleavage site (SKGR↓SLIG) is conserved.

1.5.1 PAR-2 activation

The general mechanism of activation of PAR involves protease cleavage at a specific site within the extracellular N-terminus which exposes a new N-terminal sequence forming a 'tethered ligand domain'. This domain binds to a specific region in the second extracellular loop of the cleaved receptor and the interaction results in signal transduction (Figure 1.5).

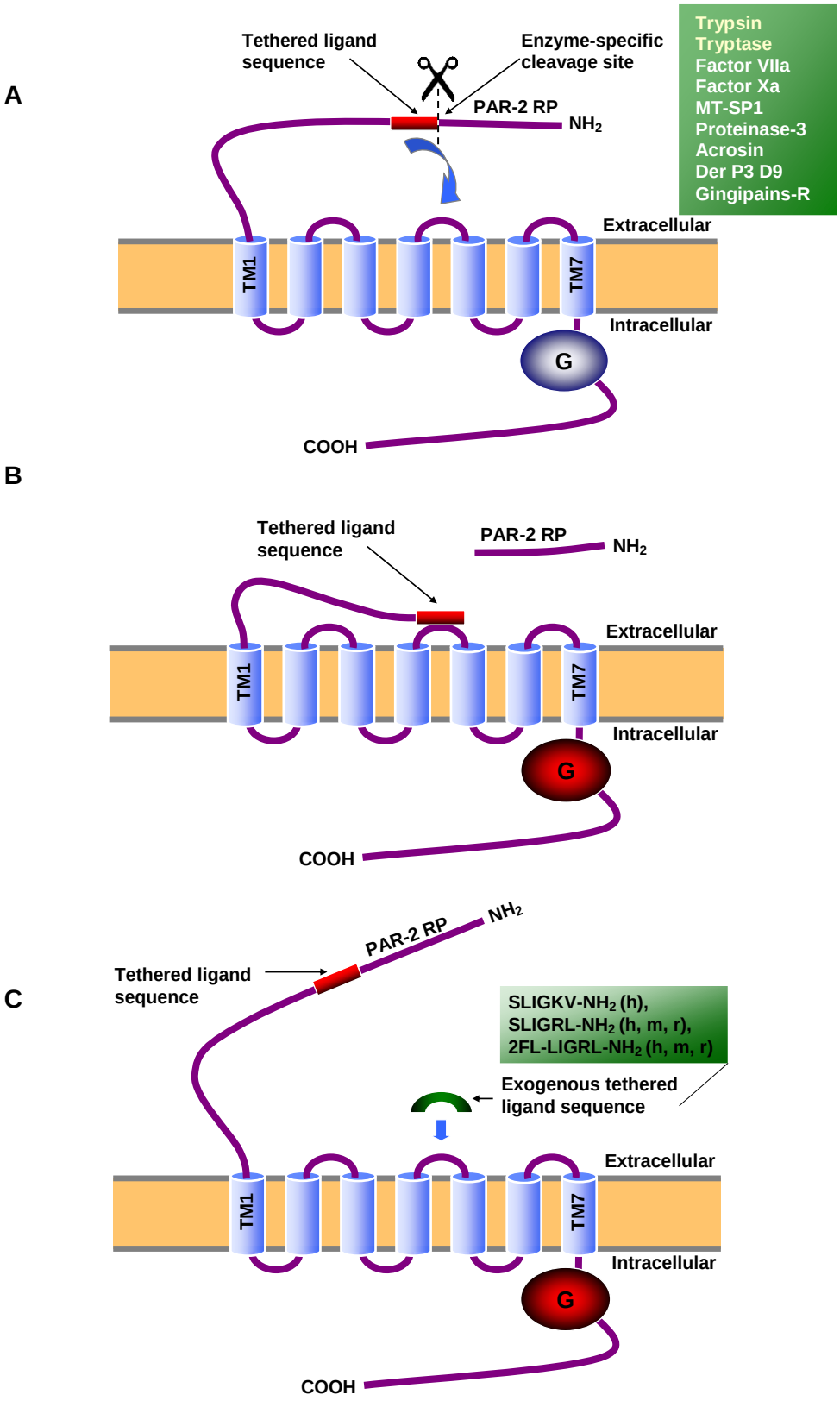

Figure 1.5 Diagrammatic representation of PAR-2 activation. (A) Excision of a PAR-2 released peptide (PAR-2 RP) from the extracellular domain by certain serine proteases results in exposure of a tethered ligand sequence, which (B) binds to the second extracellular loop of the receptor; (C) PAR-2 may be also stimulated by an exogenous peptide with the tethered ligand sequence (shown for human, h; mouse, m; rat, r).

The function of the amino-terminal fragment that is removed by proteolysis is unknown. However, there is the potential for it to have biological activity. The analogue peptide of PAR-1 has been reported to induce platelet-endothelial cell adhesion in a human saphenous vein endothelial cell model [145]. The peptide released from PAR-1 has a greater potency than thrombin or other stimuli and act through mechanisms that involve the platelet GPIIb-IIa (integrin $\alpha_{IIb}\beta_3$) receptor. It will be important to examine if the corresponding peptide of PAR-2 also has biological actions.

Several proteases can induce activation of PAR-2 in addition to trypsin and tryptase. These include factor VIIa, factor Xa, proteinase-3, membrane type-serine protease-1 (MT-SP1), acrosin, dust mite serine proteases Der p3 and Der p9, gingipain-R [141], chitinase from bacteria and fungi [146], and human epidermal kallikrein-related peptides 5 and 14, KLK5 and KLK14 [147]. Other proteases such as chymase [148], cathepsin G and elastase on the other hand, can inactivate PAR-2 by cleavage at another site. In humans the 46 amino acid residues forming the extracellular N-terminus are cleaved by trypsin and tryptase at $SKGR^{36}\downarrow S^{37}$LIGKV exposing the tethered ligand SLIGKV. In mice, cleavage is at $SKGR^{34}\downarrow S^{35}$LIGRL exposing the tethered ligand SLIGRL [143] and only two amino acids are different in those that follow the trypsin cleavage site at the carboxyl end. Direct activation of PAR-2 without receptor cleavage can be elicited by synthetic peptides which correspond to the tethered ligand domain [141] (illustrated in Figure 1.5 C).

1.5.2 PAR-2-induced intracellular signalling

PAR-2 is widely expressed in epithelial cells, endothelial cells, fibroblasts, myocytes, neurons and astrocytes. Activation of PAR-2 produces many responses including cellular differentiation, proliferation, and the production and release of various cytokines from different cell line including human keratinocytes and human airway epithelium such as IL-6, GM-CSF, eotaxin and IL-8 [149-152]. Although PAR-2 signalling has not been studied to the same extent as for other PARs, several pathways are implicated and these are summarised in Figure 1.6.

PAR-2 coupling to the heteromeric G-proteins $G\alpha_q/G_{11}$ results in activation of phospholipase C (PLC) which in turn generates inositol triphosphate (IP3) and

diacylglycerol (DAG), leading to mobilization of calcium and activation of protein kinase C (PKC) [90]. In *Xenopus* oocytes intracellular signalling provoked by trypsin may include pertussis toxin (PT)-sensitive calcium signalling, suggesting that a G_0/G_i-dependant transduction mechanism has a potential role in PAR-2 signalling as has been described with PAR-1 [153]. This finding is at variance with the results of studies with a PAR-2 transfected normal rat kidney cell line transformed by Kirsten murine sarcoma virus (KNRK) cells and enterocytes in which it has been reported that PAR-2 activation by peptide agonists did not result in signalling through G_i [154].

PAR-2 activation results in a cell-type specific activation of several kinase cascades which may be independent on PKC (e.g. extracellular signal regulated kinase; ERK) or partially regulated by PKC (e.g. the mitogen-activated protein kinase; MAPK family: c-Jun N-terminal kinase; JNK, p38MAPK and nuclear factor kappa B; NF-κB [155] alongside its regulating kinase I kappa B kinase; IKK) [156]. An important role for β-arrestins has been suggested by the activation of ERK1/2 [154]. The protein kinase pathways involved differ between studies and depend on the cell type and PKC subtype [155]. PAR-2 can in addition increase c-fos levels, which are associated with tyrosine phosphorylation of SHP-2, which has been claimed to play a role in PAR-1-induced mitogenic signalling [90].

In enterocytes and transfected epithelial cells, activation of PAR-2 results in release of arachidonic acid and formation of prostaglandin (PG) E_2 and $PGF_{1\alpha}$ through activation of phospholipase A_2 and cyclooxygenase (COX) [157]. PAR-2 activation has been found to induce redistribution of cell membrane-bound Jun activation domain-binding protein 1 (Jab-1) to the cytosol where it binds and phosphorylates the c-Jun NH_2-terminal activation domain. Activated c-Jun travels to the nucleus where it binds to a transcription factor activator protein-1 (AP-1) motif, initiating gene expression. This in turn can control PAR-2 triggered inflammatory responses and the release of pro-inflammatory mediators [158]. Studies to date have involved investigation of defined signalling processes in cells with calcium flux as a primary read-out. Investigation of changes in global gene expression could give new insight into the signalling processes.

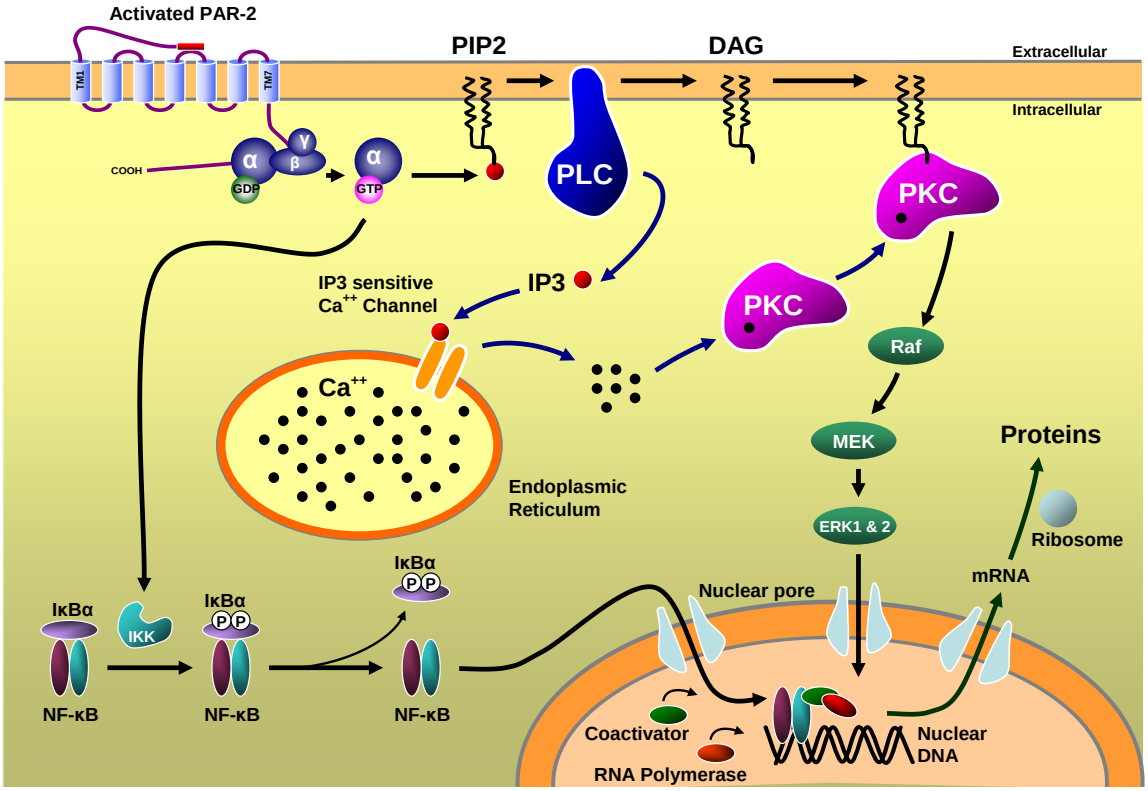

Figure 1.6 Diagrammatic representation of PAR-2 signalling pathways. Abbreviations: G protein subunits α, β and γ, guanosine diphosphate GDP, guanosine triphosphate GTP, phosphatidylinositol 4,5-bisphosphate PIP2, phospholipase C PLC, diacylglycerol DAG, inositol 1,4,5-triphosphate IP3, protein kinase C PKC, I κ B kinase IKK, inhibitory protein I κ B α, nuclear factor kappa B NF- κ B, raf kinase Raf, mitogen activated protease kinase MEK, extracellular signal-regulated kinases 1&2 ERK1 & 2. This summarises data presented in several studies [90, 153, 154, 156-158].

1.5.3 Regulation of PAR-2 signalling

PAR-2 is a single use receptor which is irreversibly activated by cleavage of the extracellular domain. The exposed PAR-2 tethered ligand domain is always ready for interaction with the second extracellular loop. Activation of PAR-2 by peptide agonists results in phosphorylation of the receptor by induction of G-protein coupled receptor kinase (GRK) and PKC. Activation of the receptor causes translocation of β-arrestins to the plasma membrane to interact with PAR-2 causing desensitization and the uncoupling of PAR-2 from heterotrimeric G-proteins [159]. At this stage β-arrestins rapidly internalize the receptor by coupling it to clathrin-coated pits in early endosomes. Detachment of PAR-2-containing clathrin-coated pits has been found to be mediated by the GTPase dynamin [160]. After this step, it has been found that most PAR-2 appears to be directed to lysosomes for degradation leading to down-regulation of PAR-2 expression.

Re-sensitization of cells with PAR-2 requires either the mobilization of Golgi stores or the synthesis of new receptors [148]. Endocytosis of PAR-2 is involved in some aspects of receptor signalling. β-arrestin-dependent endocytosis is required for MAPK cascade activation in which β-arrestins act as a scaffold that recruits and organizes components of MAPK into endosomes [154]. Certain proteases can also down-regulate PAR-2 function, through an ability to 'disarm' PAR-2, cleaving at a non-receptor activating site, that results in removal of the tethered ligand domain. Although these disarmed receptors can still interact with peptide agonists, they have lost their ability to be activated by proteases [161]. Tryptase can cleave PAR-2 at the Lys^{41} ↓Val^{42} site in addition to the other activation site but, the activating cleavage at Arg^{36} ↓Ser^{37} (SKGR^{36}↓S^{37}LIGKV) appears to be favourable [102].

1.6 PAR-2 and inflammation

PAR-2 has been proposed to have unique roles in inflammation and has been implicated in the normal functioning of the airways, intestine, cardiovascular system, nervous system and musculoskeletal systems, and in differentiation of skin. PAR-2 is widely expressed in many cell types including epithelial cells, fibroblasts, smooth muscle cells of the airways, and vascular endothelium in addition to mast cells, eosinophils, monocytes, macrophages and neutrophils

[161, 162]. The degree to which PAR-2 may have a role in inflammation and allergy is not clearly understood. Some studies have been suggested predominantly pro-inflammatory actions, while for others anti-inflammatory actions have been reported. The differences in response to PAR-2 activation may depend on the extent of PAR-2 activation, the model studied or species employed, or the tissue target or cells. Potential actions of PAR-2 agonists are summarised in Figure 1.7.

Potential anti-inflammatory actions of PAR-2 have been proposed in studies of epithelial and endothelial cells. Activation of PAR-2 in epithelial cells can result in the release of nitric oxide (NO) and PGE_2 [163, 164] which have been suggested to increase mucus secretion, ciliary beating, intercellular adhesion and water escape to the lumen. In endothelial cells, mediators generated as a result of PAR-2 activation such as NO, prostacyclins or endothelin 1 (ET1) may be responsible for vasodilatation and increased local blood flow, as well as inhibit neutrophil activation and infiltration, and inhibition of platelet aggregation [165, 166], although an increased production of von Willebrand factor has been reported [167]. PAR-2 activation by trypsin on primary spinal afferent neurons has been reported to stimulate arteriolar dilatation and hyperaemia through the release of CGRP, and to increase venular permeability through the production of SP and neurokinin A (NKA) [168].

PAR-2 activation has been reported to mediate arterial and venous dilatation in healthy human subjects *in vivo* [169] and perfused rat kidney models [170]. On the other hand, vasoconstriction has been reported following addition of PAR-2 activating peptides to isolated rat pulmonary artery [171] or human umbilical vein [172]. PAR-2 activation by the peptide agonist (SLIGRL-NH_2) may be involved in the protection against caerulein-induced intrapancreatic damage in rats through modulating MAP kinase and MAP kinase phosphatase signalling [173]**.** In contrast, it has been reported that PAR-2 peptide agonist SLIGRL-NH_2 worsening inflammatory reaction in bile salt- and secretagogue-induced pancreatitis in C57BL/6 mice [174].

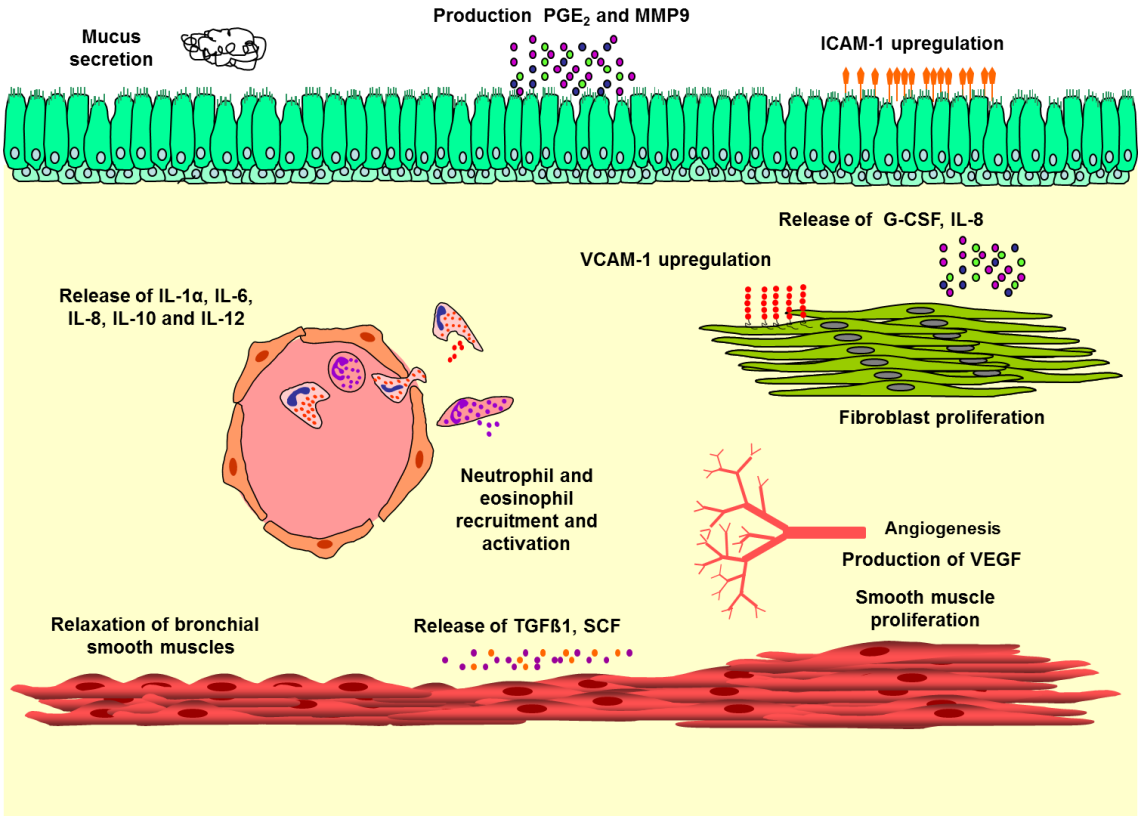

Figure 1.7 Diagrammatic representation of the potential contributions of PAR-2 activation in inflammatory processes. PGE_2, prostaglandin E 2; MMP9, matrix metallopeptidase 9; ICAM-1, intercellular adhesion molecule 1; G-CSF, granulocyte colony-stimulating factor; VCAM-1, vascular cell adhesion molecule 1; IL, interleukin; VEGF, vascular endothelial growth factor; TGFβ1, transforming growth factor beta; SCF, stem cell factor.

A role for PAR-2 activation in processes of tissue repair has been described. PAR-2 stimulation has been reported to stimulate smooth muscle cell and endothelial cell proliferation [167], induce the production of the pro-angiogenic VEGF [175] and to improve the integrity of endothelial cell barrier *in vitro* as described in a HUVEC cell model [176]. Activation of PAR-2 can stimulate the proliferation of lung fibroblasts and airway smooth muscle cells [162] and can lead to the release of PGE_2 and matrix metalloproteinase 9 (MMP9) from airway epithelial cells. The PAR-2 peptide agonist SLIGKV-NH_2 has been found to induce the proliferation of cells of a human mucoepidermoid carcinoma (h292) cell line and cultures of primary bronchial epithelial cells [177].

A contribution by PAR-2 activation to the defense against microorganisms has been reported. In human monocytes infected with influenza A virus, PAR-2 activation by the activating peptide trans-LIGRLO-NH_2 has been reported to enhance the anti-viral actions of INFγ [178] inducing a decrease in virus replication, the attraction of T lymphocytes and monocytes, and an increase in surface expression of CD64 (FcγRI and αVβ3). In a murine model of *P. aeruginosa*-induced pneumonia, PAR-2 knockout mice have been found to have decreased in INFγ levels in broncho-alveolar lavage (BAL) fluid, compared with that in wild-type infected mice where high levels of TNF-α, total protein concentration and neutrophil infiltration in the airway lumen [179]. Neutrophils and macrophages derived from PAR-2 deficient mice have been reported to have reduced phagocytic ability, while those derived from wild-type mice have enhanced phagocytic activity following activation of PAR-2 with the peptide agonist SLIGRL.

The pro-inflammatory effects of PAR-2 activation may result from release of certain cytokines which can activate immune cells and stimulate leukocyte accumulation in the tissues. In isolated human eosinophils, trypsin or the PAR-2 peptide agonist SLIGKV-NH_2 have been reported to stimulate the degranulation and production of superoxide anion [180] and the addition of tryptase can induce IL-8 release [181]. PAR-2 activation stimulated by the peptide agonist SLIGKV-NH_2 in neutrophils can result in morphological changes with an increase in CD11B/CD18 expression [182]. PAR-2 activation has been

reported to stimulate an increase in PAR-2 expression and IL-8 production in *H. pylori* infected gastric epithelial cells [183].

Addition of trypsin or the PAR-2 peptide agonist SLIGKV-NH_2 to human dermal microvascular endothelial cells has been found to result in an increase in calcium signalling and up-regulation of IL-6 and IL-8 expression [184]. Tryptase has been postulated to have a role in production of chronic inflammation through activation of basal PAR-2 in addition to the luminal PAR-2, where there is disruption of the intercellular tight junction, for example by eosinophil-derived major basic protein during allergic reactions [164]. PAR-2 stimulation by peptide agonist SLIGRL-NH_2 has been reported to induce production of cytokines such as IL-8, IL-6 and also PGE_2 from keratinocytes [185]. Human epidermal kallikrein related peptides 5 and 14 (KLK5 and KLK14) can activate PAR-2 *in vitro* which may contribute to skin inflammation, epidermal barrier repair and pruritus [147]. An increase in IL-8 production has been reported in human oesophageal epithelial cells incubated with by trypsin [186].

Intraperitoneal injection of the PAR-2 peptide agonist SLIGRL-NH_2 has been reported to cause significant accumulation of leukocytes in the peritoneum of rats [187] but their precise cell types were not enumerated. Although injection of trypsin has been reported to result in accumulation of neutrophils and eosinophils in the peritoneum of mice, SLIGRL the PAR-2 peptide agonist was not found to replicate this effect when administered intranasally into the lungs or injected into the mouse peritoneum [162]. Although there is some evidence that PAR-2 may be up-regulated in the epithelium of bronchial biopsy of asthmatic patients, as revealed by immunohistological staining [188], it has also been reported that there may be no increase in PAR-2 mRNA and protein expression in asthmatic patients compared to control subjects [189, 190]. Deficiency in PAR-2 expression has been reported to be associated with a decrease of eosinophilic inflammation in a murine model of asthma [191]. The PAR-2 peptide agonist SLIGRL-NH_2 stimulated an increase leukocyte rolling and in numbers of adherent leucocytes in wild-type mice, a process that delayed in PAR-2 deficient mice [192]. Mucin secretion has been reported to be weakly stimulated when PAR-2 is activated in human bronchial epithelial cell lines [193]. Infiltration of leukocytes in BAL fluid has been found after activation of

PAR-2 in wild type mice [194], while decreases in eosinophil numbers in BAL fluid and serum IgE levels in PAR-2 knockout mice have been observed. Allergen challenge has been found to produce high levels of eotaxin and the accumulation of eosinophils in BAL fluid in ovalbumin sensitizated wild-type mice, but not the PAR-2 knockout mice [191]. Activation of PAR-2 with trypsin or SLIGKVD-NH_2 in isolated blood eosinophils has been reported to result in morphological changes, and the release of cysteinyl leukotrienes and reactive oxygen species [190]. PAR-2 activation has been found to inhibit keratinocyte growth [195].

It has been suggested that the elevated luminal proteases may induce the activation of PAR-2 in inflammatory bowel syndrome (IBS) and ulcerative colitis [196]. Supernatants from colonic biopsies from IBS patients, which have high tryptase and trypsin levels have been reported to induce calcium mobilization in mouse dorsal root ganglion neurons from wild-type mice but not PAR-2 knockout mice [197]. A decrease in leukocyte trafficking, adhesion and expression of adhesion molecules (ICAM, VCAM and α-M) has been reported in colonic samples of PAR-2 knockout mice [198]. In a murine model of osteoarthritis, cartilage damage and subchondral bone formation have been observed to be minimal in PAR-2 deficient mice, an use of a PAR-2 blocking mouse monoclonal antibody (SAM-11) has been also reported to be protective in wild-type mice [199]. Disruption of the PAR-2 gene in C57BL/6 mice has been reported to inhibit chronic arthritis induced by injection of Freund's complete adjuvant into the joint space and peri-articular [200] while PAR-2 gene expression has been found to be upregulated in inflamed tissues when investigated by staining for a β-galactosidase activity reporter gene. In addition, activation of PAR-2 by intra-articular injection of the PAR-2 peptide agonists SLIGRL-NH_2 or 2-furoyl-LIGKV-OH has been found to induce joint swelling and hyperaemia.

1.7 PAR-2 as a target for tryptase

There is a growing awareness of the range of actions of tryptase, as a stimulus for cytokine release, cell proliferation and inflammation, the precise mode of action of this protease is unclear. While the contribution of tryptase could depend on its catalytic activation or inactivation of various substrates which may participate in inflammatory processes, the biological actions of tryptase

have been postulated to be mediated predominantly by activation of PAR-2. Although Molino and colleagues (1997) have reported that purified tryptase can cleave and activate PAR-2 [102], direct activation of PAR-2 by tryptase has not been consistent observation [201]. Tryptase has been reported to have lower potency than trypsin in the activation of PAR-2 [134], but in tissues with low trypsin expression, local release of high concentrations of tryptase from mast cells in inflammatory conditions such as asthma (and tryptase resistance to endogenous protease inhibitors) has been suggested to be capable of inducing extensive PAR-2 activation.

Evidence implicating PAR-2 in mediating the actions of tryptase has come from the findings that this receptor is abundantly expressed on cells or tissues on which tryptase can exert changes in cell function. Effective antagonists of PAR-2 have not been available, but many findings with peptide agonists or with trypsin are reminiscent of those with tryptase (Table 1.3). The PAR-2 peptide agonist SLIGKV-NH_2 has been found to replicate the effects of tryptase on calcium signalling [202] and proliferation [203] in human airway smooth muscle cells. Similarly, SLIGKV-OH can mimic the tryptase-induced proliferation of human conjunctival fibroblasts [204]. Human tryptase has been found to stimulate proliferation of rat skeletal myoblasts. Contribution of PAR-2 activation has been derived from increased levels of phosphorylated ERK 1/2, the PAR-2 activation marker in cells treated with tryptase, the effect which mimicked by trypsin.

Cyclooxygenase 2 (COX-2) has been reported to be involved in PAR-2 signalling and inhibition of COX-2 has been found to blunt the effect of tryptase on proliferation [205]. Similarly, human tryptase has been reported to enhance proliferation of human fibroblasts with induction of COX-2 mRNA expression and increased prostaglandin J_2 (PGJ_2) synthesis. The proliferative effect of tryptase has been found to be replicated by SLIGKV and abolished by blocking the COX-2 inhibition [206]. Tryptase and trypsin have been reported to stimulate release of lactoferrin and IL-8 from human neutrophils presumably, the effect which replicated by PAR-2 peptide agonists tc-LIGRLO-NH_2 and SLIGKV-NH_2 [207].

Table 1.3 Comparison of the actions of PAR-2 activators.

Effect	Cell / Tissue	Tryptase	Peptide agonists of PAR-2	Trypsin
Accumulation of inflammatory cells *in vivo*	Peritoneum	Neutrophilia and eosinophilia (m) [10]	Neutrophilia and eosinophilia (r) [187] but ↓ (m) [162]	Neutrophilia and eosinophilia (m) [162]
	Lung	Leucocytes (m) [125]	Leukocytes (m) [194]/ No effect (m) [162] or ↓ (m) [162]	n/a
	Skin	Neutrophils and eosinophils (gp) [11]	n/a	n/a
Production or secretion of mediators	Mast cells	Histamine (h) [208] Degranulation (h) [10]	No effect [208]	Histamine (h) [208]
	Neutrophils	Lactoferrin, IL-8 (h) [119]		
	HEEC	n/a	n/a	IL-8 [186]
	HUVEC	IL-8, IL-1β [105]	IL-1a, IL-10, IL-12 and IL-8 [169]	
	HDMEC	n/a	up-regulation of IL-6 and IL-8 [184]	
	PAR-2-KNRK cells	n/a	PGE_2 [209]	
	ASM cells	IL-8 [210], TGFβ1 and SCF (h) [137]	No effect (h) [210]	n/a
	Bronchial epithelial cell lines	IL-8 (h) [129]	n/a	n/a
	Eosinophils	Degranulation (h) [123]	No effect (h) [123] / IL-8 release (h) [181, 190] / degranulation and production of superoxide anion (h) [180]	
Cell function	Macrophages	n/a	↑ phagocytosis (m) [179]	n/a
	Neutrophils	n/a	Morphological changes, ↑ CD11B/CD18 expression (h) [182] and ↑ phagocytosis (m) [179]	n/a
	Eosinophils	n/a	Morphological changes (h) [180]	
	Monocytes	n/a	Enhanced INFγ-induced anti-viral effects (infected with influenza A virus, h) [178]	No effect [178]
Vascular permeability	Skin	↑ (gp) [10], induction of wheals (sh) [127]	n/a	n/a
Upregulation of adhesion molecules	Various	ICAM-1 (bronchial epithelial cell lines, h) [129]	ICAM-1 (primary keratinoctes, h) [211] VCAM-1 (bronchial fibroblasts, h) [212]	ICAM-1 (HUVEC and *in vivo*, r) [213]

↑, increase; h, human; r, rat; m, mouse; gp, guinea pigs; sh, sheep. MC, mast cells; IL, interleukin; HEEC, human oesophageal epithelial cells; HUVEC, human umbilical vein cells; HDMEC, human dermal microvascular endothelial cells; PAR-2-KNRK, PAR-2 transfected normal rat kidney cell line transformed by Kirsten murine sarcoma virus cells; ASM, airway smooth muscle; ICAM-1, intercellular adhesion molecule 1; VCAM-1, vascular cell adhesion molecule 1. n/a, not available.

The PAR-2 peptide antagonist FSLLRY-NH_2 has been developed as inactive, partial-reverse sequence PAR-1 activating peptide [214] and has been found to be able to block PAR-2 activation by trypsin *in vitro*. However, it was not able to prevent PAR-2 stimulated calcium signalling induced by SLIGRL-NH_2 or trypsin cleavage of the PAR-2 N-terminal epitope in PAR-2-KNRK cells [215]. FSLLRY-NH_2 has been reported to cause decrease in the proliferative effects [216] as well as induction of phosphorylation of ERK 1/2 from mitogen-activated protein kinase signalling, and collagen synthesis [217] induced by tryptase on adult cardiac fibroblasts. However, an increase in PAR-2 protein, as determined by western blot induced by tryptase has not been found to be altered in the presence FSLLRY-NH_2. In bone marrow stromal cells obtained from patients with acute myeloid leukaemia, addition of FSLLRY-NH_2 was found to inhibit the upregulation of VEGF and the increased phosphorylation of ERK1/2 and p38MAPK induced by tryptase [218].

Evaluation of the actions of tryptase in PAR-2 knockout mice has been studied on only limited scale. PAR-2 knockout C57BL/6J mice has been reported to be resistant to joint swelling and inflammation induced by Intra-articular injection of β-tryptase, and co-administration of a tryptase inhibitor (4-amidino phenyl pyruvic acid, APPA) has been found to prevent Freund's complete adjuvant induced chronic arthritis in wild-type mice [219]. It will be important to examine other pro-inflammatory actions of tryptase in PAR-2 deficient mice in order to determine more clearly the potential contribution of PAR-2 to the actions of tryptase.

While there have been several studies that are consistent with the idea that PAR-2 activation is a key process by which tryptase exerts its actions, several studies have not supported this concept. Thus for example, tryptase has been reported to induce production of IL-8 in airway smooth muscle cells while SLIGKV-NH_2 has failed to replicate this effect [210]. Histamine release from human airway mast cells can be stimulated by tryptase or trypsin but not by PAR-2 agonists even after addition of a proteinase inhibitor (amastatin) to the dispersed lung cells and there is little evidence for PAR-2 expression in mast cells [208]. Tryptase-induced activation, release of eosinophil peroxidase and beta-hexosaminidase from peripheral blood eosinophils from asthmatic

patients has not been reported by treating cells with PAR-2 peptide agonist SLIGRL-NH_2 [123].

Tryptase, like agonists of PAR-2, can induce profound changes in cell function which are consistent with having key roles in disease. Though frequently presented as an important molecular target for tryptase, the precise contribution of PAR-2 in mediating the cellular actions of this abundant product of mast cell activation remains to be established.

1.8 Hypothesis

From our current knowledge we can hypothesize that:
Mast cell tryptase has a crucial role in development of allergic inflamation through activation of PAR-2 and PAR-2 cleavage peptide may contribute to that role.

1.9 Aim of the study

The aim of this study has been to determine the roles of human mast cell tryptase and PAR-2 activation in inducing inflammation in appropriate *in vitro* and *in vivo* models.

In seeking to achieve this objective, it was planned to :

1. Investigate the pro-inflammatory actions of human mast cell tryptase in PAR-2 deficient mice *in vivo.*
2. Determinate the effects of tryptase and PAR-2 agonist on global gene expression in human endothelial cells.
3. Evaluate PAR-2 and its cleavage product as a mean by which tryptase may act as an inflammatory mediator.

Chapter 2.
Material and General Methods

Chapter 2. Material and General Methods

2.1 Materials

2.1.1 Chemicals

Buffers and stock solutions were kept at room temperatures unless otherwise specified. De-ionized water (dH_2O) obtained by a reserve osmosis based system (Milli-Q Biocel Water Purification System, Millipore, Billerica, MA, USA) was used in preparation of most of solutions and buffers. Reagents and chemicals are listed below;

The following were purchased from Sigma (Poole, Dorset): Glycerol, 4-(2-hydroxyethyl)-1-piperazineethanesulphonic acid (HEPES), ethanol (absolute), sulphinpyrazone, TRI Reagent®, 2-(N-morpholino) ethanesulphonic acid (MES), dimethyl sulphoxide (DMSO), N-α-benzoyl-D,L-arginine-p-nitroanilide (BApNA), Trizma® base, sodium chloride (NaCl), bovine serum albumin (BSA), sulphinpyrazone, Tween® 20, sodium dodecyl sulphate (SDS), glycine, ammonium sulphate $(NH_4)_2SO_4$, urea (electrophoresis grade), casein from bovine milk, magnesium chloride ($MgCl_2$), ethylenediaminetetraacetic acid (EDTA), potassium hydroxide (KOH), elastin, N-succinyl-Ala-Ala-Ala-p-nitroanilide, ethidium bromide, agarose, guanidine hydrochloride (GuHCl), imidazole, dithiothreitol (DTT), tricine (NT), formaldehyde, H_2O_2, carbonate-bicarbonate buffer, tetramethyl benzidine (TMB), sodium phosphate, isopropanol, gamma globulin, acetonitrile (ACN), trifluroacetic acid (TFA), trypan blue 0.4 %, propidium iodide (PI), methylene blue, hydrochloric acid (HCl), calcium ionophore A23187, sodium azide, bromophenol blue, gelatin, collagenase, porcine pancreatic elastase; type II-A, trypsin, leupeptin; tryptase inhibitor and ultra-low molecular weight marker.

A 30 % acrylamide/Bis solution, tetrametyletylenediamine (TEMED), blotting grade blocker non-fat dry cow's milk and ammonium persulphate $(NH_4)_2S_2O_8$ (APS) from Bio-Rad (Hemel Hempstead, Herts), methanol, sodium hydroxide (NaOH), glycerol, H_2SO_4 and glacial acetic acid from Fisher Scientific (Loughborough, Leicestershire). Fluro-3 AM florescence dye, MagicMarker™ XP western standard, NuPAGE® LDS Sample buffer 4x and sample reducing agent 10x were from Invitrogen were from Invitrogen (Inchinnan, Paisley). Coomassie brilliant blue (G250) was from LKB (Bromma, Sweden). Calcium chloride (CaCl2)

and Triton X-100 were from BDH Ldt. (Poole, Dorset). Piperazine-1, 4-bis (2-ethanesulphonic acid) (PIPES) buffer obtained from RefLab (Copenhagen, Denmark). Hyper ladder™ I was from Bioline Ltd. (London). The 50bp DNA Ladder obtained from New England Biolabs Ltd. (Hitchin, Hertfordshire). PageRuler™ Plus prestained protein ladder obtained from Fermentas (Thermo Scientific, Wilmington, MA, USA). SLIGKV-NH_2 (the PAR-2 peptide agonist) and LSIGLV-NH_2 (the PAR-2 scrambled peptide) were from Peptide International (Louisville, KY, USA). 160719A-5 a selective inhibitor of tryptase was a kind gift from Sanofi-Aventis (Bridgewater, NJ, USA). *Pichia pastoris* supernatant was a kind gift from Roche Pharmaceuticals (Welwyn Garden City, Hertfordshire). Heparin agarose type 1, butyl Sepharose™4 fast flow and Hitrap™ IgM purification HP column were from GE Healthcare (Little Chalfont, Buckinghamshire). BioSep 3000 size exclusion column was from Phenomenex (Macclesfield, Cheshire). Gold-β-mercaptoethanol mix (Stratagene) and ZORBAX® Extend-C18 reverse phase column were from Agilent Technologies (Austin, TX, USA). Talon metal affinity resin was from Takara Bio Europe/Clontech (Saint-Germain-en-Laye, France).

2.1.2 Culture media

Foetal calf serum (FCS), phosphate-buffered saline (PBS), 100x penicillin-streptomycin-glutamine (PSG), 0.5 % trypsin-EDTA 10x, minimum essential medium (MEM), Dulbecco's modified Eagle's medium (DMEM), enzymatic-free/Hank's based cell dissociation buffer and Hank's balanced salt solution (HBSS) 10x; containing calcium and magnesium were from GIBCO, Invitrogen (Inchinnan, Paisley). Goat serum, Luria Bertani (LB) agar, super optimal broth (SOC) medium, endothelial cell growth medium (contains foetal calf serum (FCS-10), endothelial cell growth supplement (ECGS/H-2), epidermal growth factor (hEGF-0.05), basic fibroblast growth factor (hbFGF-0.5) and hydrocortisone (HC-500) were from PromoCell (Heidelberg, Germany).

2.1.3 Molecular biology kits

Primers for IL-8 and IL-1β were obtained from Eurofins MWG/Operon (Ebersberg, Germany). The RNA extraction kit (RNeasy mini kit) was from Qiagen (Crawley, West Sussex). Precision qScript reverse transcriptase kit, primers; used for confirmation of microarray results and 2X qPCR Mastermix were from Primer Design (Millbrook, Southampton). The silver staining kit was

from Bio-Rad. Supersignal® West Pico chemiluminescent substrate was from Pierce (Thermo Fisher Scientific, Cramlington, Northumberland). The bicinchoninic acid protein assay kit (BCA1 and B9643) was from Sigma. The rapid Romanowsky stain pack HS705 was from Raymond A Lamb (Eastbourne, East Sussex). The QCL-1000 chromogenic LAL (50-647U) was obtained from Lonza (Slough, Berkshire). The 3, 3'-diaminobenzidine (DAB) peroxidase substrate kit and VECTASHIELD Mounting Medium were from Vector Laboratories (Peterborough, Cambridgeshire). Toxin Sensor™ was obtained from GenScript (Piscataway, NJ, USA). The anti-Ly-6G-biotin mouse neutrophil antibody and anti-biotin MicroBeads were from Miltenyi Biotec. Bromocresol green (BCG) Albumin (QuantiChrom™) Assay Kit reagent was from BioAssay Systems (Hayward, CA, USA). The MSD® SULF0-TAG NHS Ester was from Meso Scale Discovery (Gaithersburg, MD, USA). The lactate dehydrogenase (LDH) cytotoxicity detection kit was from Roche Diagnostic GmbH (Mannheim, Germany). The specific sandwich ELISA kits (human CXCL8/IL-8, human IL-1β/IL-F2, human TNF-α/TNFSF1A and human sICAM-1/CD54) were obtained from R&D systems (Minneapolis, MN, USA). Ambion® WT Expression kit was from Ambion Applied Biosystems (Austin, TX, USA). Affymetrix WT terminal labeling kit was from Affymetrix (Santa Clara, CA, USA). Isopropyl-β-D-thio-galactoside (IPTG), BugBuster protein extraction reagent, benzonase nuclease enzyme and pET-52(+) plasmid were from Novagen, Merck Chemicals (Nottingham, Nottinghamshire). Mastermix (MM) (ImmoMix) was from Bioline (London), Zymoclean™ Gel DNA Recovery Kit was from ZymoResearch (Irvine, CA, USA) and XL1-blue competent cells were obtained from Stratagene.

2.2 Purification of tryptase from a yeast expression system

Tryptase was purified from yeast (*Pichia pastoris*) expression system, employing a method adapted from that of Niles et al. (1998) [220]. Sequential purification of tryptase was performed by hydrophobic interaction chromatography followed by heparin affinity chromatography. The methods depend on the ability of recombinant tryptase to bind to hydrophobic groups and heparin. A BioSep-Sec-S-3000 size exclusion column was employed in high-pressure liquid chromatography (HPLC) for the final polishing stage of the purification.

A column with 25 ml of butyl Sepharose was regenerated by washing with two to three bed volumes of buffer A (10 mM MES, 1 M $(NH_4)_2SO_4$, 0.5 M NaCl, 10% (v/v glycerol), pH 6.1) at a rate of 1 ml/min. At room temperature (22°C) the supernatant of *Pichia pastoris* cells (100 ml) was filtered and loaded at a flow rate of 1 ml/min. Washing of the column to remove non-bound protein with buffer A, was followed by elution of tryptase by addition of elution buffer B (10 mM MES, 0.2 M NaCl, 10 % (v/v) glycerol, pH 5.5). Fractions of 5 ml were collected and tryptase activity was determined using a chromogenic substrate (*vide infra*). The column was washed with ten bed volumes of 70 % ethanol followed by four bed volumes of 1 M NaOH, and two bed volumes of distilled water at a flow rate of 40 ml/h.

Working in a 4°C cold cabinet, a column containing 25 ml heparin-agarose was regenerated by washing with five to ten bed volume of buffer B at a rate of 1 ml/min, before tryptase rich fractions of the butyl Sepharose column were loaded. Non-bound proteins were removed by washing with three to ten bed volumes of buffer B. Tryptase was eluted using buffer B mixed with 0 to 75 % buffer C (10 mM MES, 2 M NaCl, 10 % (v/v) glycerol, pH 6.1). Fractions of 5 ml of tryptase were collected and tryptase activity determined. The column was washed with two bed volumes of 2 M ammonium sulphate followed by three bed volumes of 1 M Tris buffer pH 8.0 containing 6 M urea, and then with three bed volumes of distilled water.

Fractions with high tryptase activity were pooled and injected into a BioSep-Sec-S-3000 size exclusion column applied to HPLC ICS 3000 pump (Dionex Corporation, Sunnyvale, CA, USA). Elution was collected in a 0.5 ml fraction volume and analyzed for tryptase activity.

2.3 Characterization of purified tryptase

Tryptase was initially characterized by detecting fractions harbouring high enzymatic activity using a specific chromogenic substrate and measuring the protein content. The purified protein was further analyzed for purity by sodium dodecyl sulphate polyacrylamide gel electrophoresis (SDS-PAGE) and staining with Coomassie blue dye or silver stain, and western blotting. Contaminating endotoxin levels were also measured.

2.3.1 Tryptase activity assay

Tryptase activity was measured by determining cleavage of the chromogenic substrate N-α-benzoyl-DL-arginine p-nitroanilide hydrochloride (BApNA) according to the procedure described by McEuen and Walls (2008) [64]. Standard tryptase assay buffer (1 M glycerol, 0.1 M Tris buffer, pH 8.0) and BApNA substrate (88.9 mM BApNA in DMSO 38.7 mg/ml) were prepared as stock solutions. A working solution of 1 mM BApNA was prepared by adding 11.2 µl of 88.9 mM BApNA to 0.989 ml standard tryptase buffer. In a microtiter plate 90 µl/well of the working solution was added to 10 µl of tryptase containing fractions. A kinetic absorbance change was measured at 410 nm for 10 minutes at 25°C in a THERMOmax micro-plate reader (Molecular Devices, Wokingham). Changes in absorbance expressed in milli-optical density units per min (mOD/min) were converted to mU/ml by multiplication of values by a factor of 3.888 (a conversion factor based on BApNA having an extinction value (ϵ) of 8800 $M^{-1}cm^{-1}$). One unit (U) was taken as the enzymatic activity that hydrolyzes 1 µmol of substrate per minute at room temperature (25°C).

2.3.2 Bicinchoninic acid (BCA) protein assay

A colorimetric protein assay using bicinchoninic acid (BCA) was employed in accordance with the manufacturer's instructions to measure protein levels in elution fractions. Serial dilutions of BSA standard were prepared covering the range 200-1000 µg/ml. The BCA working reagent was prepared by adding 19 ml bicinchoninic acid solution 25.7 µM (containing sodium carbonate 188.7 µM, sodium tartrate 8.2 µM and sodium bicarbonate 11.3 µM in 0.1 M NaOH, final pH 11.25) (Reagent A) to 0.38 ml copper sulphate pentahydrate 4 % solution (Reagent B) and mixed until the BCA working reagent was a uniform, light green colour. In a 96-well microplate (Greiner Bio-One), the BCA working reagent was added at a ratio of 8:1 to standards, blank, and unknown samples (i.e. 200 µl BCA working reagent was added to 25 µl of sample) and mixed gently. Plates were covered and sealed with film, incubated at 37°C for 30 minutes and then allowed to cool to room temperature. The OD was measured at 450/590 nm and for each assay a separate standard curve was prepared. The specific activity of the purified tryptase was expressed as units activity of enzyme per milligram of total protein content i.e. U/mg.

2.3.3 SDS-PAGE

Aliquots of 10 µl from positive fractions were mixed with sample buffer and reducing agent and heated to 70°C for 10 min. Samples were applied on a NuPAGE BisTris 4-12 % gradient gel (Invitrogen) with pre-stained molecular weight marker™ XP and Magic Marker. Gels were stained with Coomassie blue stain (0.15 % Coomassie blue (G250) in 10 % acetic acid, 40 % methanol and 50 % dH_2O) and de-stained after 30 minutes with the de-stain solution (10% acetic acid, 40 % methanol and 50 % dH_2O) or stained using a silver staining kit according to the manufacturer's instructions. Gels were photographed using a Molecular Imager GS-800 calibrated densitometer (Bio-Rad).

2.3.4 Western blotting

The electrophoresed proteins were transferred to a nitrocellulose membrane. The membrane was washed with PBS and non-specific binding was blocked for 1 h with 5 % non-fat dry cow's milk in PBS-Tween 0.05%. The membrane was washed three times with PBS-Tween for 5 min each and incubated with anti-tryptase monoclonal antibody AA5 at a dilution of 1:5000 for 1 h at room temperature with continuous shaking. After washing, the membrane was incubated with rabbit polyclonal anti-mouse antibody conjugated to horseradish peroxidase (HRP) (in a 1:10,000 dilution, DakoCytomation, Ely, Cambridgeshire) for 1 hour at room temperature. Reactive bands were visualized using Supersignal® west pico chemiluminescent substrate (Pierce, Thermo Fisher Scientific) or 3, 3'-diaminobenzidine (DAB) peroxidase substrate kit, and bands of high density were photographed using a VersaDoc™ imaging system (Bio-Rad).

2.3.5 Endotoxin assay

Endotoxin levels in the purified tryptase were measured using a Limulus Amebocyte Lysate (LAL) QCL-1000 kit from Lonza (Slough, Berkshire) following the manufacturer's guidelines in a microplate based technique. A standard ranging from 0.1 to 1.0 EU/ml was applied in the water supplied. The reaction was stopped with 25 % glacial acetic acid. In order to detect lower levels of endotoxins, highly sensitive chromogenic LAL endotoxin assay kit, Toxin Sensor™ from GenScript (Piscataway, NJ, USA) was used in a microplate based technique with a standard curve covering range from 0.005 to 0.1 EU/ml. Aliquots of 100 µl of standard or samples were mixed with equal volume of

LAL and incubated for 45 min at 37°C. After incubation, aliquots of 100 of substrate were added to the mix and incubated for 6 min at 37°C.
The reaction was stopped by sequential addition of 500 µl of the reconstituted colour-stabilizers 1, 2 and 3 provided in the kit. The absorbance was measured at a wavelength of 550nm with distilled water as blank.

2.4 Mouse studies

2.4.1 Animals

Colonies of knockout transgenic C57BL/6 mice lacking the PAR-2 gene (PAR-$2^{-/-}$) and the corresponding wild type mice (PAR-$2^{+/+}$), which had been modified as described by Ferrell et al. (2003) [200], were a gift from Kowa Company (Tokyo, Japan). Animals employed in in these studies, with a weight range of 25-35 g, were housed in standard cages and maintained with food and water available ad libitum in a thermo neutral environment. In addition to the C57BL/6 strain, BALB/c wild-type mice were studied so as to compare findings more directly with published reports employing this mouse strain. Studies with animals were conducted according to the regulations of the Home Office, UK and were covered by licence number PPL30/2564.

2.4.2 Mouse tail biopsy genotyping

Genotyping for mouse tail biopsy was performed for samples obtained according to the approved Animal Study Proposal (ASP) through licensed animal house specialists. Three samples from each genotype were obtained and stored at -80°C until processed. Tissue was homogenized by samples using a RiboLyser™ homogenizer (Hybaid Ltd., Ashford, Middlesex) in 1.5 ml Lysing Matrix D tubes (MP Biomedicals, Solon, OH, USA) with TRIzol.

Confirmation of presence of the gene for PAR-2 was confirmed by performing the PCR using the following primers; 5′-ATGCGAAGTCTCAGCCTGGCG-3′ and 5′-GAGAGGAGGTCGGCCAAGGCC-3′ to yield a 380-bp PCR product. The PCR was generally performed for 35 cycles with initial denaturation at 95°C for 5 min, annealing at 51°C then for 2 cycle/min and extension at 72°C/cycle (3 min), and a final extension (last cycle) at 72°C for 10 min. Absence of the PAR-2 gene was tested by detection of neomycin gene using the following primers; NeoFwr 5'GAGGAAGCGGTCAGCCCATT3' and NeoRev 3'TCTTCCTATTGACTAAACGG5' with amplicon size of 281bp. The PCR was

generally for 33 cycles with initial denaturation 95°C for 10 min, annealing at 68°C for 1 min and 30 s extension at 72°C, and a final extension (last cycle) at 72°C for 10 min. The PCR was concluded by cooling down to 4°C. PCR products were analysed immediately or stored at 4°C until further analysis. PCR products were separated on a 2 % agarose gel and visualized by ethidium bromide staining.

2.4.3 Study design

Animals were injected intra-peritoneally (ip) with a 0.9 % saline vehicle control or with recombinant β-tryptase; either in the active form or inactivated by heat or addition of protease inhibitors, inhibitors alone, protease activated receptor peptide agonist (SLIGRL-NH_2) or a peptide with the same amino acids but with a 'scrambled' sequence (LSIGRL-NH_2) or protease activated receptor released peptide (PAR-2 RP). Agents were injected in a total volume of 500 µl per mouse and in a concentration range of 0.01 to 1 µg/ml. Tryptase was handled with care to avoid spontaneous inactivation. Tryptase was kept on ice and diluted with saline immediately before injection of the animal. Inactivation was performed by incubation of tryptase with 10 µg/ml leupeptin for 1 h on ice or with 160719A-5 a selective inhibitor of tryptase (Sanofi-Aventis, Bridgewater, NJ, USA) (Ki 39 Nm) 50 µg/ml. The degree of inhibition was assessed by a chromogenic substrate BApNA.

2.4.4 Peritoneal lavage

At 6, 12 and 24 hours following injection, mice were weighed and sacrificed by cervical dislocation. After swabbing the abdominal skin with 70 % ethanol, a midline incision of the abdomen was made and 5 ml saline injected into the peritoneum. Abdominal massage was performed for 30 seconds then saline was collected into tubes maintained on ice. Total numbers of nucleated cells were determined using an improved Neubauer haemocytometer with 0.4 % trypan blue. The peritoneal lavage fluid was centrifuged at 300g for 10 minutes at 4°C. The supernatant was aspirated and stored at -20°C. Cell pellets were resuspended in minimum essential medium with 5 % FCS and cell number was adjusted to 10^6 cell per ml. Cytocentrifuge preparations were made using a Cytospin 3 (Shandon Southern, Runcorn) with aliquots of 100 µl of cell suspension and slides left to air dry overnight. One slide for each sample was stained with eosin/methylene blue stain (Rapid Romanowsky)

according to the manufacturer's instructions. Differential cell counts were performed blindly on randomly coded data counting a minimum of 500 cells per slide for at least 5 fields using a Standard 20™ microscope (100X/1.25 oil lens, Carl Zeiss, Göttingen, Germany). Codes were broken and data from animals injected with the same agent were pooled and analysed together. A schematic diagram of the procedures employed is shown in Figure 2.1.

2.5 Gelatin zymography

Supernatant from peritoneal lavage fluid was centrifuged at 1000g for 1 minute and 15 µl added to 5 µl of 2x non-reducing sample buffer (4 % SDS, 0.125 M Tris-HCl pH 6.8, 0.003 % bromophenol blue and 20 % glycerol) and applied to 8 % polyacrylamide gel containing gelatin.

After electrophoresis gels were incubated overnight at 37°C in MMP proteolysis buffer (50 mM Tris-HCl pH 7.8, 0.5 mM NaCl, 50 mM $CaCl_2$), then stained with Coomassie blue stain (0.15 % Coomassie blue (G250) in 10 % acetic acid, 40 % methanol and 50 % dH_2O) and destained after 30 minutes with destain solution (10 % acetic acid, 40 % methanol and 50 % dH_2O). Gels were photographed using a Molecular Imager GS-800 calibrated densitometer (Bio-Rad). Densitometric analysis of bands was performed according to average or peak pixel density and relative quantity.

As a positive control for MMP2 and MMP9 activity, a supernatant from the human fibrosarcoma cell line (HT1080) was employed as described by Togawa et al. (1999) [221]. HT1080 cells were cultured in Dulbecco's modified Eagle's medium (DMEM) with 10% foetal bovine serum (FBS) and penicillin-streptomycin-glutamine (PSG) at 37°C in humidified air with 5 % CO_2. When cells were confluent, they were detached using trypsin-EDTA (GIBCO) and the actions of trypsin were stopped by addition of medium when detachment was complete. Cells were centrifuged, washed with the medium and subcultured in 25 cm^3 TC culture flasks (Orange Scientific, Braine-L'Alleud, Belgium).

Confluent cells were washed twice with warmed phosphate buffered saline (PBS) pH 7.4 then incubated overnight with serum-free medium. The medium in flasks was aspirated and new serum-free medium added. After 48 hours the supernatant was collected.

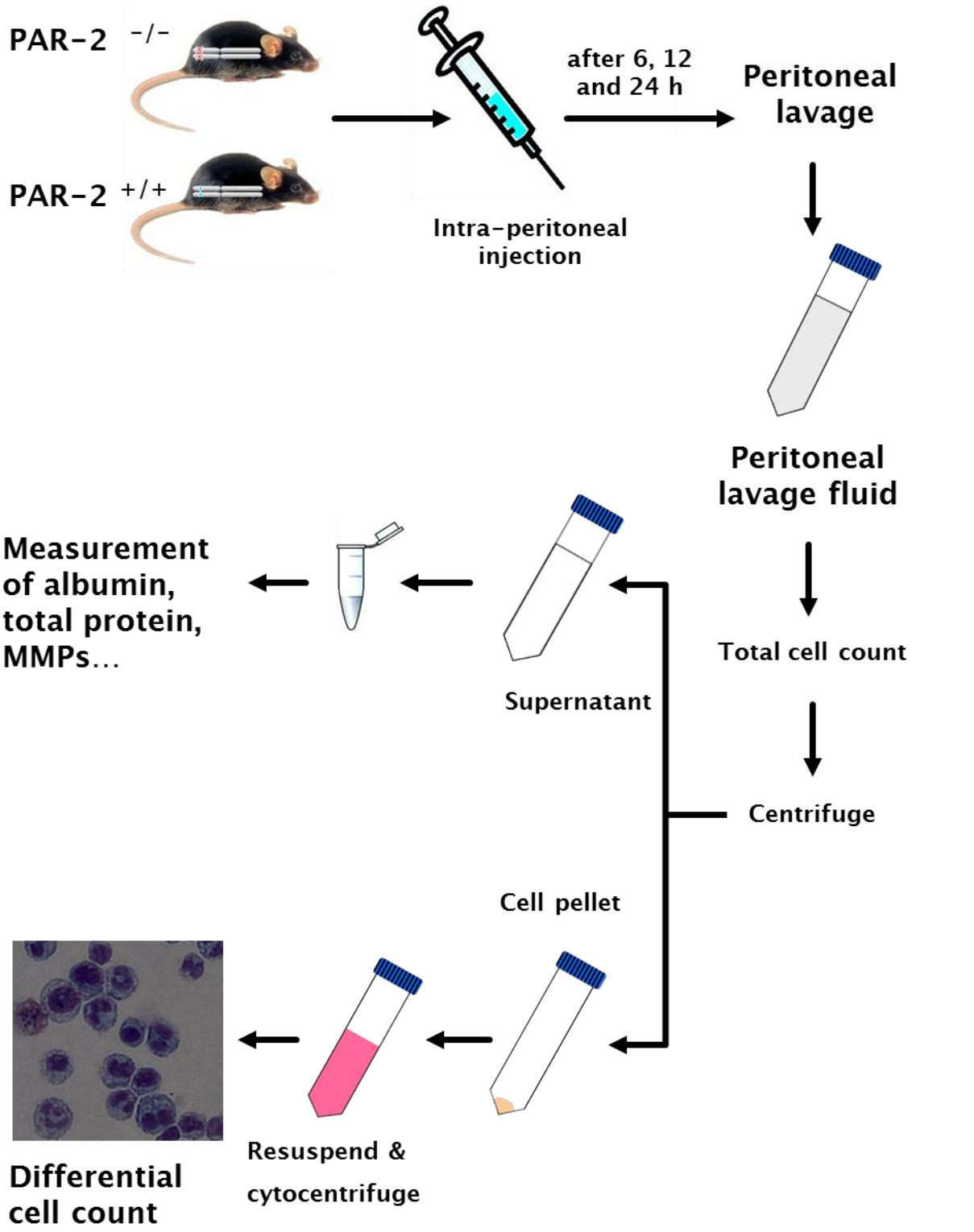

Figure 2.1 Schematic representation of the studies involving injection of mice with tryptase.

2.6 Stimulation of neutrophils

In order to examine the potential contribution of neutrophils to the response of mice to tryptase, peritoneal cells were collected from naive mice and from mice which had been injected intraperitoneally with β-tryptase (0.5 µg/mouse) or casein (0.5 ml of 9 % solution/mouse). The casein for injection was prepared as described by Watt et al. (1979)[222] with 9 g casein hydrolysate slowly dissolved in 100 ml PBS pH 7.2 containing 0.9 mM $CaCl_2$ and 0.5 mM $MgCl_2$ which had been heated to 70-90°C. The solution was boiled until all casein was dissolved (approximately 10 min) and then autoclaved (turning it to a pink coloured solution) and it was stored sterile at 4°C. After 24 h, mice were weighed and sacrificed by cervical dislocation. Peritoneal lavage was performed as described above.

2.6.1 Immuno-magnetic purification of neutrophils

A schematic diagram of the procedures employed is shown in Figure 2.2. Cells were passed through nylon mesh (30 µm, BD Falcon, Erembodegem, Belgium) in order to remove cell clumps. The cell number was determined, the cell suspension centrifuged at 300g for 10 minutes at 4°C and the supernatant decanted. The cells (10^8) were resuspended in 200 µl buffer (0.5 % BSA, 2 mM EDTA in PBS pH 7.2). A biotinylated antibody specific for the surface antigen Lymphocyte antigen 6G (LY-6G) on mouse neutrophils (Miltenyi Biotec, Bisley) was added at 50 µl per 10^8 cells, mixed well and incubated for 10 minutes at 4°C. A 150 µl aliquot of the buffer was mixed well with anti-biotin MicroBeads (100 µl per 10^8 cells, Miltenyi Biotec) and incubated for 15 minutes at 4°C. Cells were washed by adding the buffer (5 to 10 ml per 10^8 cells) and centrifuged at 300g for 10 minutes at 4°C, and the supernatant was aspirated. Cells were resuspended in the buffer (500 µl with up to 10^8 cells).

A ferromagnetic LS column (Miltenyi Biotec) was placed in the magnetic field of the MidiMacs Separator and prepared by rinsing three times with 3 ml buffer. The cell suspension was applied to the column and unlabelled cells were collected. The column was washed three times with 3 ml buffer once the column reservoir was empty, and the column removed from the separator and collection tubes set up.

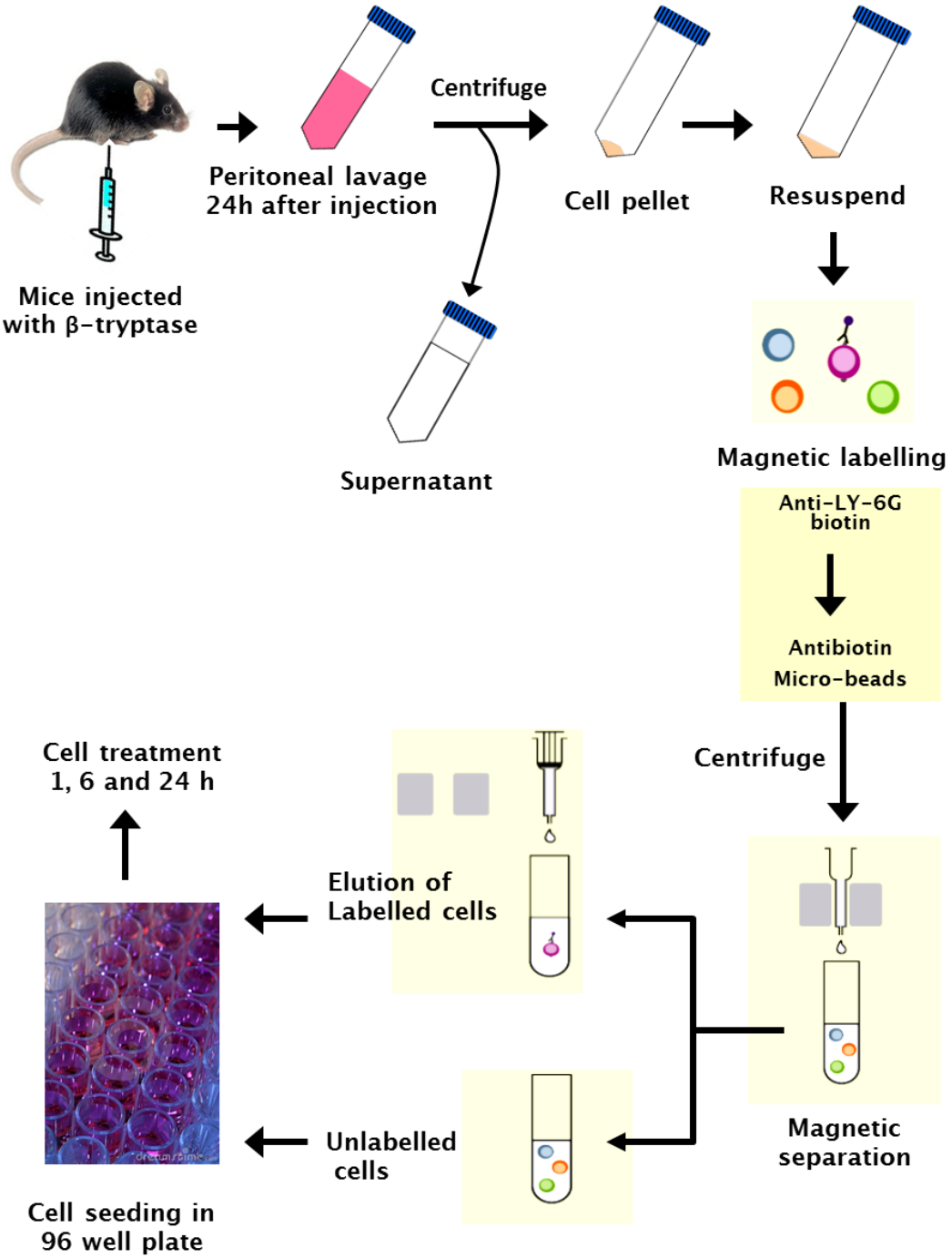

Figure 2.2 Schematic representation of magnetic cell sorting procedure with mouse neutrophils.

Labelled cells were immediately flushed twice with 4 ml buffer by applying the plunger supplied with column. The cell number was determined and the cell suspension was centrifuged at 300g for 10 minutes at 4°C, and the supernatant aspirated. The cell pellet was resuspended in RPMI 1640 conditioned medium and seeded at a density of 10^6 cells/well in 24 well tissue culture plates (Greiner Bio-One; Stonehouse, Gloucestershire).

2.6.2 Treatment of peritoneal lavage preparations

Sorted cell populations were treated with tryptase (either active or heat-inactivated for 20 minutes at 94°C) or other compounds. At 1, 6 or 24 hours after treatment, supernatants were collected for gelatin zymography.

2.7 Albumin assay and total protein assay

Quantitative colorimetric albumin bromocresol green (BCG) assay kits (QuantiChrom, BioAssay Systems, Hayward, USA) with a detection range from 0.1 mg/ml (1.5 µM) to 50 mg/ml (750 µM) were employed to determine the albumin concentration in peritoneal lavage fluid. Standard preparations of BSA were dissolved in distilled water at concentrations from 0 to 50 mg/ml. A 5 µl aliquot of sample or diluted standard was transferred to wells of a clear bottom 96-well plate. A 200 µl aliquot of working reagent was added to each well and the plate was tapped lightly to mix.

The plates were incubated for 5 minutes at room temperature and the optical density was read between 570-670nm (peak absorbance at 620nm) using a Thermo Max plate reader (Molecular Devices). The OD of the blank was subtracted from OD values obtained and a standard curve was constructed by plotting the OD values against standard concentrations. Albumin concentrations in samples were determined using the standard curve. A colorimetric BCA protein assay was employed in accordance with the manufacturer's instructions as described before (section 2.2.4) to measure protein levels in peritoneal lavage fluid.

2.8 Histamine determination

An automated glass fiber based technique was employed to determine levels of histamine in peritoneal lavage fluid. Supernatants of peritoneal lavage fluid were loaded into wells of pre-coated FiberPlate assay plates (RefLab,

Copenhagen, Denmark) and Piperazine-1, 4-bis (2-ethanesulphonic acid) (PIPES) buffer added in a total volume of 50 µl/well. The plates were covered with film and incubated for 60 minutes at 37°C. Plates were washed with dH_2O, knocked upside down on tissue paper to remove residual water and kept in the dark at room temperature prior to final analysis for histamine in the Reference Laboratory.

2.9 Measurement of elastase activity

A pilot study using the chromogenic substrate N-Succinyl-Ala-Ala-Ala-p-nitroanilide was employed to determine elastase activity in peritoneal lavage fluid. An aliquot of 35 µl peritoneal lavage fluid supernatant was added to 1.8 ml substrate solution in 0.1 M 4-(2-hydroxyethyl)-1-piperazineethanesulphonic acid (HEPES) buffer pH 7.5 containing 0.5 NaCl and 10 % DMSO at 25°C. Porcine pancreatic elastase (type II-A) was used as a positive control.

In a preliminary study, it was found that elastin failed to dissolve completely in 0.2 M Tris buffer pH 8.8 and the creamy white suspension produced was not suitable for zymography. For this reason ethanolic extraction of soluble elastin from insoluble elastin suspension was performed according to the method of Moczar et al. (1980)[223]. The elastin was solubilised using ethanolic potassium hydroxide (1 M KOH in 80% ethanol) at 37°C for two hours. In order to remove excess alkali, extracts were dialyzed against water overnight at 4°C, the dialysis tube (Sigma) retaining proteins >12 kDa. The solubilised elastin recovered has been termed κ-elastin and the high molecular weight fraction (< 50 KDa) is composed of elastin polypeptides that have been reported to have similar properties to that of α-elastin [223]. The κ-elastin was added to a concentration column (Milipore, Watford) and centrifuged three times at 800g for 30 minutes. The solution was filtered to remove any debris or remnants of insoluble elastin. A 10-12 % SDS-PAGE gel was run under reducing conditions at 150 V to examine the results of elastin solubilisation, and then total protein content was assayed using Bradford Ultra reagent (Expedeon, Harston). Elastin zymography was carried out according to the procedure described by Forough et al. (1998)[224]. Samples were electrophoresed on a 10-12 % SDS-polyacrylamide gel containing 1 mg/ml soluble κ -elastin under non-reducing conditions at 150 V. After electrophoresis, the gels were washed in 2.5 %

Triton X-100 for 30 min to remove SDS. The gels were then incubated at 37°C in 50 mM Tris buffer, pH 7.8, containing 10 mM $CaCl_2$ for at least 20 h and stained with 0.002 % Coomassie brilliant blue (G250) in 10 % acetic acid, 40 % methanol and 50 % dH_2O.

2.10 Cloning of PAR-2 released peptide (PAR-2 RP)

PAR-2 RP is formed of 36 amino acids which are encoded by 108 bp DNA (illustrated in Figure 2.3). The cDNA was produced commercially (GeneArt, Regensburg, Germany). Primers were designed and prepared commercially with one forward sequence (5'-CAT CCA TGG GTC GTA GCC CGA GCC- 3') and two reverse sequences (5'-GTG ATG GTG ATG ACC ACG GCC TTT GC- 3' and 5'-GAG CGG CCG CTT AAT GGT GGT GAT GGT GAT G- 3'; MWG Operon, Ebersberg, Germany).

PCR was first performed using cDNA of PAR-2 RP with the forward and first reverse primers in PCR tubes maintained on ice. The cDNA was shaken well then diluted 1 in 50 to give a concentration of 4 ng/µl. In a total reaction volume of 25 µl, dH_2O was added to the cDNA 0, 1, 2 or 4 µl, with 0.2 µl of each primer and 12.5 µl of master mix (MM) (ImmoMix, Bioline, London). Tubes were micro-centrifuged for 2 seconds and the tubes were placed in a Peltier thermal cycler (PTC-225, DNA engine tetrad, MJ Research, Waltham, USA) for 1.5 hour with 35-40 cycles for the plasmid at an annealing temperature 55°C. The presence of PCR product was confirmed by running on 2 % agarose gel with 1 µl of ethidium bromide. Samples were prepared for loading onto the gel by mixing 4 µl with 1.5 µl loading buffer (Bioline) on mixture paper for each running chamber. Electrophoresis was for 30-60 minutes and then the gel photographed with a digital camera (PC 1130, Cannon, Uxbridge) attached to a benchtop UV transilluminator (UVP, Cambridge) in which ethidium bromide stained DNA appeared as white bands. Results of the first PCR were not satisfactory, so were repeated at annealing temperatures of either 57 or 60°C.

A

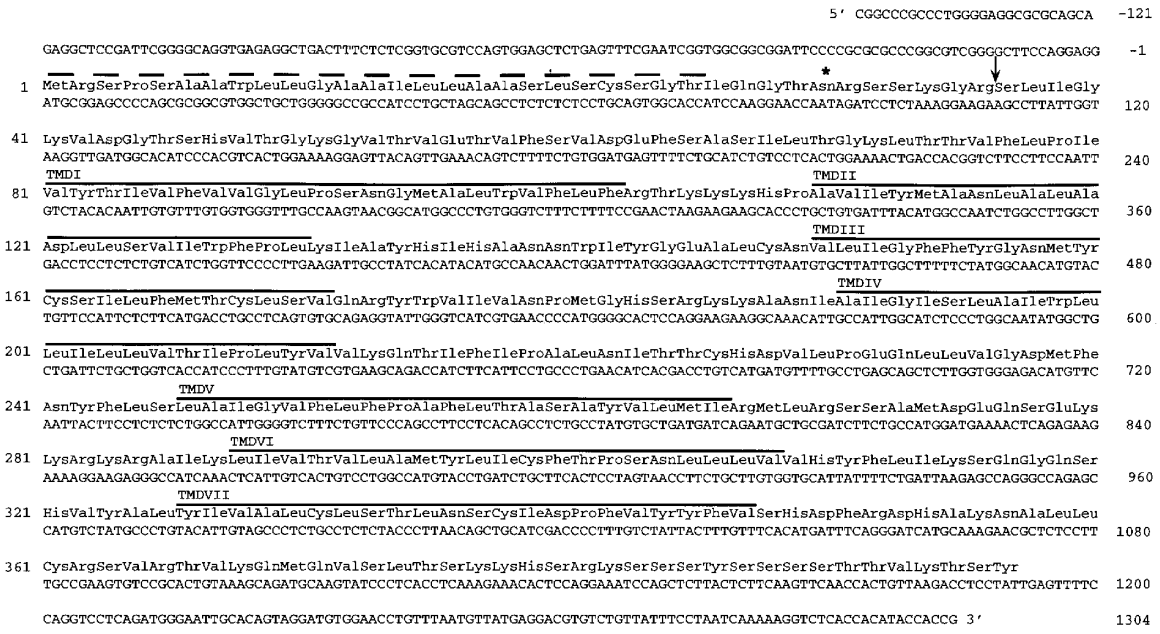

B

ATGCGGAGCCCCAGCGCGGCGTGGCTGCTGGGGGCCGCCATCCTGCTAGCAGCCT
CTCTCTCCTGCAGTGGCACCATCCAAGGAACCAATAGATCCTCTAAAGGAAGA

MetArgSerProSerAlaAlaTrpLeuLeuGlyAlaAlaIleLeuLeuAlaAlaSerLeuSerCysSerGly
ThrIleGlnGlyThrAsnArgSerSerLysGlyArg

Figure 2.3 (A) Predicted protein sequences and cDNA of human PAR-2. Solid lines indicate predicted transmembrane domains, the broken line indicates putative signal peptide, the arrow indicates the trypsin cleavage site, and the star * indicates a putative glycosylation site. Left-hand numbers refer to amino acids and right-hand numbers refer to nucleotides. PAR-2 RP is highlighted, adapted from Bohm et al. (1996) [144]. (B) Nucleotide and amino acid sequence of PAR-2 RP.

The first PCR product was passed down a cleaning column from ZymoResearch (Irvine, CA, USA). The bands (108–110 bp) were cut and DNA binding buffer (ZymoResearch) was added and the mixture centrifuged for 30 s at 600 g. Washing buffer (ZymoResearch) was added twice and centrifuged after each addition. The column was centrifuged to remove excess methanol and DNA was eluted by adding 10 µl H_2O and centrifuged. The quantity of DNA was measured using NanoDrop® ND-1000 spectrophotometer (Thermo Scientific, Wilmington, USA).

The second PCR was performed using 10 µl of the first PCR product, with the forward and the second reverse primers employed in a similar way to that carried out for the first PCR at an annealing temperature of 65°C. The second PCR product was passed down a cleaning column (ZymoResearch) and the bands (120 bp) were excised and DNA cleaned and recovered. In a total volume of 50 µl, 10 µl of pET-52(+) plasmid (Novagen, Merck Chemicals) or PCR products were digested with 0.5 µl *Not* I and *Noc* I restriction enzymes (as seen in the vector sequence map Figure 2.4) in 5 µl 10x buffer 3 (provided in the kit), 0.5 µl 100x BSA and 33.5 µl dH_2O. The DNA/enzyme mixture was prepared in a total volume of 50 µl and incubated overnight at 37°C.

The second PCR product was passed down the cleaning column as described above and pET-52b(+) plasmid was cleaned by gel recovery. The bands were cut and agarose dissolving buffer (ADB) (ZymoResearch) was added and heated to 55°C for 10 minutes. The dissolved mixture was transferred to the column supplied, centrifuged washed and eluted as above. The quantity of DNA was measured using a NanoDrop® ND-1000 spectrophotometer (Thermo Scientific). According to the quantity and the molecular weight (MW) of the second PCR product and pET-52b(+), the ratio of the ligation mixture was calculated. In a total volume of 20 µl, 4 µl of plasmid and 1 µl of insert (5 M) were mixed with 1 µl T4 ligase, 2 µl buffer and 12 µl dH_2O for 10 minutes at room temperature.

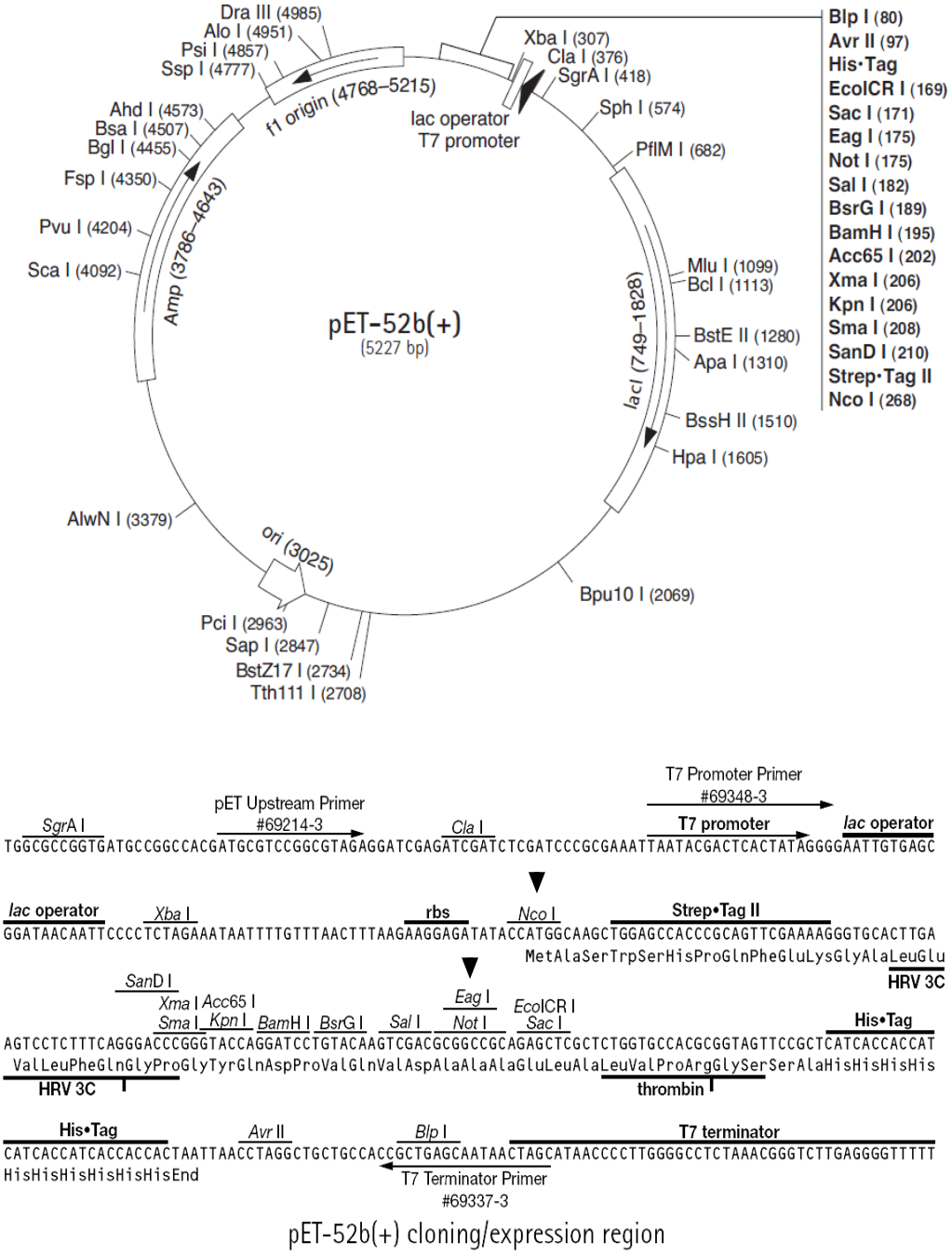

pET-52b(+) cloning/expression region

Figure 2.4 The pET-52b(+) vector map. Arrows refer to the restriction enzymes used in ligation (adapted from manual of Novagen, Merck Chemicals, Nottingham, Nottinghamshire).

The ligation mixture was transformed into XL1-blue competent cells from Stratagene (Agilent Technologies, TX, USA) by adding 1.5 µl of ligation reaction to 50 µl of XL1-blue competent cells for 30 minutes on ice. The mixture was heat shocked at 42°C for 45 s, kept for 2 minutes on ice, and 100 µl super optimal broth containing glucose (SOC) was added. The mixture and negative control (without insert) were spread over Luria Bertani Agar/ Ampicillin (LB/Amp) plates and incubated overnight at 37°C. Colonies were tested by PCR (with an annealing temperature of 49°C) and suitable colonies were cultured overnight again on LB/Amp plates.

The recombinant pET-52b(+) plasmid was purified from selected colonies. A 2 µl aliquot of Gold-β-mercaptoethanol mix (Stratagene) was added to 100 µl BL 21-Codon Plus competent *E.coli* cells (Stratagene). A 50 µl aliquot was used for transformation and the other 50 µl was kept at – 80°C. A 1 µl aliquot of recombinant pET-52b(+) was added to 50 µl of BL 21 cells and incubated for 30 minutes on ice. The mixture was heat-shocked at 42° for 25-40 s and kept for 2 minutes on ice. A 100 µl aliquot of SOC medium was added and a 1/2 dilution and also a 1/10 dilution of this mixture were added to a LB/Amp plates. The plates were incubated overnight at 37°C, and expression was monitored. Colonies that showed the fastest growth were selected and cultivated overnight in LB/Amp media. Then 0.5 ml of cultured BL 21 cell culture was cultured in 50 ml LB/Amp medium in a 250 ml sterile conical flask. Glycerol was added (85 % final volume) to the competent cell suspension, and the stock solution stored at – 80°C.

Colonies were cultured separately in LB/Amp medium in 250 ml sterile conical flasks (50 ml/flask). Flasks were incubated in an orbital shaker incubator at 250 rpm at 37°C for 3 hours. The optical density was monitored at 600 nm every hour until an OD of 0.6 was reached. Isopropyl- β -D-thio-galactoside (IPTG) (50 µl) was added to three flasks (the fourth flask remained as a control without IPTG) then left for 3 h at 30°C (a suboptimal temperature for proteases). Aliquots of 1ml of suspension were collected every hour and centrifuged at 1,000 g for 5 min. The supernatants were discarded and cell pellets were stored at –20°C. After three hours cells were centrifuged in 50 ml sterile tubes at 1,000 g for 25 minutes, then supernatants were discarded and cell pellets were stored at –20 °C.

BL 21-codon plus competent E. coli cells were lysed to induce release of PAR-2 RP by resuspending cell pellets in 3 ml BugBuster protein extraction reagent with 3 µl benzonase nuclease enzyme (Novagen, Merck Chemicals). The mixture was incubated in a rotating mixer for 20 minutes at room temperature. Cells were centrifuged at 2,000 g for 35 minutes to remove insoluble debris. Cell pellets were kept for the further purification of inclusion bodies and supernatants were collected in 2 ml tubes and stored at – 20 ºC until purification.

The inclusion bodies from lysates were purified by adding 1 ml of 6 M GuHCl and centrifuged at 1,000 g for 10 minutes. The presence of PAR-2 RP in the *E. coli* lysate was investigated by dot blotting. Cell lysates were applied to a nitrocellulose membrane (Whatman, Dassel, Germany) in a quantity of 50 µl per well in Bio-Dot apparatus (Bio-Rad). Samples were left to impregnate the membrane under gravity for 30 min, 50 µl PBS was added and the membrane dried using a suction pump for 1 min.

The dot blot apparatus was disassembled and the membrane was washed once with PBST. The non-specific binding on the membrane was blocked with 5 % non-fat dry cow's milk in PBST solution for 1 h at room temperature. The membrane was washed three times with PBST for 5 min each and incubated with a 1 in 2000 dilution of monoclonal antibody conjugated with peroxidase against the poly-histidine tag (Sigma) in the PAR-2 RP (clone HIS-1) for 2 h at room temperature. The signal was detected using SuperSignal West Pico chemiluminescent substrate (Thermo Scientific) and the image was captured using a VersaDoc™ imaging system.

PAR-2 RP was purified using Talon metal affinity resin (Takara Bio Europe/Clontech, Saint-Germain-en-Laye, France). One ml was loaded onto a 20 ml column and washed three times with the washing buffer (300 mM NaCl, 150 mM HEPES, pH 7.0). The cell lysate was applied to the column four times, and the column washed three times with 20 ml washing buffer. PAR-2 RP was eluted by adding 2 ml of elution buffer (300 mM NaCl, 50 mM HEPES, pH 7.0 and 150 mM imidazole), and 1 ml fractions of the eluant were collected in separate 2 ml tubes. The efficiency of purification was tested by dot blotting as described above.

2.11 Polyacrylamide gel electrophoresis

The peptide corresponding to PAR-2 RP (custom synthesized by Activotec, Cambridge) could not be detected on SDS-PAGE gels of up to 20 %. A special tricine gel was developed according to the protocols from the laboratories of Professor Richard W. Roberts, Department of Chemistry, University of Southern California, CA, USA [225] and Professor David Baker, Department of Biochemistry, University of Washington, WA, USA [226] and these allowed visualization of proteins below 5 kDa. A 16 % resolving gel was prepared using 6 M urea with 3.33 % tricine gel buffer (3 M Tris and 0.23 % SDS, pH 8.45). To polymerize the gel, 100 µl 10 % ammonium persulphate $(NH_4)_2S_2O_8$ (APS) and 25 µl tetrametyletylenediamine (TEMED) were added. A 5 % stacking gel was used and samples were loaded after mixing with 2x tricine sample buffer (1 M Tris-HCl, pH 6.8 with 24 % (v/v) glycerol, 8 % (v/v) SDS, 0.02 % (w/v) Coomassie blue G-250 and 0.2M DTT). The gel was run in Anode Buffer (0.2 M Tris-HCl, pH 8.9) loaded in the bottom of the electrophoresis tray and Cathode Buffer (0.1 M Tris-HCl, 0.1 M tricine and 0.1 % SDS) loaded on top of the wells. Gels were stained with Coomassie blue G-250 in 10 % acetic acid, 40 % methanol and 4 % formaldehyde [227] and de-staining was performed in a mixture of 100 ml acetic acid, 450 ml dH_2O and 450 ml methanol.

2.12 Detection of antibodies specific for PAR-2 RP

Antibodies previously produced against PAR-2 were examined for their ability to bind PAR-2 RP using dot blotting, western blotting, and direct and indirect ELISA procedures. The antibodies examined were Rabbit Antisera K and L which had been prepared against a peptide with residues 29-42 (^{29}TNRSSKGR↓SLIGK^{42}V) of human PAR-2 N-terminus extracellular domain, M and N which had been prepared against a peptide with residues 213-235 (VKQTIFIPALNITTCHDVLPEQL) of human PAR-2 N-terminus extracellular domain and O and P first 90 residues of extracellular domain of rat PAR-2 respectively (Aslam, 2003). In addition mouse monoclonal antibodies (P2A, P2B, P2C, and P2D) were employed (all of IgM class), which had been prepared against peptides corresponding to residues 37-52 and to residues 29-42 of human PAR-2 extracellular domain [228]. All antibodies used were diluted in PBS.

Dot blotting was applied as described previously in section 2.10 using 50 µl of PAR-2 RP (250 µg/ml), polyclonal rabbit anti-mouse conjugated to HRP (DakoCytomation) in a dilution of 1/1,000 as the secondary antibody for detection of the monoclonal antibodies, and anti-rabbit IgG conjugated to HRP (Sigma) in a dilution of 1/1000 as the secondary antibody for detection of rabbit polyclonal antibodies. Western blotting was employed to detect PAR-2 RP separated on 6 M urea tricine gels, following transfer to nitrocellulose membranes using semi-dry transfer apparatus (Bio-Rad) at 20 V for 1 h. The primary antibodies (monoclonal P2A, P2B, P2C, and P2D and rabbit antisera K, L, M, N, O and P) were each added at a dilution of 1/100 and secondary antibodies were added as described for the dot blotting procedure.

PAR-2 RP in concentrations from 0 to 1,000 ng/ml in coating buffer (carbonate-bicarbonate buffer) were applied in a volume of 100 µl/well to ELISA plates (Costar, New York, USA) and incubated overnight at 4°C. Plates were washed for 5 min three times with PBS-T washing buffer and blocked with 3 % BSA. Monoclonal antibodies or rabbit antisera were added (diluted 1/2) or IgM iso-type control antibody was added for 1 h at room temperature. Plates were washed as before and secondary antibodies were added at a dilution of 1/10,000 for 1 h at room temperature. After washing, a freshly prepared substrate solution (100 ml citrate-phosphate substrate buffer pH 5.5, 34 µl H_2O_2 (30 %) and 34 mg tetramethyl benzidine (TMB) in DMSO) was added in a volume of 50 µl/well and left for 5 minute in the dark. When a satisfactory colour was observed, a stop solution (2 M H_2SO_4) was added in a volume of 25 µl/well. The optical density was read at wavelengths 450 and 595 nm.

On the basis of the results of dot blotting, western blotting and direct ELISA, rabbit antisera and monoclonal antibody were selected for the development of sandwich ELISA for PAR-2 RP. ELISA plates were coated as above with rabbit antisera in the coating buffer in a dilution of 1/10 and incubated overnight at 4°C. After blocking with 3 % BSA, PAR-2 RP was applied in concentrations from 0 to 1000 ng/ml in PBS or PBS-T or NaCl (0.05 or 0.1 or 0.2 M) for 1 h at room temperature. One monoclonal was employed in a dilution of 1/100 as the detecting antibody, followed by anti-mouse IgM/HRP as the secondary antibody in a dilution of 1/10,000 for 1 h at room temperature.

2.13 Detection of PAR-2 RP in clinical samples

Sample collection and procedures with human subjects had the approval of Southampton and South West Hampshire Research Ethics Committee (Reference 363/02). Employing the ELISA protocol described above, PAR-2 RP levels were measured in clinical samples. Serum and other body fluids that were tested included, broncho-alveolar lavage, nasal lavage and synovial fluid, and also culture supernatants from human umbilical vein endothelial cells (HUVEC) and human bronchial epithelial cells (16HBE). Parallelism of dilution curves was examined and samples were spiked with preparations of PAR-2RP.

In addition to ELISA, the MSD assay technology platform was used to detect PAR-2 RP in clinical samples. In the MSD system the protein or a capture antibody is non-specifically adsorbed on the carbon surface of a MULTI-ARRAY™ plate and the detection was performed with antibody labeled with MSD SULFO-TAG™ reagent, an electro-chemiluminescent label (ECL). A voltage applied to the plate electrodes causes the label bound to the electrode surface to emit light and the intensity of the emitted light is taken as a measure of the amount of the protein of interest that is present in the sample. The signal generated from this interaction was detected using a Sector™ Imager 2400 (Meso Scale Discovery (MSD), Gaithersburg, MD, USA). Aliquots of 5 µl PAR-2 RP or clinical samples in PBS with 0.015 % Triton X-100 were loaded using tenfold serial dilutions with the highest concentration of 500 ng/ml in MSD's uncoated standard one spot MULTI-ARRAY™ 96 well plate (MSD) and incubated unsealed overnight at 4°C. Plates were blocked using 3 % BSA in Base (wash) Buffer (PBS with 0.2% Tween 20) for 1 h at room temperature. After washing three times with 150 µl buffer for 5 min each, mouse P2A monoclonal antibody (in the form of hybridoma culture cell supernatant) was applied in 1:100 dilution, 25 µl/well for 1 h at room temperature. Plates washed as before and aliquots of 25 µl anti-mouse goat SULFO-TAG antibody were added in a concentration of 0.2 ng/ml for 1 h at room temperature. The antibodies were diluted in base buffer with 1% BSA. The unbound antibody was washed as before and Reading Buffer 4 (MSD) was added 150 µl/well and plates kept at room temperature until reading. Signals were detected using a Sector™ imager 2400 powered with Discovery Workbench 3.0 software and expressed as ECL signal referred to the intensity of light emitted after stimulation of the

electrode in each well. In another set of experiments the SULFO-TAG P2A was used alone as a detecting antibody at a concentration of 1 µg/ml.

2.14 Purification of mouse monoclonal P2A antibody from hybridoma cell culture supernatant

P2A was purified from hybridoma cell culture supernatant using ammonium sulphate precipitation followed by a thiophilic affinity based chromatography. At first, the culture supernatant pH was maintained by adding 1M Tris-HCl pH 8.0 (1 part to 10 parts sample). The P2A was precipitated by slowly adding a saturated solution of ammonium sulphate to the supernatant until 50 % final saturation was reached and slowly stirred overnight at 4°C. The solution was centrifuged in Beckman J2- HS high speed centrifuge (Beckman Coulter Ltd., High Wycombe) at 10,000 g for 30 min at 4°C, supernatant decanted and cell pellet was dissolved in 10 ml column binding buffer, and stored at - 20°C. The sample was prepared for the next purification step by adding 0.8 M ammonium sulphate gradually and passing through by 0.45µm filter.

A Hitrap™ IgM purification HP column from GE Healthcare was prepared by washing with a Binding Buffer (20 mM sodium phosphate with ammonium sulphate 0.8M, pH 7.5) followed by Elution Buffer (20 mM sodium phosphate, pH 7.5) and finally Regeneration Buffer (20 mM sodium phosphate, pH 7.5 with 30 % isopropanol) five column volumes each. The column was equilibrated with five column volumes of the Binding Buffer. Sample was diluted five times in Binding Buffer and applied to two connected columns (each of one ml column volume) slowly by syringe at a rate of 1 ml/min. Unbound material was removed by washing the column with fifteen column volumes of Washing Buffer, and the P2A eluted by application of twelve column volumes Elution Buffer. Fractions of 1 ml volume were collected and stored at 4°C until further analysis. The column was regenerated using seven column volumes of Regeneration Buffer, re-equilibrated with five column volumes Binding Buffer and followed by five column volumes of 20 % ethanol for reservation.

The total protein content in fractions was detected using a bicinchoninic acid protein assay kit (BCA) using a standard curve derived from the absorbance values with a range of concentrations of gamma globulin from 0 to 10 mg/ml at 550 nm wavelength. Fractions with high protein content were further

analyzed using SDS-PAGE electrophoresis. Samples were applied on a 4-12 % gradient gel under reducing conditions and after heating to 95°C for 10 min. Gels were stained with silver staining kit according to the manufacturer's instructions or transferred to a nitrocellulose membrane using the western blotting technique described before. The membrane was blocked for 1 h with 5 % non-fat dry cow's milk in PBS-Tween and the presence of P2A was detected with polyclonal rabbit anti-mouse immunoglobulin HRP antibody. Antibody reaction was visualized using 3, 3'-diaminobenzidine (DAB) peroxidase substrate kit and bands of high density were photographed using a VersaDoc™ imaging system. P2A antibody positive fractions were collected and concentrated using a filter device Centricon Ultracel YM100 concentration column with 100,000 NMWL molecular weight membrane cut off (Amicon Bioseparation, Millipore). Glycerin was removed from the membrane by washing twice with 2 ml dH_2O water and centrifugation at 1,000 g for 5 min. The eluted fractions were applied in 2 ml volume to the column and centrifuged at 1,500 g for 1 h using a fixed angle rotor until about 100 µl remained above the membrane. The column was reversed and centrifuged at 1,000 g for 5 min followed by washing twice with 200 µl PBS at 1000g for 5 min each. Concentrates were collected in one tube and total protein content was measured as before and stored at 4°C until further analysis.

2.15 Labelling of mouse monoclonal antibody

In order to use mouse P2A monoclonal antibody to detect PAR-2 RP in the MSD immunoassay system, P2A was labelled with SULFO-TAG. MSD® SULF0-TAG NHS Ester is an amine-reactive, N-hydroxysuccinamide ester that can readily be coupled under mild basic conditions to primary amine groups (e.g. lysine-containing proteins) of proteins forming a stable amide bond. In preservative free PBS, pH 7.2, the P2A antibody was diluted to a concentration of 1 mg/ml. The stock solution of 3 nmol/µl was prepared by adding 50 µl dH_2O cold water to 150 nmol lyophilized ester powder and vortexed gently to ensure dissolution. The volume of SULFO-TAG NHS Ester stock solution required for tagging the antibody was calculated according to the protein content of antibody sample and optimal ratio of ester to protein (i.e. challenge ratio of 20:1 or 100:1) according to the following equation:

SULFO-TAG reagent required (nmol)

$$= 1000 \times \left(\frac{\text{Protein Concentration (mg/ml)}}{\text{Protein MW}} \right) \times \text{Challenge ratio x Volume of protein in solution } (\mu l)$$

Using the previous value, the volume of SULFO-TAG stock solution required for the labeling reaction was calculated:

$$\text{MSD SULFO-TAG } (\mu l) = \frac{\text{SULFO - TAG reagent required (nmol)}}{\text{concentration of MSD SULFO - TAG stock solution (nmol/}\mu l)}$$

The ester was added to the antibody solution and incubated for 2 h at room temperature in a foil covered 2 ml tube. The excess ester was removed by dialysis of the coupled antibody solution using Slide-A-lyser 20K dialysis cassettes (Pierce) overnight at 4°C in 500 ml PBS with 0.05 % sodium azide and repeated for another 1 h in the morning. The molar protein concentration was determined as described previously. The absorbance of the SULFO-TAG antibody conjugate was measured by adding 50 µl of the solution in a microtiter 96-well plate at a wavelength of 450nm.
The effectiveness of the labeling procedure was determined by calculating the labeling incorporation ratio as follows:

(A) Protein concentration; $\frac{\text{Protein concentration (mg/ml)}}{\text{MW protein}} =$ M

(B) Label concentration; $\frac{OD_{450}}{15{,}400} =$ M

M = moles per liter
15,400 M^{-1} cm^{-1} = Extinction coefficient of the labeling ester
Labeling Incorporation Ratio (SULFO-TAG label: protein) = B/A

The reactivity of the tagged P2A compare to the non-tagged, hybridoma cell supernatant and that of rabbit serum P2 to synthetic PAR-2 RP was tested by dot blotting using the method described above. Serial dilutions of synthetic PAR-2 RP were used for generating a standard curve with the SULFO-TAG P2A conjugate as detecting antibody in the MSD immunoassay system.

2.16 Stability of PAR-2 RP

The potential of proteases to degrade PAR-2 RP was examined by dot blotting, by separation on 6 M urea tricine gels and by sandwich ELISA as described previously. Samples of 50 µl PAR-2 RP at 250 µg/ml were incubated with an equal volume of active and heated trypsin 0.06 µg/ml or active and heated tryptase at 80 mU/ml at time points ranging from 0 to 24 h. In a separate experiment, PAR-2 RP at a concentration of 1 µg/ml was incubated with 50 mU/ml tryptase or 100 U/ml trypsin for 2 h at 37°C. Aliquots of 25 µl of PAR-2 RP with or without incubation with protease were injected into a BioSep-Sec-S-3000 size exclusion column (Phenomenex) in HPLC at 4°C with a 0.5 ml/min flow rate, and fractions monitored at 214 nm. PAR-2 RP was eluted in 45 % acetonitrile with 0.1 % trifluoroacetic acid. PAR-2 RP degradation was also examined using a ZORBAX® Extend-C18 reverse phase column (Agilent) with a 1 ml/min flow rate and screening fractions at 254 nm wavelength at room temperature. PAR-2 RP was eluted in 85 % methanol in water or by gradient elution of acetonitrile from 10 to 100 % with 0.05 % trifluoroacetic acid.

2.17 Effects of tryptase and PAR-2 RP on human endothelial cells

2.17.1 Culture of umbilical vein cells (HUVECs)

All procedures employing HUVECs were approved by Southampton and South West Hampshire Research Ethics Committee (Reference 241/01). Umbilical cords and placenta were collected at birth and kept at 4°C. The cord was cut under sterile conditions under a hood as soon as possible and washed with pre-warmed PBS (37°C). Blood clots were removed, and the tissues checked for damage. The umbilical vein was defined and pre-warmed 1 % collagenase in PBS (37°C) was injected slowly using a 20 ml plastic syringe (BD Plastipak, Oxford); and the cord was incubated for 15-30 minutes at 37°C. The contents of the cord were collected in 50 ml sterile Falcon tubes (Greiner Bio-One) and centrifuged at 150g for 10 minutes. Supernatant was discarded and cell pellets resuspended in 10 ml pre-warmed endothelial cell culture medium (PromoCell, Heidelberg, Germany) containing a 10 % penicillin-streptomycin-glutamine mixture (GIBCO, Invitrogen), and cultured in a 75 cm^2 TC culture flask (Orange Scientific) at 37°C in humidified air with 5 % CO_2. After overnight incubation

the medium was aspirated and cells washed three times with warm PBS and new medium added.

HUVECs are adherent cells and grow in monolayers. Cells were allowed to grow to confluence, changing media every 48 hours. Upon reaching 80–90 % confluence, HUVECs were detached using trypsin-EDTA medium for 1 to 2 min at 37°C. Detachment was observed at a magnification of 100x using an inverted microscope (Leica Microsystems, Wetzlar, Germany). After 80 % of cells were detached, the actions of trypsin were stopped by adding complete medium. Cells were collected in a sterile 50 mL tube and centrifuged at 150g for 10 minutes. The supernatant was discarded and cell pellets resuspended in pre-warmed fresh medium. Cells maintained at 37°C in humidified air with 5 % CO_2.

2.17.2 Cell counting

Viability of cell were tested by adding 10 µl of the cell suspension to 90 µl of trypan blue 0.4 % and mixed by aspirating with a pipette. In a cleaned improved Neubauer haemocytometer, the cover-glass moistened with water and 10 µl of the mixed cell suspension was added to both counting chambers. The mean number of viable (bright) cells and non-viable (stained) cells in the four areas of the counting chamber were calculated, multiplied by dilution factor (10) and the correction factor (10^4) to obtain the number of cells per ml.

$$\text{Number of cells/ml suspension} = \left(\frac{\text{Number of cells counted}}{4}\right) \times \text{Dilution factor} \times 10^4$$

For gene expression studies, HUVECs were resuspended in the medium above containing 2 % FBS, loaded in a 24-well culture plate pre-coated with gelatin (0.1 %, Greiner Bio-One) at a density of 10^5 cells per well and incubated for 24 h at 37°C in humidified air with 5 % CO_2.

2.17.3 Characterization of HUVECs

The identity of HUVECs was confirmed by immunocytochemistry with fluorescent labelled antibodies. HUVECs were loaded on 8-well chamber slides (Nunc, Fisher Scientific) at a density of 30–50 x 10^3 cells per chamber and incubated for 24 h at 37°C in humidified air with 5 % CO_2. When 90 %

confluence was achieved, cells washed twice with PBS and fixed in ice-cold 100 % methanol for 20 minutes. Cells were washed as before and blocked with 10 % goat serum for 1 h at room temperature. After washing, cells were incubated for 1 h at room temperature with monoclonal antibody P2A specific for PAR-2 antibody (culture supernatant diluted 1:30, Aslam, 2003) or mouse monoclonal anti-human von Willebrand factor (vWF) antibody (1:50 dilution, DakoCytomation) as primary antibodies. Fluorescein isothiocyanate (FITC)-conjugated anti-mouse goat (1:68 dilution, Sigma) was used as the secondary antibody for 1 h at room temperature. For nucleic acid staining, cells were incubated with 1-3 µg/ml propidium iodide (PI) for 5 minutes. Cells were washed, chambers removed and slides mounted with VECTASHIELD Mounting Medium (Vector Laboratories). Cover-slips were applied, sealed with nail polish and left to dry in the dark at room temperature for 2 h. Slides were stored in the dark at 4°C, and cells were and photographed using AxioSkop 2 Plus™ fluorescence microscopy with AxioCam™ camera (Carl Zeiss).

2.18 Endothelial cells and treatments

Possible cytotoxic actions of the cell treatments were investigated using methylene blue cytotoxicity assay and by measurement of lactic dehydrogenase (LDH). These will be discussed separately.

2.18.1 Methylene blue cell counting

HUVEC were cultured as before, detached and seeded in 100 µl/well medium in a flat bottom 96-well culture plate in two sets; one with 2-fold dilutions of untreated cells prepared with the highest cell density at 2.5 x 10^5 cell/well and treated cells were added at a density of 50 x 10^3 cell/well. Cells were incubated at 37°C in humidified air with 5 % CO_2 overnight. Triton-X 100 (1 %) in PBS was added and plates were centrifuged at 250g for 10 min. The supernatant was aspirated (and stored at 4°C for LDH assay) and cells fixed with addition of 100 % cold methanol (100 µl/well) and plates were incubated for 30 min at 4°C. Methanol was decanted, cells were washed twice with PBS and then left to dry at room temperature. A volume of 50 µl of 1 % methylene blue was added to each well and incubated at room temperature for 30 min. The plates were washed with tap water, left to dry at room temperature and 100 µl/well of ethanol: HCl (1:1, v:v) was added. The absorbance was measured at 595 nm with a microplate reader. The standard curve was generated by plotting the OD

values of the standard wells against the cell number. From the standard curve the cell number of the unknown wells was determined and data was expressed as the percent decrease in cell number for each treatment.

2.18.2 Measurement of lactic dehydrogenase (LDH)

A colorimetric cytotoxicity detection kit (LDH) (Roche Diagnostic GmbH) was used to detect the levels of LDH in supernatants of the cell culture. Plates were centrifuged again as mentioned above to obtain cell free supernatant. In accordance with the manufacturer's guidelines, a 50 µl/well substrate mix was prepared and loaded in a clear bottomed assay plate. An equal volume of the supernatant was added to each well and incubated for 30 min in the dark at room temperature. An aliquot of 50 µl of 1 M acetic acid was added to each well to stop the breaction and the absorbance was measured at 490/595nm. The OD values were plotted in comparison to that with 1 % Triton X-100 (100 % LDH release) after subtraction of values of the background (the substrate mix alone).

2.19 RNA extraction

2.19.1 Qiagen RNeasy

RNA extraction was performed using a silica-based membrane column combined with microspin technology under strict conditions to prevent contamination. Supernatant from HUVECs culture were decanted and preserved at -20°C until further analysis. Cells were washed twice with ice cold PBS and disrupted by adding 350 µL RLT lysis buffer for each well (containing guanidine-thiocyanate) and mixed gently for homogenization by pipetting for 30 s. The cell lysate was either stored at -80 °C or used right away in the Qiagen kits. In accordance with the manufacturer's guidelines, RNA in the cell lysate was precipitated by adding an equal volume of 70 % ethanol and mixing well by pipetting. Samples, including any precipitate, were transferred to the RNeasy mini spin columns placed in 2 ml collection tubes, the lid closed gently and centrifuged at 8,000 g for 15 s using Heraus Fresco 17 ultracentrifuge (Thermo Scientific). The flow-through was discarded and the spin column was washed with 700 µL of RW1 buffer (containing ethanol) by centrifugation as before. The flow-through was decanted and the spin column washed twice with 500 µL RPE buffer by centrifugation at 8,000 g 15 s first and then for 2 min. The spin column was placed in a new collection tube and centrifuged at

full speed for 1 min to remove any residual flow-through from the column. To elute the RNA, the spin column was placed in a 1.5 ml RNase-free collection tube, 50 µL of RNase-free water was added, left for 10 min, and centrifuged at 8,000 g for 1 min. The RNA was stored at -80 ºC or used straightaway in cDNA synthesis.

2.19.2 RNA Quantification

RNA quantity and purity was tested by measuring the optical density of extracted RNA samples using a NanoDrop® ND-1000 spectrophotometer (Thermo Scientific) at RNA-40 mode. The machine was calibrated by application of 1 µL RNase-free water and absorbance readings of blank samples were measured at 260 nm and 280 nm wavelengths. The concentration of nucleic acid in the samples was expressed as ng/µL based on absorbance at 260 nm. The ratio of 260 nm and 280 nm absorbance readings (A260/A280) was considered as a primary indicator for purity of the nucleic acid from contaminant proteins, and a ratio of 1.8 to 2.0 was considered acceptable. The presence of other contaminants including solvents and salts (e.g. phenolate ion, thiocyanate), in addition to organic compounds in the samples was estimated by the ratio A260/A230, and values greater than 1.8 were accepted. The average yield of RNA was 20-30 ng/µl.

2.20 Reverse-transcribed polymerase chain reaction (RT-PCR)

A 100 ng quantity of RNA was used as a template for transcribing into cDNA. The cDNA was synthesized using a Primer Design Precision qScript reverse transcriptase kit according to the manufacturer's instructions. In a 0.2 ml thin walled tube, random nanomer and oligo-dT primers were added to the RNA sample in a total reaction volume of 10 µl and gently mixed by vortex. Primers were annealed to RNA by heating up to 65ºC for 5 min in a thermocycler (Eppendorf Mastercycler, Cambridge) and immediately cooled down on ice. RNA was reverse transcribed by incubating with reverse transcriptase enzyme and nucleotides in a 10x reaction buffer in a total reaction volume of 20 µl. Tubes mixed briefly by vortex, heated up to 55ºC for 20 min and reaction was stopped by incubation at 75ºC for 15 min using a thermocycler. The cDNA was stored at -20ºC until use.

2.21 Design of primers

RNA Primers were designed using a web based ProbeFinder program v2.45 selecting an optimal combination of human Universal ProbeLibrary (UPL) probe and a gene-specific primer set at Roche applied science web site [229], and obtained from Eurofins MWG/operon (Ebersberg, Germany). The genomic mRNA sequence was obtained from Gene Bank (National Center for Biotechnology Information, NCBI) and the nucleotide sequence was exported in the FASTA form. Primers were optimized to have annealing temperatures between 59 and 61°C, the length was set at 18-27 nucleotides and the PCR amplicon was 60 to 150 bp long. Primers that bound close to exon-exon splice junctions were chosen, thereby facilitating amplification of intron-spanning targets (so as to eliminate false positive signals from residual genomic DNA). The PCR efficacy was optimized so that the annealing temperature could be accurately matched. Primers to the whole amplicon were tested for specificity using the Basic Local Alignment Search Tools (BLAST®). The oligonucleotides used in the qPCR shown in Table 2.1.

2.22 Reference genes

Housekeeping genes are typically endogenous constitutive genes that are required for basic cellular function or structure and used as reference genes in all quantitative studies. Gene expression was normalized in respect to the control genes glyceraldehyde-3-phosphate dehydrogenase, GAPDH[24, 230] and β-actin, ACTB[231] (PrimerDesign, Southampton). When these two genes were examined, it was determined that they had not changed significantly in the various experiments conducted.

2.23 Real time polymerase chain reaction (rtPCR)

2.23.1 Principle

Real time or quantitative polymerase chain reaction (rtPCR or qPCR) amplify and at the same time allow quantification of DNA sequences targeted. The quantity can be either an absolute number of copies or a relative number when normalized to DNA input or additional normalizing genes. The procedure follows the general principle of polymerase chain reaction but the amplified DNA is detected as the reaction progresses in real time and not at the end of reaction.

Table 2.1 Primer pairs used in qPCR reactions for the study of IL-8 and IL-1β expression in HUVECs

Primer	Accession Number	Tm	%GC	Sequence	Amplicon size
IL-8 F	NM_000584	59	55	AGACAGCAGAGCACACAAGC	62bp
IL-8 R		60	56	ATGGTTCCTTCCGGTGGT	
IL-1β F	NM_000576.2	60	50	TACCTGTCCTGCGTGTTGAA	76bp
IL-1β R		60	35	TCTTTGGGTAATTTTTGGGATCT	

Two common methods for detection of products in rtPCR are the use of sequence-specific DNA probes consisting of oligonucleotides that are labelled with a fluorescent reporter which hybridize with its complementary DNA target, or the use of a non-specific fluorescent dye, e.g. SYBR green, which binds with any double-stranded DNA to give fluorescence. To ensure accuracy in the quantification, it is necessary to normalize expression of a target gene to constitutively expressed housekeeping genes. This can correct possible differences in RNA quantity or quality across experimental samples. A special thermocycler provided with a sensitive camera is used to detect the fluorescence in reaction tubes or wells in a plate at frequent intervals during the reaction.

2.23.2 Reaction setup and Optimization protocol

Primers were diluted with nuclease-free water according to the manufacturer's instructions. In a total reaction volume of 10 µl, 2X qPCR Mastermix buffer, primer pairs and cDNA template were mixed in a thin walled 0.1 µl tube and loaded into a Corbett Rotor-gene 6000™ thermocycler (Corbett Life Science, Qiagen, Crawley, West Sussex). To minimize pipetting error, samples were run in triplicate in at least three different experiments. Samples were prepared in a volume 10 % greater than required. All reagents used were optimized for quality and reproducibility. Melting curves of the amplicons were examined for contamination and specificity (one peak per each amplicon). Following investigation of time course concentration dependent effects, a comparative study of gene expression was performed.

The thermal profile of the PCR consisted of three steps: Taq polymerase activation, cycling and melting curve analysis. Enzyme activation was performed at 95°C for 10 min and followed by 45-50 cycles of PCR. Each PCR cycle included denaturing at 95°C (15 s), annealing at 57°C (60 s) and extension at 72°C (30 s). The melting curve was generated with a stepped temperature transition from 57 to 95°C with a rise of 1°C/5 s for each step.

2.24 Measurement of levels of cytokines in the supernatant of HUVEC cultures

The effect of various agents on the production of IL-8, Il-1β and TNF-α from HUVECs was investigated by measuring the cytokine levels in culture

supernatants with specific sandwich ELISA kits for human CXCL8/IL-8, IL-1β and TNF-α/TNFSF1A (R&D Systems, Abingdon, Oxfordshire). In accordance with the manufacturer's instructions, ELISA microplates were coated with 100 µl of a cytokine-specific mouse anti-human antibody diluted in PBS, sealed and incubated overnight at 4°C. Plates were washed three times with 0.05 % Tween® 20 in PBS and blocked for 1 h with 150 µl per well 1 % BSA in PBS blocking buffer. After washing, samples or standard in blocking buffer (50 µl) were loaded and incubated for 2 h at room temperature. Standard concentrations were loaded at seven points in two fold serial dilutions with 1000 pg/ml as the highest concentration. Plates were washed as before and 50 µl biotinylated goat anti-human cytokine-specific detecting antibody diluted in the blocking buffer was loaded at the recommended concentration for 2 h at room temperature. The washing step was repeated and 50 µl of Streptavidin-HRP diluted 1:200 in blocking buffer was added to each well and incubated for 20 min at room temperature away from direct light. After washing, a freshly prepared substrate solution (consisting of 100 ml citrate-phosphate substrate buffer pH 5.5, 34 µl H_2O_2 (30 %) and 34 mg tetramethyl benzidine (TMB) in DMSO) was added in a volume of 50 µl/well and left for 20 minute in the dark. When a satisfactory colour was observed, a 2 M H_2SO_4 stop solution was added in a volume of 25 µl/well. The optical density was read at 450/595nm.

2.25 Microarray studies

2.25.1 DNA microarray hybridization

Total cellular RNA extracted from three independent experiments with HUVECs was used in microarray studies. The whole microarray hybridization was performed at the Genomic Centre, King's College London. RNA quantity was measured using a NanoDrop® ND-1000 spectrophotometer (Thermo Scientific). It was ensured that the A260/A280 ratio was 1.8-2.1 and the A260/A230 ratio was more than 1.0. The integrity of RNA was evaluated by microfluidic analysis, applying RNA samples to RNA 6000 Nano LabChip® Kit (AgieInt) and data was analyzed using Eukaryote Total RNA nano chips (Version 2.6) software (Agilent) in accordance with the standard protocol using an Agilent 2100 Bioanalyzer instrument. Agilent 2100 Expert Software was used to analyze and display results. An RNA Integrity Number (RIN score) depending on algorithmic analysis of the entire electropherogram was generated for each sample on a scale of 1-10 (1=lowest; 10=highest) as an indication of RNA quality. The

concentration of RNA in samples was calculated and the [28s/18s] rRNA ratio was also produced. The thermal profile used as described in the protocol guidelines in a Peltier Thermal Cycler (PTC-225, DNA engine tetrad, MJ Research, Waltham, USA).

Using an Ambion® WT Expression kit (Ambion Applied Biosystems, Austin, TX, USA) according to the standard protocol, total RNA was converted into complementary RNA (cRNA) and cDNA synthesized. The first-strand cDNA was synthesized from total RNA using reverse transcriptase, followed by formation of the second-strand cDNA using DNA polymerase. Antisense cRNA was formed from the second-strand cDNA template by *in vitro* transcription (IVT) using T7 RNA polymerase. The cRNA synthesized was purified using nucleic acid binding magnetic beads supplied with the kit, and cRNA yield estimated using a NanoDrop® ND-1000 spectrophotometer (Thermo Scientific) and size distribution was examined using an Agilent 2100 bioanalyser. A sense-strand second-cycle cDNA was synthesized from the antisense cRNA using reverse transcriptase with random primers, and the antisense cRNA template was degraded by addition of RNase H to the samples. The cDNA synthesized was purified using a nucleic acid binding magnetic beads technique and cRNA yield and size examined as described above.

The single sense-stranded cDNA was fragmented and labeled using the Affymetrix WT terminal labelling kit (Santa Clara, California, USA) using fragmentation and terminal labelling Master Mix respectively following the protocol for thermal profiling. The labelled sense-strand cDNA was hybridized with the hybridization cocktail and applied into Human Gene 1.0 ST cartridge arrays (Affymetrix) using standard protocols and incubated for 17 h at 45°C in a GeneChip Hybridization Oven 460 at 60 rpm. The arrays were washed and stained using a GeneChip Fluidics Station 450, and scanned using an Affymetrix GeneChip Scanner 3000 7G. A schematic diagram of the procedures employed is shown in Figure 2.5

2.26 Confirmation of microarray results

The expression profile for the genes chosen was investigated using real-time PCR, and cell expression of certain adhesion molecules was tested by immunocytochemistry, flow cytometry and ELISA.

2.26.1 Real-time RT-PCR

In order to confirm microarray study results, fifteen primers' forward and reverse mix from PrimerDesign were employed in a real time PCR reaction (Table 2.2). Primers were diluted with nuclease-free water according to the manufacturer's instructions. The cDNA templates of the three experiments used in microarray were pooled for each treatment. The quantity and purity of cDNA were tested using a NanoDrop® ND-1000 spectrophotometer (Thermo Scientific). Samples were run in triplicate and in a total reaction volume of 20 µl with 2X qPCR Mastermix, primer mix and cDNA template mixed in 384-well plates; and loaded into a LightCycler® 480 thermocycler (Roche GmbH, Mannheim, Germany). A volume 10 % more than required was employed so as to minimize pipetting errors.

The thermal profiling of the PCR consisted of three steps: Taq polymerase activation, cycling and melting curve analysis. Enzyme activation was performed at 95°C for 10 min, followed by 50 PCR cycles. Each PCR cycle included denaturing at 95°C (15 s), annealing at 60°C (60 s) and extension at 72°C (30 s). A melting curve was generated with a temperature transition from 50 to 98°C, with a ramp rate of 0.06°C/s.

2.26.2 Immunocytochemistry

Immunocytochemistry was performed with tryptase-treated HUVECs for the adhesion molecules: inter-cellular adhesion molecule 1 (ICAM1, CD54), vascular cell adhesion molecule 1 (VCAM-1) and epithelial cell adhesion molecule (EpCAM, CD11a), and integrin alpha L chain (ITGAL, CD326). HUVECs were cultured and stained with immunofluorescent dye as described before. Mouse monoclonal antihuman CD54-FITC (1:50 dilution), mouse anti-human CD106-FITC (1:10, AbD Serotec), mouse monoclonal antihuman CD326-FITC (1:11 dilution) and mouse monoclonal antihuman CD11a (1 µg/ml) were used as primary antibodies. FITC-conjugated goat anti-mouse immunoglobulin (1:64 dilution, Sigma) was used as the secondary antibody. For nucleic acid staining, cells were incubated with propidium iodide (PI). Slides were kept in the dark at 4ºC. Cells were viewed and photographed using fluorescence microscopy.

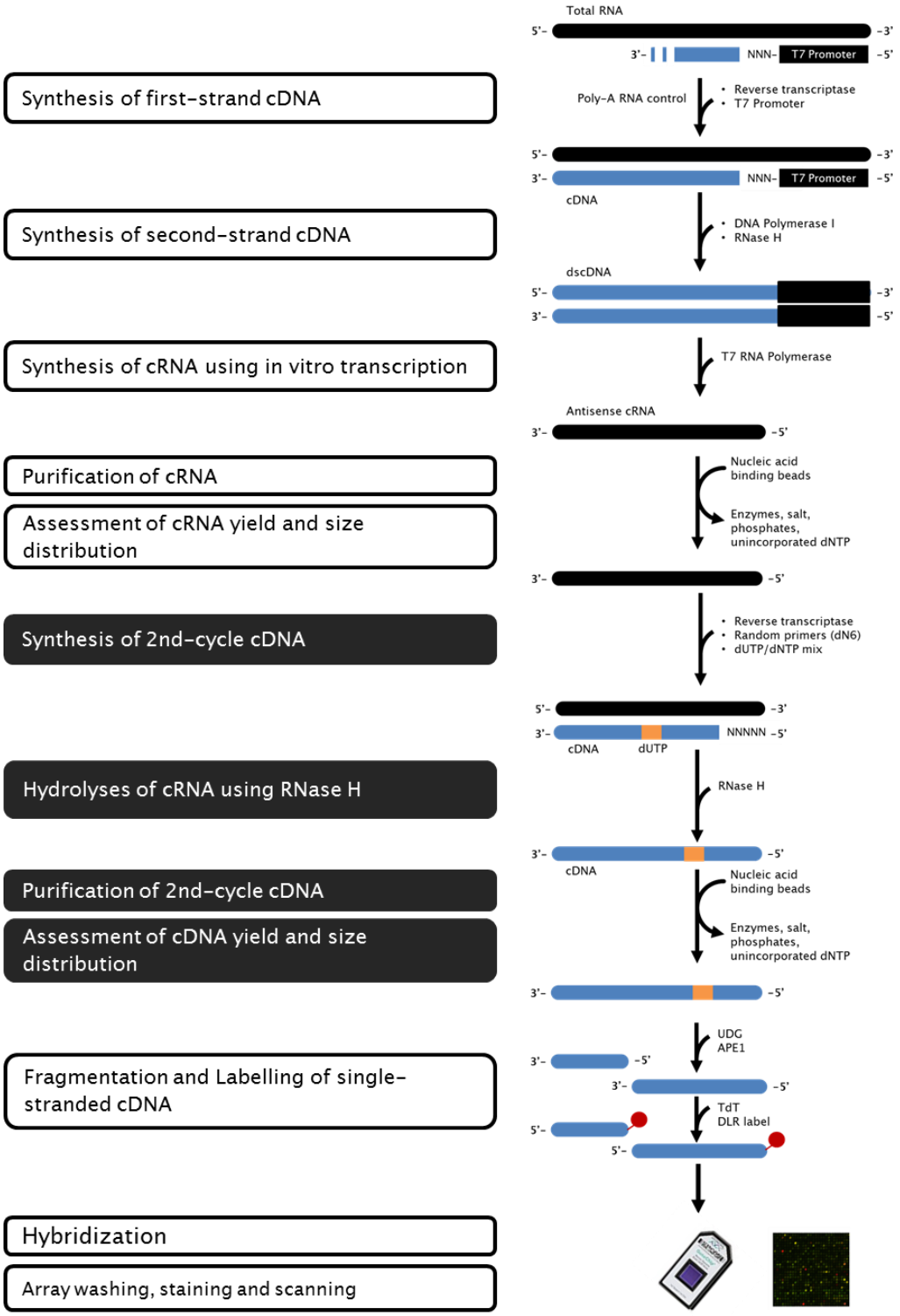

Figure 2.5 Schematic representation of microarray workflow. cRNA: complementary RNA, dscDNA: double stranded complementary DNA, RNase H: Ribonuclease H, UDG: Uracil-DNA Glycosylase, APE1: Human Apurinic/Apyrimidinic Endonuclease 1, TdT: Terminal deoxynucleotidyl transferase, DLR: Biotin-11-dXTP Analog (a DNA labeling reagent). Adapted from Ambion® WT Expression and Affymetrix WT terminal labelling kits manuals.

Table 2.2 Primer pairs used in qPCR for confirmation of findings of microarray studies with HUVECs

Primer	Accession Number	Tm	% GC	Sequence	Amplicon size
CXCL10 F	NM_001565	71.6	57.1	CAGAGGAACCTCCAGTCTCAG	93bp
CXCL10 R		56.3	45.5	GGTACTCCTTGAATGCCACTTA	
EPCAM F	NM_002354	55.5	39.1	TGTTATTGTGGTTGTGGTGATAG	89bp
EPCAM R		56	43.5	CCTTCTCATACTTTGCCATTCTC	
GDF3 F	NM_020634	56.6	45	ATGTTTGTGTTGCGGTCAGT	87bp
GDF3 R		56.5	45.5	GGGGTTGTCATTCCAATCCTTA	
ICAM1F	NM_000201	56.1	55	CCTATGGCAACGACTCCTTC	111bp
ICAM1R		55.2	61.1	TCTCCTGGCTCTGGTTCC	
IL-2 F	NM_000586	55.8	38.5	CCTATCACTCTCTTTAATCACTACTC	107bp
IL-2 R		55.5	42.9	GTTTGTGACAAGTGCAAGACT	
IL-3 F	NM_000588	56.8	39.1	GGACATCAAAAACAGCAGAACTT	87bp
IL-3 R		56.7	52.6	GCCGCAGGAAAAGGTGAAA	
IL-6 F	NM_000600	55.5	42.9	GCAGAAAACAACCTGAACCTT	116bp
IL-6 R		55.6	42.9	ACCTCAAACTCCAAAAGACCA	
ITGAL F	NM_001114380	56.3	50	TCTGCCTGAACCTTCCATCT	128bp
ITGAL R		56.3	55	CGTGTGCTTTGAGGGAGTAG	
LXN F	NM_020169	56.1	29.6	GAAGACACATGGTATAAAATGGTAAAA	108bp
LXN R		55.6	29.6	AGATGCTATATTATGAAGTAGAATGGT	
SELE F	NM_000450	56.4	45.5	TTCTTGCCTACTATGCCAGATG	123bp
SELE R		56.5	47.6	AGGAAAGGGAACACTGAGTCT	
SMAD2 F	NM_005901	55.8	36	AGATCCATAATGAATCCAGAACTTC	127bp
SMAD2 R		55.9	34.6	GAAGAAAAATCTAAAAGCCCTCTATG	
TLL1 F	NM_012464	56.8	45.5	GGTGAATGTGAAATGGGAGTCT	108bp
TLL1 R		57.2	37.5	GCAAGTGGAAATAATGAAGCTGAA	
TNFAIP3 F	NM_006290	57	45	AACATTTTGCTGCTGCCTCA	113bp
TNFAIP3 R		57	47.6	TCCTTCAAACATGGTGCTTCC	
TNFRSF9 F	NM_001561	56.9	43.5	CTCACCTACCATCCATCAAGTTT	90bp
TNFRSF9 R		56.7	37.5	GCACAGGATAGACAAATTGACAAT	
VCAM-1 F	NM-001078	56.7	34.6	CAGGCTAAGTTACATATTGATGACAT	116bp
VCAM-1 R		58	60	GAGGAAGGGCTGACCAAGAC	

2.26.3 Flow cytometry

HUVECs were harvested as described before and cells at the second passage were seeded into a 6-well culture plate at a density of 3-5 x 10^5 cells per well. Cells were starved in serum free medium for 24 h followed by incubation with tryptase or other agents for 16 h in serum free medium. Supernatant was aspirated and stored at 20°C until further analysis. Cells were washed once with PBS and detached by adding enzyme-free/Hank's based cell dissociation buffer (GIBCO, Invitrogen) at 1 ml per well and incubated for 30 min at 37°C. Detached cells were collected into a 15 ml tube and centrifuged at 300g for 5 min. Supernatant was discarded and cell pellets were washed once with PBS/BSA 1 % solution (Ca^{2+} and Mg^{2+} free) and centrifuged as before. The density was adjusted to 1 x 10^6 cells per ml by adding PBS/BSA. Aliquots of 100 µl of cell suspension (~1 x 10^5 cells) were loaded into 5 ml polystyrene round bottom tubes (Becton Dickson, NJ, USA) and kept on ice.
Cells were incubated with mouse anti-human CD54 (ICAM-1; 20 µl/5x10^5 cells; 1:5 dilution, AbD Serotec), mouse anti-human CD326 (EpCAM; 1:11 dilution, Miltenyi Biotec Ltd., Bisley, Surrey) or mouse anti-human CD106 (VCAM-1; 1:10 dilution) monoclonal FITC-conjugated antibodies for 30 min. Cells were washed twice with 2 ml PBS/BSA and centrifuged at 300g for 5 min each time. Other aliquots of cell suspension were incubated with mouse monoclonal anti-human CD11a (integrin alpha L chain, LFA-1; 1:100, AbD Serotec) antibody for 30 min, washed twice and centrifuged as before, followed by secondary anti-mouse IgG whole molecule-FITC conjugated antibody developed in goat (1:64 dilution, Sigma) for 15-30 min on ice. Cells were washed twice as before and centrifuged at 300g for 5 min each time. The dead cells were labelled by adding aliquots of 2 µl of 1 µg/ml propidium iodide (PI) stock solution to each tube. Mouse isotype IgG1-kappa (1:100 dilution, Sigma) and mouse IgG2a (1:100 dilution, AbD Serotec, Kidlington, Oxfordshire) were used as the corresponding controls. Subsequently cells were resuspended into 300 µl PBS/BSA solution and fluorescence was determined using a BD FACSCalibur™ flow cytometer (Becton Dickinson). Data acquisition was performed using BD CellQuest Pro version 5.2.1 Software with background and viability gate adjustment. Cell parameters were adjusted to 5000 events and the histograms of positive cells were compared to the isotype control.

2.26.4 Analysis modules

Using Rotor-Gene 6000 Series Software v1.7.87, the relative quantification of gene expression was calculated according to the ΔΔCt method. A threshold for detection of fluorescence above background and Ct, the number of PCR cycles at which fluorescence from a sample crosses the threshold was determined. The Ct values of various treatments were normalized to the reference genes and calibrated in respect to non-treated cell control samples. Relative quantification (RQ), expressed as fold change, was calculated according to the following formula:

$RQ = 2^{-\Delta\Delta Ct}$ i.e. (2 to the power of minus Delta Delta CT)

Where:

Ct = cycle threshold

$\Delta\Delta Ct = \Delta Ct_{\text{Treated sample}} - \Delta Ct_{\text{Untreated sample}}$

$\Delta Ct = (Ct_{\text{\_Target gene}} - Ct_{\text{\_Reference gene}})$

Reaction efficiency was calculated with consideration of reaction efficiency of the target and the endogenous reference genes to be close to each other as possible.

2.26.5 Soluble Intracellular Adhesion Molecule 1 (sICAM1) ELISA

The effect of tryptase on production of sICAM-1 by HUVECs was investigated by measuring levels in HUVEC culture supernatants using specific sandwich ELISA kits (human sICAM-1/CD54; R&D Systems). In accordance with the manufacturer's instructions (and as described before in section 2.21), microplates were coated with a mouse anti-human sICAM-1 antibody diluted in PBS and incubated overnight at 4°C. Plates were washed three times with 0.05 % Tween® 20 in PBS and blocked for 1 h with 1 % BSA in PBS blocking buffer. After washing, samples or standard in blocking buffer were loaded and incubated for 2 h at room temperature. Standard concentrations of recombinant human sICAM-1 were loaded in two-fold serial dilutions (with the highest concentration of 2000 pg/ml; seven concentrations). Plates were washed as before and biotinylated sheep anti-human sICAM-1 antibody (diluted in the blocking buffer) was added at the recommended concentration for 1 h at room temperature. The washing step was repeated and Streptavidin-HRP diluted in blocking buffer was added and incubated for 20 min at room

temperature away from direct light. After washing, a freshly prepared substrate solution was added and left for 20 min in the dark. The reaction was stopped by adding 2 M H2SO4. The optical density was read at 450/595nm.

2.27 Calcium mobilization assay

HUVECs were loaded in a 96-well black calcium assay plate (Greiner Bio-One) at a density of 40 to 50 x 10^3 cells per well and incubated overnight at 37°C in humidified air with 5 % CO_2. Cells were washed once with pre-warmed PBS and incubated for 35 min in the dark at 37°C with fluro-3 AM florescent dye in complete medium (5 mL medium containing 100 µL HEPES buffer pH 7.0, 5 µl 0.25 M sulphinpyrazone and 50 µL 2.5 mg/ ml fluro-3 AM. Cells were washed once with challenge buffer (88 ml dH_2O, 10 ml 10x Hank's buffered salt solution (HBSS), 2 ml 1 M HEPES buffer pH 7.0, 1.333 mL 7.5 % BSA sterile and 100 µL 0.25 M sulphinpyrazone dissolved in DMSO) and 25 µl was left per well for another 20 min in the dark at 37°C.

Calcium mobilization was measured using FlexStation II equipment (Molecular Devices). The flex mode was operated using the default settings with single wavelength detection. The excitation wavelength was set at 486nm, and emission at 538 nm with a cut-off of 530 nm. After 20 s baseline readings, agents were added and fluorescence was detected for 120-300 s with a 1.52 s interval. The compound plate was loaded with the reagents under investigation (at double concentration; 100 µl per well). The assay was performed at least twice for each agent added.

Data were expressed as relative fluorescence units (RFU) per second and analysis included plotting the maximum induced calcium responses (peaks), as fluorescence change, versus the concentration. The half-maximal effective concentration values (EC50) were estimated from the concentration-response curve.

2.28 Statistics

Where Kruskal-Wallis analysis indicated significant differences between groups, for the preplanned comparisons of interest, the Mann-Whitney U test was used, and $p < 0.05$ was taken as significant. The degree of association between variables was analyzed by calculation of Spearman's coefficient of rank correlation (r_s). SPSS version 18 software was used for analysis of data and preparing graphs. $P<0.05$ was taken as significant. Microarray data for 35,000 genes were analyzed using Qlucore Omics Explorer (Version 2.1) bioinformatics software (Qlucore AB; Lund, Sweden) and the contribution of significant genes in biological pathways was analyzed using MetaCore™ (Version 2.5) Software (GeneGo; Carlsbad, CA, USA). A fold-change >1.5 or <-1.5 and a P value of < 0.05 was taken as evidence for differentially gene expression and a list of differentially expressed gene was generated. One-way ANOVA test was employed for multiple group comparisons, and unpaired Student's t-test was employed for investigating differences between two groups.

Chapter 3.

Results

Chapter 3. Results

3.1 Overview

Tryptase, the most abundant protease of the human mast cell, has been implicated as a key mediator of allergic disease. It can interact with numerous cell types to induce changes associated with inflammation and remodelling. The precise mechanisms involved are unclear; though roles for PAR-2 have been proposed. In the following section we have investigated the potential contributions of PAR-2 in the inflammatory changes induced by tryptase in the mouse as well as in cultured cells *in vitro*. In order to explore the role of PAR-2 in mediating the actions of tryptase, PAR-2 knockout C57BL/6 mice were employed. Inflammatory reactions in response to the injection of tryptase into mouse peritoneum were examined by investigating of the patterns of cell accumulation, as well as measuring MMP, albumin and total protein concentrations.

Endothelial cells were selected for investigation of mechanisms underlying cell accumulation. The actions of tryptase on endothelial cells that were studied included the potential to stimulate release of cytokines, altered global gene expression and calcium mobilisation. As the PAR-2 N-terminal released peptide cleaved from the exodomain (PAR-2 RP) has been little examined previously, attempts were made to measure its levels in biological fluids, and its potential role in inflammatory processes was studied.

3.2 Purification of tryptase from a yeast expression system

Tryptase was successfully purified from the culture supernatant of a *Pichia pastoris* yeast expression system through hydrophobic interaction chromatography with butyl Sepharose, followed by heparin agarose affinity chromatography with a salt gradient and was eluted between 1.04 to 1.29 M NaCl (Figure 3.1). When a BioSep-Sec-S-3000 size exclusion column was employed in HPLC for the final polishing stage of the purification, the elution position for tryptase fractions (as monitored by BApNA substrate cleavage) was consistent with it having a molecular weight of 132 KDa for the active tetrameric form (Figure 3.2 A).

On investigating the purity of tryptase in fractions of high tryptase activity on Coomassie blue and silver stained SDS-PAGE gels, a single band was observed corresponding to 35 kDa (Figure 3.2 B, C). This is consistent with that of the monomeric form of tryptase. The identity as tryptase was confirmed by western blotting with the tryptase-specific monoclonal antibody AA5 (Figure 3.2 D). The specific activity of the β-tryptase preparations employed ranged from 9-12.2 U/mg where 1 unit was taken as the amount of tryptase that can cleave BApNA to release 1 µmol p-nitroanalide per min at 25°C. The endotoxin levels as assayed by the LAL assay were less than 0.08 EU/1U tryptase in all preparations used in the study.

3.3 Mouse model of peritoneal inflammation

3.3.1 Tryptase-induced cell accumulation

Injection of tryptase into the peritoneum of wild type and PAR-2 deficient mice had little effect on the total number of nucleated cells recovered up to 24 h afterwards in peritoneal lavage fluid (Table 3.1). Various cell types were enumerated and identified in peritoneal lavage fluid of mice injected with tryptase (Figure 3.3). Tryptase injection was associated with a substantial increase in neutrophil numbers in wild type mice at 24 h (Figure 3.4).

There was a similar pattern of neutrophilia in the PAR-2 deficient mice. Relative numbers of eosinophils, lymphocytes, macrophages and mast cells appeared to be little affected by injection of tryptase. There were no significant differences between the two mouse strains in the numbers of other cells types in the peritoneum.

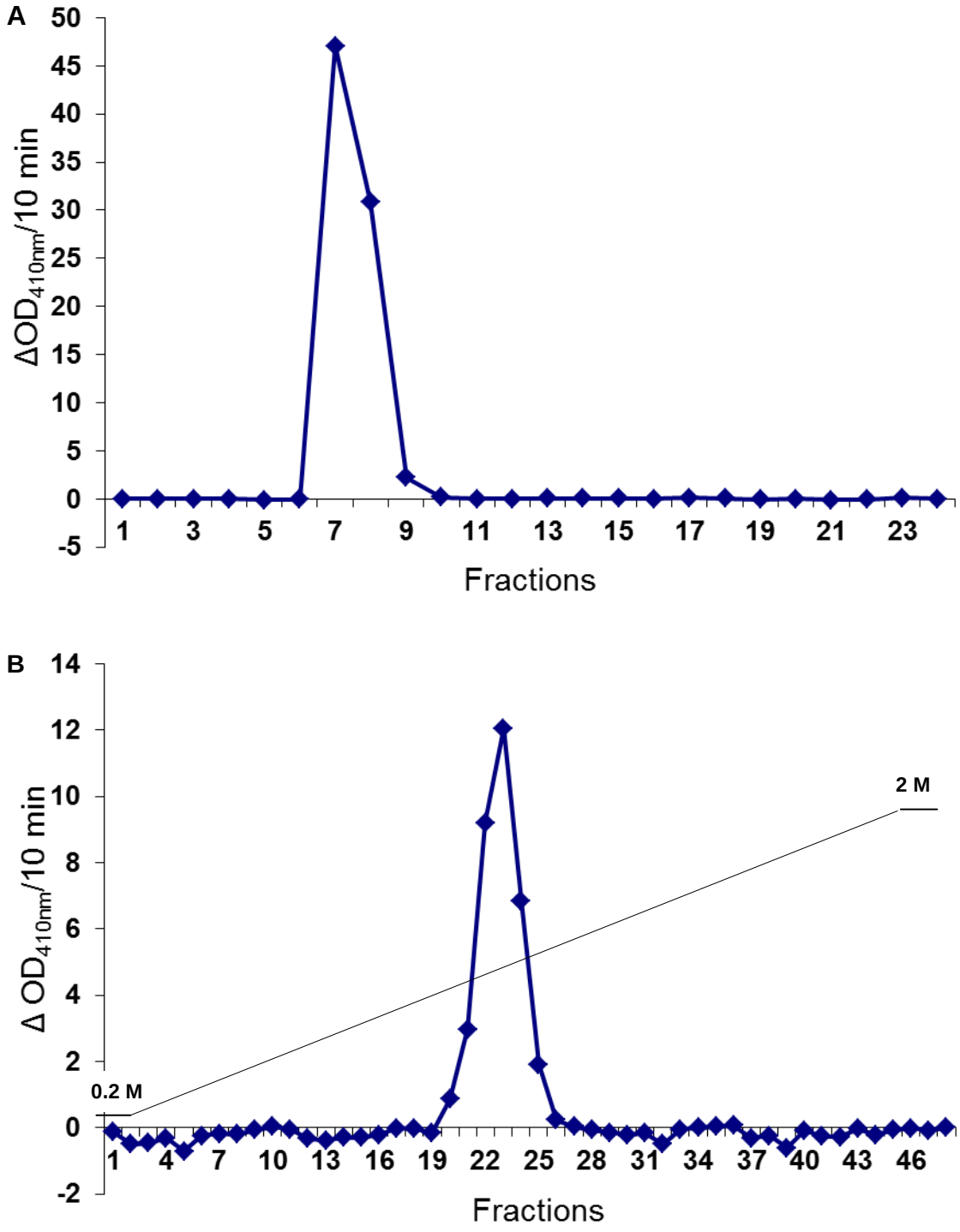

Figure 3.1 BApNA cleaving activity in fractions of supernatant from a yeast expression system for tryptase that had been (A) applied to a butyl Sepharose hydrophobic interaction column, (B) a heparin agarose affinity column, eluting with a salt gradient (0.2–2.0 M).

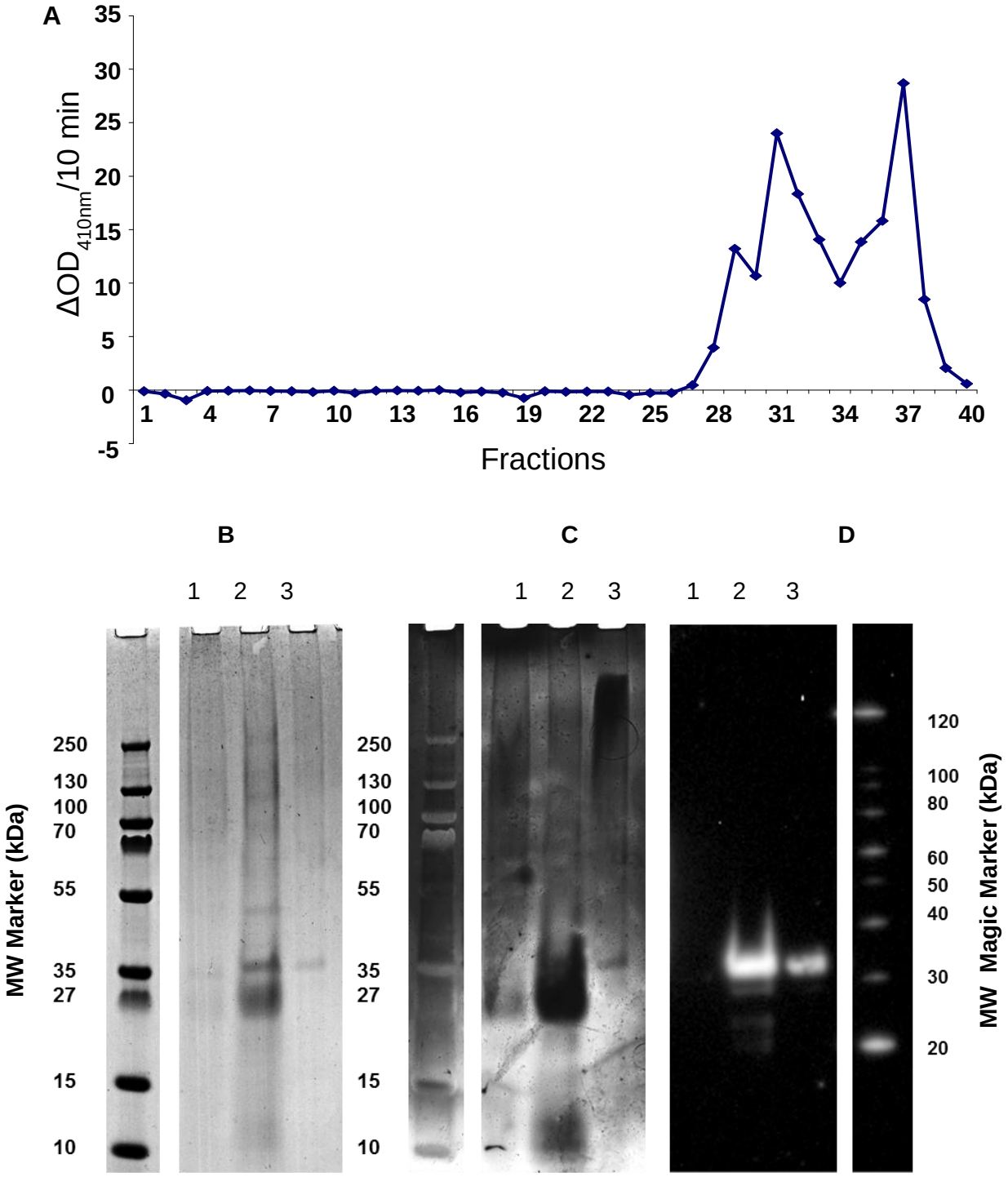

Figure 3.2 (A) BApNA cleaving activity in fractions of supernatant from a yeast expression system for tryptase that had been applied to a BioSep-Sec-S-3000 size exclusion column in HPLC. (B) SDS-PAGE stained with Coomassie blue dye or (C) silver stain, and (D) western blot of tryptase. Lane 1, total yeast cell supernatant; lane 2, tryptase rich fractions eluted from a butyl agarose column; lane 3, eluted from a heparin-agarose column. Molecular weight (MW) markers are indicated.

Table 3.1 Total cell numbers in peritoneal lavage fluid obtained from C57BL/6 mice following injection of tryptase (0.5 µg/mouse) at 6, 12 and 24 h.

Time	Mice Strain	Saline	Tryptase
6 h	PAR 2 $^{+/+}$	1.9 (0.82–3.03)	1.56 (0.96–1.76)
	PAR 2 $^{-/-}$	4 (1.99–4.41)	3.94 (2.35–7.11)
12 h	PAR 2 $^{+/+}$	3.82 (2.97–4.87)	2.25 (1.43–3.08)*
	PAR 2 $^{-/-}$	5.22 (3.93–7)	4.55 (3.15–8.61)
24 h	PAR 2 $^{+/+}$	3.6 (3.06–4.59)	4.11 (2.44–7.32)
	PAR 2 $^{-/-}$	4.43 (3.03–5.65)	3.95 (3.21–5.52)

Median values (lower/upper quartile) x 10^6. * $P<0.05$, compared with the response in the saline injected group with 6–10 mice per group (Mann–Whitney U test follows Kruskal–Wallis test for each time point).Total numbers of live nucleated cells were determined using an improved Neubauer haemocytometer with 0.4 % trypan blue.

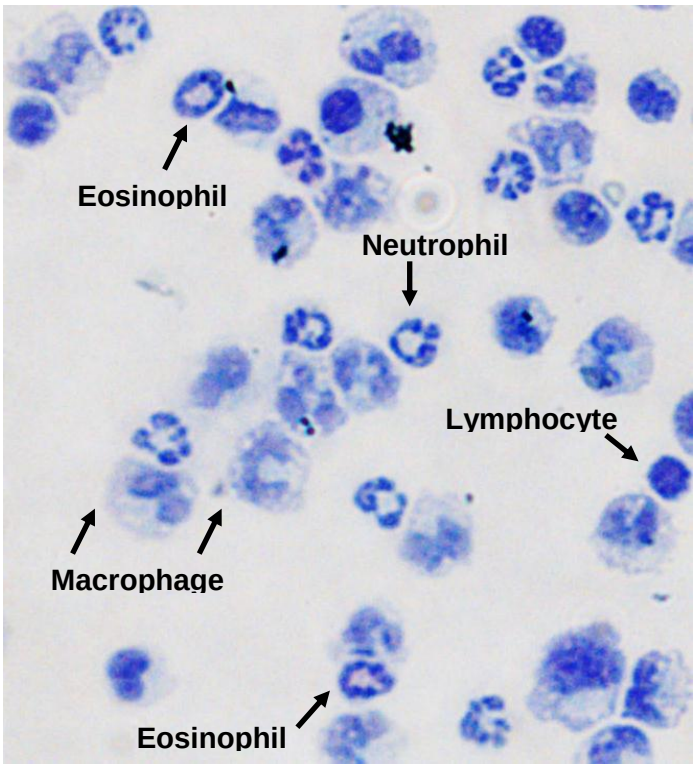

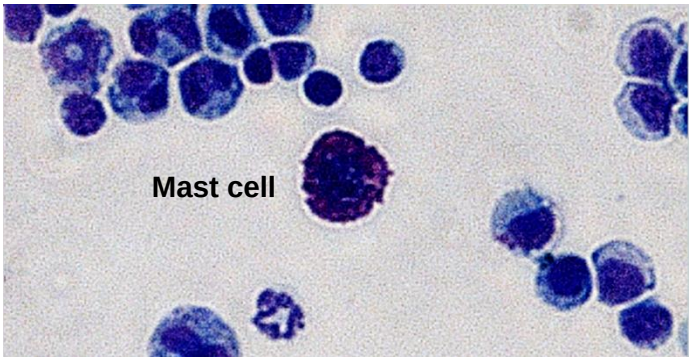

Figure 3.3 Cytocentrifuge preparation of cells recovered by peritoneal lavage from C57BL/6 mice 24 h following injection of tryptase (0.5 µg/mouse). Examples of specific cell types are indicated. Cells were stained with eosin/methylene blue stain (Rapid Romanowsky).

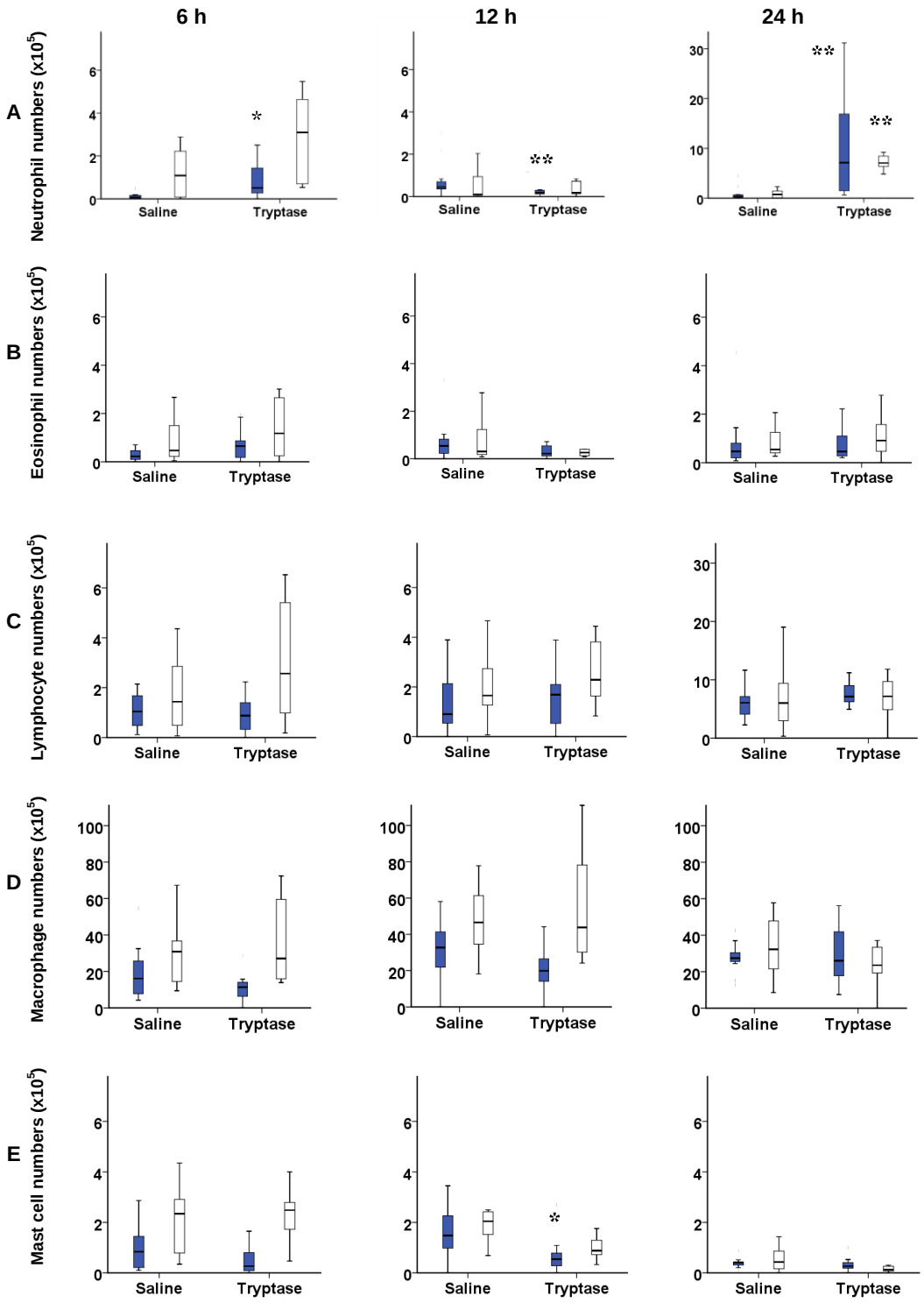

Figure 3.4 Numbers of (A) neutrophils, (B) eosinophils, (C) lymphocytes, (D) macrophages and (E) mast cells in peritoneal lavage fluid from C57BL/6 mice 6, 12 and 24 h following intraperitoneal injection of tryptase (0.5 µg/mouse) in PAR-2 knockout (PAR-$2^{-/-}$) (open boxes) and wild-type (PAR-$2^{+/+}$) mice (blue boxes). Data are displayed as box and whisker plots with 6-10 mice per group, showing the median values, the inter-quartile range and range. * $P<0.05$, ** $P<0.005$ compared to saline injected group (Mann-Whitney U test follows Kruskal-Wallis test for each time point).

As the pattern of cell accumulation in mice of the C57BL/6 strain differed from that reported previously following injection of human lung tryptase in BALB/c mice [11], a comparison was made between the responses of C57BL/6 and BALB/c mice injected with recombinant tryptase under the same conditions. Injection of tryptase in the peritoneum of BALB/c mice was associated with increases in numbers of neutrophils, eosinophils, lymphocytes, macrophages and mast cells as well as in the total number of cells, compared with those in the saline-injected group (Figure 3.5). This contrasted with the findings in the C57BL/6 mice, which exhibited neutrophilia alone. There was little alteration in the extent of tryptase-induced neutrophilia between the two mouse strains. Total cell numbers as well as numbers of macrophages, mast cells and eosinophils were all higher in the BALB/c mice when compared with those in the C57BL/6 mice. On the other hand, the degree of tryptase-induced accumulation of lymphocytes was greater in the C57BL/6 than BALB/c mice.

Heat-inactivation of tryptase was associated with a significant reduction in numbers of neutrophils compared with the saline- and tryptase-injected groups (Figure 3.6 and Figure 3.7). Similar results were found with the selective tryptase inhibitor SAR160719A-5 and to limited extent with leupeptin (data not shown).The peptide agonist of PAR-2 SLIGRL-NH_2 failed to replicate the actions of tryptase, and the control peptide employed actually stimulated a small increase in certain numbers of cell types (Table 3.2). Injection of PAR-2 RP was associated with a small decrease in numbers of lymphocytes and mast cells compared with those in the saline-injected mice, and an apparent increase in eosinophil numbers.

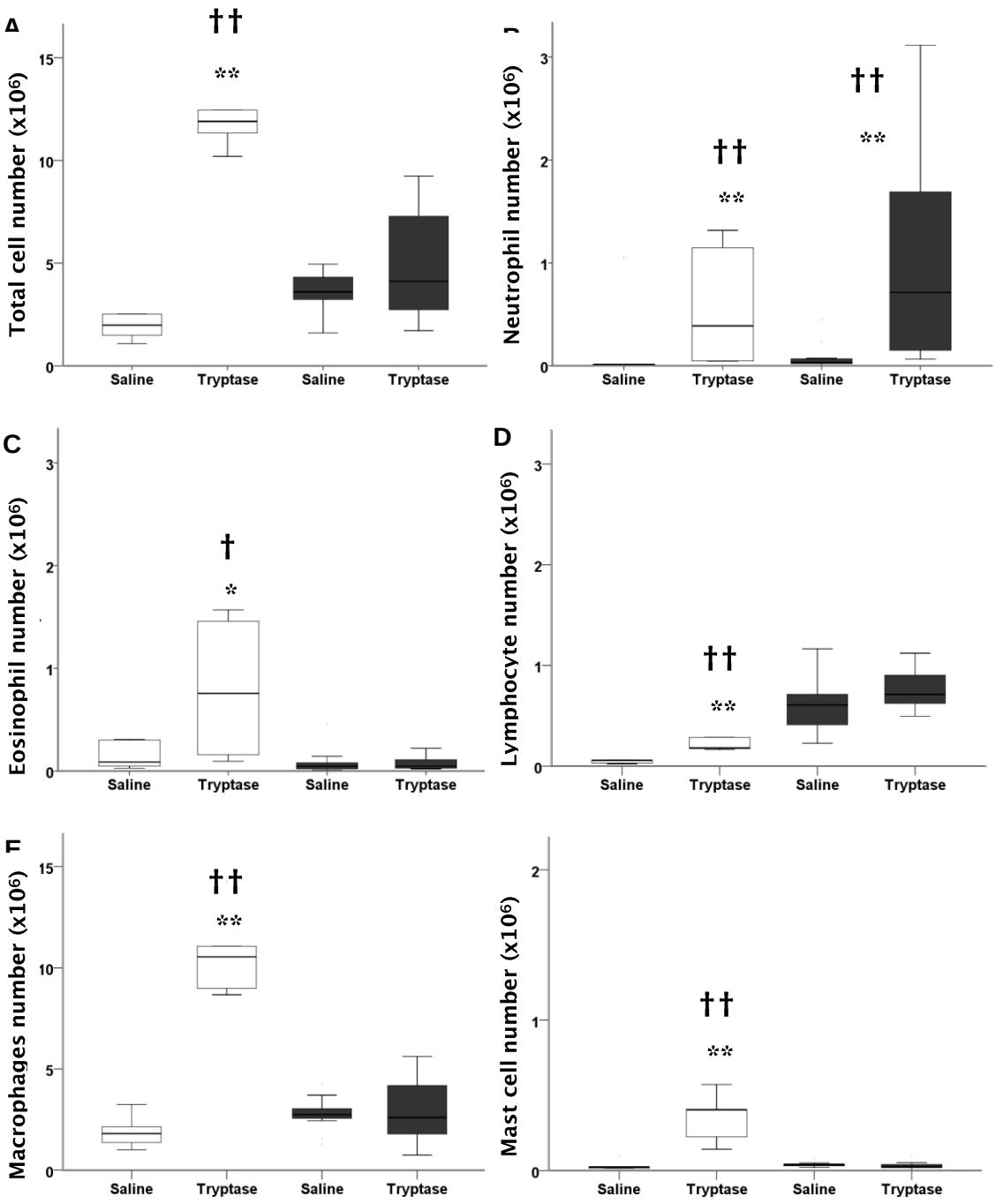

Figure 3.5 Total numbers of (A) nucleated cells, (B) neutrophils, (C) eosinophils, (D) macrophages, (E) lymphocytes and (F) mast cells recovered from the peritoneum of C57BL/6 (filled bars) and BALB/c (open bars) mice 24 h following injection of 0.5 µg/mouse tryptase. N=5-12 mice per group. * P<0.05, ** P<0.005 compared with response in saline injected mice and † p<0.05, †† p<0.005 compared with response in BALB/c mice (Mann-Whitney U test follows Kruskal-Wallis test).

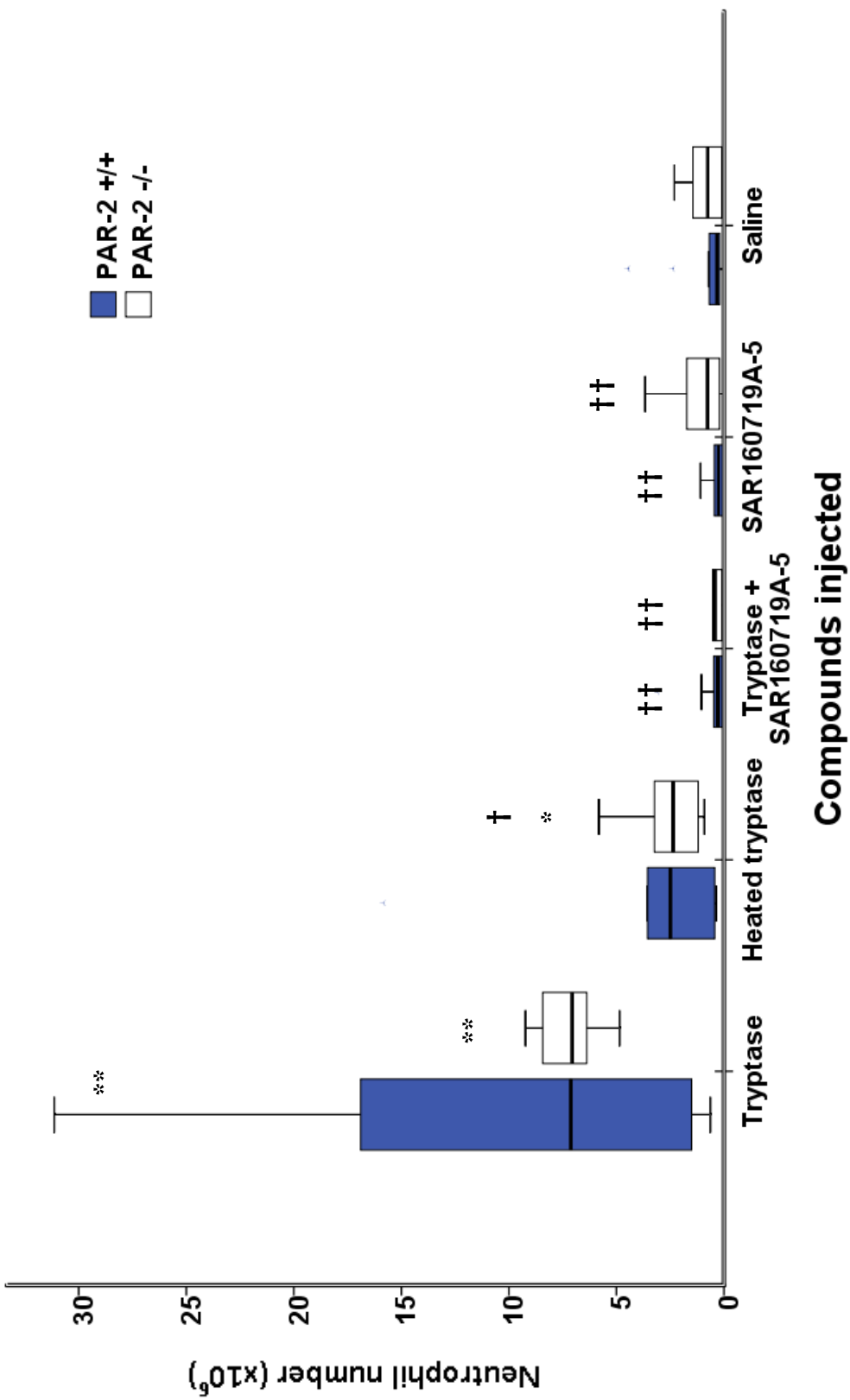

Figure 3.6 Neutrophil numbers in peritoneal lavage fluid from PAR–2 knockout (PAR–$2^{-/-}$) and wild–type (PAR–$2^{+/+}$) C57BL/6 mice 24 h following injection of tryptase (0.5 µg/mouse), heated tryptase, tryptase pre–incubated with the selective inhibitor SAR160719A–5, the inhibitor alone and the saline vehicle. * P<0.05 ** P<0.005 compared to saline–injected group, †P<0.05 ††P<0.005 compared to tryptase–injected group (Mann–Whitney U test follows Kruskal–Wallis test).

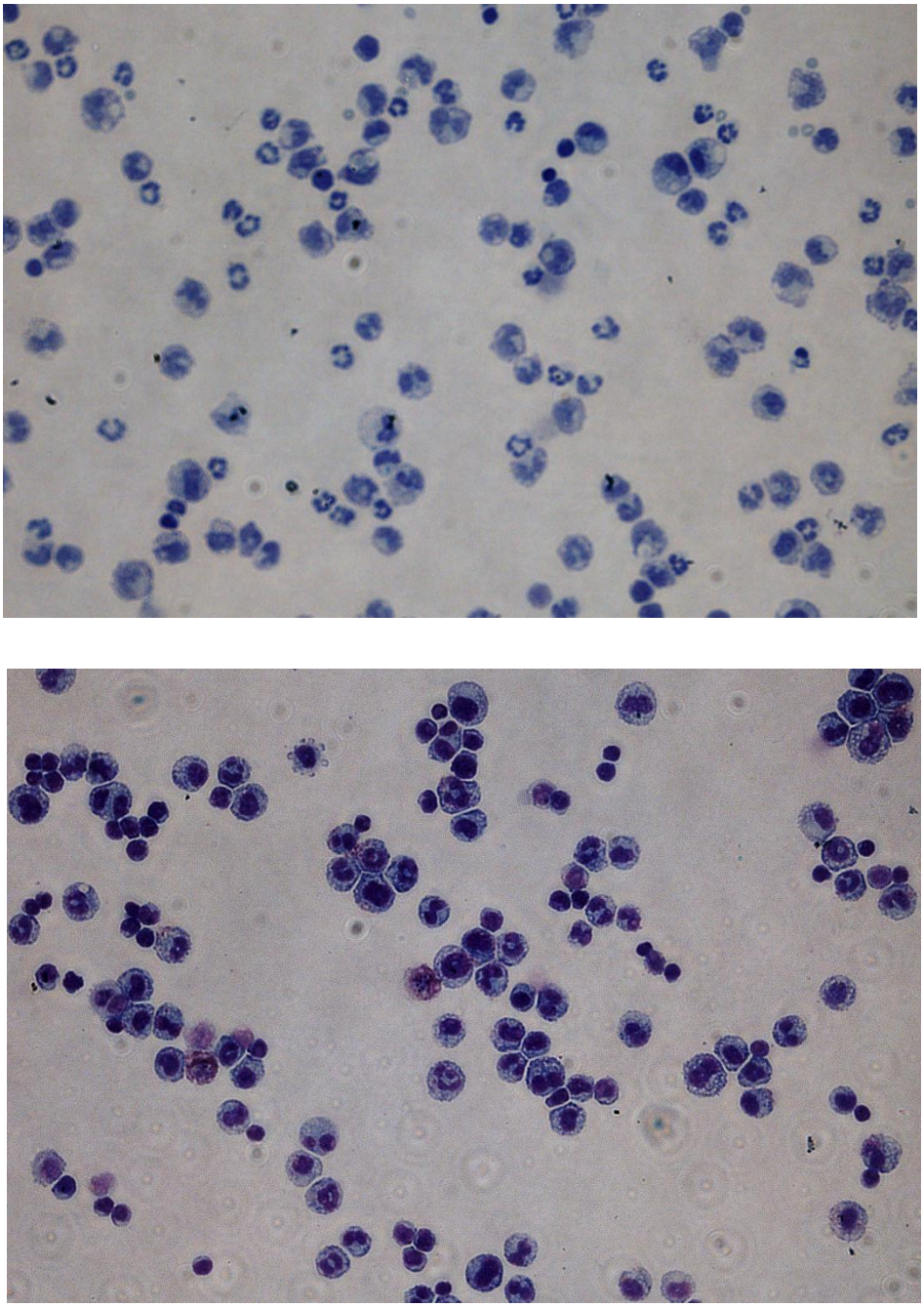

Figure 3.7 Cells in peritoneal lavage fluid collected from mice 24 h following injected with (A) tryptase (0.5 µg/mouse) or (B) saline. Neutrophilia is a feature in the tryptase-injected mice, while macrophages predominant in the saline control-injected mice. Cells were stained with eosin/methylene blue stain (Rapid Romanowsky).

Table 3.2 Effects on total and differential cell counts in peritoneal lavage fluid from mice 24 h following injection of of the PAR-2 agonist SLIGRL-NH_2 (0.5 µg/mouse), the scrambled peptide LSIGRL-NH_2 (0.5 µg/mouse), or the PAR-2 (0.5 or 50 µg/mouse) released peptide (PAR-2 RP) in wild type and PAR-2 deficient C57BL/6 mice.

Compounds injected	Mouse strain	Total cells	Neutrophils	Eosinophils	Lymphocytes	Macrophages	Mast cells
Saline	PAR 2 $^{+/+}$	3.6	0.03	0.05	0.61	2.74	0.04
	PAR 2 $^{-/-}$	4.43	0.08	0.05	0.6	3.23	0.04
Tryptase	PAR 2 $^{+/+}$	4.11	0.71**	0.05	0.71	2.60	0.03
	PAR 2 $^{-/-}$	3.95	0.71**	0.09	0.72	2.36	0.01
SLIGRL-NH_2	PAR 2 $^{+/+}$	4.02	0.05††	0.13* ††	0.35†	2.98	0.04
	PAR 2 $^{-/-}$	4.13	0.08††	0.1	0.55	2.53	0.05†
LSIGRL-NH_2	PAR 2 $^{+/+}$	3.57	0.25**	0.28** ††	0.24** ††	3.02	0.02*
	PAR 2 $^{-/-}$	6.31** †	0.06††	0.05	0.38†	5.74** ††	0.16**†
PAR-2 RP (0.5 µg/mouse)	PAR 2 $^{+/+}$	2.56	0.05††	0.18**††	0.08** ††	2.15	0.01**
PAR-2 RP (50 µg/mouse)	PAR 2 $^{+/+}$	2.79	0.04††	0.09	0.2** ††	2.45	0.01** †

Median values are shown (x10^6) for 10-12 mice each group. * P<0.05, ** P<0.005, compared with response in the saline-injected group and †P<0.05, ††P<0.005, compared with the response in the tryptase-injected group (Mann-Whitney U test follows Kruskal-Wallis test for each cell type).

3.3.2 Gelatin Zymography

Inflammatory processes involve activation of pro-MMP to MMP which contributes to the turnover and degradation of the extracellular matrix proteins, as well as processing a number of bioactive molecules. Tryptase has been reported to activate pro-MMP3 [7] and the active form (MMP3) has found to degrade cross-linked fibrin [8]. Neutrophil accumulation at site of inflammation is controlled by many mediators including fibrin degradation products [9] in addition to complement fragments (C5a, C3a), lipid mediators (LTB_4, PAF) and chemokines [10]. For these reasons the presence of MMPs were investigated to give an insights into other aspects of inflammatory reaction in response to tryptase.

In developing gelatin zymography methods for the analysis of alterations in MMP activity in mouse peritoneal lavage fluid, the human fibrosarcoma cell line HT1080 was employed as a positive control. HT1080 cells treated with medium containing foetal calf serum (FCS) elicited two bands corresponding to the active form of MMP9 at about 100 kDa, and the MMP9 pro-form at 105 kDa (Figure 3.8). In addition there were weak bands corresponding to the MMP2 pro-form at about 65kDa. As FCS alone (in the absence of cell supernatant) also appeared to contain pro-MMP9 and pro-MMP2, the cells were cultured in serum-free conditions. In the absence of FCS, bands corresponding to mature active MMP9 (but not the pro-form) and the pro- and active forms of MMP2 were observed. Occasionally bands at a lower molecular weight were also observed (Figure 3.9) which may reflect the presence of degradation products.

In the saline-injected mice, bands were observed for MMP2 but not for MMP9. Tryptase injection, on the other hand, was associated with the presence of bands for both MMP2 and MMP9 (particularly in PAR-2 knockout mice). When the intensity of the bands was expressed digitally, a progressive increase in levels was observed 6 h to 24 h after injection of tryptase for both MMP9 (Figure 3.10) and MMP2 (Figure 3.11). Injection of saline was associated with the absence of MMP9 activity at those time points and with low levels of MMP2. There was little difference between the wild-type and the PAR-2 knockout mice in MMP9 levels, but MMP2 activity appeared higher in PAR-2 knockout mice.

Heat treatment of the tryptase abolished the tryptase-induced increase in MMP9 and MMP2 levels. Incubation of tryptase with the selective inhibitor

SAR160719A-5 also abolished the actions of tryptase on MMP9 and MMP2 levels. The PAR-2 agonist SLIGRL-NH_2 and the non-PAR-2 activating control peptide had little effect in this model. Similarly PAR-2 RP did not alter activity of MMP2 and MMP9 in peritoneal lavage fluid (Figure 3.12).

The pattern of findings with MMP9 and MMP2 activity in PAR-2 knockout mice (Figure 3.12 A, B) was similar to that in the wild-type mice. MMP2 activity was greater in the PAR-2 knockout mice than in the wild type, but this was not seen with MMP9.

On the other hand there was a close correlation between levels of MMP9 and MMP2 for both the wild type mice (r_s= 0.882, n = 33 $p<0.005$) and for the knockout mice (r_s= 0.975, n = 30 $p<0.005$) either separately, or when both groups of animals were analysed together (Figure 3.13). The activity of MMP9 was correlated with the number of neutrophils recovered from the peritoneum of wild-type mice (r_s= 0.452, n = 33, $p<0.005$) and for the knockout mice (r_s= 0.360, n = 30, $p<0.005$) either separately, or when both groups of animals were considered together (Figure 3.14). Similarly the activity of MMP2 was correlated with the number of neutrophils recovered from the peritoneum of wild type mice (r_s= 0.335, n = 33, $p<0.005$) and the knockout mice (r_s= 0.328, n = 30, $p<0.005$) either separately, or when both groups of animals were considered together (Figure 3.15). Associations were not observed between MMP2 or MMP9 levels and the numbers of any of the other cell types enumerated.

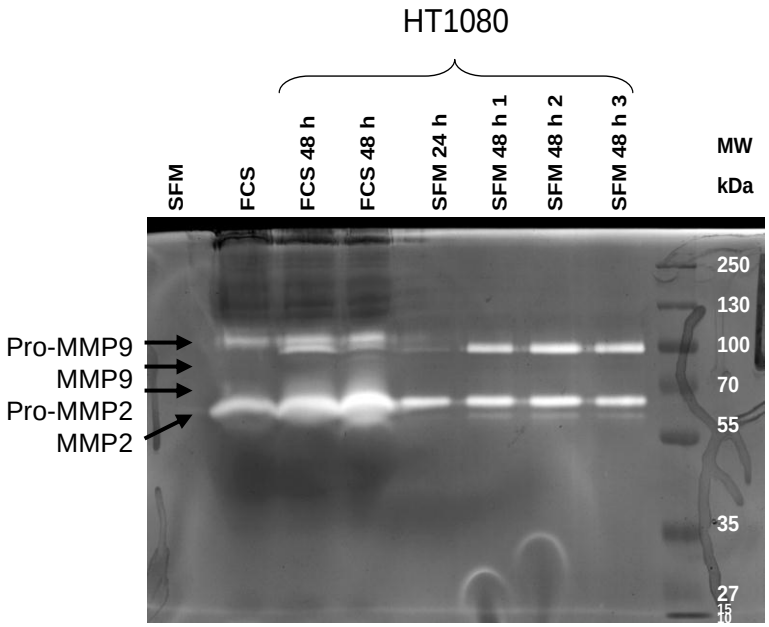

Figure 3.8 Gelatin zymography indicating clear bands for MMP2 and 9 (pro and mature forms) from supernatants of HT1080 cells incubated with foetal calf serum (FCS) or serum free medium (SFM) for 24 or 48 h. FCS and SFM were added alone as controls. Molecular weight (MW) markers are indicated.

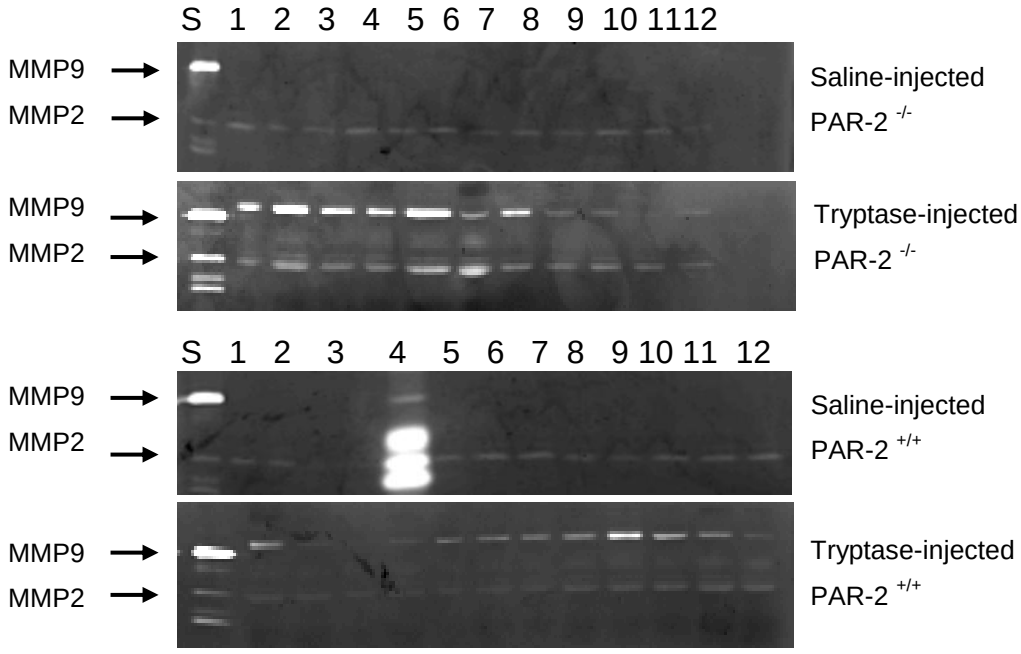

Figure 3.9 Gelatin zymography showing the presence of MMP2 and 9 in a standard preparation of HT1080 supernatant (S) and supernatants from peritoneal lavage fluid from mice 24 h after injection of saline or tryptase (mice 1 to 12).

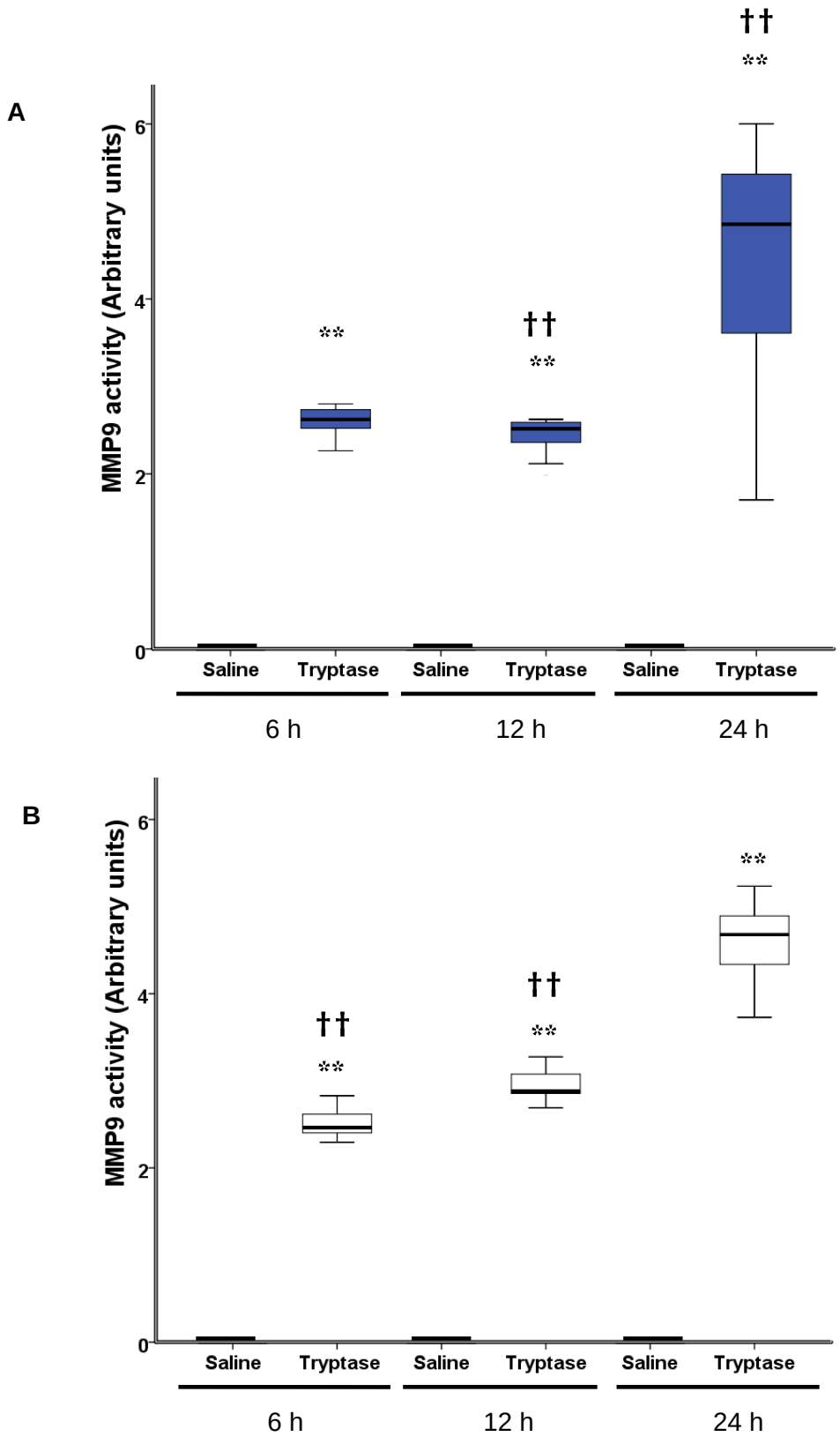

Figure 3.10 MMP9 activity in peritoneal lavage fluid from (A) wild type and (B) PAR-2 knockout mice 6, 12 and 24 h following intraperitoneal injection of tryptase (0.5µg/mouse). † P<0.05 †† P<0.005 (compared with response to tryptase-injected mice at 24 h), * P<0.05 ** P<0.005 (compared with response in the saline-injected mice at 24 h). Mann-Whitney U test follows Kruskal-Wallis test.

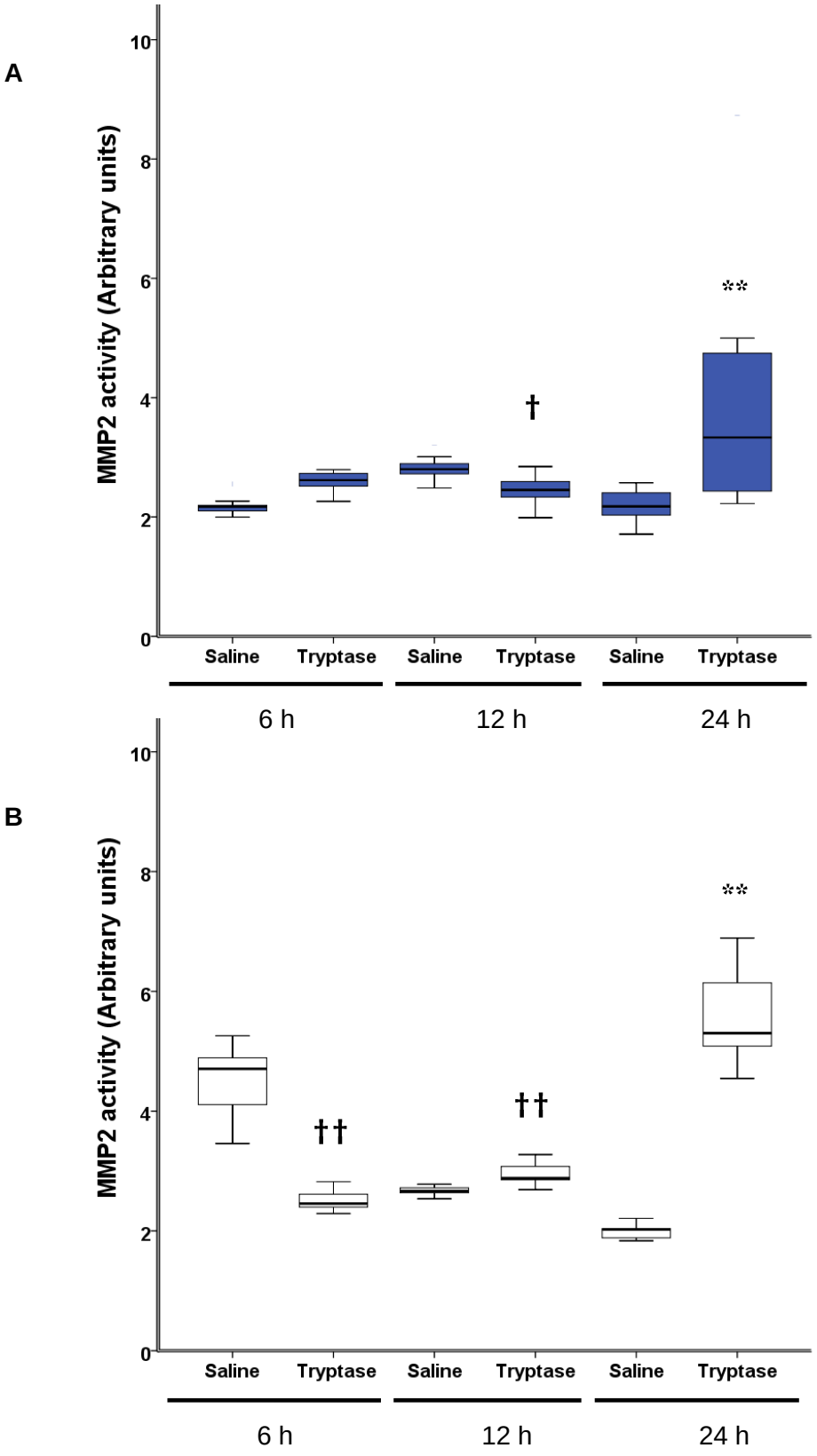

Figure 3.11 MMP2 activity in peritoneal lavage fluid from (A) wild type and (B) PAR-2 knockout mice 6, 12 and 24 h following intraperitoneal injection of tryptase (0.5µg/mouse). † P<0.05 †† P<0.005 (compared with response to tryptase-injected mice at 24 h), * P<0.05 ** P<0.005 (compared with response in the saline-injected mice at 24 h). Mann-Whitney U test follows Kruskal-Wallis test.

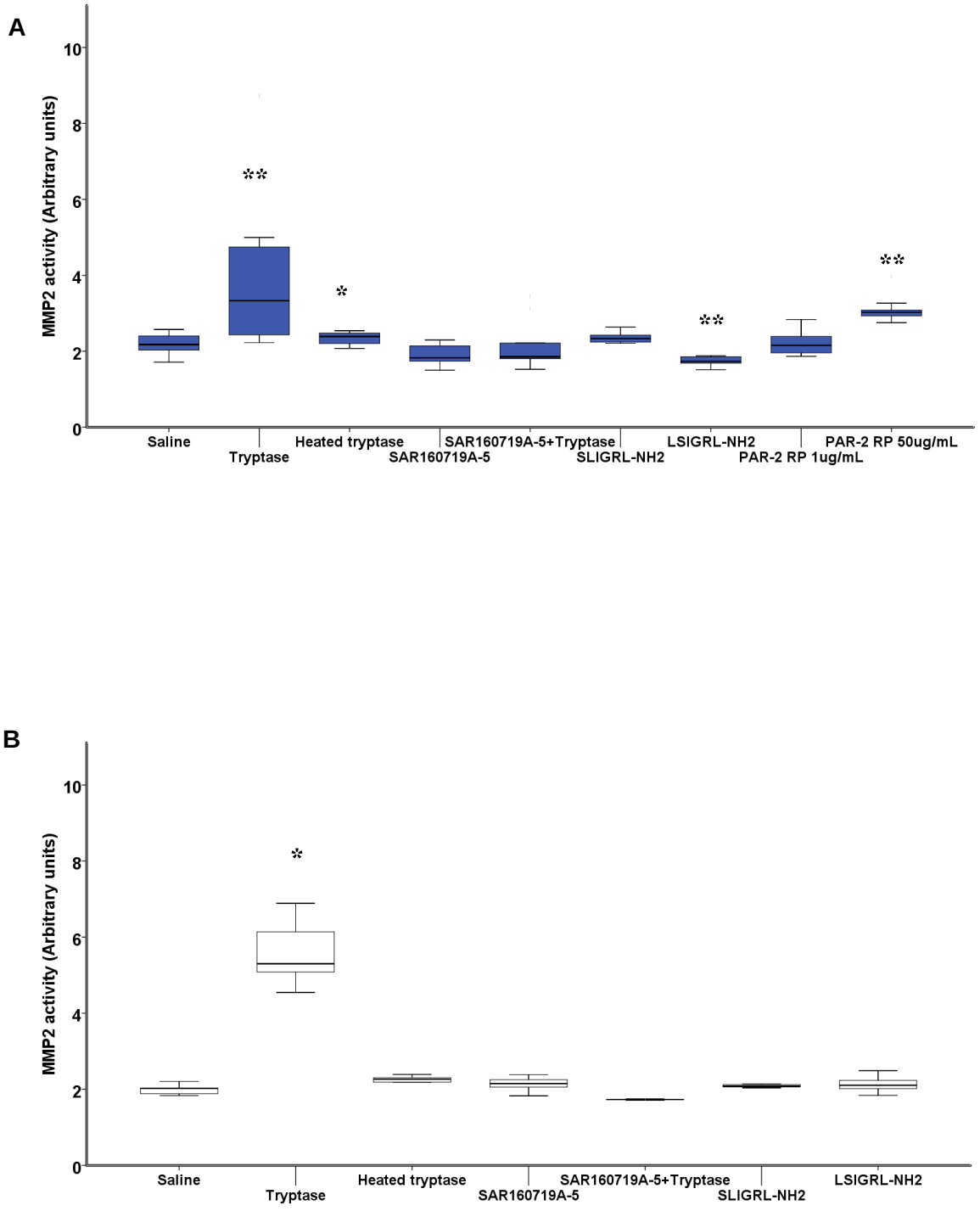

Figure 3.12 MMP2 levels in peritoneal lavage fluid from (A) wild type and (B) PAR-2 knockout mice 24 h following intraperitoneal injection of various compounds. * P<0.05 ** P<0.005 (compared with response in the saline-injected mice at 24 h).

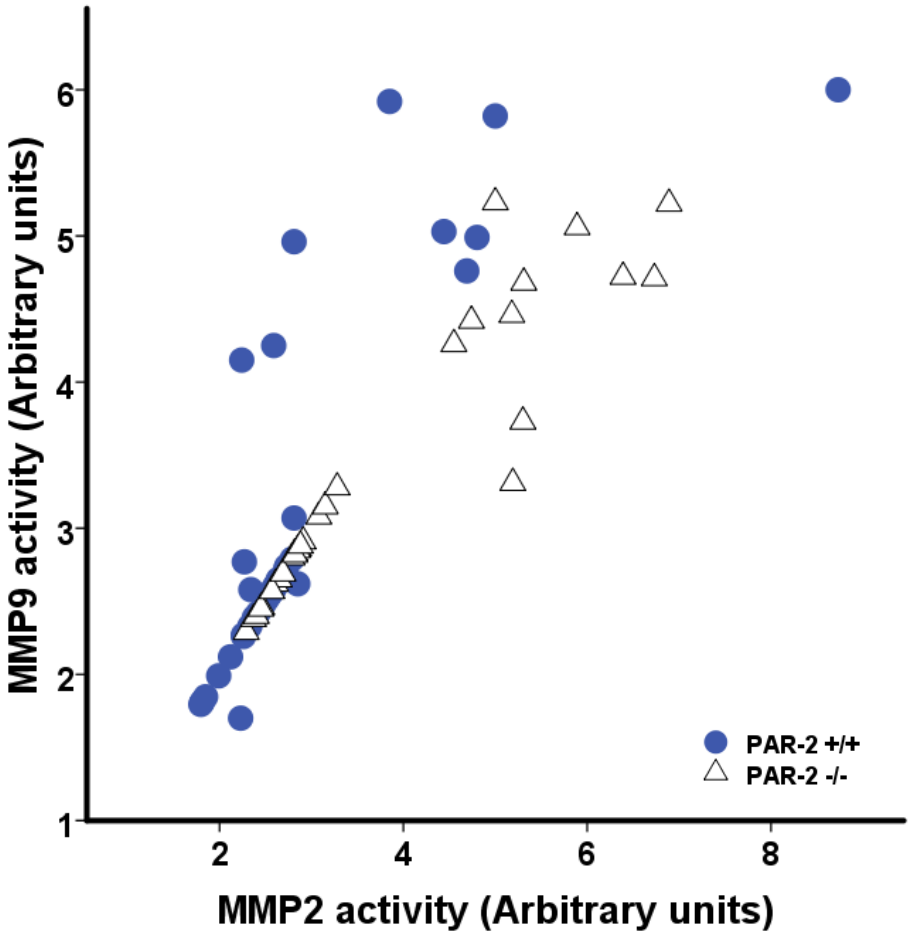

Figure 3.13 Association between MMP2 and MMP9 levels in peritoneal lavage fluid from C57BL/6 mice 6, 12 and 24 h following intraperitoneal injection of tryptase (0.5 µg/mouse). r_s = 0.902, n = 63, P<0.005.

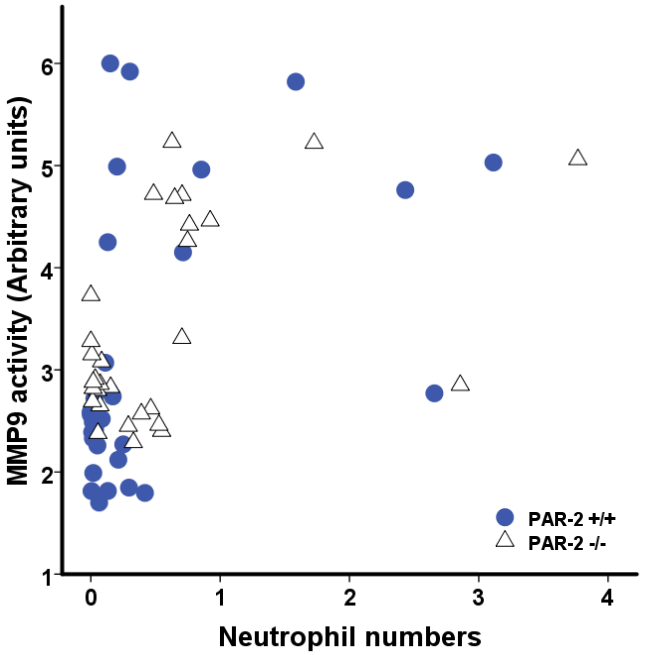

Figure 3.14 Association between MMP9 levels and neutrophil accumulation in peritoneal lavage fluid from C57BL/6 mice 6, 12 and 24 h following intraperitoneal injection of tryptase (0.5 µg/mouse). r_s = 0.440, n = 63, P<0.005.

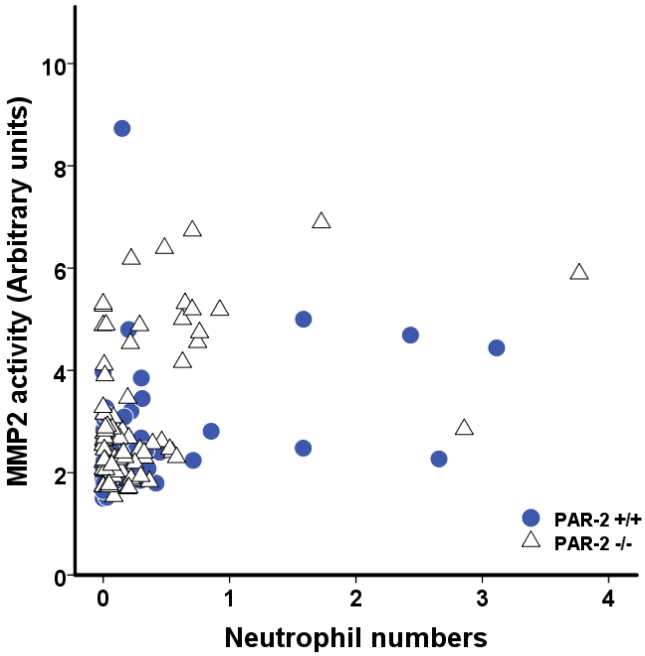

Figure 3.15 Association between MMP2 levels and neutrophil accumulation in peritoneal lavage fluid from C57BL/6 mice 6, 12 and 24 h following intraperitoneal injection of tryptase (0.5 µg/mouse). r_s = 0.363, n = 63, P<0.005.

3.3.3 Collection of neutrophil-rich and neutrophil-depleted cell populations from mouse peritoneal lavage fluid

Injection of tryptase or casein into the peritoneum of mice resulted in the accumulation of neutrophils. Sorting of peritoneal lavage fluid cells by positive selection with magnetic beads allowed effective separation of cells into neutrophil-rich (containing 88 % neutrophils) and neutrophil-depleted cell populations. Gelatin zymography revealed the presence of MMP9 but not MMP2 in supernatants of peritoneal cells *in vitro* for up to 24 h. There was relatively little MMP9 in the supernatant of cells from naïve mice (data not shown). The neutrophil-rich cell population of tryptase-injected mice produced substantially more MMP9 than the neutrophil-depleted cell population from these mice. Treatment of either neutrophil-rich or neutrophil-depleted cell populations with tryptase *in vitro* was not associated with alterations in levels of MMP9 in cell culture supernatants (Figure 3.16). Similar data was obtained with cells recovered from the peritoneum of casein-injected mice. The release of MMP9 appeared to be constitutive and was unaffected by addition of tryptase. Measurement of MMP9 levels by densitometry of gels indicated that MMP9 release was predominantly in cells of the neutrophil-rich population at all time points examined (Figure 3.17).

3.3.4 Albumin assay

A hallmark of inflammatory responses is microvascular leakage and oedema. Increased vascular permeability induced by inflammatory mediators facilitates movement of large protein molecules (including albumin, globulin and fibrinogen) [11]. The measurement of albumin levels in the inflammatory filtrate was taken as a measure of vascular permeability. Measurement of albumin in the peritoneal lavage fluid of mice showed a significant increase in albumin concentration 24 h after injection of tryptase (compared with injection of saline; Figure 3.18). Heating of tryptase abolished the tryptase-induced effect on albumin concentration while PAR-2 RP failed to reproduce the effects of tryptase. No differences were observed in albumin levels in lavage fluid from wild-type and PAR-2 knockout mice. At 6 h or 12 h following injection of tryptase, the albumin levels in the peritoneal lavage fluid were not significantly different from those in the saline-injected mice (data not shown).

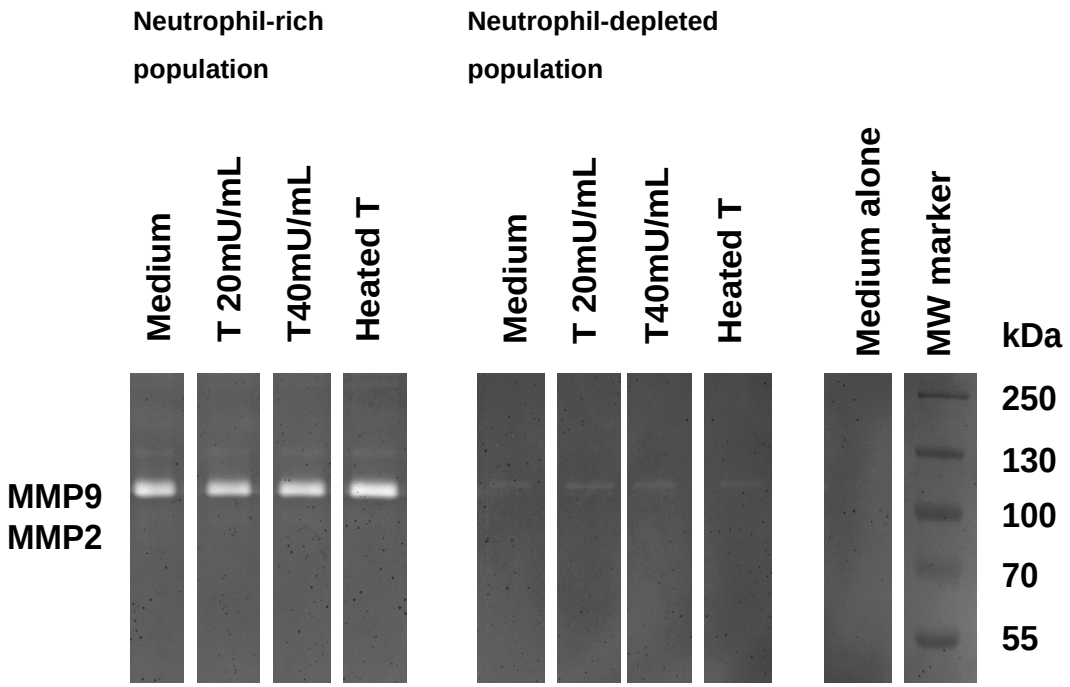

Figure 3.16 Gelatin zymography for neutrophil-rich and neutrophil-depleted peritoneal lavage cell populations (or medium alone) isolated from mice 24 h following injection of 0.5 µg/mouse of recombinant tryptase. Culture supernatants were collected at 1 h following addition of tryptase (T) at 20 or 40 mU/ml, heated tryptase 40 mU/ml or medium alone. The positions of molecular weight markers are shown.

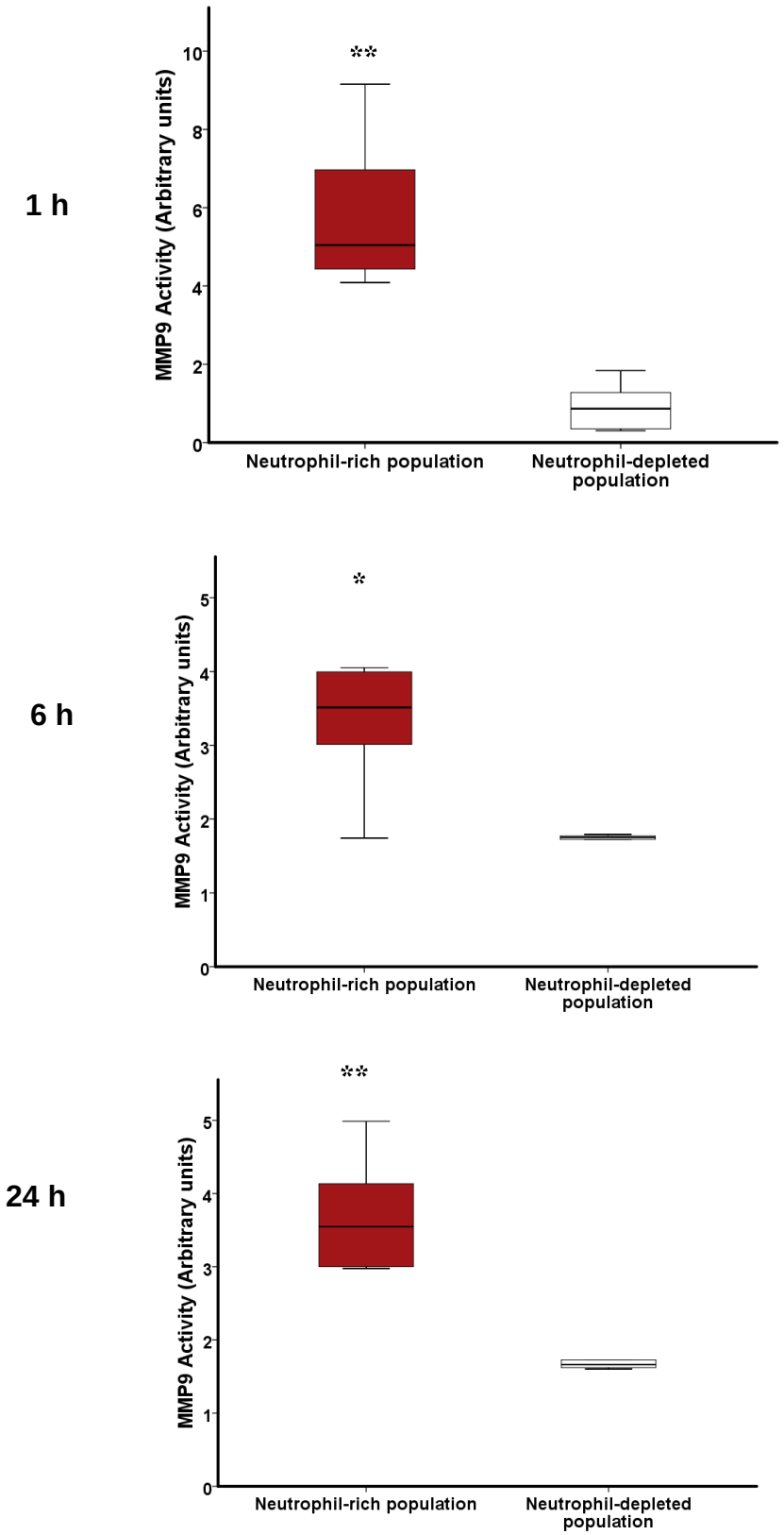

Figure 3.17 MMP9 activity in culture supernatants of neutrophil-rich and neutrophil-depleted cell populations (n = 6) maintained in culture for 1, 6 or 24 h. Median, inter-quartile range and range are indicated.* P<0.05, ** P<0.005 compared with the neutrophil-depleted cell population (Mann-Whitney U test).

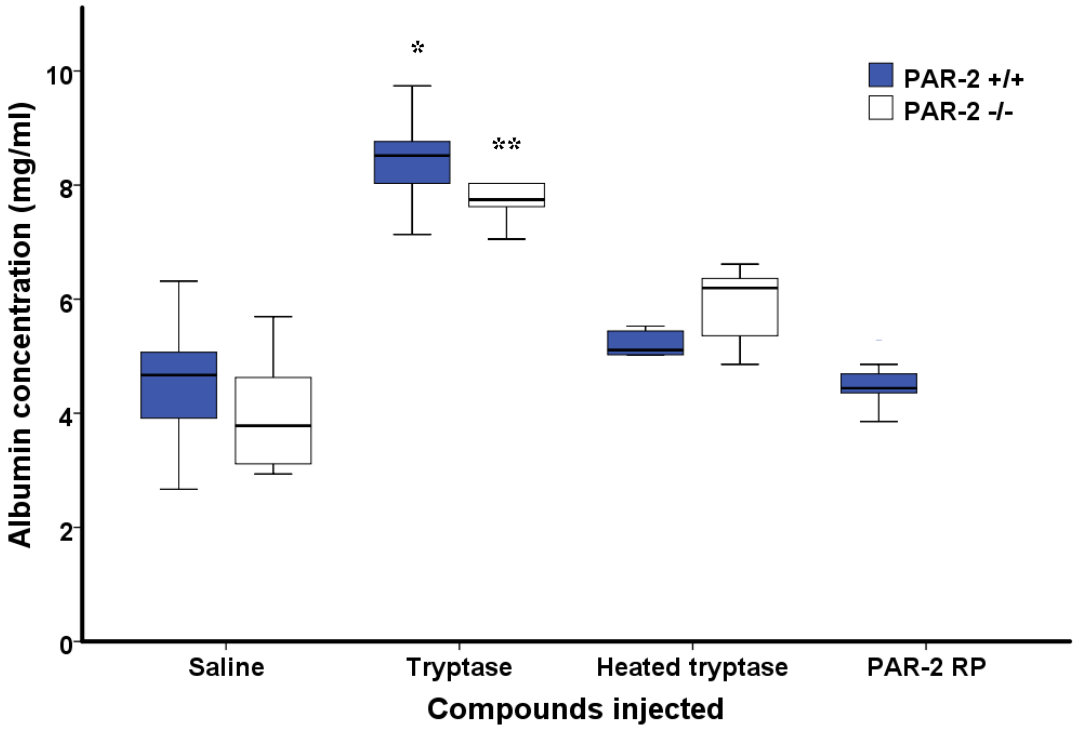

Figure 3.18 Albumin levels in peritoneal lavage fluid from C57BL/6 mice 24 h following injection with tryptase (0.5 µg/mouse). Median, inter-quartile range and range are indicated.* P<0.05, ** P<0.005 compared to saline-injected group (Mann-Whitney U test follows Kruskal-Wallis test).

3.3.5 Total protein assay

The total protein concentration in peritoneal lavage fluid as detected by BCA binding did not differ between mice injected with tryptase, PAR-2 agonist or PAR-2 RP at 24 h (Figure 3.19). Similarly no differences in protein concentration were detected at 6 h or 12 h (data not shown). There was no association between concentrations of albumin and total protein levels in mouse peritoneal lavage fluid (Spearman coefficient of rank correlation).

3.3.6 Histamine in peritoneal lavage fluid

In order to investigate peritoneal mast cell activation and degranulation in mice model, we measured the levels of histamine in the peritoneal lavage fluid. At 24 h following injection of mice with 0.5 µg tryptase, the histamine concentration in supernatants of peritoneal lavage fluid was significantly reduced, an effect not seen with heated tryptase (Figure 3.20). There was a trend for mast cell numbers to be reduced at the 24 h following injection of tryptase, but this did not reach statistical significance (Figure 3.21).

3.3.7 Measurement of elastase activity

Neutrophil elastase is serine protease secreted from neutrophils as well as macrophages and playing an important rolein host dfense against bacteria and in connective tisssue remodeling [232]. Ethanolic extraction allowed successful solubilisation of elastin, and on 12% SDS-PAGE the effective solubilisation was demonstrated (Figure 3.22). With elastase as a positive control in elastin zymography, there were bands at 28 and 22 kDa (Figure 3.23). However, supernatants from peritoneal lavage fluid from mice of both the saline and tryptase-treated groups failed to show any bands. Similarly, no elastase activity was detected on elastin zymography in supernatants from cultured neutrophil-rich or neutrophil-depleted cell populations.

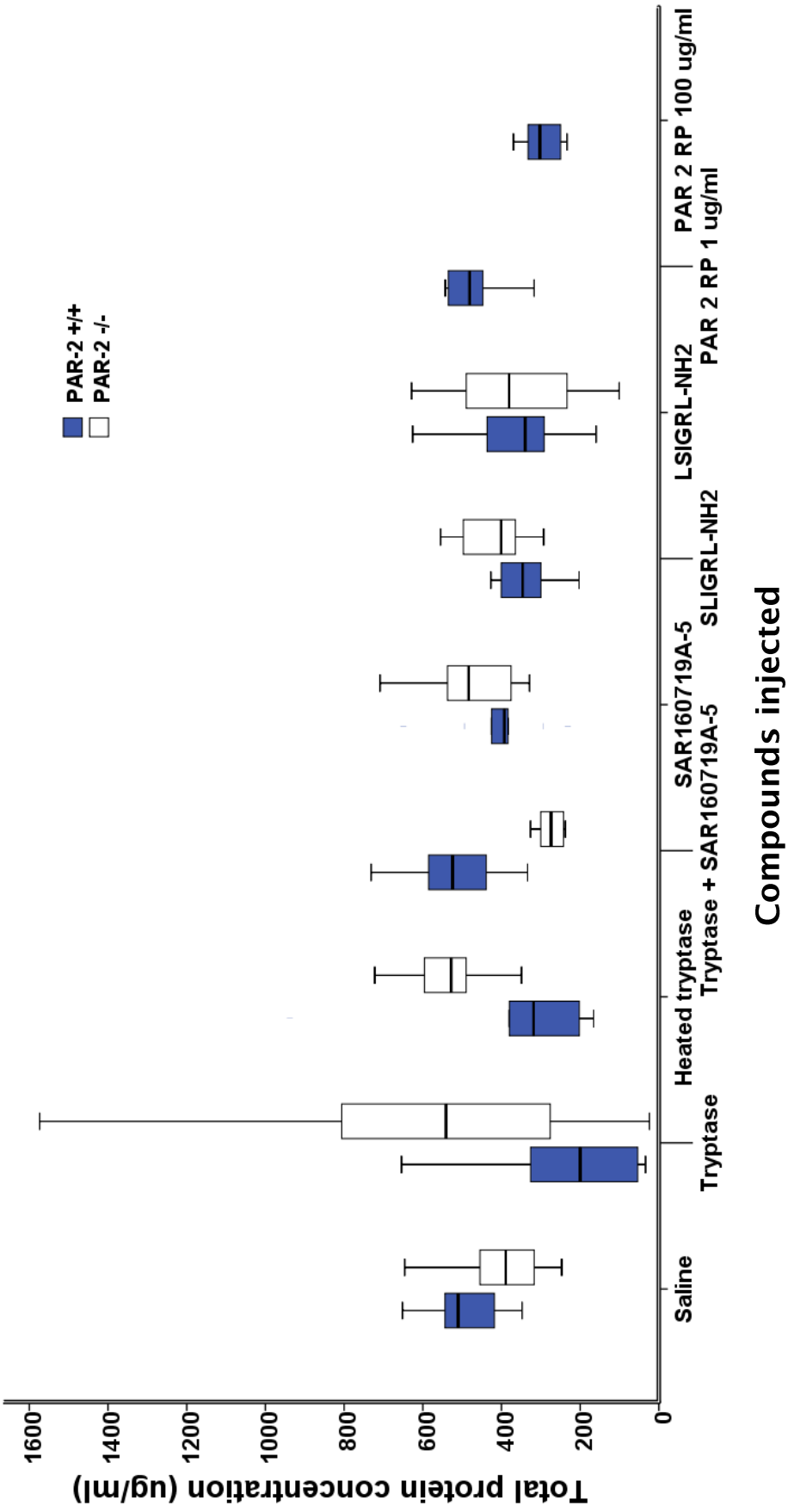

Figure 3.19 Total protein levels in peritoneal lavage fluid from C57BL/6 mice 24 h following injection with tryptase (0.5 µg/mouse) and other compounds. (Mann–Whitney U test follows Kruskal–Wallis test).

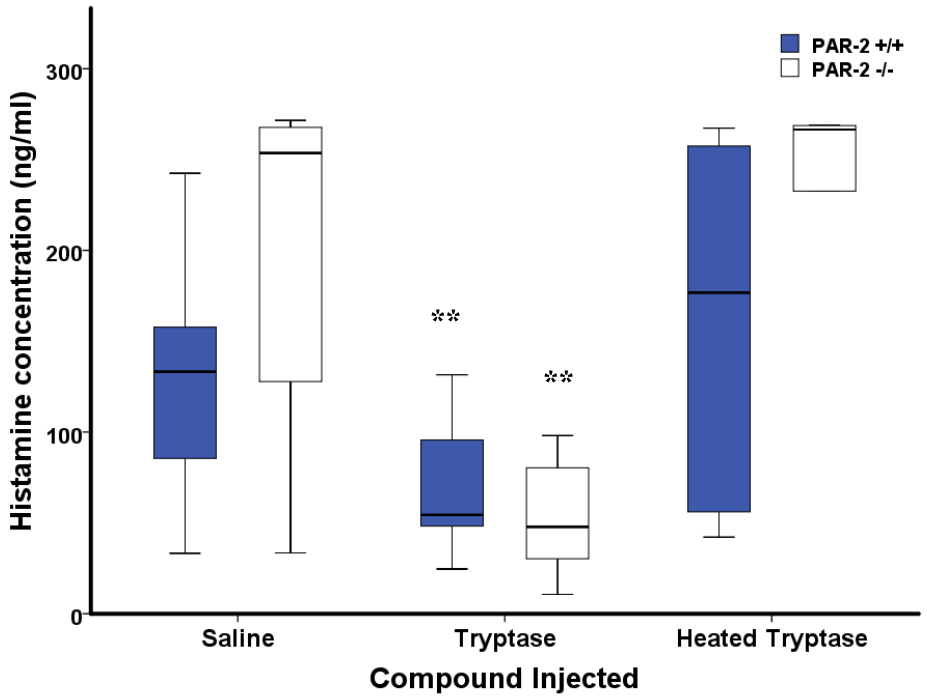

Figure 3.20 Histamine concentration in peritoneal lavage fluid supernatant from C57BL/6 mice 24 h following injection of tryptase (0.5 µg/mouse). ** $p<0.005$ compared with the saline injected group (Mann–Whitney U test follows Kruskal–Wallis test).

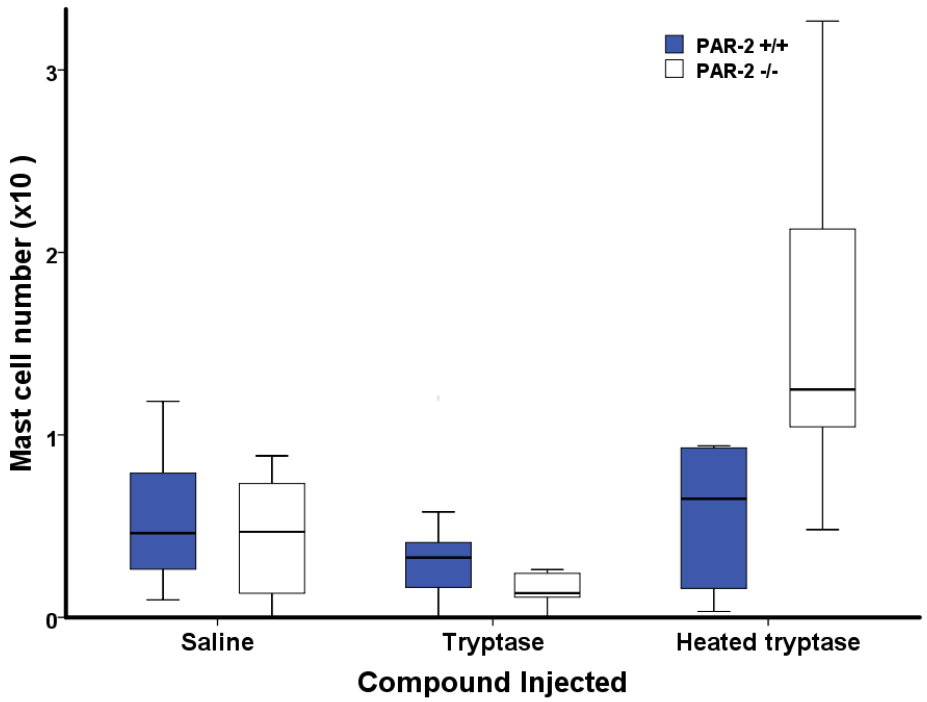

Figure 3.21 Mast cell numbers recovered in peritoneal lavage fluid from C57BL/6 mice 24 h following injection of tryptase 0.5 µg/mouse. Mann–Whitney U test follows Kruskal–Wallis test.

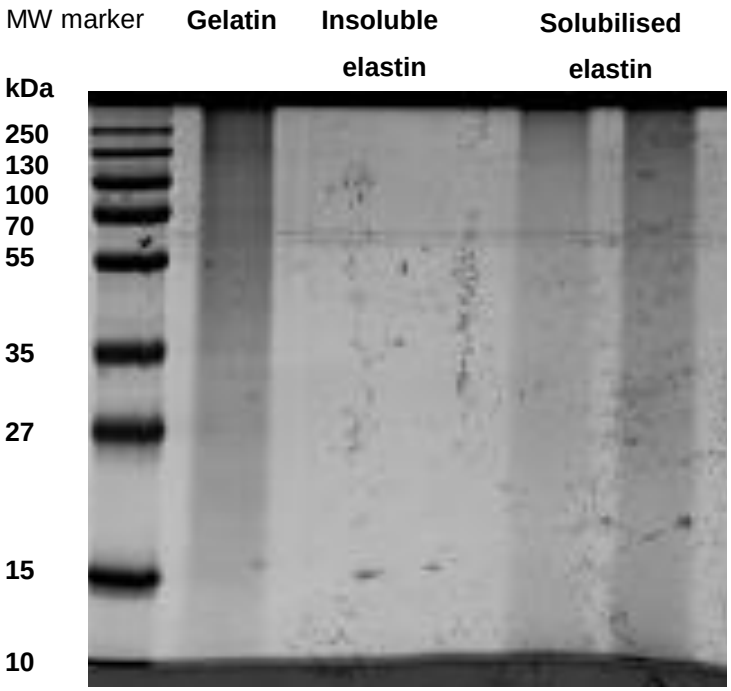

Figure 3.22 SDS-PAGE (12 %) of gelatin, insoluble elastin and solubilized elastin (as performed by ethanolic KOH extraction of insoluble elastin). Molecular weight marker is indicated.

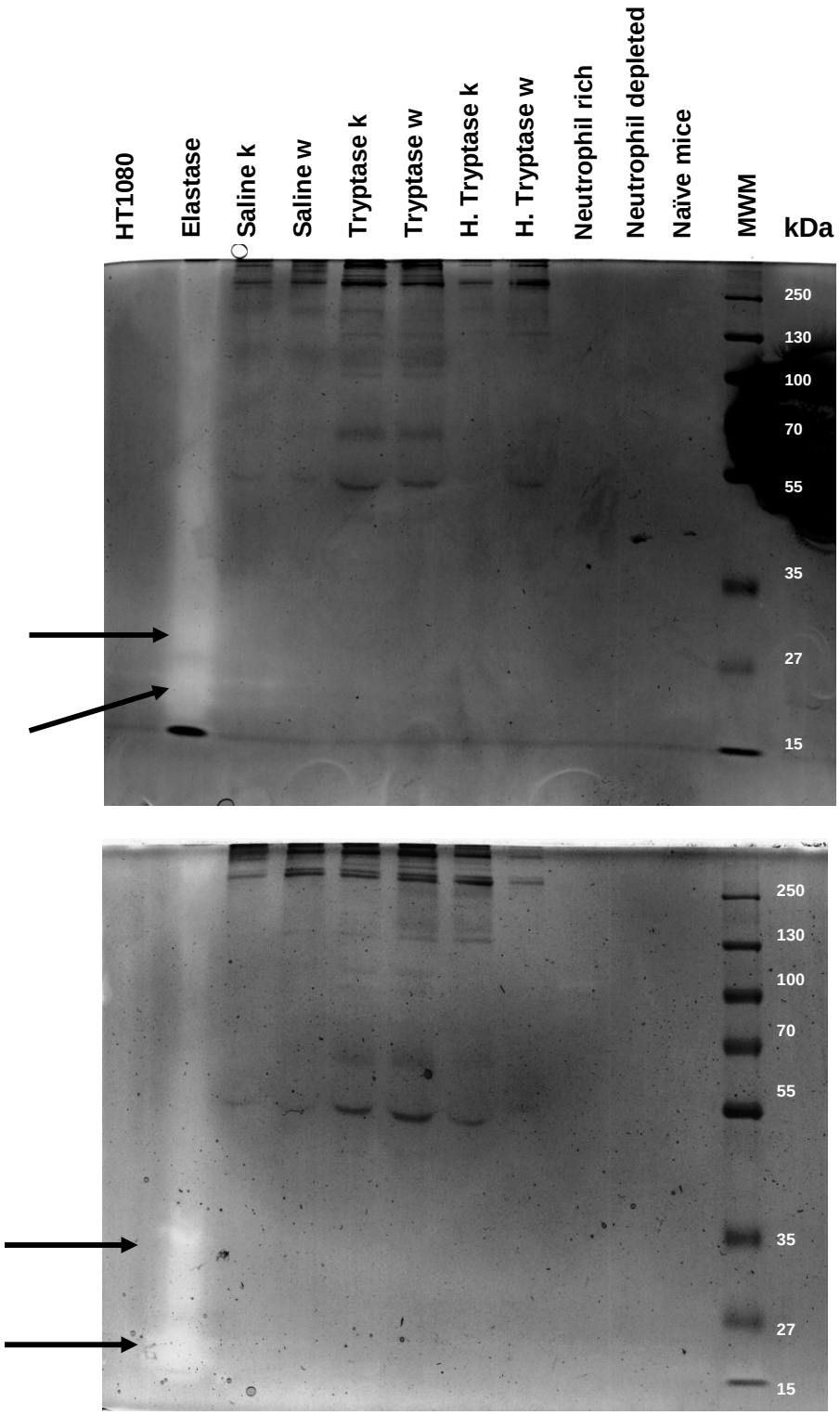

Figure 3.23 Elastin zymography using (A) 8% and (B) 10% gels for peritoneal lavage fluid from mice following treatment with saline, tryptase or heated (H) tryptase both PAR-2 knockout (K) or wild-type (W) mice and cell culture supernatant from neutrophil-rich, neutrophil-depleted cell populations or cells from naïve mice. Arrows indicate two bands of elastin digestion by elastase.

3.4 Effects of tryptase and PAR-2 RP on human endothelial cells

3.4.1 Characterization of HUVECs

Endothelial cells are widely distributed cells and playing an important role in leukocytes transimmigration into tissues through cytokine production and expression of adhesion molecules. Although primary endothelial cells had the advantage to be without pathological changes that found in other cell lines, a great concern should be taken about the purity of cell culture. Using immunocytochemistry with fluorescent labelled antibodies, HUVEC cell suspensions were found to be composed of more than 99 % of endothelial cells. When monoclonal specific antibody was used and von Willebrand antigen appeared as granular staining in more than 99 % of cells (Figure 3.24 A). The appearance was that of a homogenous population of HUVECs with very little contamination with other cells. There was a high degree of PAR-2 expression which appeared as diffuse green florescence staining of HUVECs with specific monoclonal antibody P2A (Figure 3.24 B).

3.4.2 Tryptase-induced IL-8 gene expression and release

In a previous study of cytokine expression in HUVECs in response to tryptase, cells were allowed to become quiescent in serum-free medium for a period of 48 h prior to incubation with various agents [128]. However, when similar conditions were applied in the present studies, cell viability was poor and the HUVECs detached from the culture flask (Figure 3.25). For this reason, various conditions for culturing HUVECs prior to challenge were explored. These included growing cells in serum-free medium or medium containing 1 % or 2 % FCS or 1 % human serum albumin. When expression of IL-8 gene expression at baseline was studied, it was found that results with 1 or 2 % FCS were similar to those with serum-free medium, or those with human serum albumin (data not shown). With medium containing 1 % or 2 % FCS, no marked difference was observed following 8 h incubation with tryptase (Figure 3.26). With TNF-α as stimulus, higher expression of mRNA for IL-8 was observed with 2 % FCS in the medium. In all subsequent studies of gene expression in HUVECs, cells were incubated in 2 % FCS.

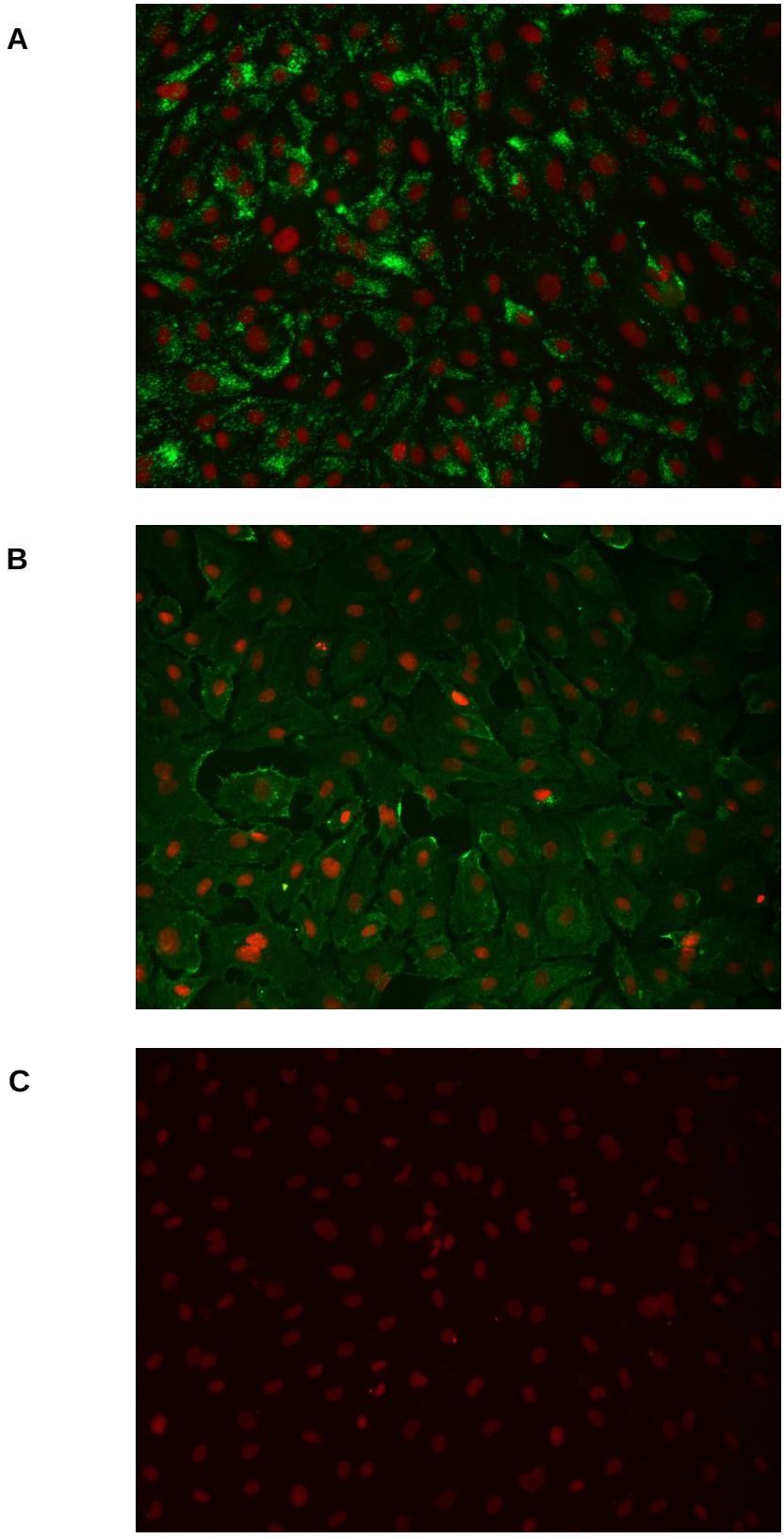

Figure 3.24 Fluorescence microscopy images of HUVECs with (A) antibody specific for von Willebrand factor or (B) PAR-2 specific monoclonal antibody P2A or (C) no antibody.

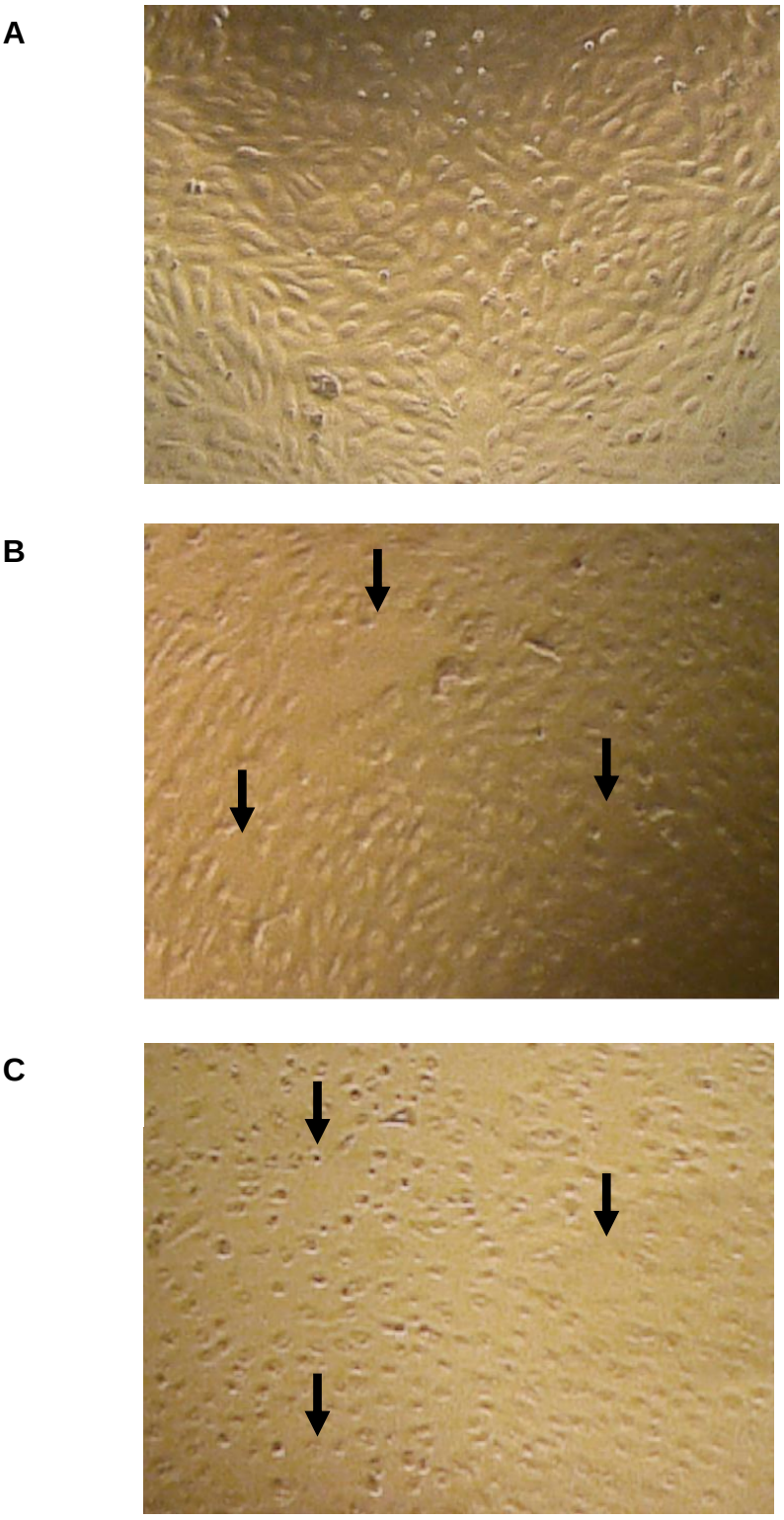

Figure 3.25 Bright field microscopy images of HUVECs cultured for 48 h with (A) 2 % FCS or (B)) 1 % FCS or (C) SFM. Arrows indicate points confluence had not been obtained.

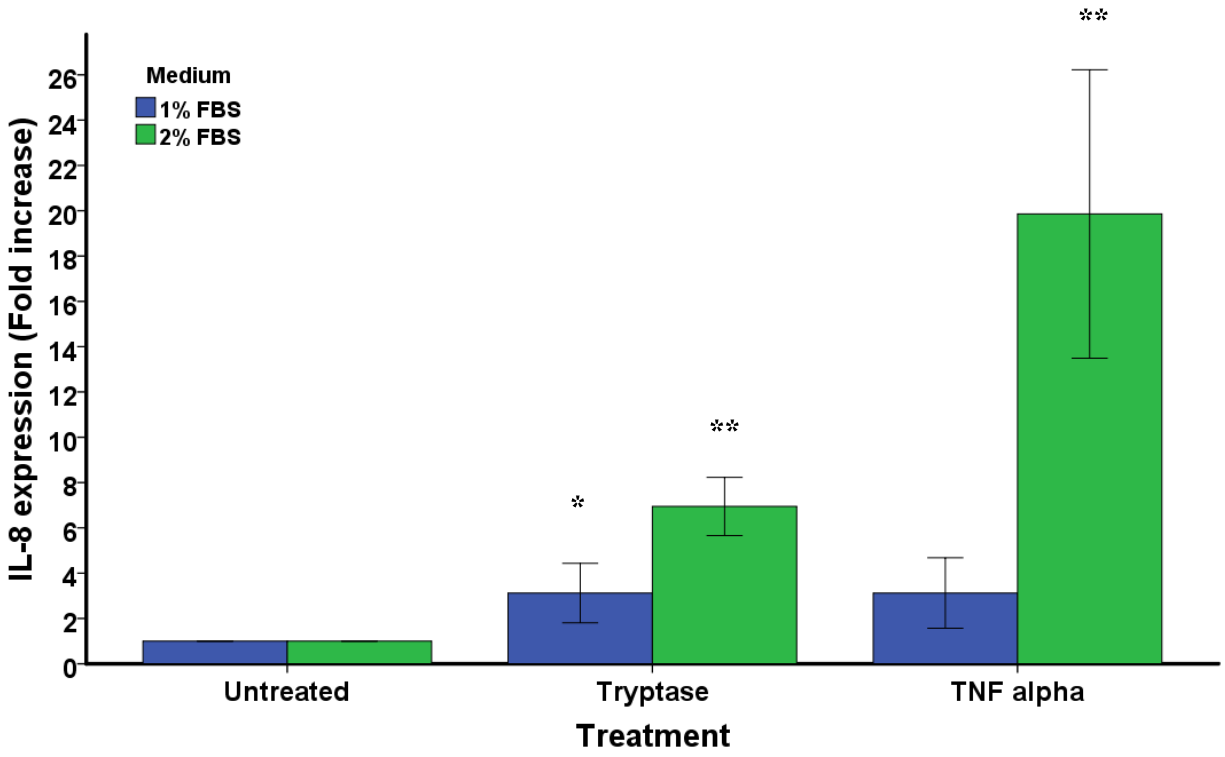

Figure 3.26 Relative IL-8 mRNA expression in HUVECs following incubation with 40 mU/ml tryptase or 10 U/ml TNF-α with 1 % FCS or 2 % FCS. Data are expressed as mean change ± standard error of means (SEM). n=3, * P<0.05, ** P<0.005 compared to the untreated cells. Mann-Whitney U test follows Kruskal-Wallis test.

Addition of tryptase at a concentration as low as 20 mU/ml provoked a small but significant upregulation of IL-8 gene expression with much greater effects at higher concentrations (Figure 3.27 A). Increased IL-8 gene expression in cells was detected after 2 h incubation with tryptase, though higher levels were apparent at later time points up to 24 h (Figure 3.27 B).

The pattern of tryptase-induced IL-8 gene expression was reflected in levels of IL-8 in the supernatants of HUVECs (Figure 3.28). At the early time points, there was little change in IL-8 concentrations in response to tryptase, though an increase of 60 % was detected at 8 h and of 120 % at 24 h. These increases in IL-8 concentration with 40 mU/ml tryptase were, however, less than the increase in IL-8 gene expression and cytokine levels measured by ELISA in separate experiments in cells incubated with 10 U/ml TNF-α for the same time points (Figure 3.28 A).

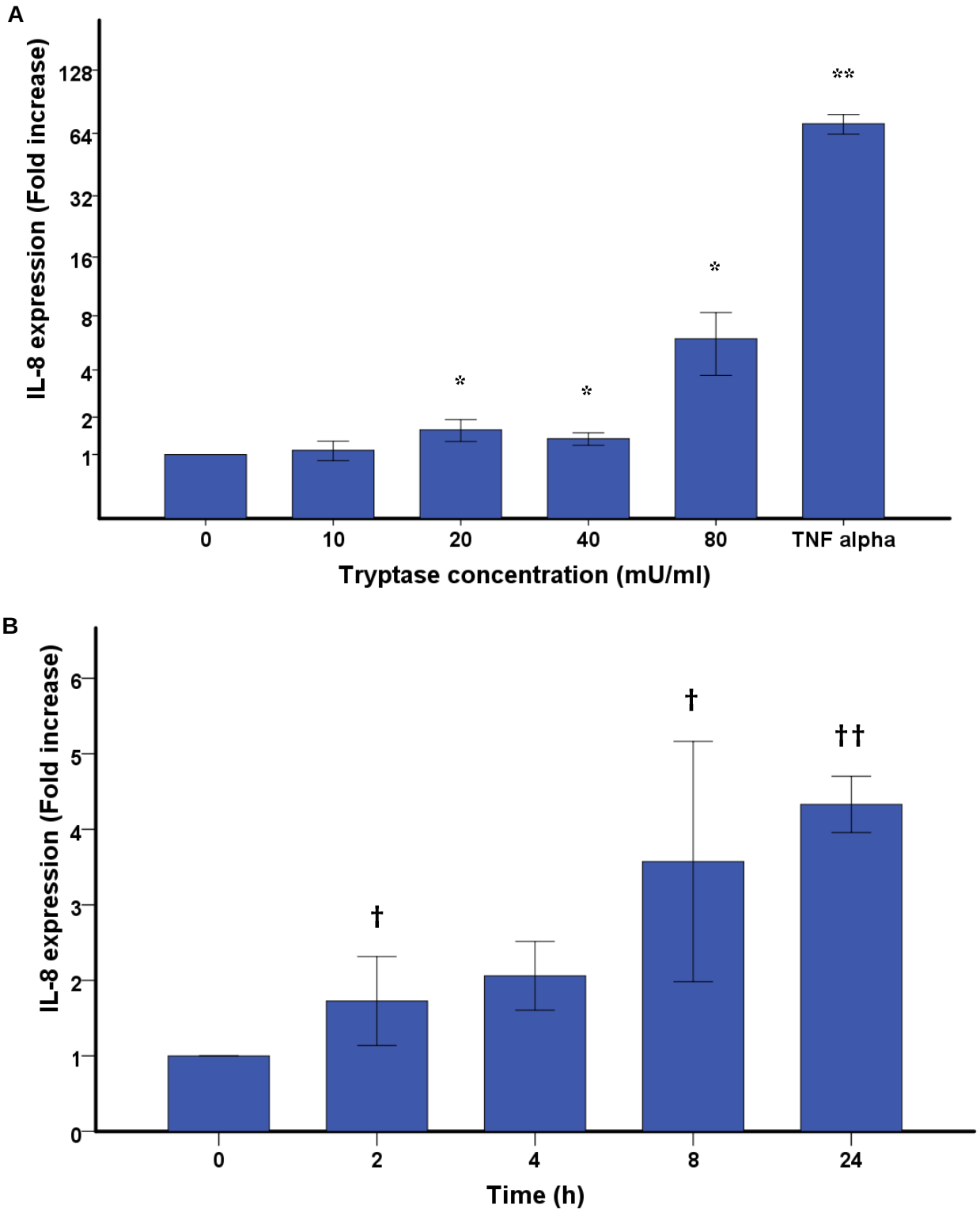

Figure 3.27 Relative mRNA expression for IL-8 in HUVECs (A) after 3 h incubation with various concentrations of tryptase or TNF-α at 10 U/ml and (B) at various time points following incubation with 40 mU/ml tryptase. Data are expressed relative to those for untreated cells * P<0.05, ** P<0.005; or those of tryptase treated cells at zero time point † P<0.05, †† P<0.005. Mean ± SEM. n=3. Mann-Whitney U test follows Kruskal-Wallis test.

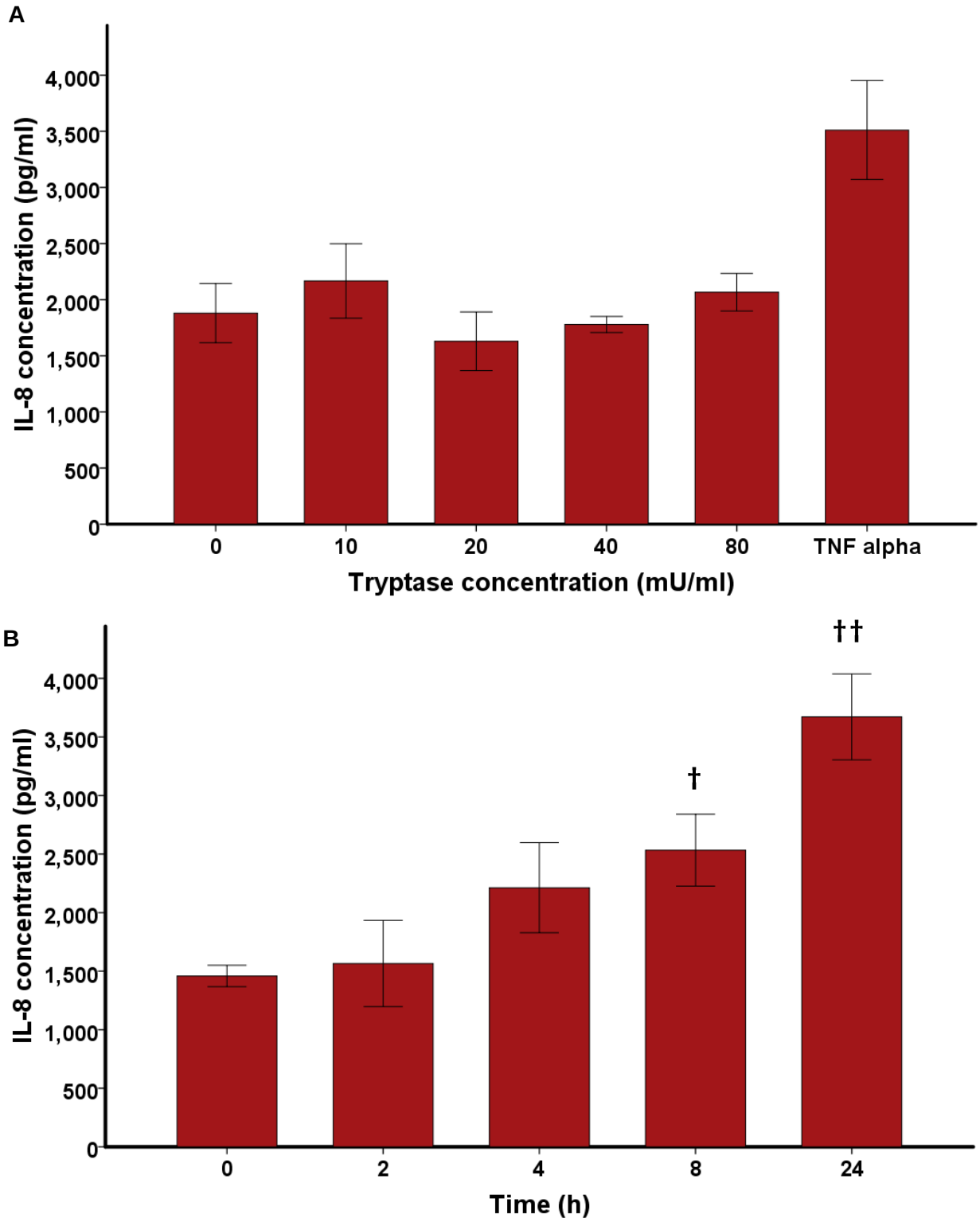

Figure 3.28 Concentrations of IL-8 in supernatants of HUVECs (A) after 8 h incubation with various concentrations of tryptase or TNF-α at 10 U/ml and (B) at various time points following incubation with 40 mU/ml tryptase. Data are expressed relative to those for untreated cells, * P<0.05, ** P<0.005005 or to zero timepoint tryptase treated cells † P<0.05, †† P<0.005. Mean ± SEM. n=3. Mann-Whitney U test follows Kruskal-Wallis test.

3.4.3 Characterization of tryptase inhibitors

Tryptase activity towards the substrate BApNA was examined after incubation with SAR160719A-5 and TdPI inhibitors at various concentrations, and for different time periods at 4°C to avoid effect of heat on tryptase. Incubation with concentrations higher than 10^{-5} M of SAR160719A-5 were able to inactivate more than 95 % of active tryptase directly after incubation, however with time tryptase regain its activity to reached about 40 % after 4 h (Table 3.3). The TdPI concentrations higher than 10^{-6} M were able to abolish activity of tryptase to about 40 % of its original activity directly after incubation and activity of tryptase decreased further to reach 20 % after 4 h. After 16 h, activity of tryptase incubated with SAR160719A-5 has not been further changed while tryptase has been to recover from inhibition mediated by TdPI inhibitors to reach 80 % of its original activity. Tryptase alone was found, as dissolved in 2 M NaCl buffer, not losing much of its activity when incubated at 4°C.

Tryptase inhibitors SAR160719A-5 and TdPI were found to be without cytotoxic actions on HUVECs over a range of concentrations at which they were effective at inhibiting tryptase at the concentrations employed. The number of cells stained with methylene blue dye 24 h following incubation with SAR160719A-5 was only reduced relative to the untreated cells at concentrations of 10^{-5} M and higher (Figure 3.29 A). Addition of TdPI whether expressed in a bacterial or baculovirus expression system, did not result in a significant decline in cell numbers even at a concentration of 10^{-5} M (Figure 3.29 B). These findings were consistent with the pattern of LDH concentrations in cell supernatants. No alterations in LDH levels were detected following 24 h incubation of SAR160719A-5, apart from at a concentration of 10^{-4} M or above (Figure 3.30 A). No increase in LDH levels was observed after incubation with TdPI inhibitors for the same period (Figure 3.30 B).

3.4.4 Catalytic dependency and role of PAR-2

Usage of tryptase inhibitors enabled us to define the role of catalytic abilities of tryptase in its pro-inflammatory actions. When tryptase at the submaximal concentration of 40 mU/ml was incubated for 8 h with HUVECs in the presence of the protease inhibitors SAR160719A-5 or TdPI at concentrations effective at inhibiting BApNA cleavage, a significant reduction in IL-8 mRNA expression

was observed (Figure 3.31 A). Neither of these inhibitors altered IL-8 gene expression when added alone.

Incubation of tryptase with TdPI was associated with little increase in IL-8 levels while incubation of tryptase with SAR160719A-5 was without effect on tryptase induced IL-8 release (Figure 3.31 B). Addition of peptide agonist SLIGKV-NH_2 and its scrambled peptide added as a control were associated with no apparent increase in cytokine expression, and PAR-2 RP had no effect on IL-8 gene expression. Similarly, PAR-2 RP, SLIGKV-NH_2 or its scrambled peptide had no effect on IL-8 cytokine levels in cell supernatants.

3.4.5 Tryptase-induced IL-1β gene expression

Tryptase stimulated IL-1β gene expression and the effect was appeared to be abolished after incubation with the protease inhibitor (Figure 3.32). Interestingly, addition of PAR-2 RP was associated with an increase in IL-1β cytokine expression of up to 10 fold, though addition of SLIGKV-NH_2 or its scrambled peptide was without effect on HUVECs IL-1β expression. The levels of IL-1β and TNF-α in HUVEC supernatants were not significantly increased after incubation with tryptase or other agents.

Table 3.3 Activity of tryptase (as percentage of initial value; 40 mU/ml) following addition of 10^{-5} M SAR160719A-5 or 10^{-6} M TdPI (expressed either in bacterial or baculovirus expression system) for various incubation periods at 4°C. n = 4, Mean ± SEM.

Time (min)	SAR160719A-5	TdPI Bacterial	TdPI Baculovirus
1	4.7 (± 4.4)	42.1 (± 15.3)	39.9 (± 17.6)
10	12.6 (± 6.3)	27.4 (± 12.0)	22.1 (± 08.9)
30	18.1 (± 14.4)	20.4 (± 12.7)	33.0 (± 12.0)
60	17.5 (± 12.7)	41.5 (± 18.8)	30.6 (± 14.1)
120	19.5 (± 6.5)	46.8 (± 11.8)	36.1 (±12.2)
240	43.1 (± 17.4)	39.4 (± 29.5)	37.2 (± 29.6)

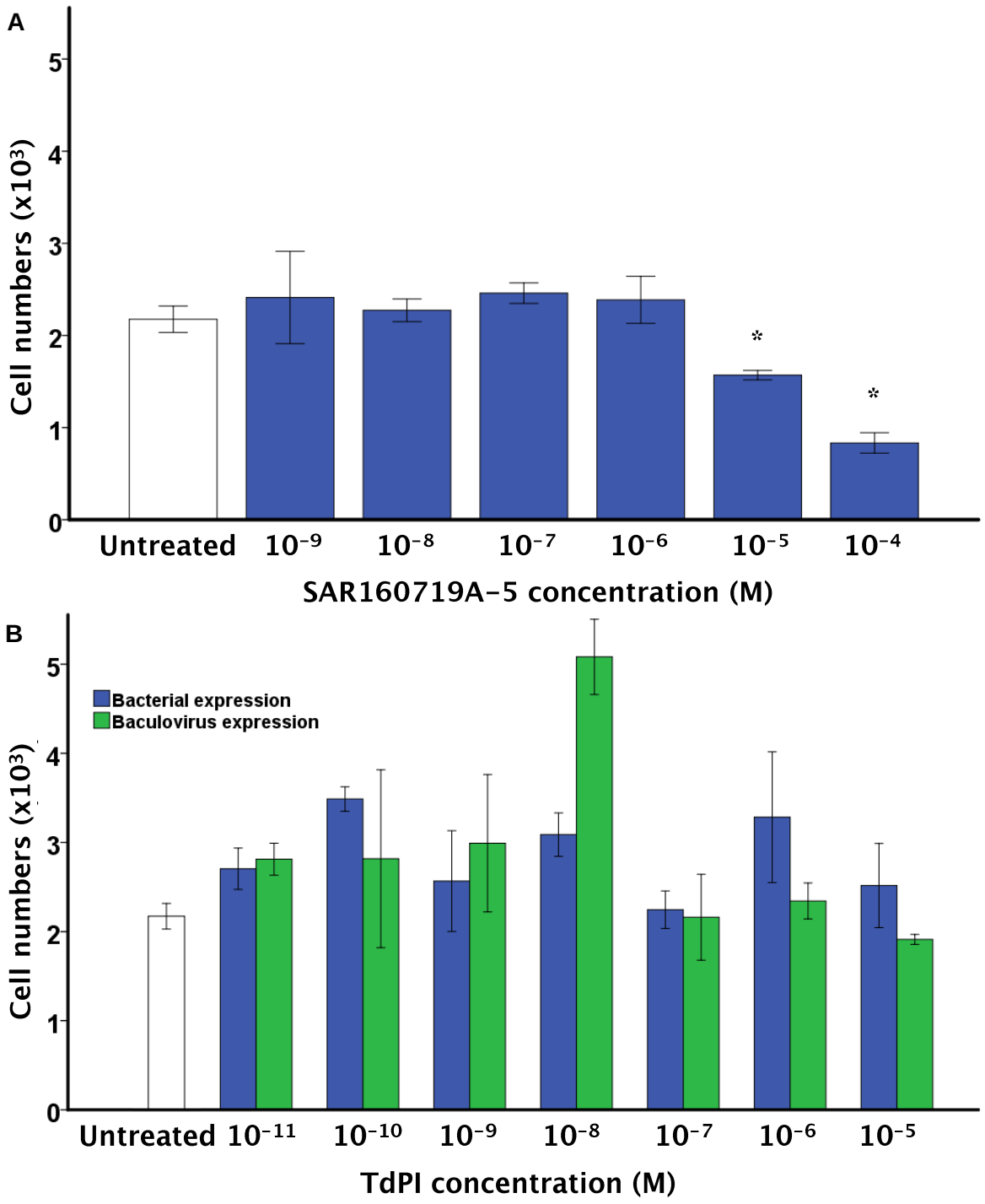

Figure 3.29 Number of HUVECs following 24 h incubation with various concentrations of the tryptase inhibitors (A) SAR160719A-5 or (B) TdPI (expressed either in bacterial or baculovirus expression system) as detected by methylene blue assay. Data are expressed as mean ± SEM. n=3,* P<0.05, compared to the untreated cells. Mann-Whitney U test follows Kruskal-Wallis test.

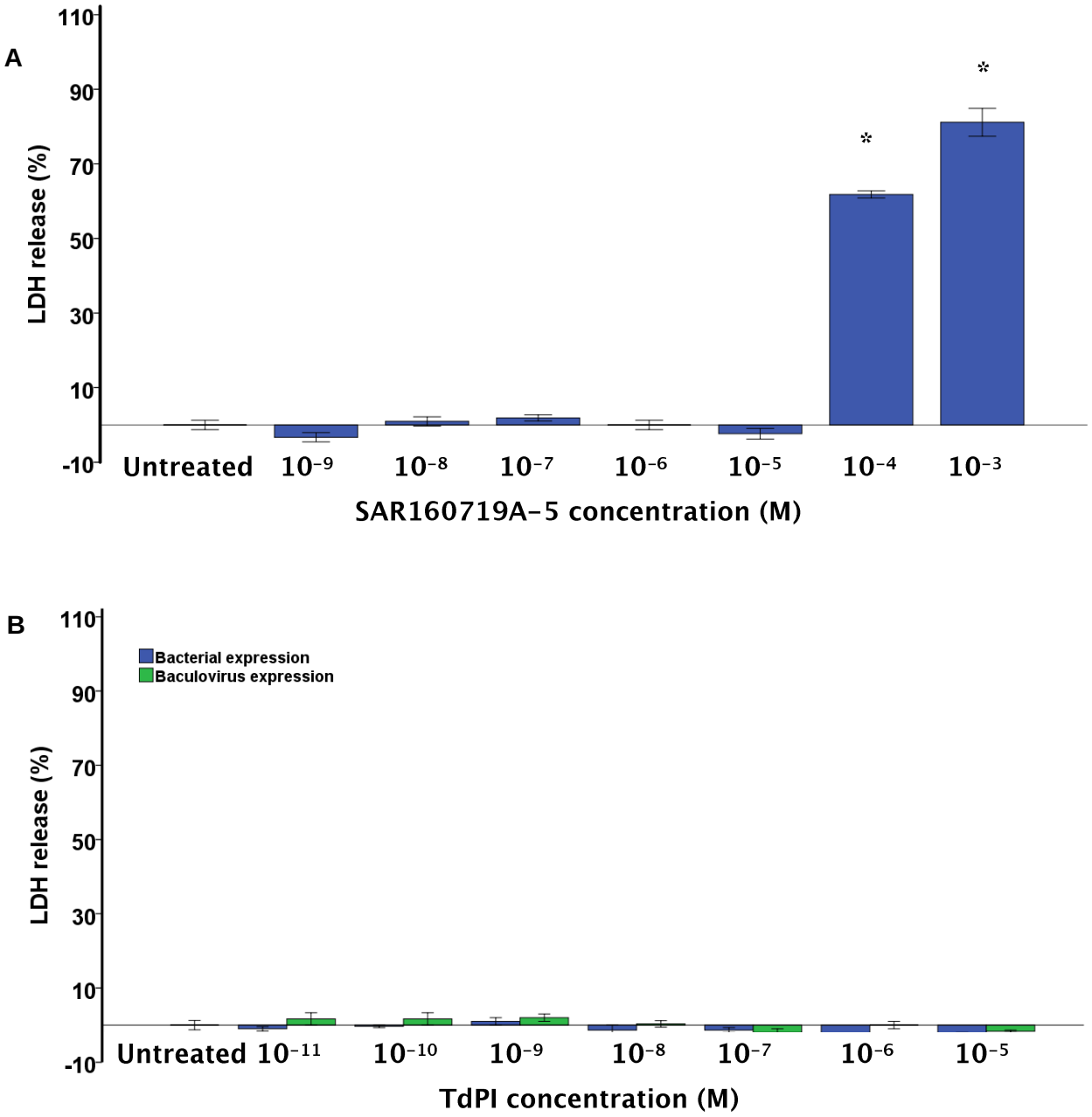

Figure 3.30 LDH release from HUVECs (expressed as a percentage of total) following 24 h incubation with various concentrations of the tryptase inhibitors (A) SAR160719A-5 or (B) TdPI (expressed either in bacterial or baculovirus expression system). Data are expressed as mean ± SEM. n=3, * P<0.05, compared to the untreated cells. Mann-Whitney U test follows Kruskal-Wallis test.

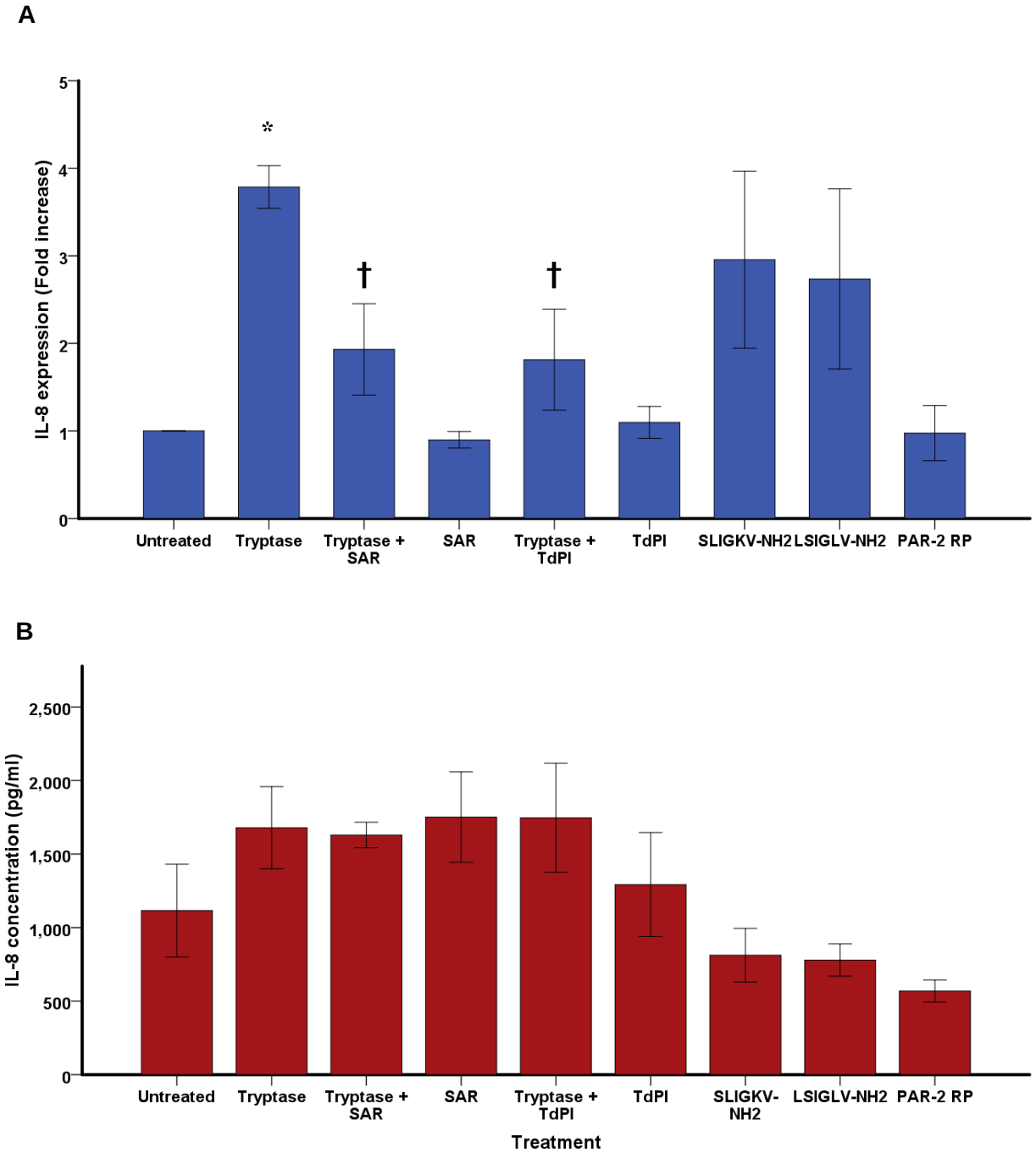

Figure 3.31 (A) Relative mRNA expression for IL-8 in HUVECs and (B) concentrations of IL-8 in cell supernatants after 8 h incubation with 40 mU/ml tryptase with or without 10^{-5} M SAR160719A-5 (SAR) or 10^{-6} M TdPI (bacterially expressed), or with 100 µM SLIGKV-NH_2 or 100 µM LSIGLV-NH_2, OR 10 U/ml TNF-α. Data are expressed mean ± SEM. n=3, * P<0.05, ** P<0.005 compared to untreated cells and † P<0.05, compared with expression in cells incubated with tryptase. Mann-Whitney U test follows Kruskal-Wallis test.

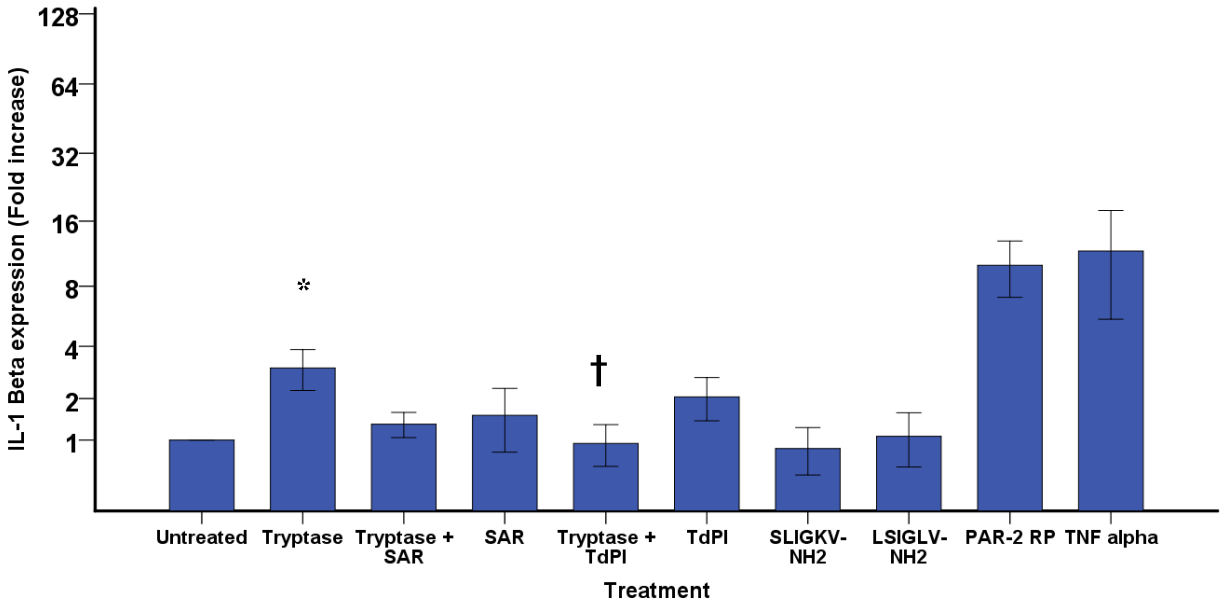

Figure 3.32 Relative mRNA expression for IL-1β in HUVECs after 8 h incubation with 40 mU/ml tryptase with or without 10^{-5} M SAR160719A-5 (SAR) or 10^{-6} M TdPI (bacterially expressed), or with 100 µM SLIGKV-NH_2 or 100 µM LSIGLV-NH_2, OR 10 U/ml TNF-α. Data are expressed mean ± SEM. n=3, * P<0.05, compared to untreated cells and † P<0.05, compared with expression in cells incubated with tryptase. Mann-Whitney U test follows Kruskal-Wallis test.

3.4.6 DNA microarray studies

The effects of tryptase on individual gene expression were studied on a limited scale. In the current study and for the first time the global gene expression of tryptase was investigated on endothelial cells. The aim of the microarray study was not only confirming the previously reported effects of tryptase, but also to explore behaviour of tryptase on the expression of global genes. In performing DNA microarray studies for global gene expression, conditions were selected on the basis of findings with qPCR and cytokine measurements. HUVECs were incubated for 8 h with tryptase at 40 mU/ml, the PAR-2 peptide agonist SLIGKV-NH_2 at 100 µM, PAR-2 RP at 100 µM or medium alone, and total cellular RNA was extracted from three independent experiments.

The quantity of total RNA recovered ranged between 17-29 ng/µl and it was of good quality as determined using a NanoDrop® ND-1000 spectrophotometer. The total RNA samples had distinct spikes corresponding to 18S and 28S rRNA subunits, the predominant form of RNA [233] indicating that RNA was not degraded. When the integrity of total RNA was investigated by running samples in an Agilent 2100 Bioanalyzer, the integrity number (RIN score) ranged from 7.9 to 9.1. RNA electrophoresis revealed two strong fluoresnce 28S and 18S bands of rRNA, with an rRNA 28s/18s ratio of 0.9 to 1.5, confirming a lack of RNA degradation (Figure 3.33). Aliquots of 500 ng of RNA were used to synthesize cDNA using a reverse transcriptase kit. When the quantity and quality of cDNA was tested using an Agilent 2100 Bioanalyzer it was found to be was satisfactory (Figure 3.34). The microarray data was summarised and normalised for each condition using the GeneSpring® Multi-Omic Analysis version 11.5 software (see Principal Component Analysis (PCA) Figure 3.35 and Figure 3.36). Robust Multichip Average (RMA) normalisation was used with background adjustment followed by quantile normalisation and finally summarisation of the data set. Quantile normalisation is a technique for making two data distributions becomes identical in statistical properties through ranking of data sets. Principal component analysis is a statistical method for determining genes that have similar, correlated patterns of expression from whole gene data. Principal component analysis reduces data dimensionality by performing a covariance analysis between factors, and was used to simplify the analysis and visualization of multidimensional data sets.

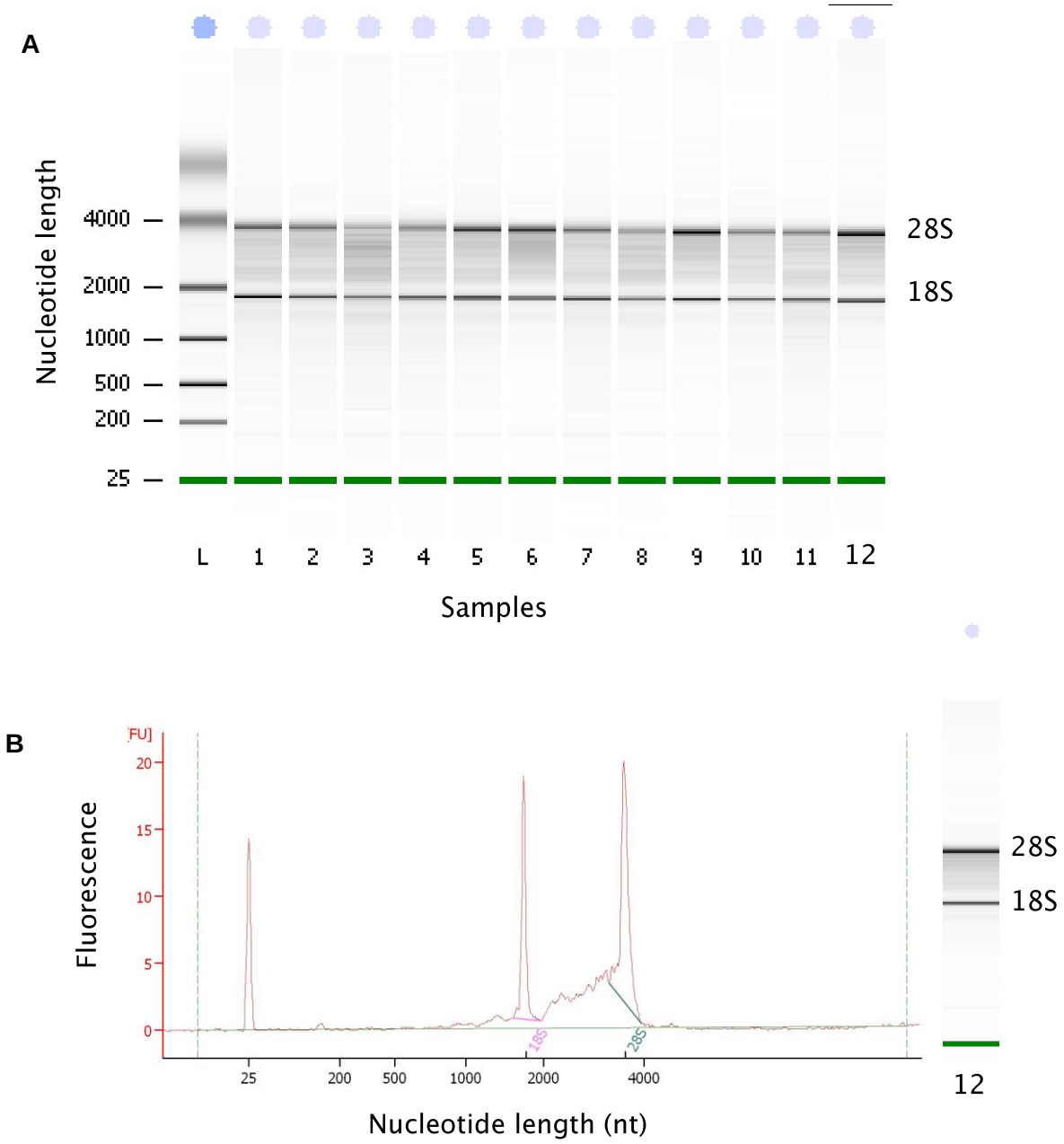

Figure 3.33 Analysis of the quality of RNA samples for DNA microarray studies by Agilent bioanalyser. (A) Electrophoresis image (gel-like) for the total RNA from 12 separate samples of HUVECs and a molecular weight ladder (L). (B) Representative electropherogram image (for sample 12) indicating 28S and 18S rRNA subunits.

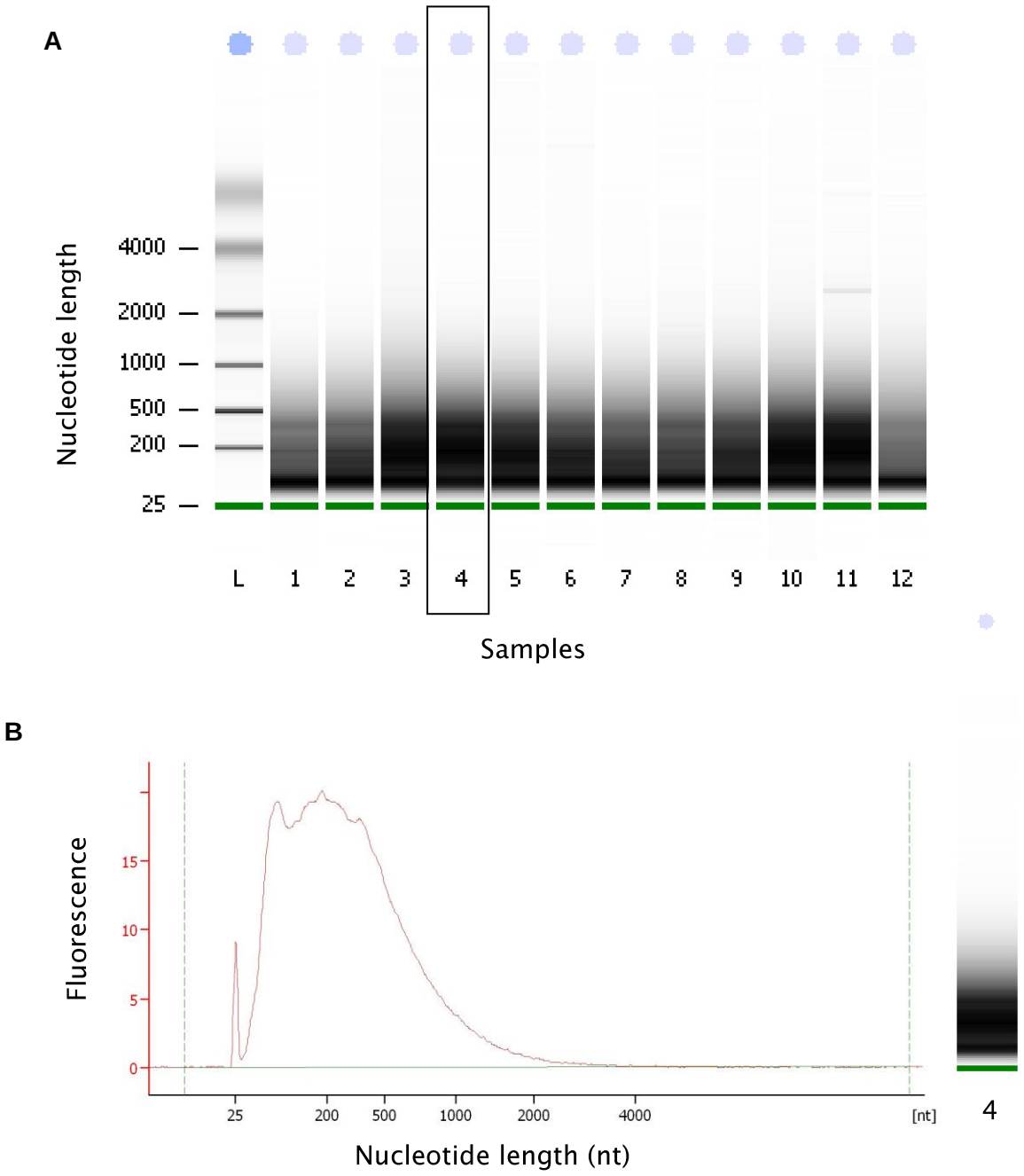

Figure 3.34 Analysis of the quality of cDNA samples for DNA microarray studies by Agilent bioanalyser. (A) Electrophoresis image (gel-like) for cDNA of 12 samples of HUVECs and a molecular weight ladder (L). (B) Representative electropherogram image (for sample 4) showing the yield and distribution of cDNA.

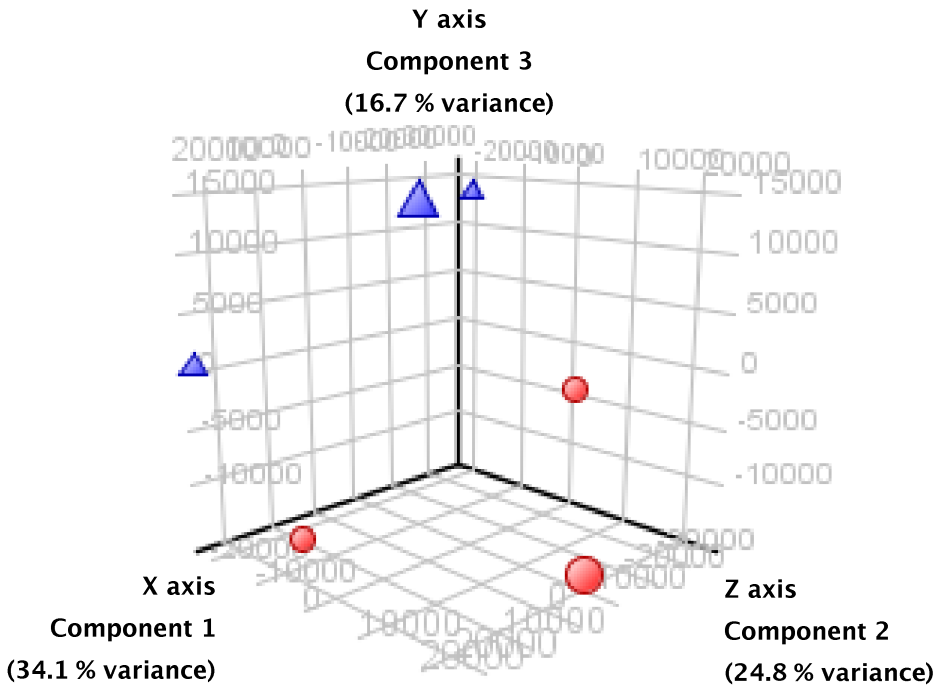

Figure 3.35 Principal component analysis of gene expression array intensity values in HUVECs. An array representing one experiment is shown as a single circle: tryptase or triangle: untreated cells, in the three-dimensional plot. The distance between points represents a measure of the dissimilarity of expression patterns between the arrays. X, Y and Z axes are represent components of analysis with 75.6 % of the total variability.

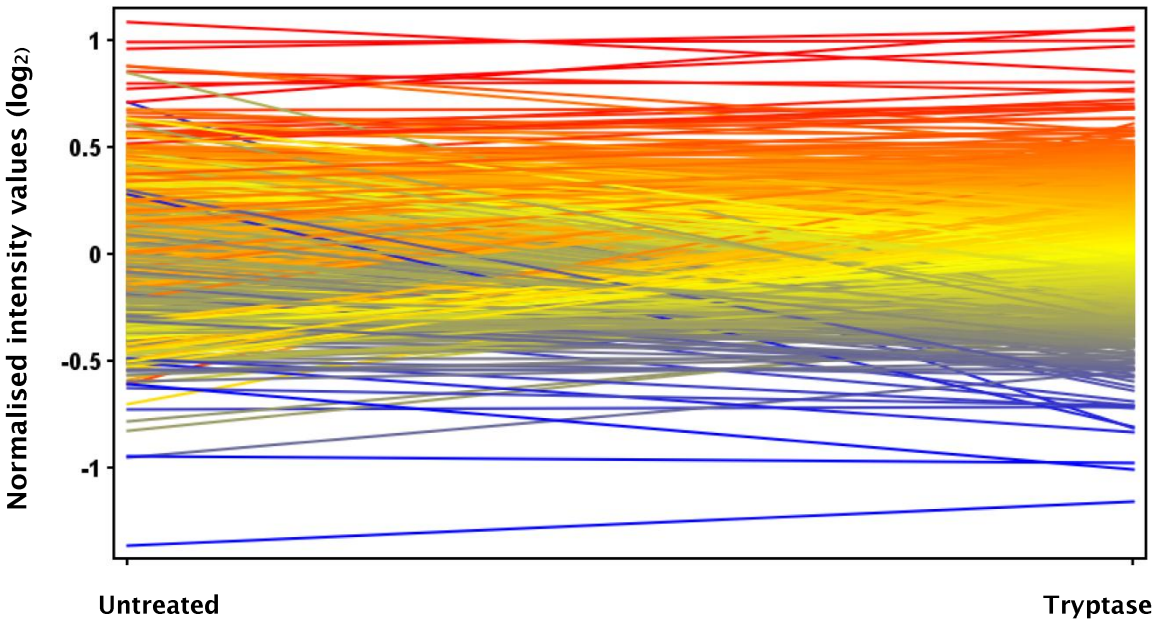

Figure 3.36 A profile plot of normalisation expression intensity value of genes for tryptase-treated HUVECs with cut off set at 20th percentile (values below were considered as noise produced by non-expressed genes). Red lines indicate the genes up-regulated, and the genes down-regulated coloured by blue in tryptase-treated cells compared to that of untreated cells. Yellow lines represent genes which have similar expression relative to that of untreated cells.

3.4.6.1 Tryptase-induced gene expression

Genes were identified where there was at least a 1.5 fold increase or decrease in gene expression following incubation of HUVECs with tryptase, PAR-2 peptide agonist or PAR-2 RP in comparison with the non-treated cells. According to these criteria, there were fifteen genes identified as apparently up-regulated and eleven genes apparently down-regulated in HUVECs on incubating cells with tryptase (Table 3.4). The list of genes identified suggests that tryptase can stimulate high expression of several adhesion molecules including vascular cell adhesion molecule 1 (VCAM-1), intercellular adhesion molecule 1 (ICAM-1), selectin E (SELE) and epithelial cell adhesion molecule (EPCAM). Also up-regulated under these conditions were growth differentiation factor 3 (GDF3), the chemokine (C-X-C motif) ligand 10 (CXCL10), tumour necrosis factor receptor superfamily member 9 (TNFRSF9) and tumour necrosis factor alpha-induced protein 3 (TNFAIP3). Incubation of tryptase with HUVECs was also associated with down-regulation of glycerol-3-phosphate acyltransferase mitochondrial (GPAM) and small nucleolar RNAs.

Application of GeneSpring® Multi-Omic Analysis version 11.5 software to explore the contribution of the differentially expressed genes in molecular pathways, suggested that that many pathways may have been involved including androgen receptor, B cell receptor (BCR), epidermal growth factor 1(EGFR1), interleukin 2 (IL-2), interleukin 3 (IL-3), interleukin 6 (IL-6), kit receptor (a member of tyrosine kinase family), NOTCH (a pathway involved in cell-cell communication), transforming growth factor beta receptor (TGFBR), TNF alpha/NF-kB and Wnt (a pathway involved in embryogenesis and cancer) (Table 3.5).

3.4.6.2 PAR-2 peptide agonist (SLIGKV-NH_2)-induced gene expression

The pattern of tryptase-induced gene expression was not reproduced when SLIGKV-NH_2 was added to cells (Table 3.6). Incubation of SLIGKV-NH_2 with HUVECs resulted in apparently high expression of mRNA for regulator of calcineurin 1 (RCAN1) and latexin (LXN). Genes which were apparently down-regulated were glycerol-3-phosphate acyltransferase, mitochondrial (GPAM), ubiquitin interaction motif containing 1 (UIMC1), taste receptor type 2, member 5 (TAS2R5), olfactory receptor [family 5, subfamily M, member 10] (OR5M10), small Cajal body-specific RNA 5, 9 and 7, and small nucleolar RNAs.

3.4.6.3 PAR-2 RP-induced gene expression

PAR-2 RP appeared to trigger up-regulation of integrin alpha L (ITGAL), TRAF and TNF receptor associated proteinTDP2 (TTRAP), small proline-rich protein 2B (SPRR2B), SEC11 homolog C (*S. cerevisiae*, SEC11C), general transcription factor IIIC, polypeptide 6, alpha 35 kDa (GTF3C6), gliomedin (GLDN) and many zinc fingers proteins (Table 3.7). PAR-2 RP treatment was associated also with apparently down-regulation of glycerol-3-phosphate acyltransferase, mitochondrial (GPAM) and small nucleolar RNAs.

Table 3.4 Gene expression profile of tryptase-treated HUVECs. Genes, their symbol and accession number are listed where there was a change in expression of greater than 1.5 fold compared to that of untreated cells. Significance is shown compared with expression in untreated cells (unpaired Student's t-test).

Gene description	Gene symbol	Accession number	*p* Value	Fold change
Selectin E	SELE	NM_000450	0.413	2.332
Vascular cell adhesion molecule 1	VCAM1	NM_001078| NM_080682	0.155	1.895
Intercellular adhesion molecule 1	ICAM1	NM_000201	0.247	1.790
Tumor necrosis factor receptor superfamily, member 9	TNFRSF9	NM_001561	0.055	1.735
Chemokine (C-X-C motif) ligand 10	CXCL10	NM_001565	0.424	1.673
Carbonic anhydrase VIII	CA8	NM_004056	0.266	1.633
Developmental pluripotency associated 3	DPPA3	NM_199286	0.123	1.628
Transmembrane 4 L six family member 19	TM4SF19	NM_138461	0.063	1.596
Tumor necrosis factor, alpha-induced protein 3	TNFAIP3	NM_006290	0.139	1.580
Tolloid-like 1	TLL1	NM_012464	0.146	1.559
Growth differentiation factor 3	GDF3	NM_020634	0.286	1.545
Epithelial cell adhesion molecule	EPCAM	NM_002354	0.007	1.525
BCL6 co-repressor-like 2	BCORL2	NM_001173413	0.353	1.521
Rho-associated, coiled-coil containing protein kinase 1 pseudogene 1	ROCK1P1	NC_000018.9| NT_010859.14	0.145	1.517
Cytochrome P450, family 4, subfamily Z, polypeptide 2 pseudogene	CYP4Z2P	NR_002788	0.142	1.501
Glycerol-3-phosphate acyltransferase, mitochondrial	GPAM	NC_001807	0.090	-1.902
Small Cajal body-specific RNA 9-like (retrotransposed)	SCARNA9L	NR_023358	0.088	-1.892
Small nuclear ribonucleoprotein polypeptide N	SNRPN	NC_000015.9| NT_026446.14	0.371	-1.673
Small nucleolar RNA, C/D box 45B | Rab geranylgeranyltransferase, beta subunit	SNORD45B| RABGGTB	NR_002748	0.053	-1.604
Chromosome 4 open reading frame 49	C4orf49	NM_032623	0.081	-1.530
Small Cajal body-specific RNA 9	SCARNA9	NR_002569	0.152	-1.529
Small nucleolar RNA, C/D box 47 | growth arrest-specific 5 (non-protein coding)	SNORD47| GAS5	NR_002746	0.129	-1.526
Ribosomal protein SA pseudogene 58	RPSAP58	NR_003662	0.023	-1.524
Small nucleolar RNA, C/D box 113-3	SNORD113-3	NR_003231	0.089	-1.521
Eukaryotic translation initiation factor 4A2	EIF4A2	NC_000003.11| NT_005612.16	0.090	-1.504

Table 3.5 Potential pathways stimulated by tryptase in HUVECs, showing numbers of genes involved and tested in the array, and the number of matched genes using GeneSpring® Multi-Omic Analysis version 11.5 software. Significance is shown compared with expression in untreated cells (unpaired Student's t-test), n.s., not significant.

Pathway	Pathway genes*	Genes tested in the array †	Matched genes††	*p* Value
Alpha 6 beta 4 integrin	53	50	48	n.s.
Androgen receptor	98	94	93	0.004
BCR	148	135	131	0.031
EGFR1	181	176	173	3.67×10^{-4}
Hedgehog (in embryo development)	24	21	21	n.s.
ID (Oncology)	30	29	28	n.s.
IL1	40	24	24	n.s.
IL2	72	58	57	0.051
IL3	76	71	71	0.003
IL4	56	49	48	n.s.
IL5	39	33	31	n.s.
IL6	66	52	52	0.011
IL7	16	16	15	n.s.
IL9	12	12	12	n.s.
Kit Receptor (tyrosine kinase family)	70	65	64	0.029
NOTCH (cell-cell communication control multiple cell differentiation)	93	74	74	0.001
TCR	140	126	121	0.061
TGFBR	200	136	136	1.10×10^{-5}
TNF-α/NF-kB	214	191	190	2.94×10^{-6}
Wnt (embryogenesis and cancer)	138	103	101	0.010
MT-heavy metal-pathway	16	14	13	n.s.

†Genes in a pathway included in the chip, †† Genes in a pathway affected by the tryptase, BCR: B cell antigen Receptor, EGFR1: Epidermal growth factor 1, ID: inhibitor of DNA binding, TCR: T-Cell Receptor, TGFBR: transforming growth factor beta receptor, n.s., Not significant.

Table 3.6 Gene expression profile of PAR-2 peptide agonist (SLIGKV-NH_2)-treated HUVECs. Genes, their symbol and accession number are listed where there was a change in expression of greater than 1.5 fold compared to that of untreated cells. Significance is shown compared with expression in untreated cells (unpaired Student's t-test).

Gene description	Gene symbol	Accession number	*p* Value	Fold change
Regulator of calcineurin 1	RCAN1	NM_004414| NM_203417| NM_203418	0.054	1.509
Latexin	LXN	NM_020169	0.070	1.496
Glycerol-3-phosphate acyltransferase, mitochondrial	GPAM	NC_001807	0.002	-5.733
Ubiquitin interaction motif containing 1	UIMC1	NC_001807	0.001	-2.343
Small nucleolar RNA, C/D box 47 | growth arrest-specific 5 (non-protein coding)	SNORD47| GAS5	NR_002746	0.017	-2.022
Olfactory receptor, family 5, subfamily M, member 10	OR5M10	NM_001004741	0.032	-1.933
Taste receptor, type 2, member 5	TAS2R5	NC_001807	0.017	-1.808
Small Cajal body-specific RNA 9	SCARNA9	NR_002569	0.046	-1.730
Small Cajal body-specific RNA 7	SCARNA7	NR_003001	0.002	-1.728
Small nucleolar RNA, C/D box 50A	SNORD50A	NR_002743	0.048	-1.682
GA binding protein transcription factor, alpha subunit 60kda	GABPA		0.016	-1.664
Small nucleolar RNA, C/D box 76 | growth arrest-specific 5 (non-protein coding)	SNORD76| GAS5	NR_003942	0.046	-1.642
RNA component of mitochondrial RNA processing endoribonuclease	RMRP	NR_003051	0.028	-1.621
Small nucleolar RNA, H/ACA box 4 | eukaryotic translation initiation factor 4A2 | eukaryotic translation initiation factor 4A, isoform 2	SNORA4| EIF4A2	NR_002588	0.044	-1.544
Lp2570	LOC10013 1796		0.021	-1.522
Small nucleolar RNA, C/D box 59B	SNORD59B	NR_003046	0.049	-1.510

Table 3.7 Gene expression profile of PAR-2 RP-treated HUVECs. Genes, their symbol and accession number are listed where there was a change in expression of greater than 1.5 fold compared to that of untreated cells. Significance is shown compared with expression in untreated cells (unpaired Student's t-test).

Gene description	Gene symbol	Accession number	*p* Value	Fold change
Tyrosyl-DNA phosphodiesterase 2 | TRAF and TNF receptor associated protein	TDP2| TTRAP	NM_016614	0.017	1.681
Small proline-rich protein 2B	SPRR2B	NM_001017418	0.030	1.662
SEC11 homolog C (S. Cerevisiae)	SEC11C	NM_033280	0.007	1.611
General transcription factor IIIC, polypeptide 6, alpha 35kda	GTF3C6	NM_138408	0.010	1.580
Gliomedin	GLDN	NM_181789	0.025	1.540
Zinc finger protein 840 (pseudogene)	ZNF840P		0.001	1.513
Uracil phosphoribosyltransferase (FUR1) homolog (S. Cerevisiae)	UPRT	NM_145052| NR_030774	0.001	1.507
Poly(A) binding protein interacting protein 1	PAIP1	NM_006451| NM_182789| NM_183323	0.041	1.506
integrin, alpha L (antigen CD11A (p180), lymphocyte function-associated antigen 1; alpha polypeptide)	ITGAL	NM_002209| NM_001114380	0.000	1.330
Glycerol-3-phosphate acyltransferase, mitochondrial	GPAM	NC_001807	0.001	-4.474

3.4.7 Confirmation of microarray findings

3.4.7.1 Real-time RT-PCR

When changes in expression of the 15 genes identified in microarray studies were investigated by real time PCR reaction an apparent higher level of expression was confirmed in the majority of cases. Using pooled cDNA from the three experiments used in microarray, tryptase-treatment of cells was found to be associated with an expression of more than two fold expression of genes for the cytokines C-X-C motif ligand (CXCL10), IL-2, IL-3 and IL-6, the adhesion molecules VCAM1, EPCAM and ICAM1, and for tumor necrosis factor alpha-induced protein 3 (TNFAIP3) and tolloid-like protein 1 (Table 3.8). There appeared to be a small increase also in expression of integrin alpha L (ITGAL), tumour necrosis factor receptor superfamily member 9 (TNFRSF9), SMAD2 and growth differentiation factor 3 (GDF3) while expression of selectin E (SELE) and latexin (LXN) genes were not affected with tryptase treatment of cells.

The pattern of gene expression was different in the SLIGKV-NH_2 treated cells where genes for IL-3, GDF3, SELE and IL-6 appeared to have been down-regulated to nearly half of the level of expression seen in untreated cells. PAR-2 RP treatment of cells appeared to result in up-regulation of genes for ITGAL, EPCAM, ICAM1, TNFAIP3 and TLL1 by more than 1.5 fold. TNF-α treatment of cells was associated with an increase of up to 65 fold in gene expression of VCAM1 and SELE, and an apparent up-regulation of expression for genes ICAM1, CXCL10 and TNFR3F9. On the other hand, TNF-α treatment did not appear to affect expression of several genes for which there was a apparent up-regulation with tryptase including EpCAM, GDF3, IL-2, IL-3, IL-6, ITGAL, SMAD2, TLL1 and TNFAIP3.

3.4.7.2 ICAM-1 expression in HUVECs

To investigate if altered gene expression was reflected in changes at the protein level, expression of the surface adhesion molecules identified was examined by immunocytochemistry and flow cytometry. At least three different experiments were conducted to explore the effect of tryptase. TNF-α, but not tryptase-treatment of cells was associated with an increase in the surface expression of ICAM-1 as demonstrated in immunocytochemistry (Figure 3.37).

Table 3.8 Relative expression on qPCR of a selected group of genes in HUVECs incubated for 8 h with tryptase, SLIGKV-NH_2, PAR-2 RP and TNF-α. Change in expression relative to that in untreated cells is shown.

	Cell treatment			
Gene	Tryptase	SLIGKV-NH_2	PAR-2 RP	TNF-α
CXCL10†	2.24*	0.77*	1.31*	1.96*
EPCAM†	2.6*	0.96	1.56	1.03*
GDF3†	1.45*	0.59*	1.02	0.47*
ICAM1†	2.91*	0.96	1.83*	4.34*
IL-2†	2.16*	0.76*	1.41*	0.89
IL-3†	2.17*	0.65*	1.24*	0.86*
IL-6	2.22*	0.65*	1.40	0.99
ITGAL†	1.93*	0.87	1.95*	1.00
LXN	0.98	1.01	1.13	0.43*
SELE†	0.97	0.41*	0.38*	51.32*
SMAD2	1.86*	1.04	1.23*	0.79*
TLL1†	2.95*	0.97	1.75	1.18*
TNFAIP3†	2.08*	0.87*	1.68*	1.03
TNFRSF9	1.71*	0.76	1.09	2.69*
VCAM1†	2.29*	1.27*	1.06	65.71*

Mean fold increase in expression, n=3. † $p < 0.05$ between all treatment conditions using Kruskal-Wallis test, * $p < 0.05$ compared to the non-treated cells using Mann-Whitney U test. ITGAL, integrin alpha L (CD11A); TNFRSF9, tumor necrosis factor receptor superfamily member 9 (CD137); IL3, interleukin 3 (colony-stimulating factor, multiple); LXN, latexin; SMAD2, SMAD family member 2; GDF3, growth differentiation factor 3; CXCL10, chemokine (C-X-C motif) ligand; IL2, interleukin 2; VCAM1, vascular cell adhesion molecule 1(CD106); EPCAM, epithelial cell adhesion molecule (CD326); SELE, selectin E; IL6, Interleukin 6 (interferon beta 2); ICAM1, intercellular adhesion molecule 1 (CD54); TNFAIP3, tumor necrosis factor alpha-induced protein 3; TLL1, tolloid-like 1.

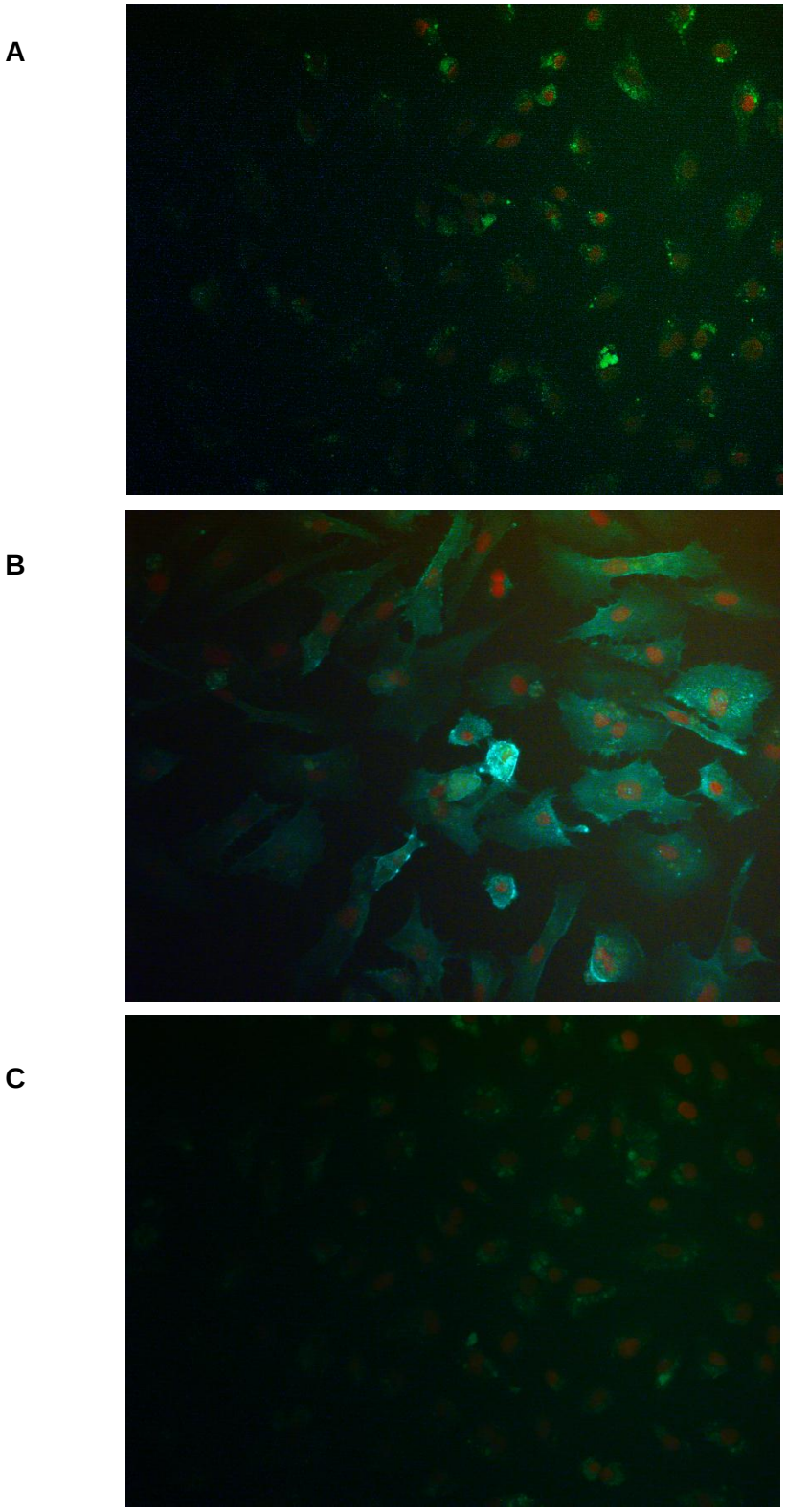

Figure 3.37 Fluorescence microscopy images of HUVECs with anti-ICAM-1 antibody after 16 h incubation with (A) 40 mU/ml tryptase or (B) 2 ng/ml TNF-α or (C) without treatment.

Depending on cell characterization and exclusion of dead cells (Figure 3.38), it was found by flow cytometry that tryptase could induce higher expression of ICAM-1, than the constitutive expression apparent on untreated cells (Figure 3.39). A marked increase in surface expression of ICAM-1 was detected following incubation of cells with TNF-α. The PAR-2 peptide agonist SLIGKV-NH_2 treatment was found to stimulate expression of ICAM-1 in cells and this was seen also with PAR-2 RP.

A marked increase in soluble intracellular adhesion molecule 1 (sICAM1) levels were detected in the supernatants of HUVECs after 16 h incubation with tryptase or TNF-α, while lower levels were detected with SLIGKV-NH_2 or PAR-2 RP. After just 1 h of incubating the cells with tryptase or TNF-α, release of sICAM-1 was not observed, suggesting that the mechanism does not involve direct cleavage of membrane-bound ICAM-1 by tryptase (Figure 3.40).

3.4.8 Expression of VCAM-1, EpCAM and ITGAL

On flow cytometry, tryptase treatment of HUVECs was associated with increased expression of VCAM-1 and EpCAM while expression of ITGAL was not altered as compared to untreated cells (Figure 3.41). Addition of TNF-α to cells appeared to stimulate a more marked increase in surface expression of VCAM-1 and ITGAL and to a lesser extent expression of EpCAM.

Treatment of cells with the PAR-2 peptide agonist SLIGKV-NH_2 was found to increase expression of VCAM-1 and ITGAL. PAR-2 RP treatment of cells was associated with an apparent increase in expression of surface molecules VCAM-1, EpCAM and ITGAL (Figure 3.42).

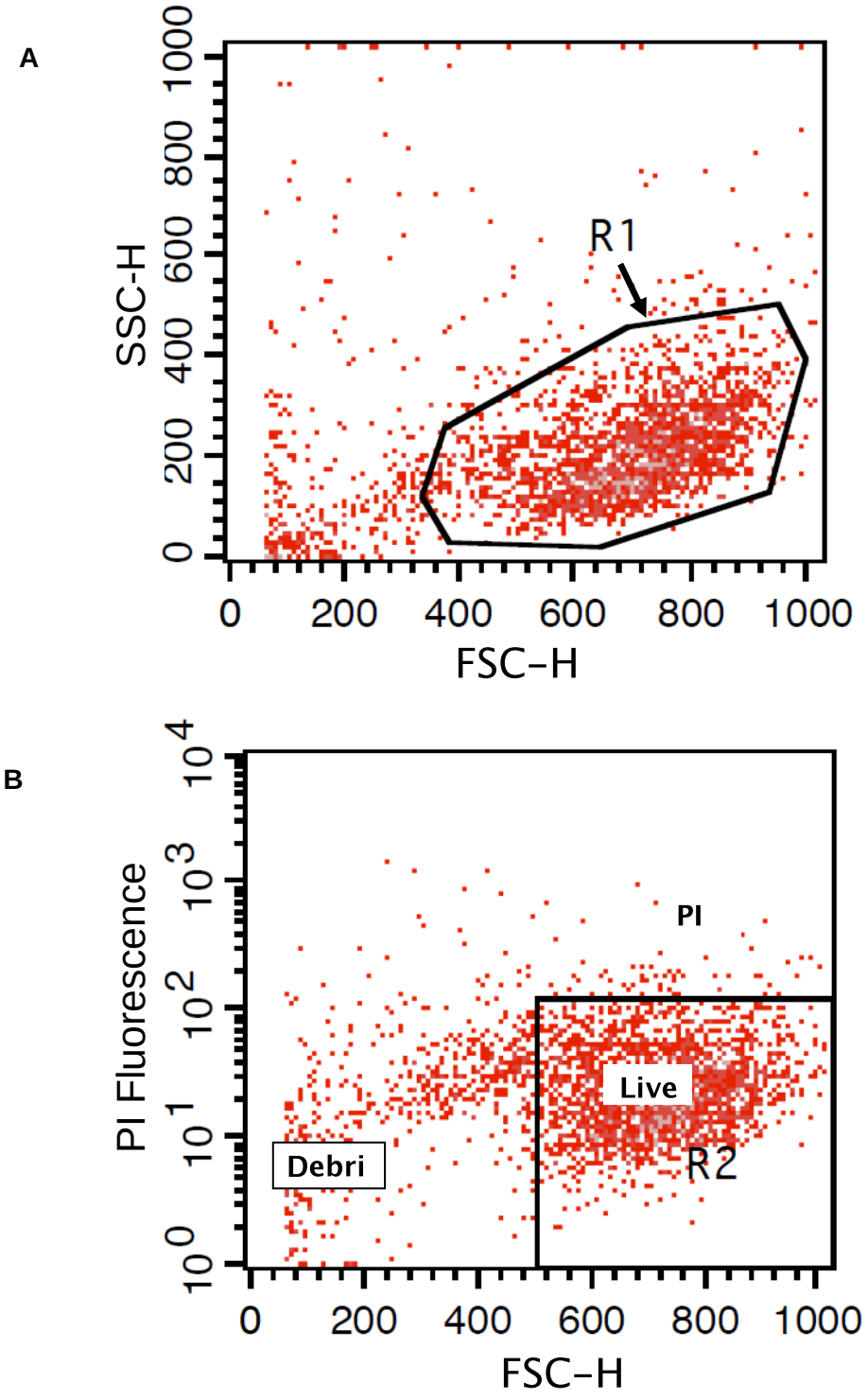

Figure 3.38 Fluorescence flow-cytometry of HUVECs. (A) with all cells outlined (region 1; R1) and (B) with live cells only outlined (region 2; R2) using 1 ng/ml propidium iodide (PI) stain. FSC-H, forward scatter height; SSC-H, side scatter height.

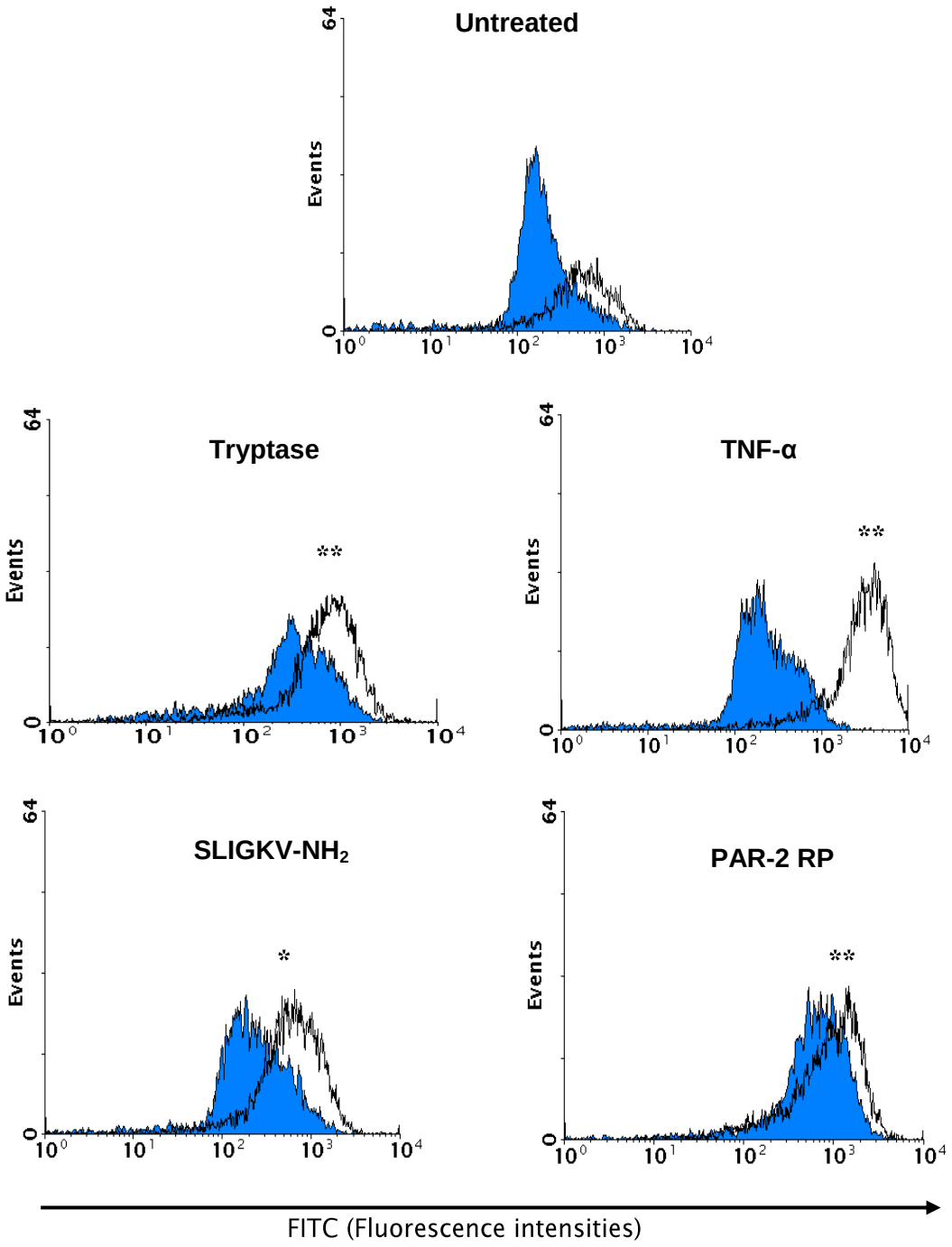

Figure 3.39 Expression by flow cytometry of ICAM-1 in HUVEC that were either untreated or incubated for 16 h with 40 mU/ml tryptase or 2 ng/ml TNF-α or 100 μM SLIGKV-NH_2 or 10 μg/ml PAR-2 RP. A shaded histogram is shown for the profile with isotype control antibody, and an open histogram for the specific anti-ICAM-1 antibody. Data is representative of three experiments. Data are analysed by two-way ANOVA. n=3, * $p < 0.05$, ** $p < 0.005$ compared with untreated cells.

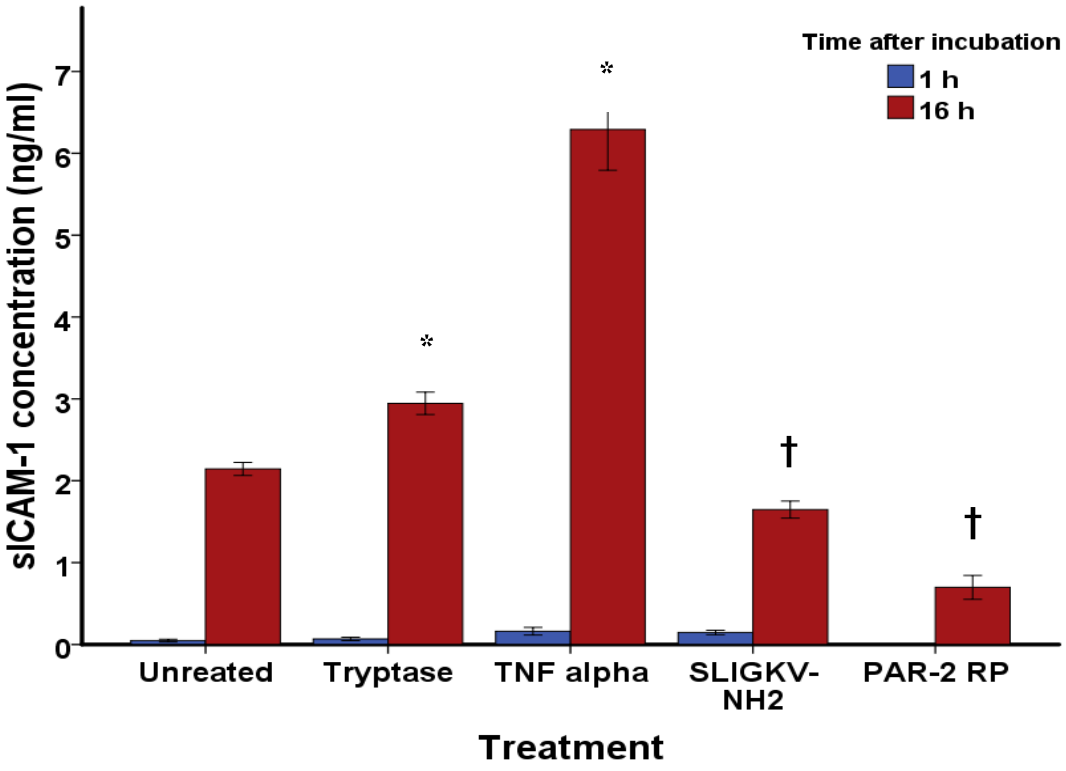

Figure 3.40 Levels of sICAM-1 in the supernatant of HUVECs after 1 h and 16 h incubation with 40 mU/ml tryptase or 2 ng/ml TNF-α or 100 µM SLIGKV-NH_2 or 10 µg/ml PAR-2 RP. Data are expressed as mean change ± SEM. n=3, * P<0.05 (greater), † P<0.05 (lower) than the untreated cells. Mann-Whitney U test follows Kruskal-Wallis test.

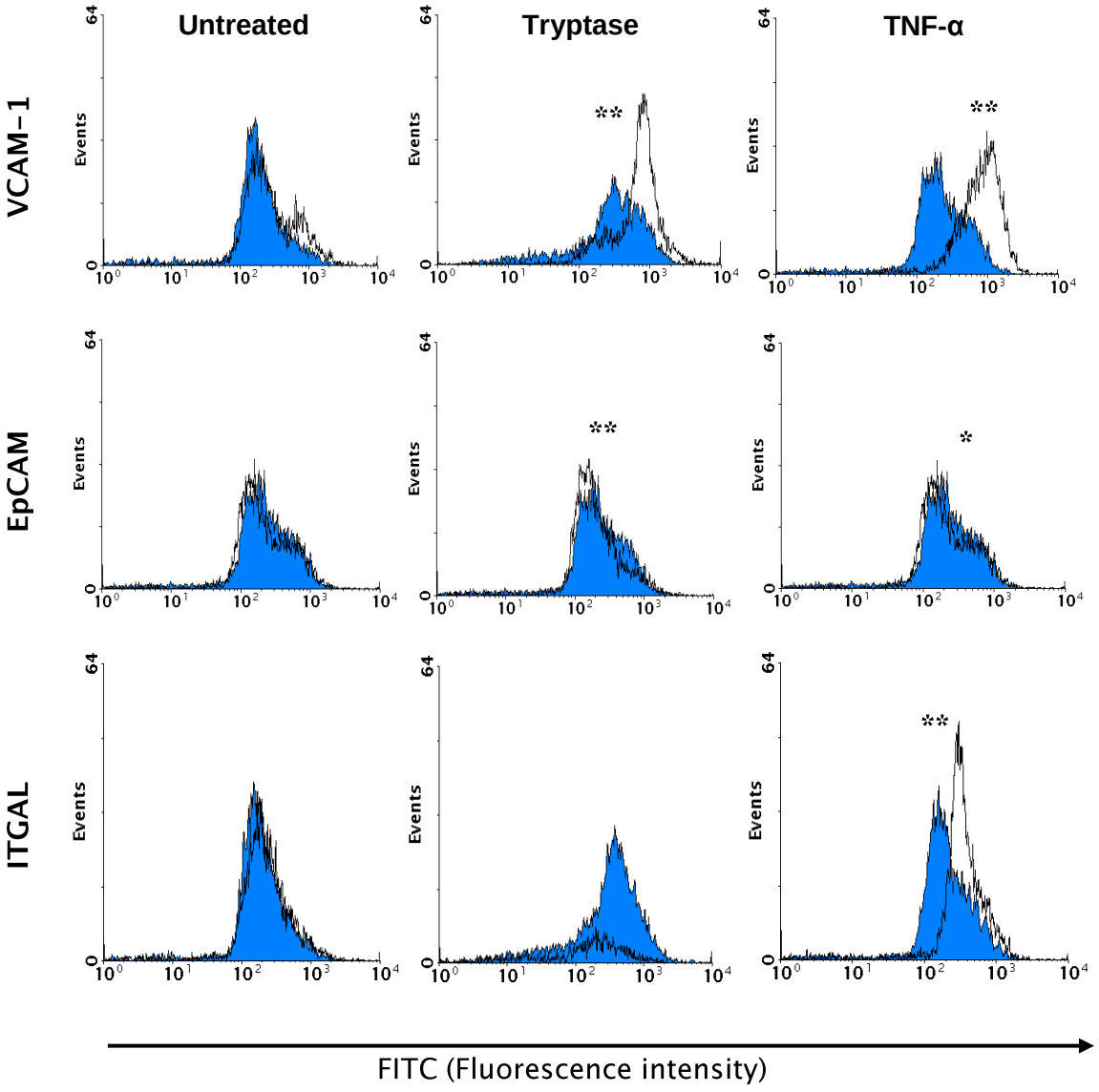

Figure 3.41 Expression by flow cytometry of VCAM-1, EpCAM and ITGAL in HUVEC that were either untreated or incubated for 16 h with 40 mU/ml tryptase or 2 ng/ml TNF-α. A shaded histogram is shown for the profile with isotype control antibody, and an open histogram for the specific antibody. Data is representative of three experiments. Data are analysed by two-way ANOVA. n=3, * $p < 0.05$, ** $p < 0.005$ compared with untreated cells.

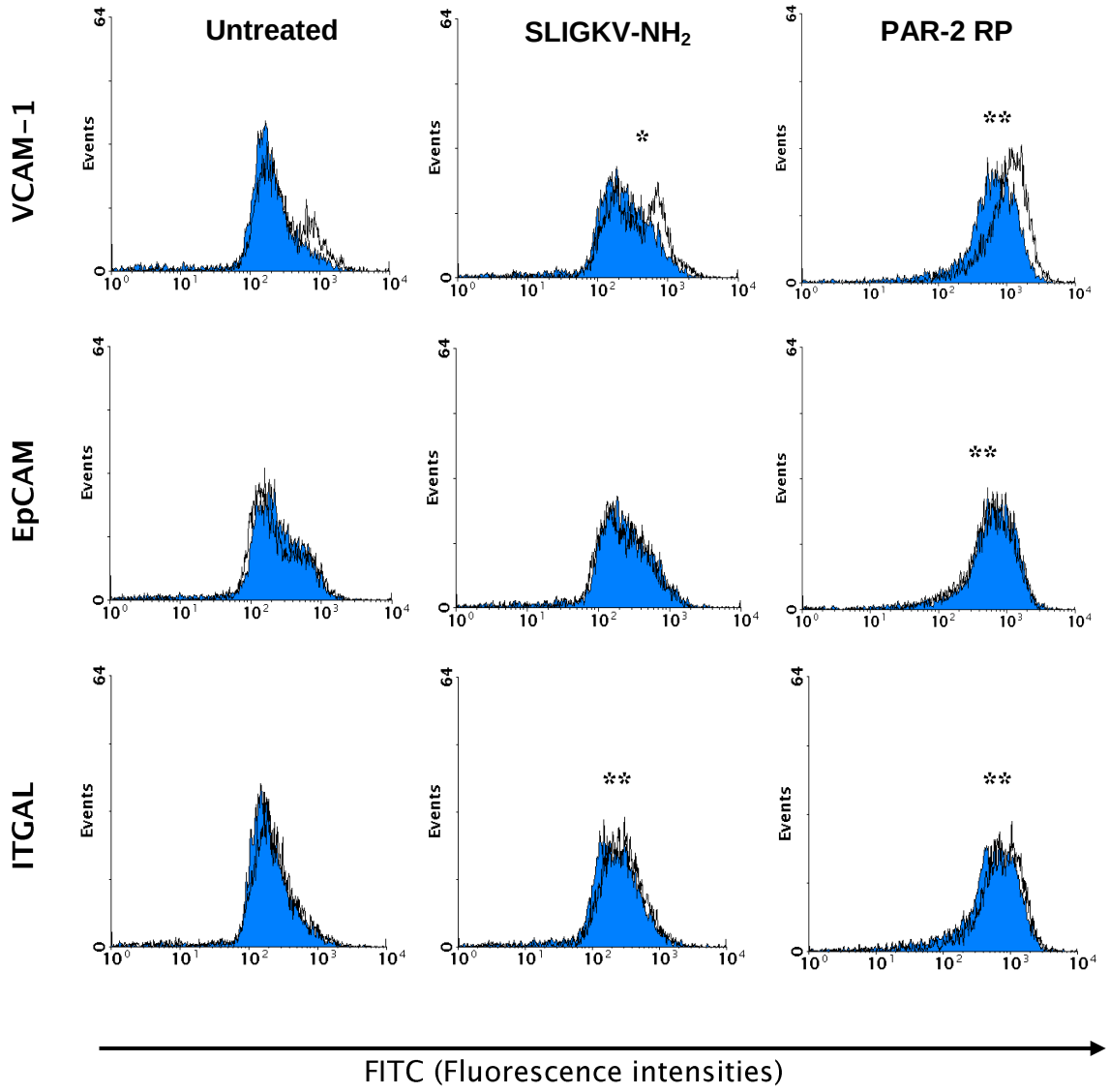

Figure 3.42 Expression by flow cytometry of VCAM-1, EpCAM and ITGAL in HUVEC that were either untreated or incubated for 16 h with 100 µM SLIGKV-NH_2 or 10 µg/ml PAR-2 RP. A shaded histogram is shown for the profile with isotype control antibody, and an open histogram for the specific antibody. Data is representative of three experiments. Data are analysed by two-way ANOVA. * $p < 0.05$, ** $p < 0.005$ compared with untreated cells.

3.4.9 Calcium mobilization studies

Calcium is common signalling mechanism of many receptors including PAR-2. Investigating of calcium mobilisation enabled us to explore the effect of tryptase on endothelial cells, and probably PAR-2, in comparison to effects of other agents including standard stimuli. Addition of calcium ionophore (A23187) to HUVECs stimulated a concentration-dependent increase in intracellular calcium as indicated by change in fluorescence on FlexStaion II equipment (Figure 3.43). The response elicited by A23187 was taken as a reference for normalisation of responses of with other agents. With fluorescence peak values normalised, a four parameters logistic (or nonlinear regression) model was used for curve fitting and calculation of the concentration giving a half maximal response (EC_{50}) (see Table 3.9). The elicited calcium flux declined to baseline levels at low concentrations but failed to do so at high concentrations.

Although the addition of tryptase stimulated a concentration-dependent increase in calcium flux, the increase was relatively small (less than 10 % of the maximal response with A23187) even at concentrations up to 100 mU/ml (500 µM); and there was little evidence for a decline to baseline levels (Figure 3.44). The PAR-2 peptide agonist SLIGKV-NH_2 showed a concentration-dependent increase in calcium mobilization (Figure 3.45) and achieved 70 % of the maximal response of A23187. A similar pattern was found after addition of trypsin to cells (Figure 3.46) which achieved just over 20 % of the maximal response stimulated with A23187. As with tryptase, PAR-2 RP stimulated mobilization of calcium, but there was a slight increase over that with tryptase and less than 15 % of the maximal response of A23187 (Figure 3.47). When compared to the basal calcium flux detected in the presence of EDTA, all agents used (even at the submaximal concentrations) elicited a significant increase in peak fluorescence, except for the PBS and LSIGRL-NH_2 controls (Figure 3.48).

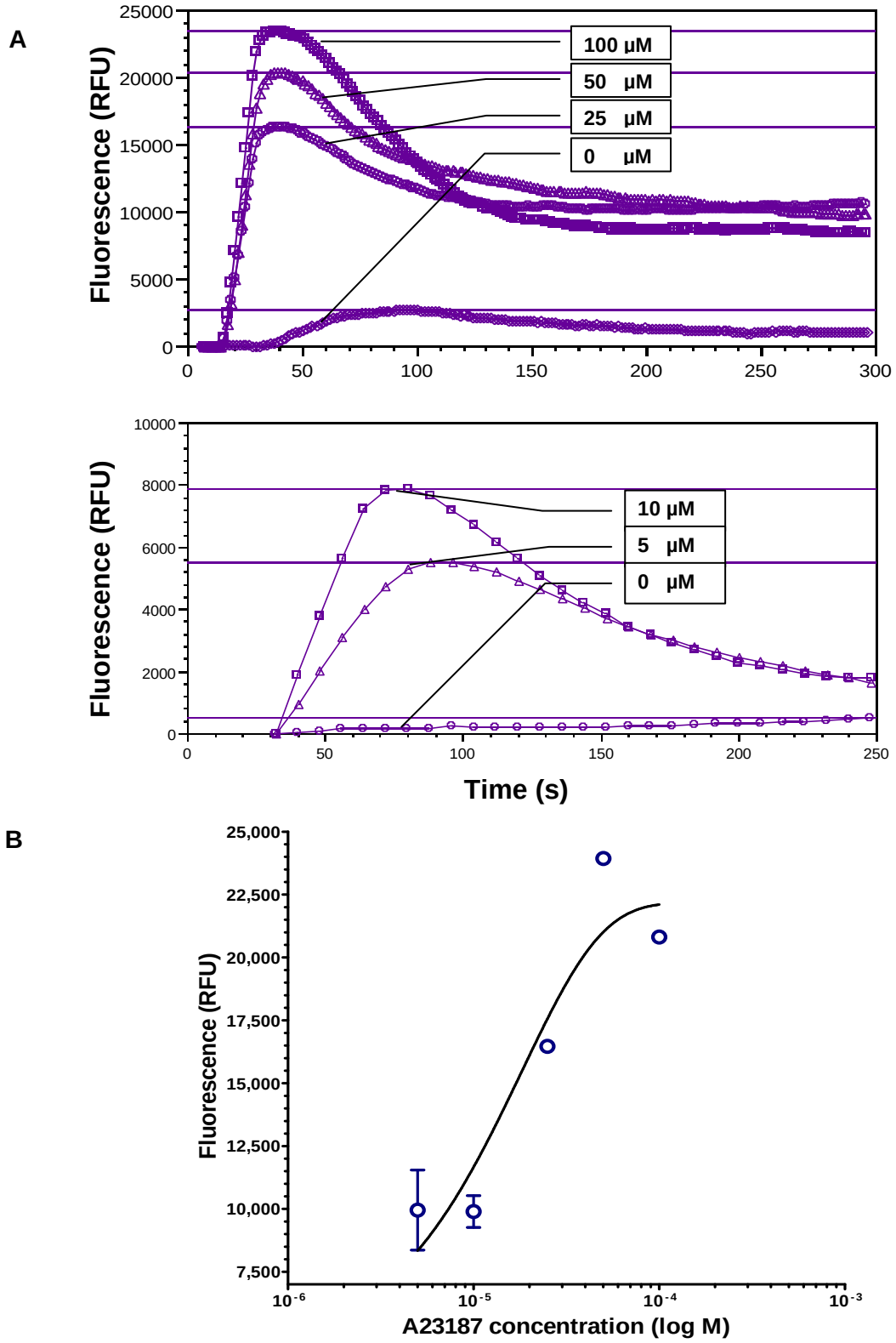

Figure 3.43 Calcium ionophore-induced calcium mobilisation in HUVECs. (A) Representative traces showing alterations in fluorescence induced by calcium ionophore A23187 at 5, 10, 25, 50 or 100 µM. (B) Peak fluorescence changes fitted to a four parameter curve. Data are expressed as mean ± SEM of five independent experiments.

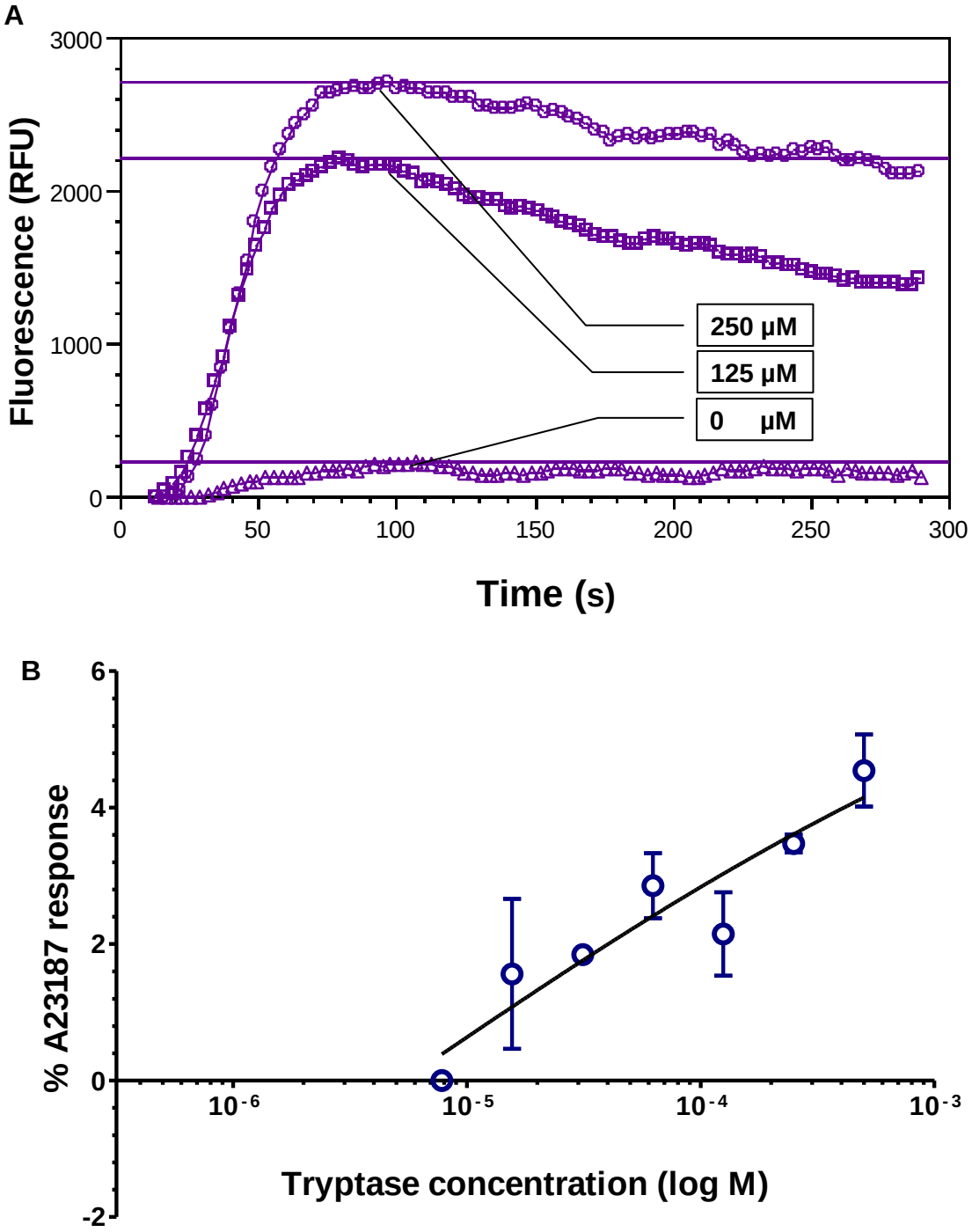

Figure 3.44 Tryptase-induced calcium mobilisation in HUVECs. (A) Representative traces showing alterations in fluorescence induced by 125 and 250 µM (25-50 mUml) of tryptase. (B) Peak fluorescence changes induced by different concentrations were normalized by the maximal response mediated by calcium ionophore A23187 (100 µM). Data are expressed as mean ± SEM of three independent experiments.

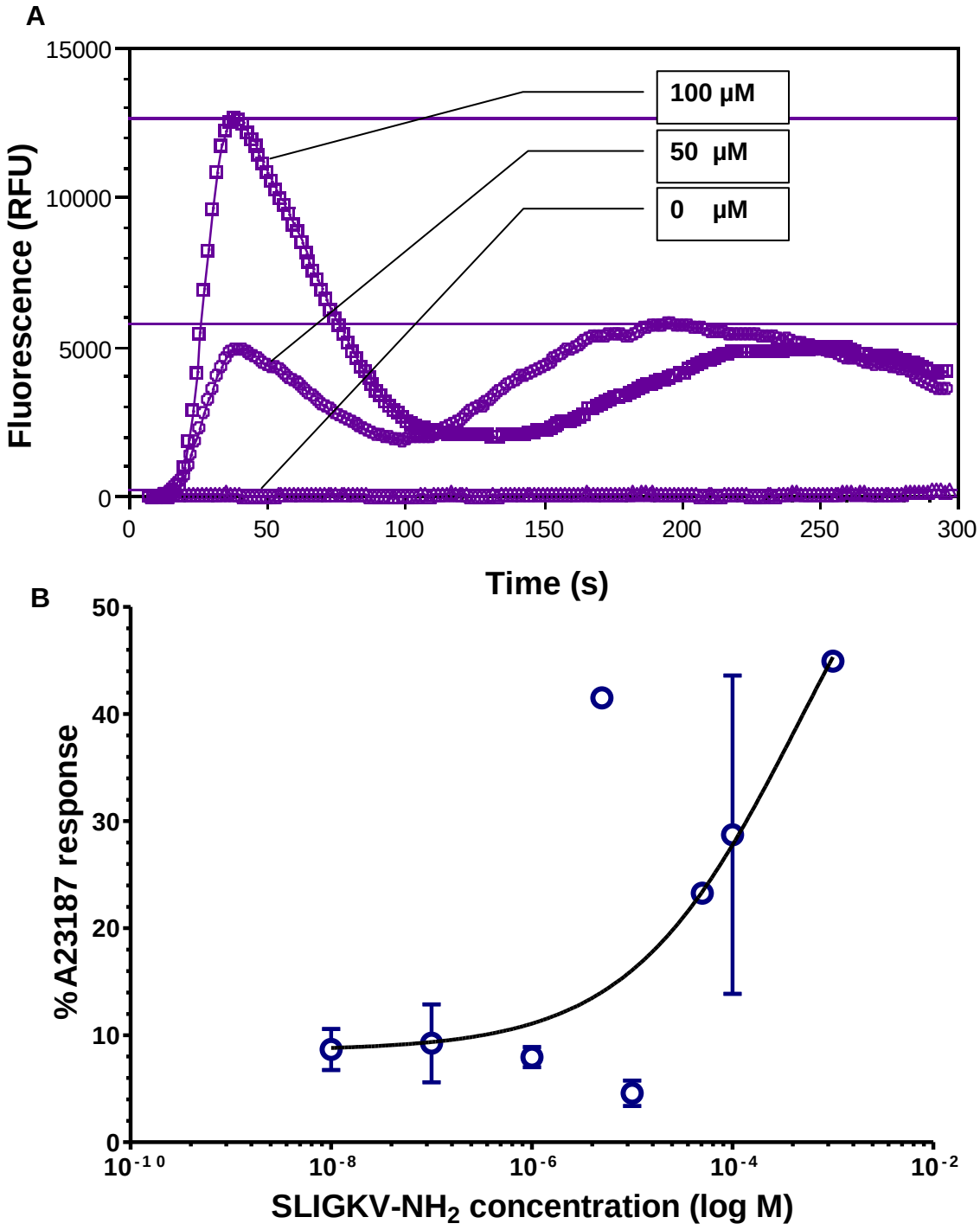

Figure 3.45 PAR-2 peptide agonist-induced calcium mobilisation in HUVECs. (A) Representative traces showing alterations in fluorescence induced by SLIGKV-NH_2 at 50 and 100 µM. (B) Peak fluorescence changes induced by different concentrations were normalized by the maximal response mediated by calcium ionophore A23187 (100 µM). Data are expressed as mean ± SEM of three independent experiments.

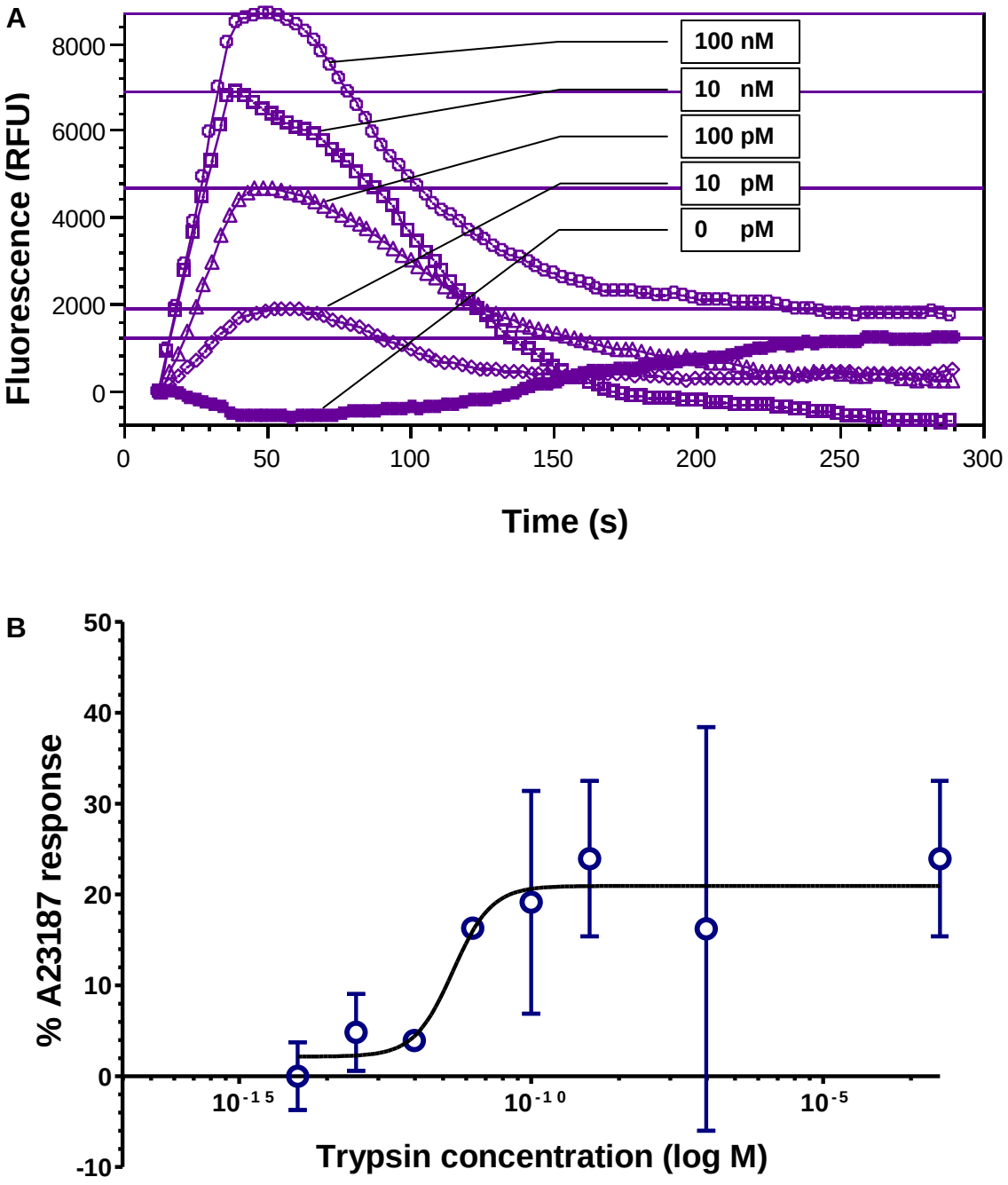

Figure 3.46 Trypsin-induced calcium mobilisation in HUVECs. (A) Representative traces of alterations in fluorescence induced by trypsin at 10 pM to 100 nM (0.3 mU/ml to 30 U/ml). (B) Peak fluorescence changes induced by different concentrations were normalized by the maximal response mediated by calcium ionophore A23187 (100 µM). Data are expressed as mean ± SEM of two independent experiments.

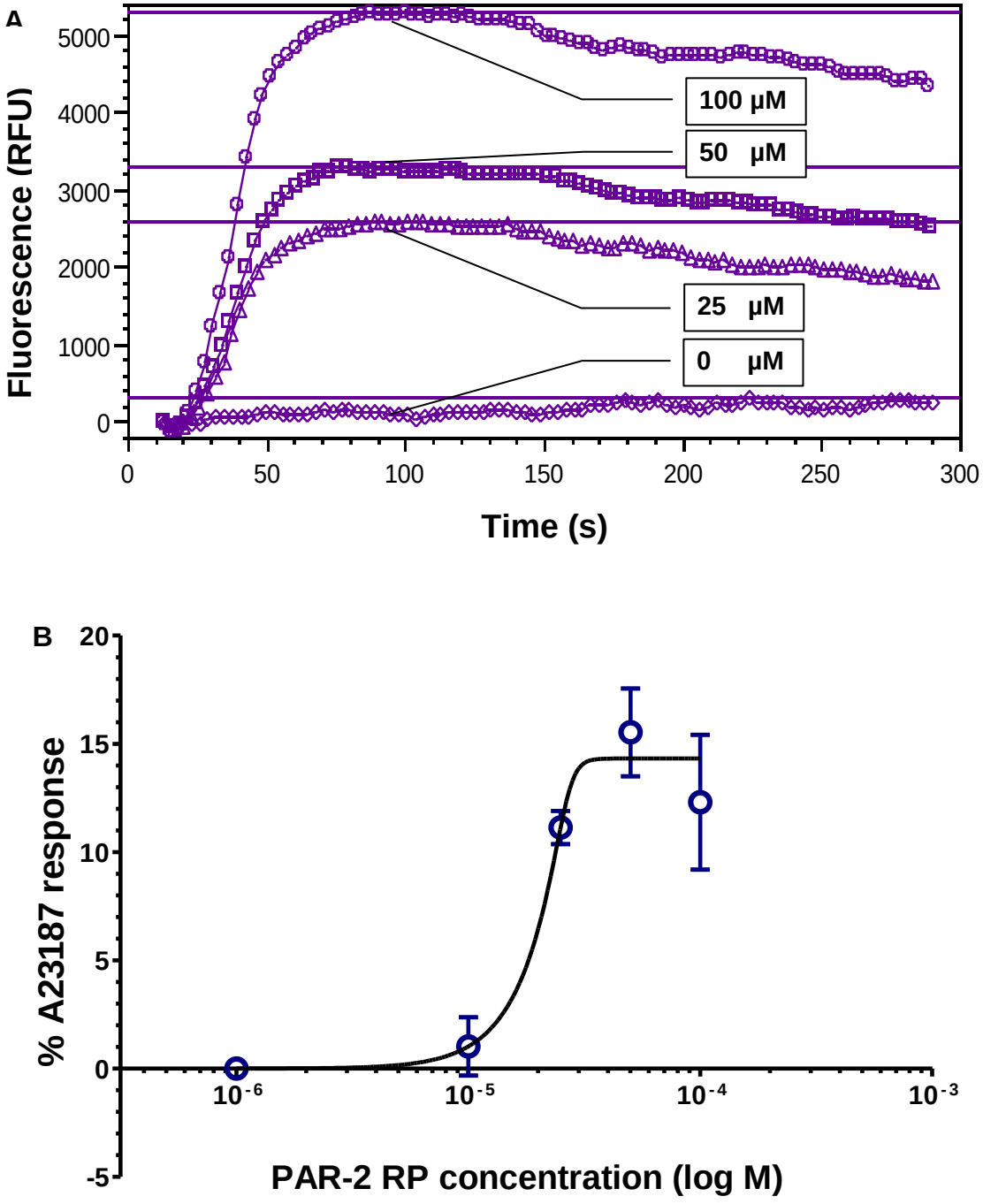

Figure 3.47 PAR-2 RP-induced calcium mobilisation in HUVECs. (A) Representative traces of alterations in fluorescence induced by PAR-2 RP at 25, 50 or 100 µM. (B) Peak fluorescence changes induced by different concentrations were normalized by the maximal response mediated by calcium ionophore A23187 (100 µM). Data are expressed as mean ± SEM of six independent experiments.

Table 3.9 Calcium flux as indicated by the maximal fluorescence response stimulated by addition of various agents to HUVECs, and that of the half maximal effective concentration (EC_{50}) as normalized to the response with calcium ionophore of A23187. RFU; reference fluorescence unit.

	Maximum response		EC_{50} response		
	Fluorescence (RFU)	% A23187 response	EC_{50} (M)	Fluorescence (RFU)	% A23187 response
A23187	22372	100	2.5×10^{-5}	16152	100
Tryptase	1916	8.6	4.9×10^{-5}	321	2
SLIGKV-NH_2	15687	70.1	4.7×10^{-4}	6354	39.3
Trypsin	5110	22.8	4.562×10^{-12}	1964	12.2
PAR-2 RP	3204	14	2.1×10^{-5}	1156	7.2

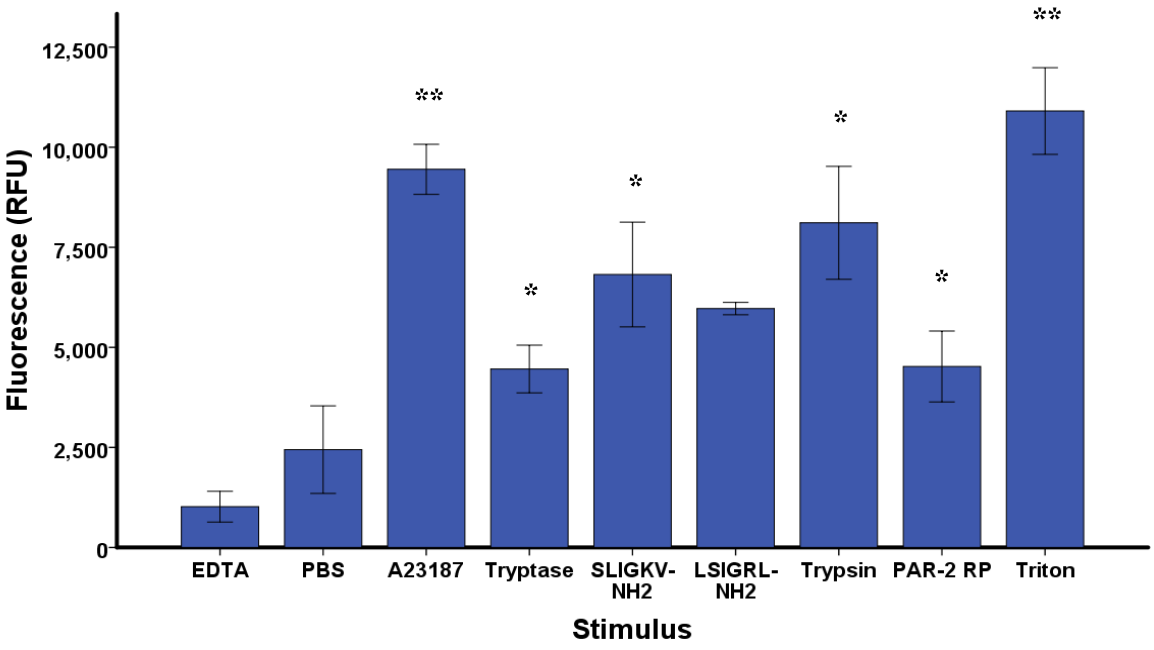

Figure 3.48 Calcium flux as indicated by peak fluorescence changes with EDTA (1 M); PBS; Triton X 100, (10 %); A23187 (5 µM); trypsin (50 µM); tryptase (100 µM); PAR-2 RP (100 µM); SLIGKV-NH_2 (100 µM) or LSIGRL-NH_2 (100 µM). Data expressed as mean ± SEM. * $P<0.05$, compared to the basal calcium levels (in the presence of EDTA at 1 M). Mann-Whitney U test follows Kruskal-Wallis test.

Pre-incubation of HUVECs with pertussis toxin for 24 h was found to decrease the mobilization of cytosolic calcium induced by tryptase. When cells pre-incubated with the PAR-2 peptide antagonist FSLLRY-NH_2 there was also a trend for decreased calcium flux with tryptase but this was significant only at the highest tryptase concentrations tested. Pre-treatment of cells with pertussis toxin or the PAR-2 peptide antagonist did not significantly reduce the calcium flux response to PAR-2 RP (Figure 3.49).

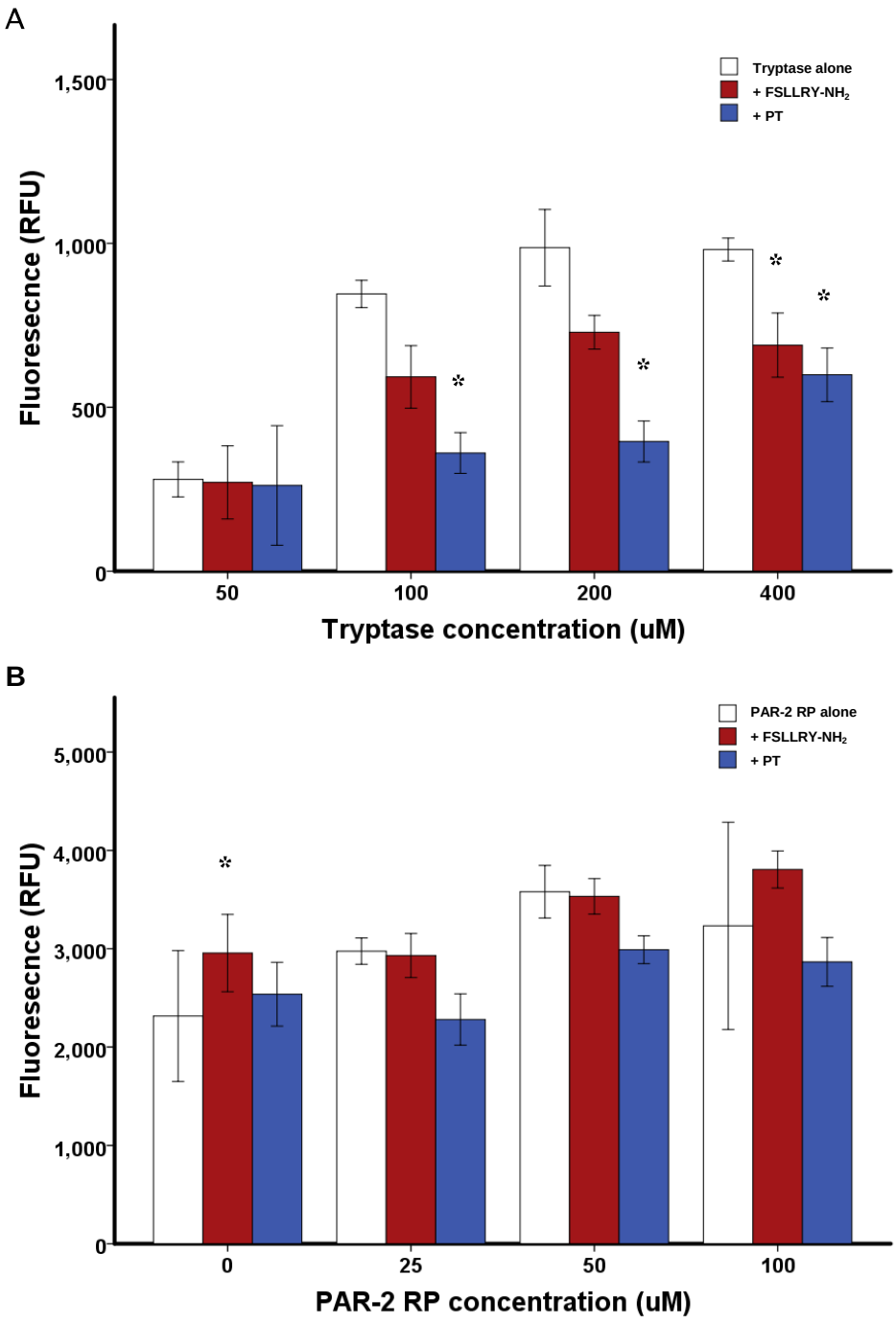

Figure 3.49 Calcium flux in HUVECs and the effect of the peptide PAR-2 antagonist FSLLRY-NH_2 (100 µM) or after blockage of G-proteins with pertussis toxin (PT, 100 ng/ml) on (A) tryptase or (B) PAR-2 RP response. Data expressed as mean ± SEM. n=3 , * P<0.05, compared to the response in cells without pre-treatment at the corresponding concentration. Mann-Whitney U test follows Kruskal-Wallis test.

3.5 The PAR-2 released peptide (PAR-2 RP)

3.5.1 Cloning of PAR-2 RP

Examination of PCR products of PAR-2 RP on 2 % agarose gel revealed bands of the predicted molecular weight (108bp) as well as some bands at higher molecular weight (Figure 3.50). Bands were cut, digested, cleaned and then inserted into pET-52b$^{(+)}$. The ligated plasmid showed bands of the predicted molecular weight (400 bp) on 2 % agarose gel (Figure 3.51) which transformed into XL-1-blue competent cells. Colonies of BL 21-codon plus competent *E. coli* expressing PAR2-RP were cultured and lysed to release the peptide. Cell lysate preparations of PAR-2 RP were purified using a Talon metal affinity resin column, monitoring the purification by dot blotting with anti-poly-his tag monoclonal antibody (Figure 3.52). On 6 M urea tricine gels, cloned PAR-2 RP peptide of the predicted size (3.6 kDa) was not detected, possibly on account of breakdown or aggregation of this peptide. For the synthetic PAR-2 RP peptide, there was a band at 3.6 kDa and a larger band was present at about 1 kDa (Figure 3.53). Attempts to perform western blotting for the cloned PAR-2 RP were unsuccessful with all of the specific antibodies tested.

3.5.2 Binding to PAR-2 RP by specific antibodies

Dot blotting with the synthetic PAR-2 RP indicated that monoclonal antibodies P2A, P2C and rabbit antiserum P2 could react, but not monoclonal antibodies P2B or P2D, or rabbit antisera K, L, M, N or O (Figure 3.54). The result of dot blotting were confirmed by western blotting as synthetic PAR-2 RP reacted with monoclonal antibody P2A and rabbit antiserum P2 but not with monoclonal antibodies P2C, P2B or P2D, or rabbit antisera K, L, M, N or O (Figure 3.55). When all antibodies were tested in direct ELISA for binding with PAR-2 RP, a positive reaction was found with monoclonal antibodies P2A and P2B and rabbit antisera K and P2, and not with the other antibodies tested. When different pairs of these antibodies were investigated in sandwich ELISA, the only combination that gave a suitable concentration response curve was with the monoclonal P2A and rabbit antiserum P2. Optimal concentrations of each antibody in an assay for PAR-2 RP were selected following comparison of several dilutions of monoclonal antibody P2A and rabbit antiserum P2 (data not shown).

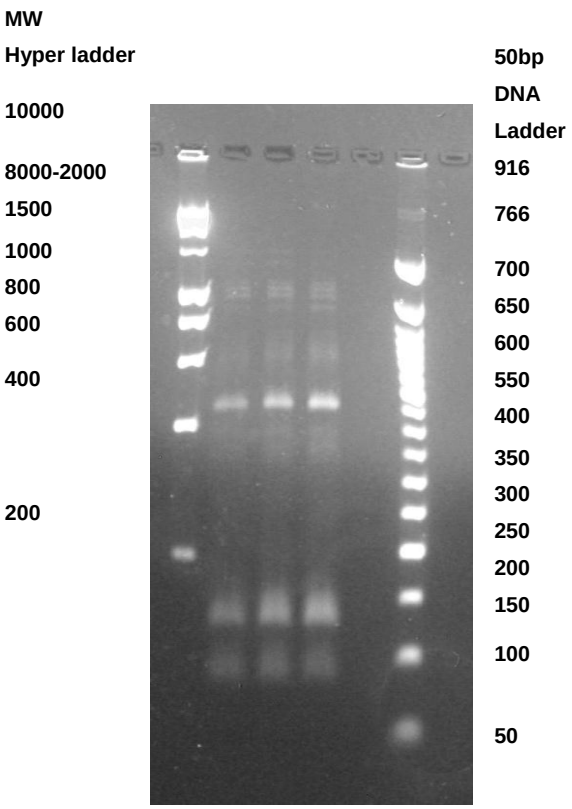

Figure 3.50 PCR product of cloned PAR-2 RP on 2 % agarose gel using two molecular weight markers (Hyper ladder I, Bioline and 50bp DNA ladder, BioLabs).

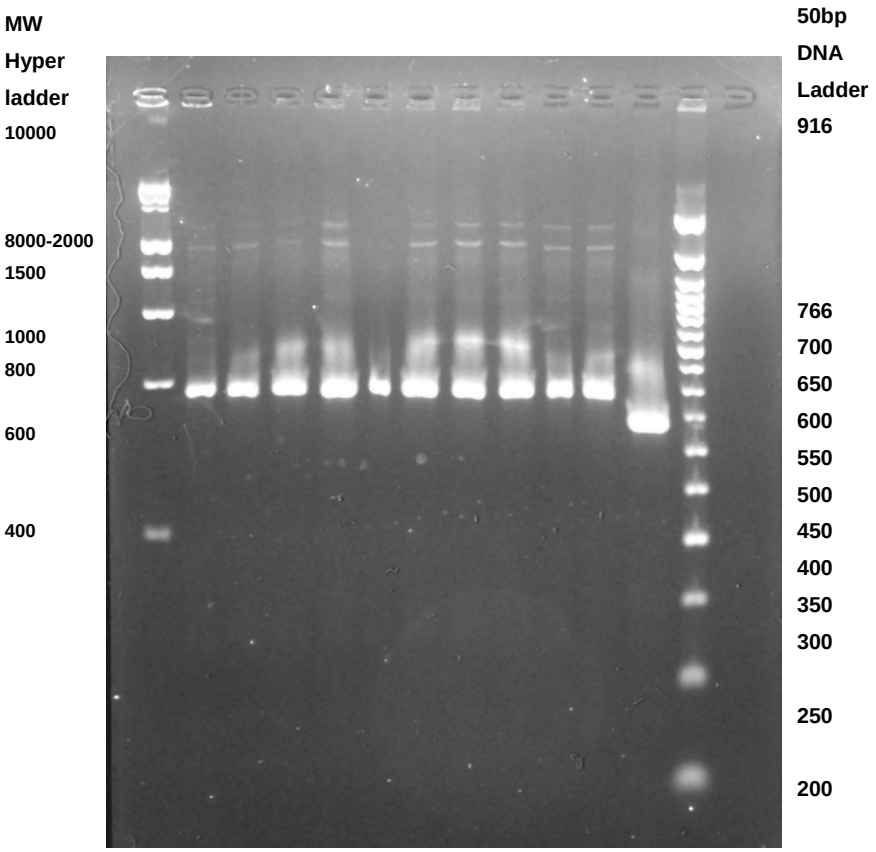

Figure 3.51 PCR product of PET 52$^{(+)}$ cell colonies on 2 % agarose gel using two molecular weight markers (Hyper ladder I, Bioline and 50bp DNA adder, BioLabs).

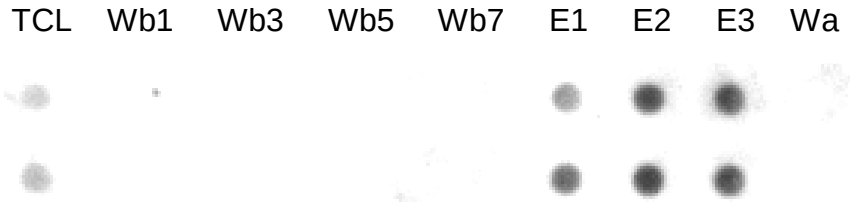

Figure 3.52 Dot blot analysis with anti-poly-his tag monoclonal antibody of total lysate (TCL) of BL21- codon plus transfected with PAR-2 RP, fractions eluted (E1, E2, E3) from the talon metal affinity resin. Dots for wash buffer, before elution (Wb) and after elution (Wa) are indicated.

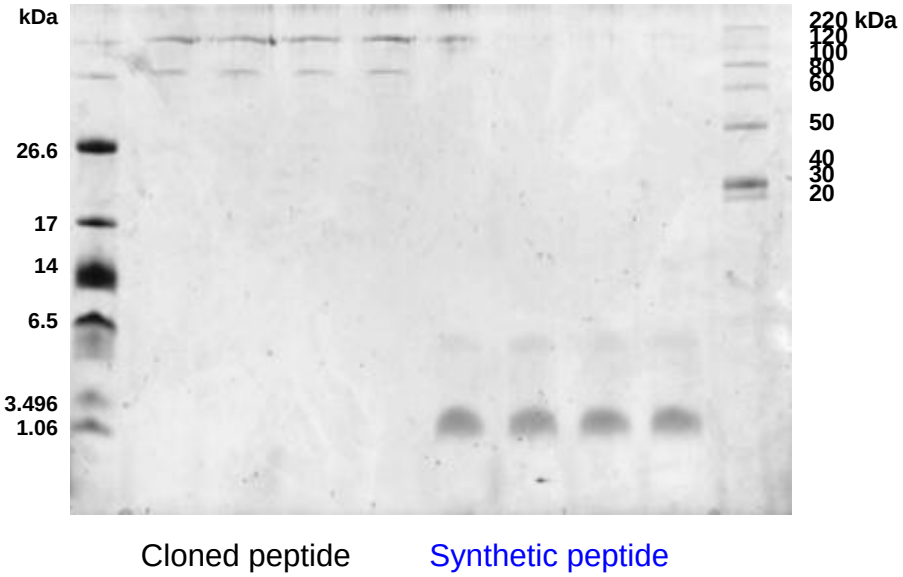

Figure 3.53 Coomassie blue stained 6M urea-tricine gel of purified preparations and the synthetic PAR-2 RP (four replicates shown for each). Molecular weight markers for the range 1.06 to 26.6 kDa and 20 to 230 kDa are shown.

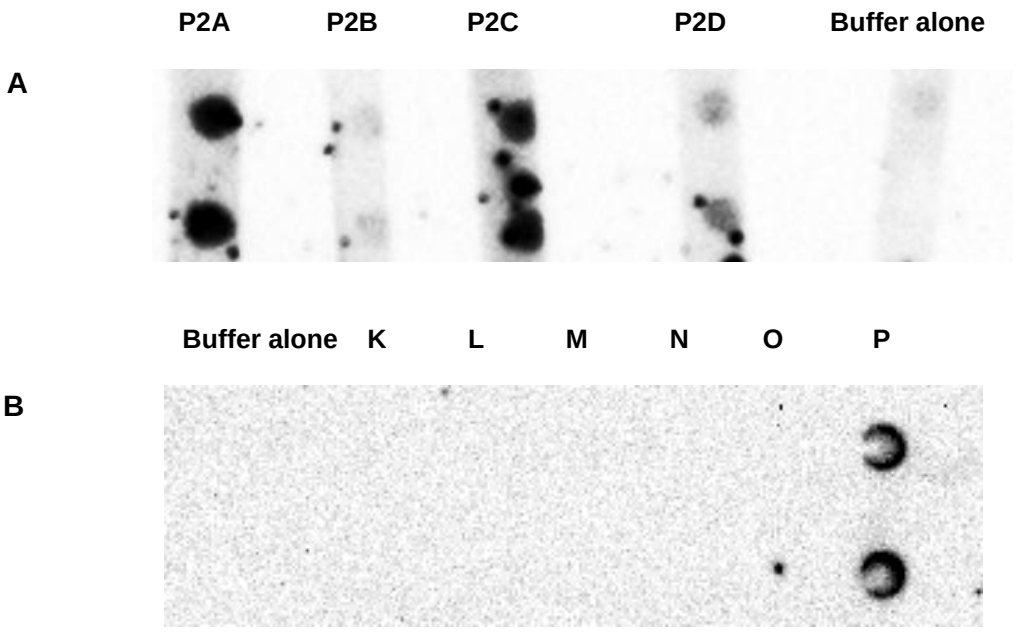

Figure 3.54 Dot blotting of synthetic PAR-2 RP with (A) PAR-2 specific monoclonal antibodies P2A, P2B, P2C and P2D, and (B) rabbit antisera K, L, M, N and P. Buffer alone was included as a negative control.

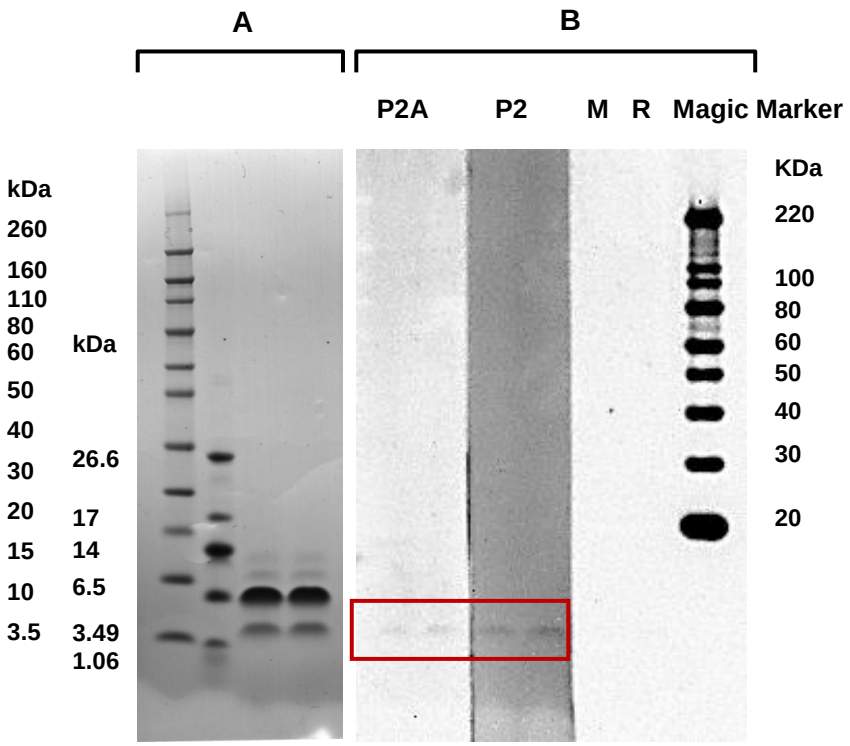

Figure 3.55 (A) SDS-PAGE and (B) western blotting of synthetic PAR-2 RP with PAR-2 specific monoclonal antibody P2A, rabbit antiserum P2 or mouse IgM (M) or rabbit IgG fraction (R) isotype controls are indicated. Molecular weight markers are indicated.

Various assay conditions were investigated including dilution of PAR-2 RP with PBS, PBS-T and various concentrations of NaCl in PBS or H_2O (Figure 3.56). A good standard curve was obtained with PAR-2 RP in 0.2 M NaCl in PBS with rabbit antiserum P2 diluted 1/100 and monoclonal detecting antibody P2A diluted 1/1000. Both the synthetic and the cloned form of PAR-2 RP reacted in the sandwich ELISA, but more consistent results were obtained with the synthetic peptide, and for this reason all subsequent experiments were performed with the synthetic peptide.

3.5.3 Purification and labelling of mouse monoclonal P2A antibody

P2A was successfully purified from hybridoma cell culture supernatant using ammonium sulphate precipitation followed by thiophilic affinity based chromatography. Four fractions with high protein content from the Hitrap™ IgM purification HP column (from 3rd to 6th) were pooled and further analyzed by SDS-PAGE. Two well defined bands corresponding to the IgM heavy chain (~ 95 kDa) and light chain (~ 20 kDa) were observed on SDS-PAGE electrophoresis and their identity was confirmed by the binding of rabbit anti-mouse immunoglobulin in western blotting (Figure 3.57). The ammonium sulphate precipitation step was of limited use in purification of P2A, with multiple bands observed for this IgM monoclonal antibody.

Following purification, monoclonal antibody P2A was concentrated and adjusted to 1 mg/ml and conjugated successfully with the MSD® SULF0-TAG NHS ester using an ester to protein ratio of 100:1. The labelling incorporation ratio of ester to protein was 15, a value which was considered suitable for effective signal emission and optimal performance (according to the manufacturer's guidelines). The P2A-ester antibody conjugate was confirmed to react with the synthetic PAR-2 RP in dot blotting (Figure 3.58). The effectiveness of the labelling process was confirmed by employing the tagged antibody to detect the whole molecule of PAR-2 in HUVEC lysates using the MSD electrochemiluminescence (ECL) detection system (Figure 3.59). The P2A-ester conjugate was found to bind in a consistent and concentration-dependent manner.

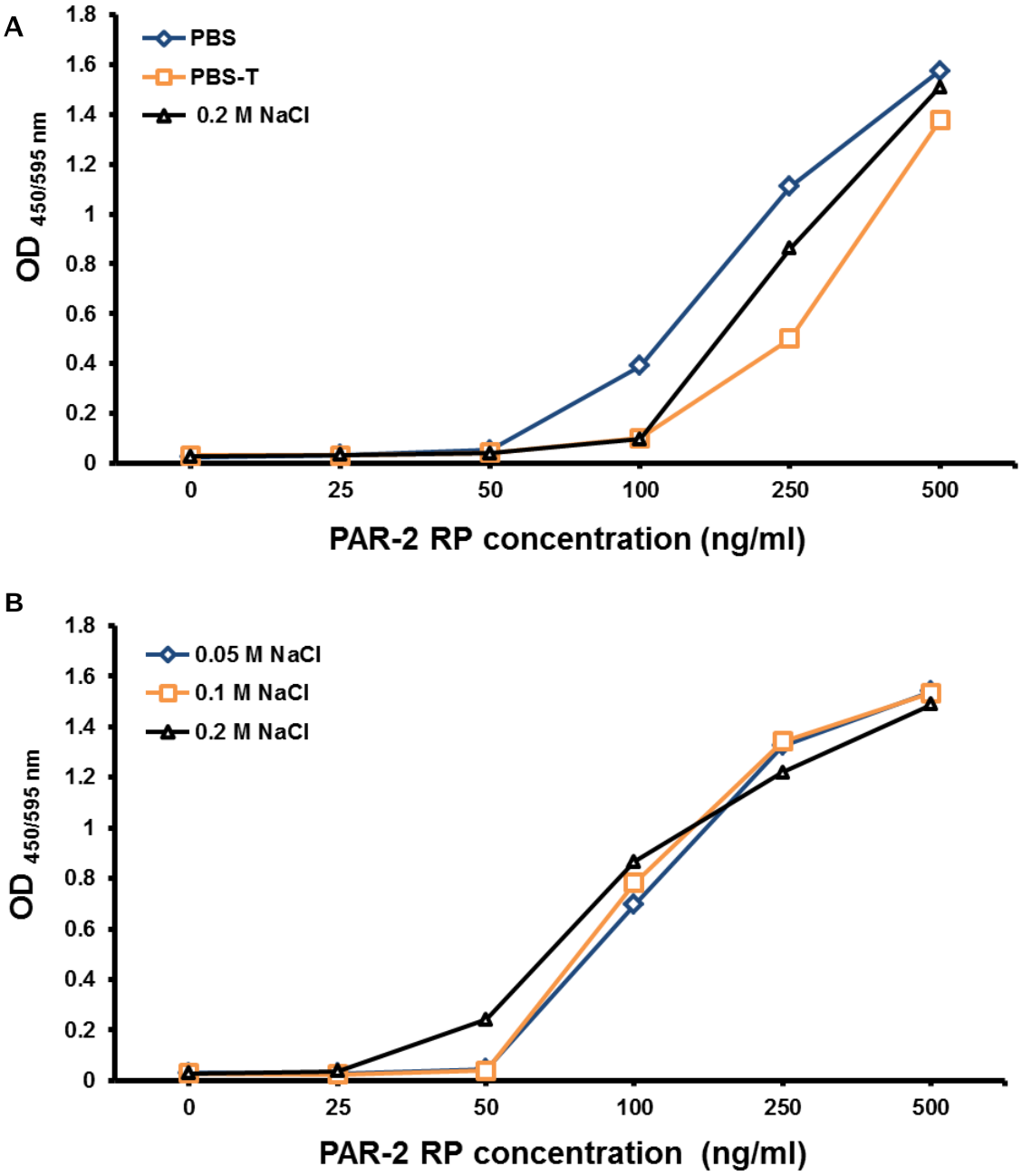

Figure 3.56 Standard curves with increasing concentrations of synthetic PAR-2 RP in sandwich ELISA with rabbit serum P2 as coating antibody and monoclonal P2A for detection. Effects of dilution of PAR-2 RP with (A) PBS, PBS with Tween 20 (PBS-T) or with 0.2 M NaCl, or with (B) 0.05 M, 0.1 M or 0.2 M NaCl. The means of duplicate measures are shown.

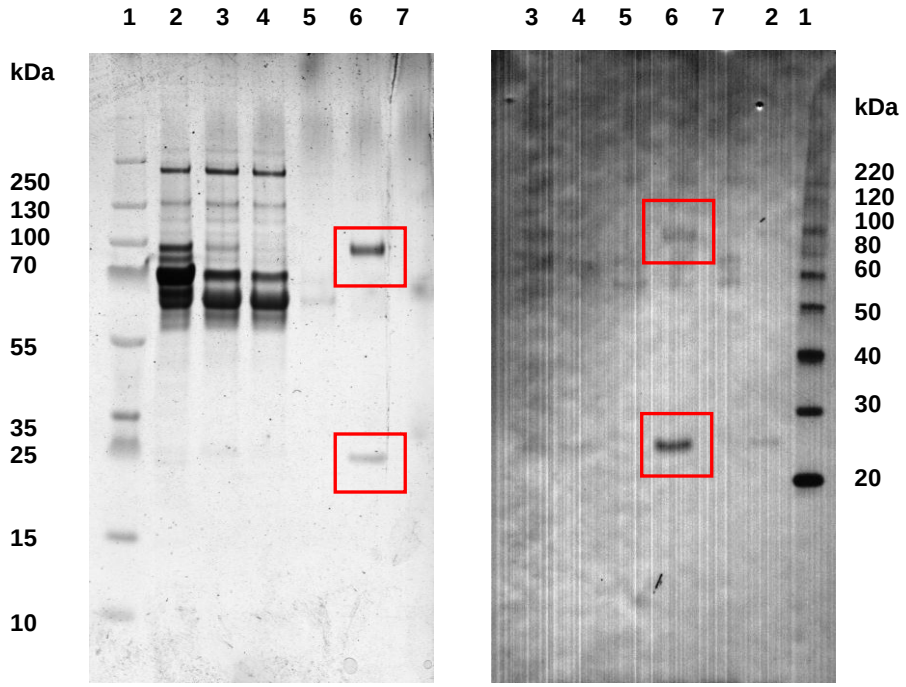

Figure 3.57 (A) Silver-stained SDS-PAGE and (B) Western blot of P2A antibody at different stages of fractionation on a HiTrap™ column. Lane 1: Molecular weight marker; lane 2: Monoclonal antibody P2A, lane 2; P2A in hybridoma supernatant; Lane 3: Fractions after ammonium sulphate precipitation; Lane 4: Flow through fractions of the column; Lane 5: wash fractions before elution; Lane 6: Eluted fractions; Lane 7: Wash fractions following elution. The IgM heavy chain (~ 95 kDa)are light chain (~ 25 kDa) and outlined using red rectangles.

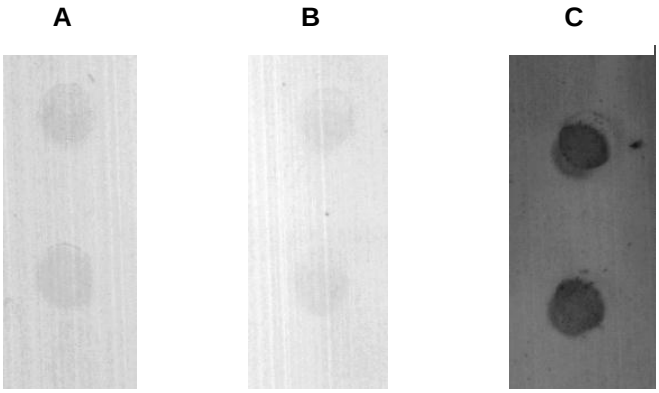

Figure 3.58 Dot blots (in duplicate) of synthetic PAR-2 RP (100 µM/ml) with (A) mouse monoclonal P2A antibody in hybridoma supernatant (1/100 dilution), (B) P2A-ester conjugate (15:1) (1/5000 dilution), and (C) rabbit antiserum P2 (1/100 dilution).

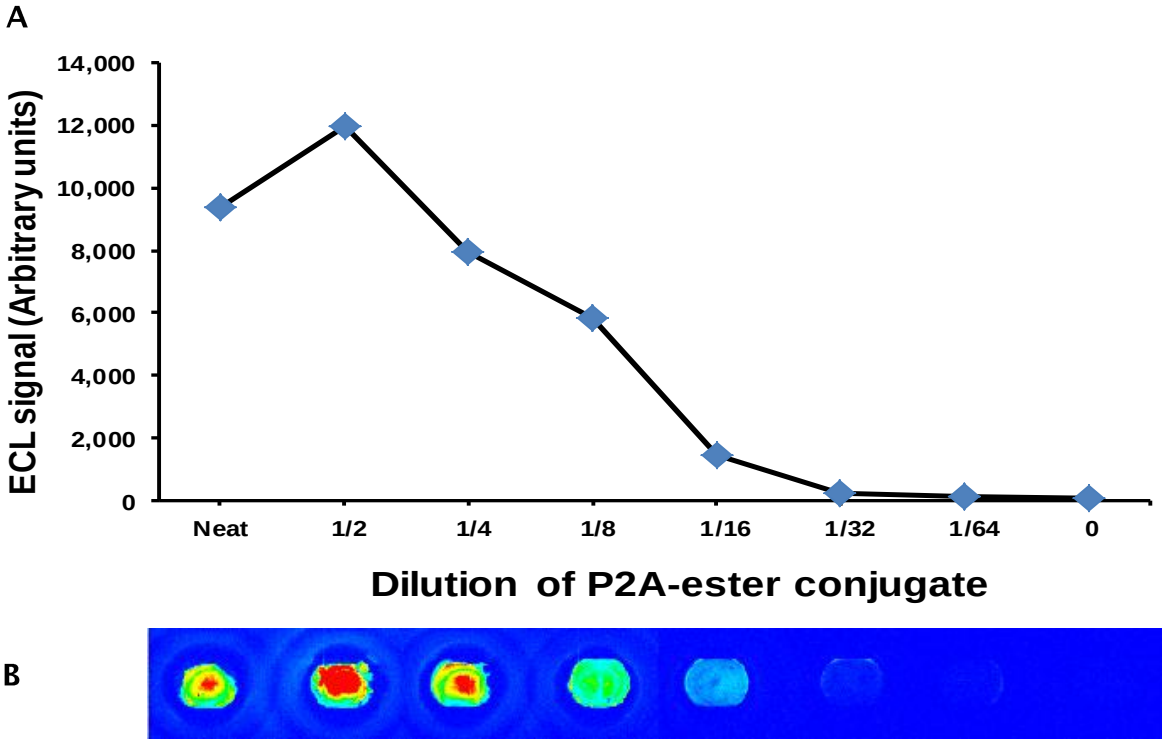

Figure 3.59 Detection of PAR-2 in a HUVEC lysate using P2A-ester conjugate in MSD ECL platform. (A) Electrochemiluminescence (ECL) signal of serial dilutions of a 1 mg/ml solution of P2A-ester conjugate and (B) the corresponding signal image. The means of duplicate measures are shown.

3.5.4 Detection of PAR-2 RP in clinical samples

The ELISA developed allowed the detection of synthetic PAR-2 RP added to buffer (Figure 3.60). However, it failed to detect PAR-2 RP in samples of cell culture supernatants including those of the 16HBE cell line, HUVECs or keratinocytes (Figure 3.60 A). The PAR-2 RP assay was affected by interference in clinical samples including serum from cases of anaphylaxis, synovial fluid from patients with osteoarthritis (Figure 3.60 B), broncho-alveolar lavage from asthmatic subjects, or nasal lavage fluid collected before and after allergen challenge in hay fever patients (Figure 3.61). In each case spiking of these samples with the synthetic PAR-2 RP led to almost complete loss of PAR-2 RP. For this reason we examined the potential for enzymatic degradation of PAR-2 RP.

As attempts to detect PAR-2 RP by ELISA were not successful, use of the MSD ECL detection platform was investigated. The standard curve generated using concentrations of the synthetic PAR-2 RP peptide had a lower limit of detection of 1000 ng/ml. In serum samples, direct reaction of P2A conjugate with PAR-2 RP resulted in a low signal which did not allow differentiation between samples from healthy or subjects with asthma or anaphylaxis (data not shown). Consistence differences on levels of PAR-2 RP in selected sputum samples were not observed and there were differences in dilution curves (Figure 3.62).

Although the ECL based MSD assay system has been reported to be unaffected by the interference caused by rheumatoid factors in an anti-drug antibody assay in serum samples, even without sample processing [234], partial removal of interference was observed when PAR-2 RP was spiked into serum samples from healthy subjects or from patients with food allergy or anaphylaxis. No marked difference was observed between samples obtained before or after food challenge (data not shown). In spite of high baseline levels, PAR-2 RP was detected in most clinical samples investigated including serum, plasma and saliva. In samples of these fluids collected from food allergic patients before and after diagnostic food challenge, differences were observed in PAR-2 RP levels (Figure 3.63). However, a consistent pattern was not observed and these pilot studies were not extended to a larger number of samples.

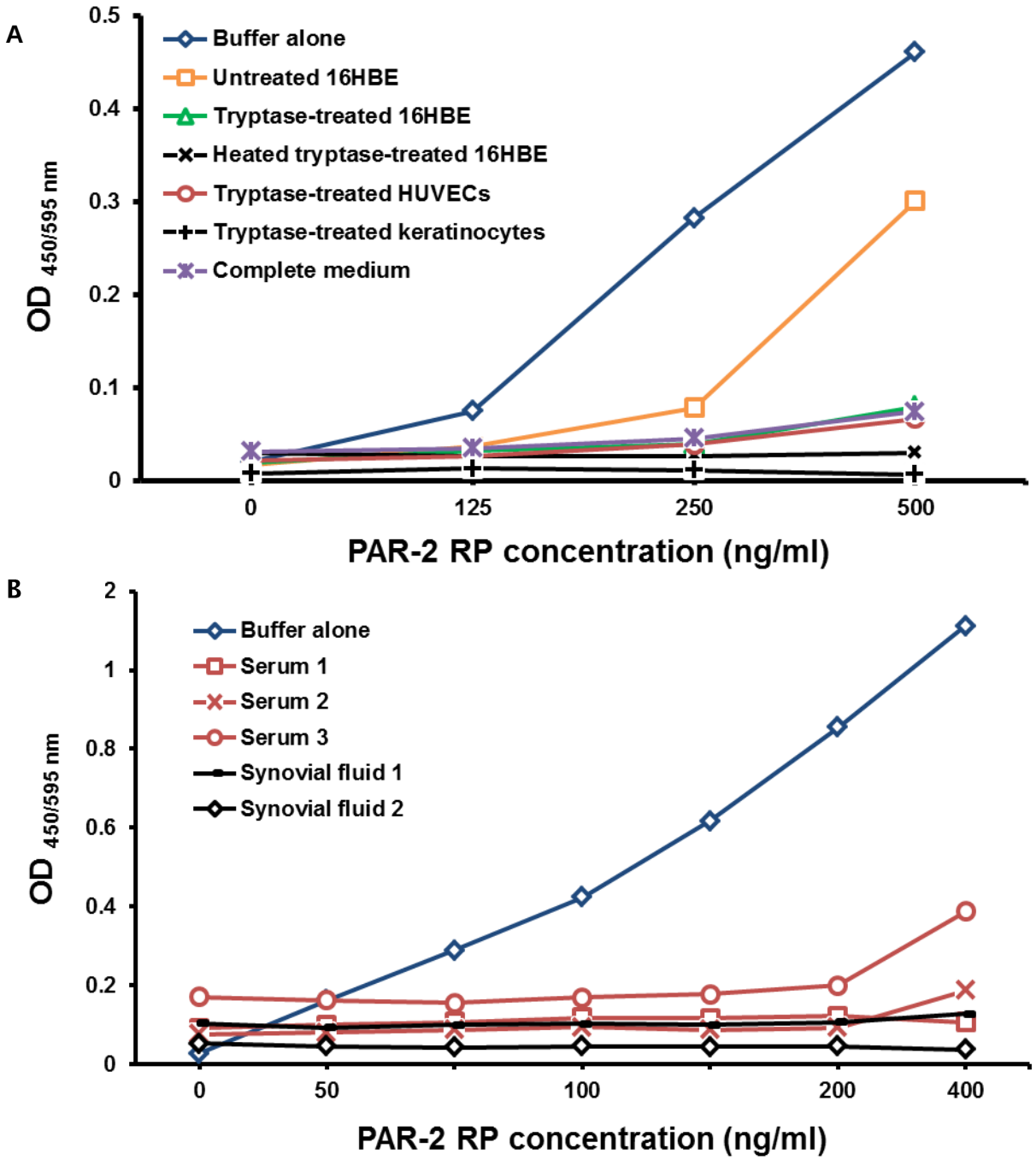

Figure 3.60 Sandwich ELISA of PAR-2 RP with rabbit antiserum P as capture antibody and monoclonal antibody P2A as detecting antibody. (A) Standard curve for PAR-2 RP diluted in 0.2 M NaCl in PBS, or spiked into culture supernatants from cells of the bronchial epithelial cell line 16HBE maintained in serum-free medium with or without incubation with tryptase (40 mU/ml) for 3 h, or with heated-tryptase for 3 h. Also examined were culture supernatants from HUVECs or keratinocytes maintained in medium with serum-free medium that had been incubated with tryptase (20 mU/ml). (B) Standard curve for PAR-2 RP in buffer alone or spiked into serum samples from cases of anaphylaxis (subjects 1, 2 and 3), or synovial fluid from cases of osteoarthritis (subjects 1 and 2). The means of duplicate measurement are shown.

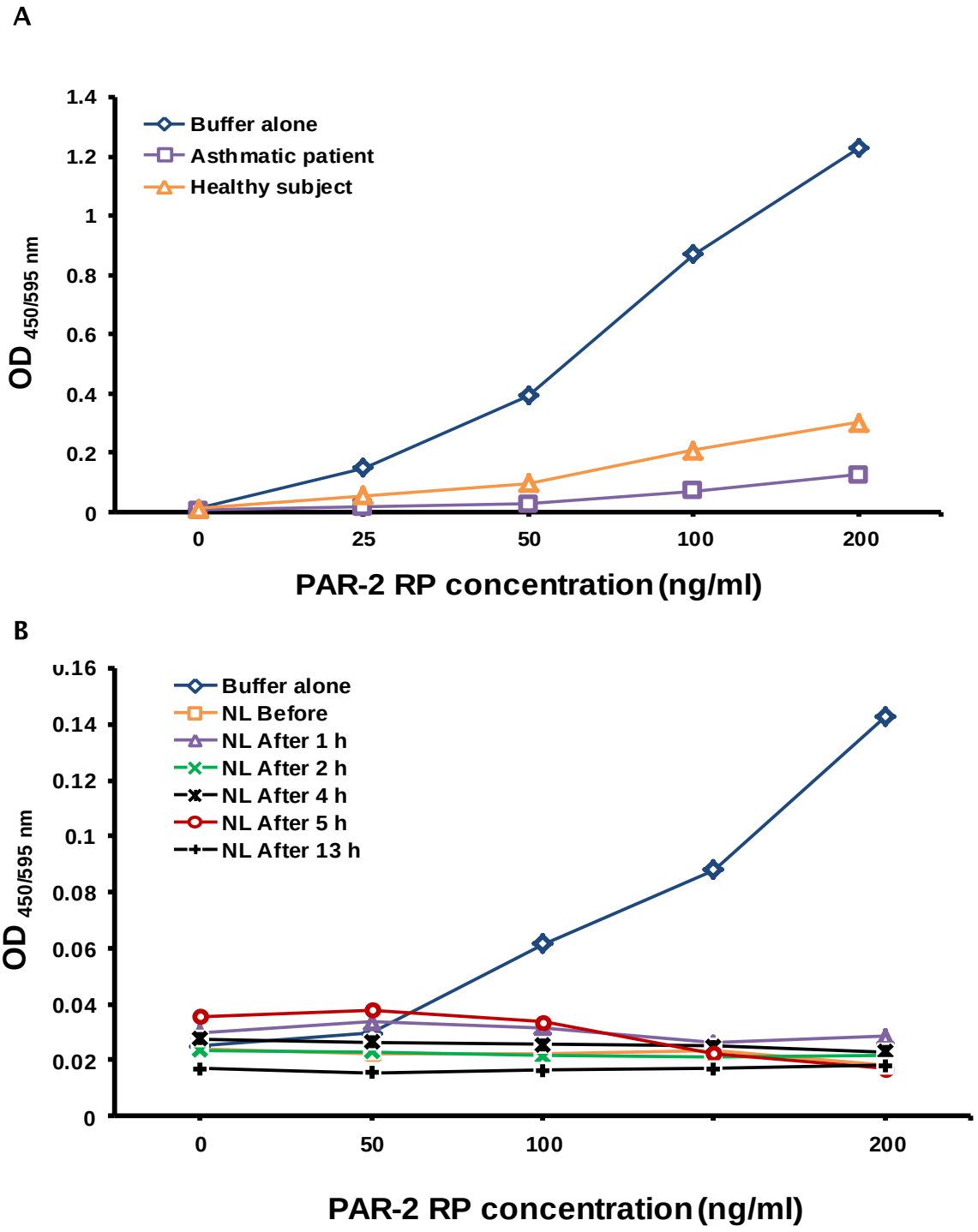

Figure 3.61 Sandwich ELISA of PAR-2 RP with rabbit antiserum P as capture antibody and monoclonal antibody P2A as detecting antibody. Standard curve of PAR-2 diluted in 0.2 M NaCl in PBS or spiked into (A) broncho-alveolar lavage from an asthmatic patient or a healthy subject or (B) nasal lavage (NL) fluid from a patient before and 1 h, 2 h, 4 h, 5 h or 13 h following grass pollen allergen challenge. The means of duplicate measurement are shown.

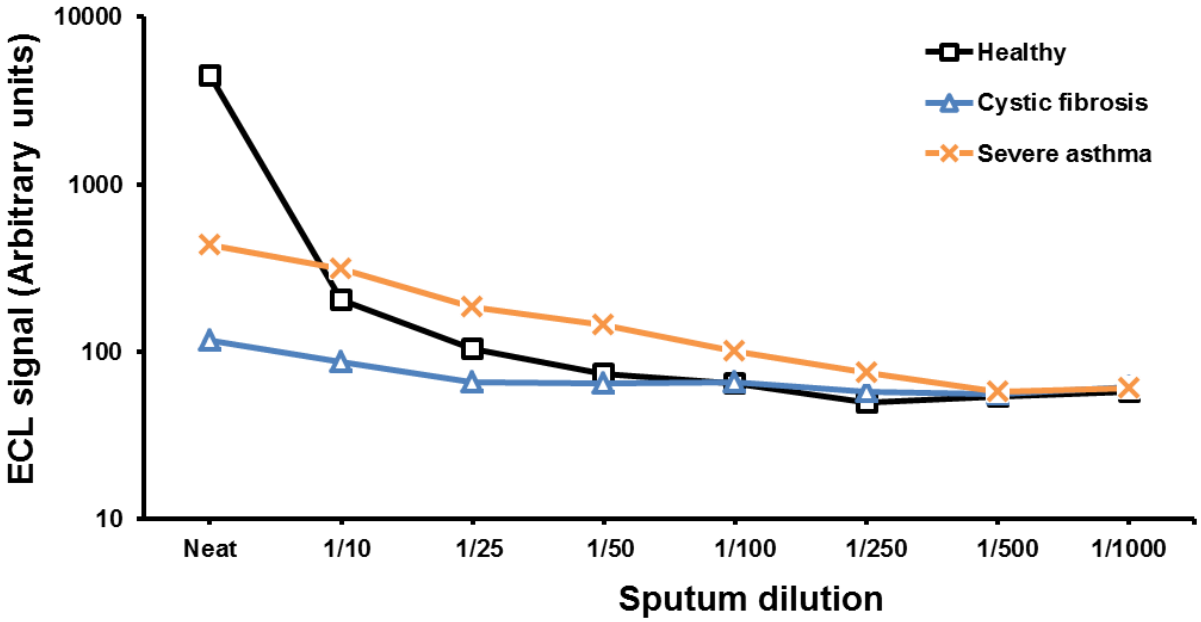

Figure 3.62 Detection of PAR-2 RP in sputum from a single healthy subject, a patient with cystic fibrosis and a patient with severe asthma with P2A-ester conjugate using MSD ECL platform. The means of duplicate measurement are shown.

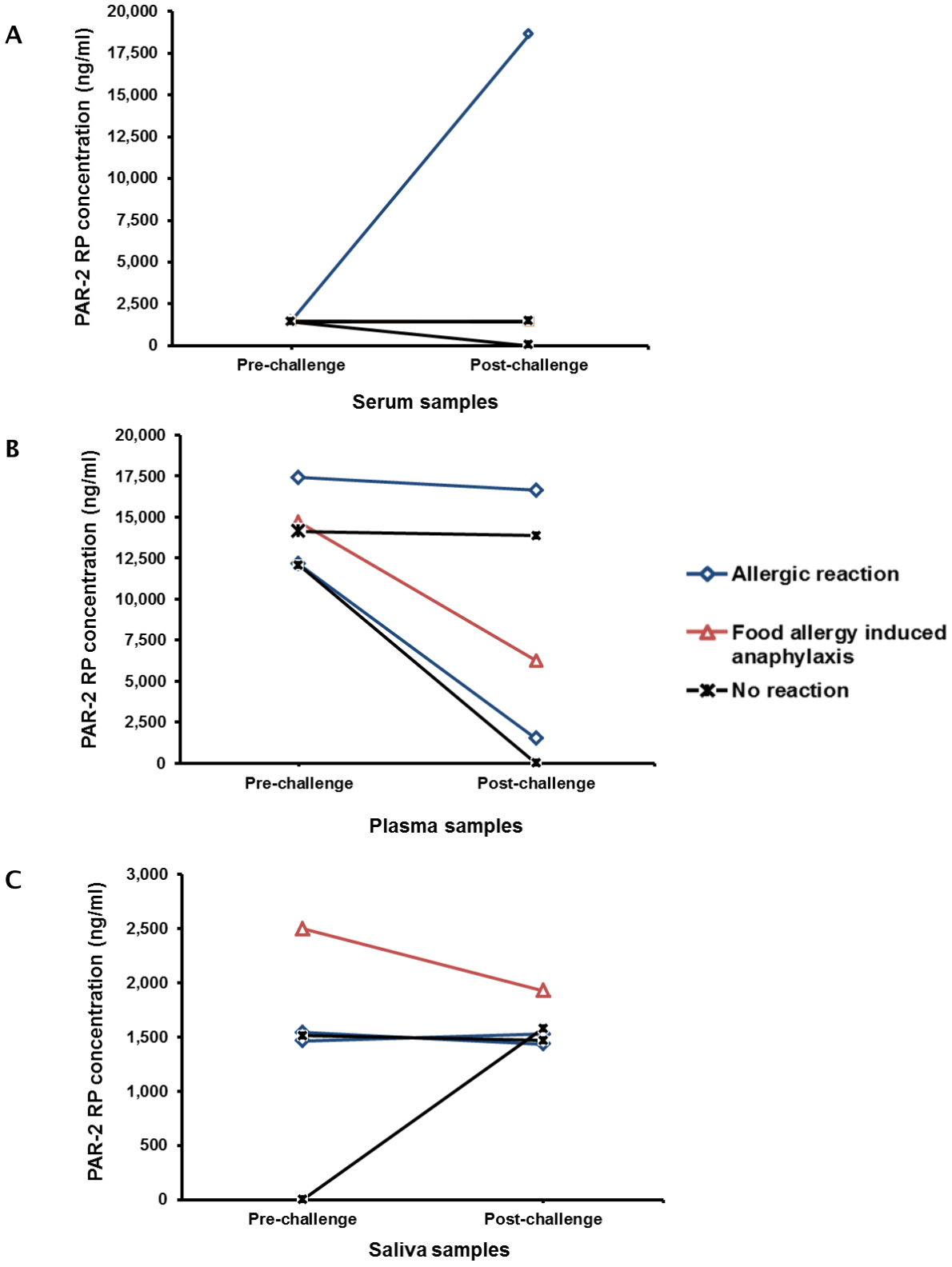

Figure 3.63 Detection of PAR-2 RP in samples of (A) serum, (B) plasma and (C) saliva (are diluted 1 in 2) from patients with history of food allergy, before and after food challenge. Two patients experienced food allergy symptoms, one patient had food allergy induced anaphylaxis patient and two patients had no reaction using the MSD ECL platform.

3.5.5 Stability of PAR-2 RP

Trypsin and tryptase are predicted to cleave PAR-2 RP at three cut points leaving a peptide with 29 amino acid length, using the PeptideCutter software programe (ExPASY Bioinformatics Resources) (Figure 3.64) [235]. By dot blotting, it was found that incubation of PAR-2 RP with either trypsin and to a lesser extent with tryptase led to loss of antigenicity (Figure 3.65). Investigation of PAR-2 RP on bis-Tris SDS-PAGE gels revealed that PAR-2 RP became aggregated into bands at 6.5 and 3.5 kDa at least under the conditions employed (Figure 3.66). Addition of trypsin resulted in the appearance of peptide bands at approximately 3.5 kDa and 1.1 kDa, a process that was apparent as early as 15 min (Figure 3.67). Degradation to a lesser extent was seen also when PAR-2 RP was incubated with tryptase, or even with buffer alone for 2 h.

When PAR-2 RP was analysed by reverse phase chromatography after 2 h incubation with proteases, a striking difference in pattern was not observed. However, there was three new peaks appeared following incubation with tryptase and six new peaks with trypsin (Figure 3.68).

Incubation of PAR-2 RP with trypsin or heating to 95°C for 10 minutes was associated with loss of the immunoreactivity to monoclonal antibody P2A when tested by ELISA (Figure 3.69). Incubation of PAR-2 RP with tryptase had a little effect on antibody binding by ELISA when investigated under similar conditions.

MR^{2}↓S^{3}PSAAWLLGAAILLAASLSCSGTIQGTNR^{31}↓S^{32}SK^{34}↓G^{35}R^{36}↓S^{37}LIGKV

Figure 3.64 Amino acid sequence of PAR-2 RP in black letters, with arrows indicating predicted cleavage points with trypsin. Amino acids in blue letters correspond to the PAR-2 RP tethered sequence.

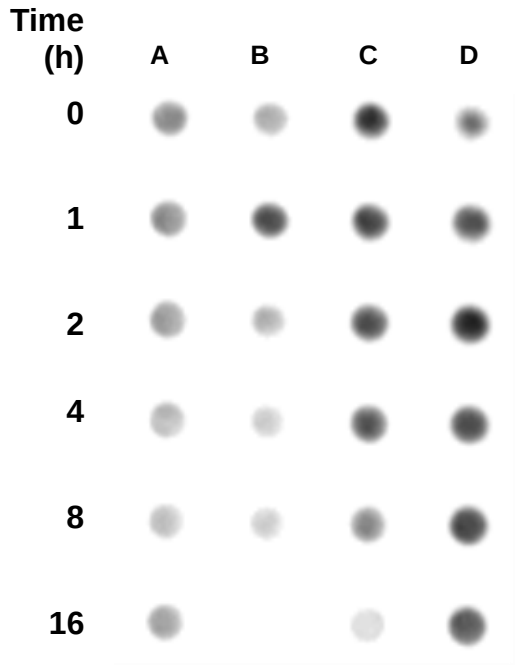

Figure 3.65 Dot blotting with antibody P2A of 10 µg/ml PAR-2 RP following incubation for up to 16 h with (A) buffer alone, (B) 100 U/ml trypsin, (C) 50 mU/ml recombinant tryptase, or (D) 50 mU/ml lung tryptase.

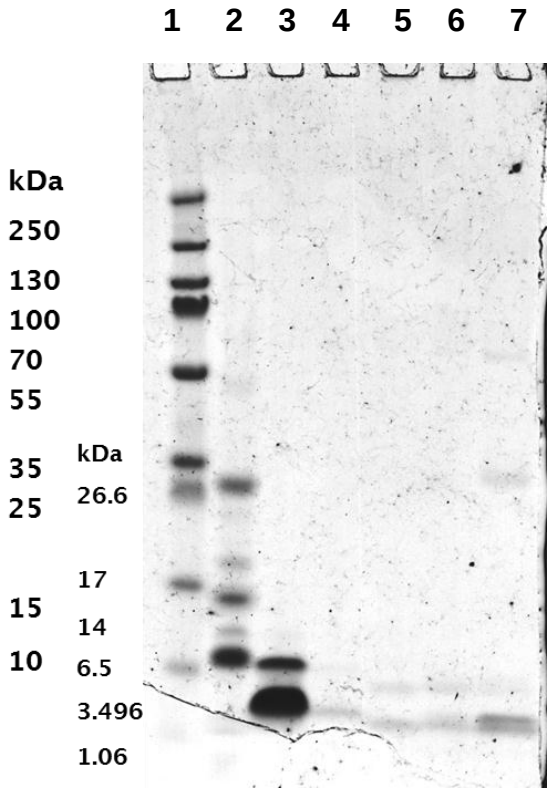

Figure 3.66 PAR-2 RP (1 mM) separated on bis-Tris SDS-PAGE 4-12 % gradient gel in non-reducing conditions after incubation with buffer alone at 37°C for 0 h (lane 3) or 2 h (lane 4), or 2 h incubation with 100 U/ml trypsin (lane 5); 50 mU/ml lung tryptase (lane 6) or 50 mU/ml recombinant tryptase (lane 7). Molecular weight markers are indicated (lanes 1 and 2).

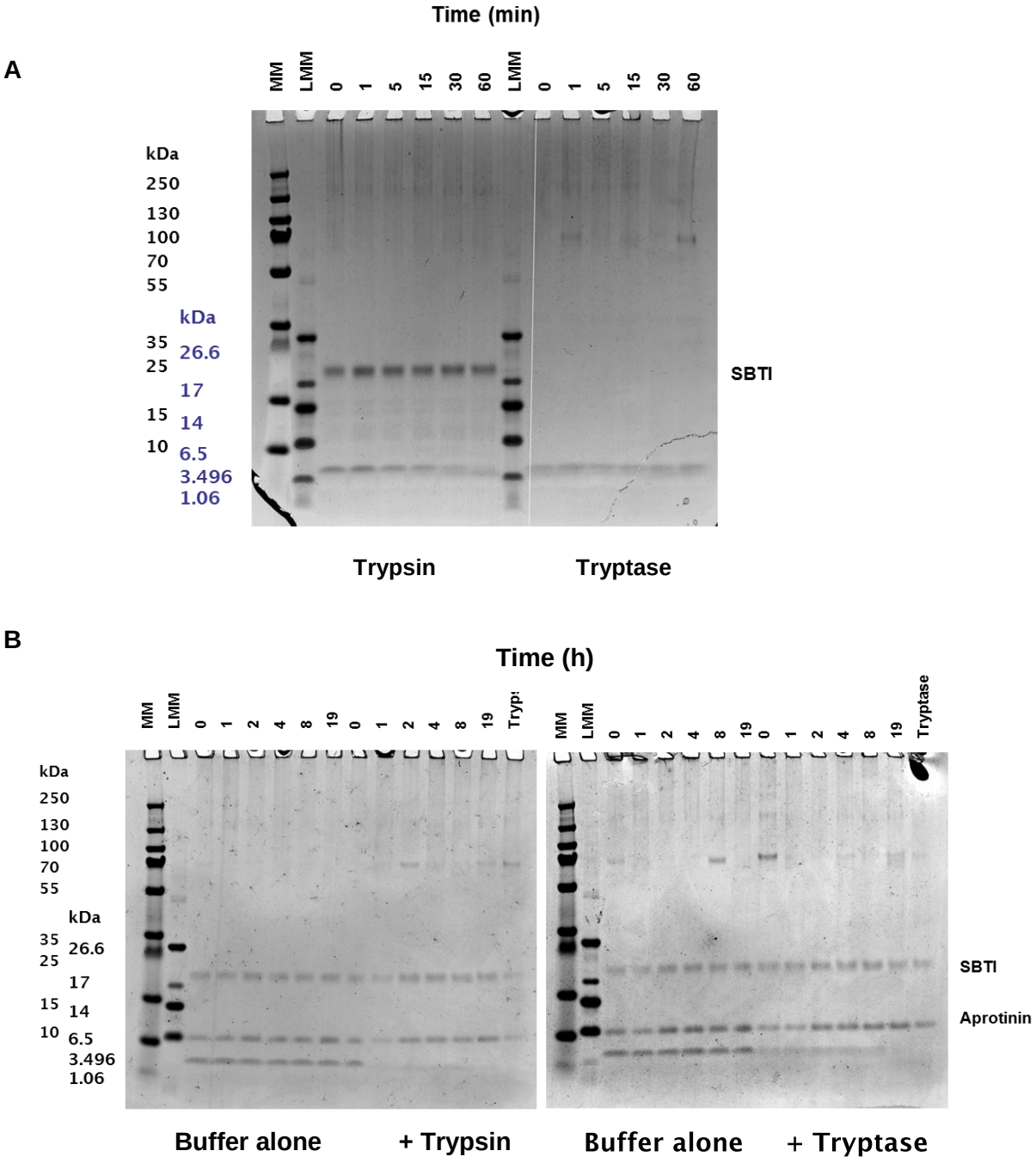

Figure 3.67 Digestion of PAR-2 RP following incubation with trypsin or tryptase for periods of (A) 0 to 60 minutes and (B) 0 to 19 h. Cleavage of PAR-2 RP by trypsin is apparent after 15 min incubation at 37°C (A) and by tryptase after 16 h (B). Bands for the protease inhibitors soybean trypsin inhibitor (STBI, 23.3 kDa) and aprotinin (6.5 kDa) are indicated as are the molecular weight markers.

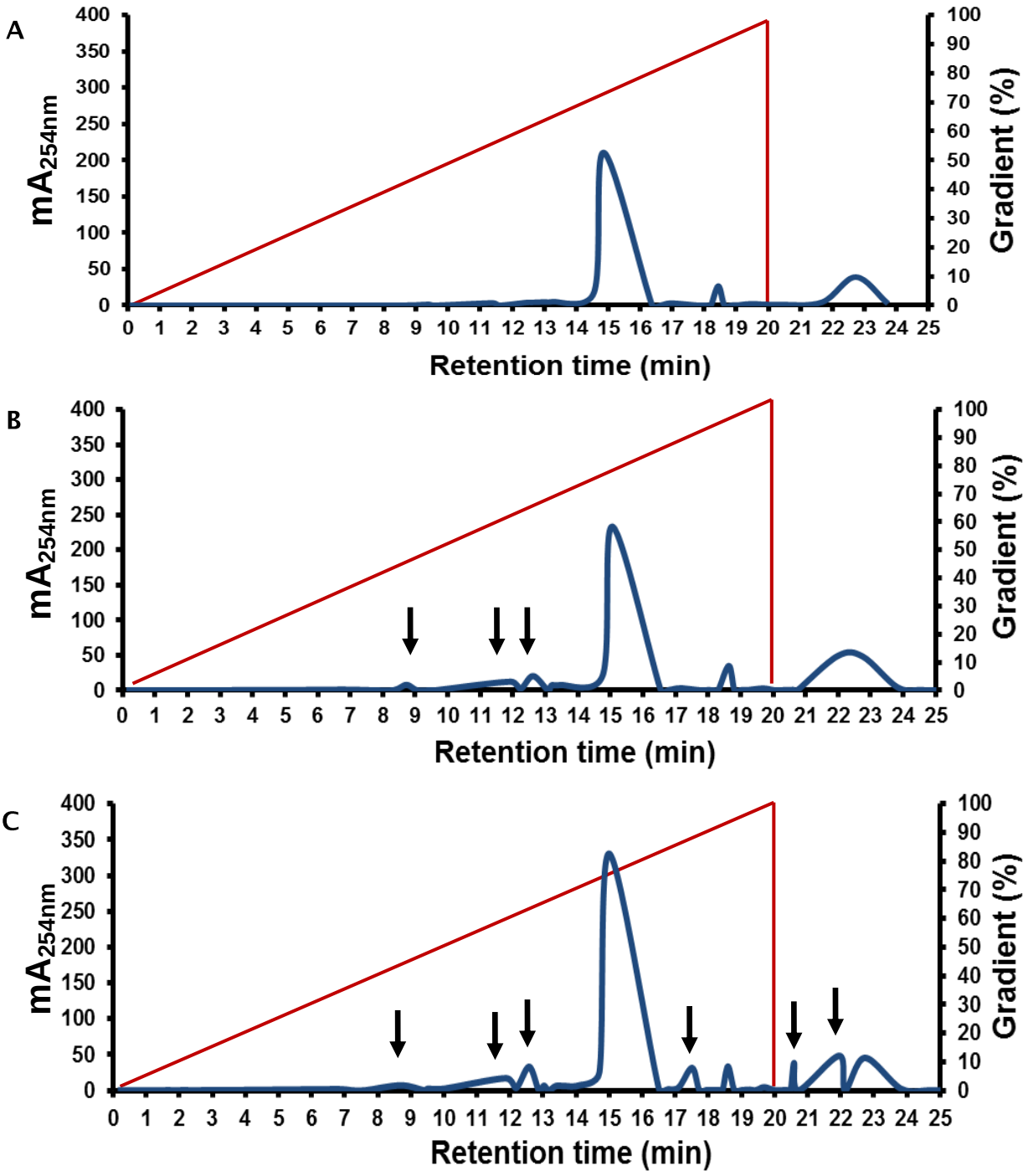

Figure 3.68 Degradation of PAR-2 RP (1 µg/ml) as analysed by reverse column chromatography following 2 h incubation with (A) buffer alone, (B) tryptase 50 mU/ml or (C) trypsin 100 U/ml at 37°C. A gradient elution of acetonitrile (0 – 100 %) into 0.05 % trifluoroacetic acid in water was employed. Arrows indicate the appearance of new peaks following incubation with proteases. mA_{250nm}, milli-absorbance unit at 254 nm.

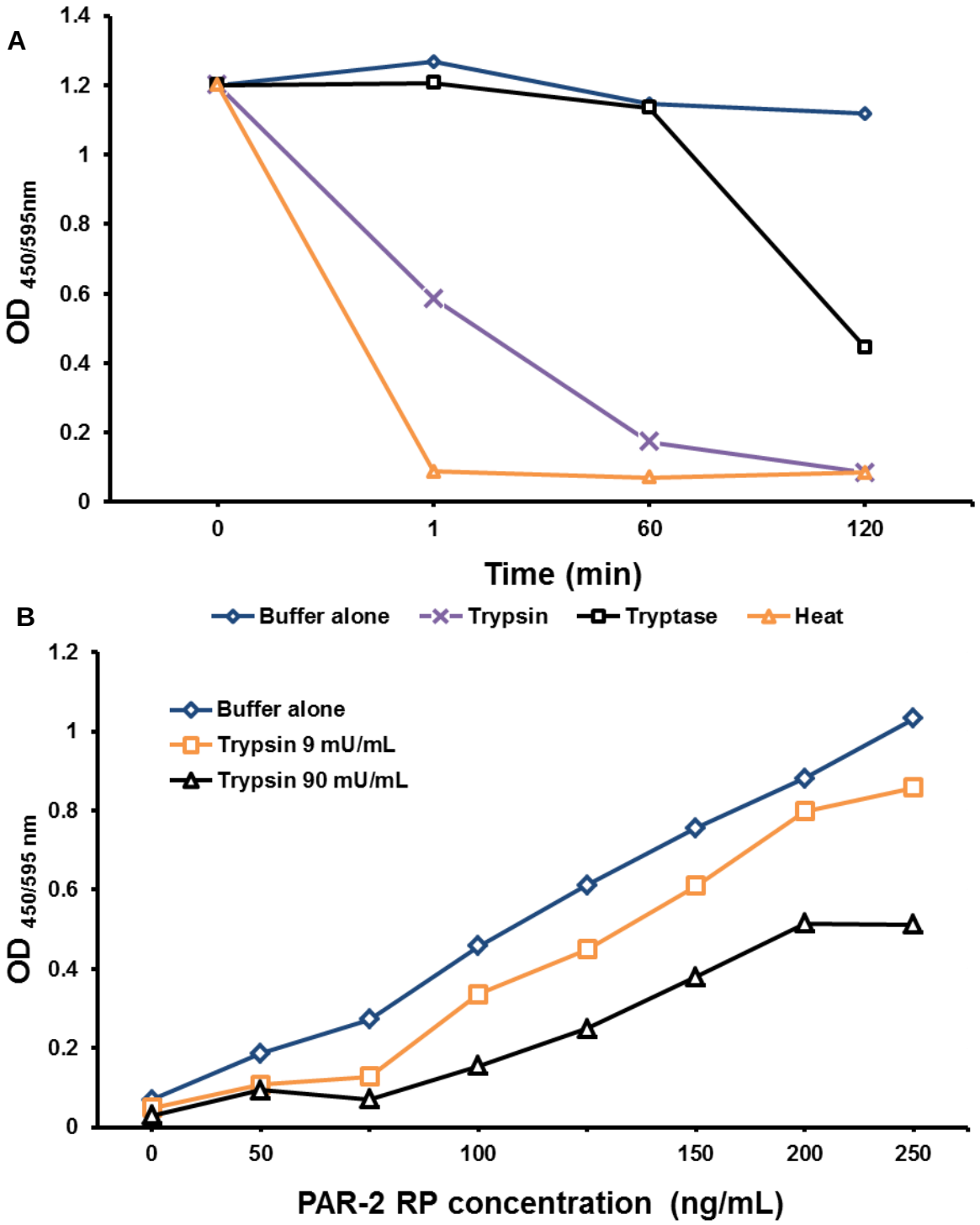

Figure 3.69 (A) Detection of PAR-2 RP by ELISA following incubation of 500 ng/ml PAR-2 RP with 900 mU/ml trypsin, 80 mU/ml tryptase or with buffer alone for up to 4 h at room temperature. The effect of heating of PAR-2 RP to 95°C for 10 min is also shown. (B) Standard curve with increasing concentrations of synthetic PAR-2 RP spiked with 9 mU/ml or 90 mU/ml trypsin.

Chapter 4.
Discussion

Chapter 4. Discussion

The present study confirms and extends the idea that mast cell tryptase has potent pro-inflammatory actions. Tryptase is able to elicit the accumulation of neutrophils in an *in vivo* model and to stimulate MMP release and microvascular leakage. At the cellular level, a key process could be the ability of tryptase to induce increased expression of adhesion molecules such as ICAM-1 and VCAM-1, and cytokines such as IL-8, IL-6 and CXCL10 from endothelial cells. The effects of tryptase appear dependant on an intact catalytic site. The activation of PAR-2, long predicted to be a principle cellular target, did not emerge as an important mechanism. While some of the actions of tryptase could be mediated by cell signalling processes triggered by cleavage of PAR-2, or even be mediated through PAR-2 RP, its seems likely that the role tryptase as a mediator of inflammation may be largely independent of PAR-2.

4.1 Actions of tryptase *in vivo*

The finding that tryptase is a potent stimulus for recruitment of neutrophils *in vivo*, provided confirmatory evidence for studies performed previously in which tryptase purified from human lung tissue was injected into the mouse peritoneum [11]. However, there were important differences from the findings of the ealier reports, and our use of PAR-2 knockout mice has provided new information on the underlying mechanisms.

Care was taken to ensure that the tryptase employed in this study was of high purity and activity. The method involved isolation of recombinant human β-tryptase from yeast expression system, using high salt extraction, heparin-agarose and butyl-agarose affinity chromatography. On SDS-PAGE, tryptase appeared as a single band whose identity was confirmed by western blotting. The endotoxin levels were extremely low, and our finding that heating the tryptase at 90ºC for 20 min abolished its proteolytic activity, would argue against any role for endotoxin in the findings obtained.

The intraperitoneal injection of C57BL/6 mice with tryptase caused neutrophilia without an increase in the number of other cell types. These results differ from the previous studies which showed an increase in numbers

of total nucleated cells and of eosinophils, as well as neutrophils in the peritoneum of BALB/c mice following intraperitoneal injection of tryptase [11, 208]. The difference would seem to be related to a difference in mouse strain rather than the tryptase injected, either recombinant or purified from human lung tissue. Injection of the recombinant form of tryptase into the peritoneum of BALB/c mice was still found to induce a pattern of cell accumulation different from that observed in the C57BL/6 mice that were used in the current study on account of the background of the PAR-2 knockout mice. In keeping with the earlier study [11], the peritoneal lavage fluid from BALB/c mice injected with tryptase had a significantly higher total nucleated cell counts. There was also an accumulation of macrophages along with significantly higher numbers of eosinophils in BALB/c mice compared to C57BL/6 mice. An increase in mast cell numbers was also observed in BALB/c animals.

The BALB/c mouse strain has been characterized as a Th2 responder, while the C57BL/6 mouse strain has been characterized as a Th1 responder [236]. The Th2-type response to allergen involves the release of IL-5, IL-13 and IL-4 which in turn stimulate B-cell differentiation and an antibody-mediated immune response. Moreover, IL-5 is a powerful eosinophil chemoattractant [237, 238]. The Th1-type cytokine response to allergen involves release of INF-γ and TNF-α which results in stimulation of macrophages and neutrophils, inducing cell-mediated immune responses [237].

Challenge of mice by ovalbumin inhalation, has been found to induce marked accumulation of neutrophils in the BAL fluid of Th1 cell reconstituted mice, while there was a selective eosinophil accumulation in BAL fluid of mice in to which Th2 cells had been transfered [239]. On the other hand, HayGlass et al. [240] have reported that there is a little difference between BALB/c and C57BL/6 in Th2 and Th1 responsiveness when mouse strains were immunized with Der p1, ovalbumin or human serum albumin. In the model of HayGlass, when either a Th1 response (induced with complete Freund's adjuvant) or Th2 response (elicited by alum) was examined, the degree of eosinophilia or neutrophilia could not be differentiated between either mouse strains [240]. There is likely to be complex interaction between these two T-cell pathways, as well as other T-helper cell subsets, and both Th9 and Th17 subsets have also been implicated [241, 242]. Our findings indicate that there are marked

differences between the two mouse strains in response to tryptase, as reflected in accumulation of different cell populations. The neutrophil accumulation into mice peritoneum was maximized after 24 h of tryptase injection, the phenomenon which previously reported [11, 208]. Building up mechanisms seems to be involved in the process of recruitment of inflammatory cells.

Intradermal injection of tryptase has been reported to induce microvascular leakage and oedema in guinea pig skin 20 minutes following injection [10]. Microvascular leakage was attributed to the ability of tryptase to stimulate release of histamine through activation of mast cells, and this was demonstrated experimentally *in vitro*. In the present study, injection of tryptase into the mouse peritoneum resulted in high levels of albumin in the peritoneal lavage fluid 24 h after of injection (but not at the 6 or 12 h timepoints studied). While increased mast cell activation may underlie the effect observed, other cell types are likely to contribute to the induction of inflammation by tryptase, and the accumulation of inflammatory cells. Mediators released from cells following their recruitment could play a role. Thus, neutrophil elastase has been reported to induce an increase in the permeability of monolayers of epithelial cell lines [243, 244]. In the present study elastase could not be detected in the peritoneal lavage fluid by elastin zymography, so support for this theory was not found. However, neutrophils can contribute to increased vascular permeability through other mechanisms. Studies on isolated perfused rat lung preparations have indicated that the adhesion of mechanically stimulated neutrophils to endothelial cells may result in increased vascular permeability with PKC-mediated intracellular signaling in the endothelial cells [245].

The tryptase-induced increases in the number of neutrophils were highly significantly correlated with MMP9 levels in the peritoneal lavage fluid. Neutrophils have been reported to have an essential role in body defense mechanisms against infection and inflammation. At least four types of granules have been described: azurophil, specific, gelatinase and secretory granules [246]. The contents of neutrophil granules are not only used intra-celluarly in phagocytosis but also used as a ready stores for mobilisation in response to inflammation [247]. As well as producing MMPs [248], neutrophils can also activate pro-forms of MMPs by the release of elastase and cathepsin G which

can cleave and activate both MMP3 and MMP9 [249]. In the present study, the neutrophil-rich cell population in the mouse peritoneum appeared to be responsible for most of the MMP9 produced in this compartment. Constitutive release of MMP9 from neutrophils demonstrated *in vitro* following their recovery from the peritoneal cavity of mice following injection of tryptase or casein.

Heating tryptase or pre-incubating this protease with the selective tryptase inhibitor SAR160719A-5 effectivly inhibited tryptase-induced neutrophilia and microvascular leakage. This suggests that the actions of tryptase in the model employed are dependent on an intact catalytic site for tryptase. With the PAR-2 peptide agonist SLIGRL-NH_2, intraperitoneal injection did not stimulate altered numbers of cells in the peritoneal lavage fluid of mice. It has been reported that intraperitoneal injection of SLIGRL-NH_2 peptide into mice can induce a decrease in the numbers of inflammatory cells that can be recovered, though intraperitoneal injection of trypsin stimulated the accumulation of inflammatory cells in the peritoneum [162]. Such findings raised the possibility that rapid degradation of the peptide agonist of PAR-2 following injection may account for lack of response, or that mechanisms other than PAR-2 activation may be involved. Studies with PAR-2 knockout mice produced support for the later idea.

The absence of a difference in response to tryptase in wild-type or PAR-2 deficient mice strongly suggests that tryptase may act through mechanisms other than PAR-2 activation. Apart from engaging PAR-2, proteases may regulate cell function in diverse other ways. Proteases could alter cell behaviour through the regulation of the growth factor receptors. The mechanisms may involve activation of a hormone-like cellular signaling through direct catalytic activity on receptors themselves (e.g. insulin receptors or insulin like growth factor-1 receptors) [250] or the release of a membrane tethered agonist e.g. heparin-binding epidermal growth factor (EGF) [251] or generation of a growth factor agonist from other precursors. Tryptase may also have a role in cytokine activation as observed with TGFβ or inactivation as mast cell-derived IL-6 which can be hydrolysed by mouse tryptase mMCP-6 [99, 134].

The strength of an *in vivo* model such as used in the present studies is that it can provide evidence for the overall effects of tryptase. However, mechanisms and precise biological roles of each cell type are not clear. The responses of specific cell type to tryptase will be affected by interaction with other cells and the local environment. Investigation of global gene expression in a single cell type *in vitro* can represent a powerful approach in exploring responses in detail to tryptase. As endothelial cells have key roles in the trafficking of inflammatory cells and in inflammation, these cells were considered particularly suitable for more in depth studies of mechanisms. An adantage in employing HUVECs is that they do not have pathological changes found in cell lines and subsequent studies were focused on these human cells.

4.2 Gene expression studies

A key contribution of tryptase in inflammatory processes could relate to its ability to stimulate the production of certain cytokines and to induce expression of adhesion molecules including ICAM-1 and VCAM-1. In the present studies it was confirmed, using highly purified recombinant tryptase that this protease can induce upregulation of mRNA for IL-8 and IL-1β in endothelial cells an observation made previously with tryptase purified from human lung tissue [128].

In previous reports, the lung derived tryptase, at a slightly higher concentration than used in the present studies was found to stimulate release of IL-8 from HUVECs [128] and from endothelial cell line, ECV304 [252]. The chemokine IL-8 is formed and stored in endothelial cells in Weibel-Palade bodies, from where it can be rapidly released upon stimulation as has been found with certain other inflammatory mediators such as histamine [253-255]. IL-8 is a potent chemo-attractant for neutrophils and eosinophils [256, 257] and a study with blocking antibodies suggested that neutrophil chemoattractant activity in supernatants of endothelial cells treated with tryptase may be attribute to the presence of IL-8 [255]. Not only can tryptase stimulate endothelial cells to release IL-8 but also cells of the epithelial cell line H292 [129] airway smooth muscle (ASM) cells [210], to a lesser extent human neutrophils [207] and human blood eosinophils [181].

The present studies suggest that tryptase stimulated *de novo* synthesis of IL-8, with up-regulation of mRNA expression within two hours of adding this protease to cells. This pattern has been previously observed in an epithelial cell line [258]. Tryptase-induced IL-8 mRNA expression in HUVECs was markedly decreased by pre-incubation of tryptase with the tryptase inhibitor SAR160719A-5 or with TdPI. There was not complete inhibition, but as found using the chromogenic substrate, there is likely to be residual tryptase activity and this could be responsible for the small changes observed. The release IL-8 into cell supernatants appeared unaffected by addition of inhibitors, though in some previous studies, tryptase-induced release has been reported to be blocked by pre-incubation of the enzyme with leupeptin or benzamidine, both of which are broad-spectrum protease inhibitors [128, 129, 258]. Residual tryptase activity after inhibition of tryptase in the present studies or perhaps loss or degradation of the inhibitor could account for the present findings with secreted IL-8.

Tryptase was effective in upregulating expression of mRNA for IL-1β but not its release from HUVECs. IL-1β does not seem to be produced constitutively by HUVECs, but only stimulated cells have been reported previously to be able to synthesise this cytokine in response to pro-inflammatory mediators such as TNF-α, LPS or even IL-1β itself [259]. Production of this cytokine is not invariably associated with its secretion from stimulated cells into medium but as described with LPS [260], integration of several stimuli may be required in the control of IL-1β release. As with mRNA for IL-8, tryptase-induced upregulation of expression of mRNA for IL-1β could be inhibited by TdPI.

IL-8 and IL-1β were selected as endothelial cell products for particular study on account of previous findings that their expression was altered by tryptase. The plan was to employ conditions suitable for studying these two cytokines, and adapt them for studies of global gene expression. It was thus a surprise that by gene microarray studies alterations in expression for neither IL-8 nor IL-1β were markedly changed. Gene arrays are generally less sensitive than quantitative PCR studies focusing on a single gene, and this indicates the need for a broad experimental approach.

Although changes in mRNA expression for IL-8 and IL-1β did not emerge from global gene microarray studies of HUVECs treated with tryptase, many of the genes identified as being upregulated are ones associated with inflammation. The list includes several cytokines including IL-2, IL-3, IL-6, IL-8 and CXCL10, and importantly also adhesion molecules genes including ICAM-1, VCAM-1, ITGAL and EpCAM.

The pattern of gene expression stimulated with tryptase appears similar in some respects to that reported for other pro-inflammatory stimuli investigated by gene microarray. Thus, addition of TNF-α to HUVECs has been found to be associated with up-regulation and production of cytokines that induce recruitment and activation of leukocytes including up-regulation of mRNA for IL-1β [128], IL-6 [24], IL-8 [24, 128, 255, 261] and GM-CSF [128]. A similar pattern of cytokine production has been reported with IL-1 which stimulated production of IL-8, IL-1α and β, IL-6, CXCL10 and MCP1 in HUVECs [262], while the profile of lipopolysaccharide (LPS) stimulated HUVECs has been noted to have similarities with that of TNF-α [263, 264].

Of the cytokines identified as being stimulated by tryptase, IL-2 is an important cytokine in development and control of T cell function [265]. Activated $CD4^+$ T-cells may be the main source of IL-2 under physiological conditions, but this cytokine has been reported to be present in the human arterial wall, and may be linked to processes involved in leukocyte adhesion and survival [266, 267]. In another report, IL-2 expression or production was not detected in resting HUVECs or in cells following stimulation with IL-1β or TNF-α [268].

IL-3 is well-established as stimulus for differentiation of multipotent haematopoietic stem cells in a synergy with IL-1, IL-6 and GM-CSF [269]. Interestingly, though increased expression of IL-3 mRNA was seen in tryptase-treated HUVECs, this has not been found in previous studies involving addition of TNF-α or IL-1β [24, 261, 262].

Tryptase has been reported to stimulate IL-6 expression in eosinophils [181] and it may be produced also in human conjunctival epithelial cells [270] and T cells [271], but this is the first report of tryptase-induced release from

endothelial cells. IL-6 has been reported to induce acute phase reactants [272] and in synergy with IL-3, stimulate growth of granulocyte, macrophage and multipotential hematopoietic progenitors and spleen cell cultures [269].

Interferon-inducible protein (IP10) or CXCL10 is a 98 amino acid peptide chemokine produced by endothelial cells, monocytes, smooth muscle cells and fibroblasts. T cells and lung mast cells have been found to express the high affinity G protein-coupled receptor CXCR3 to which it binds [273, 274]. CXCL10 has been reported to play an important role in recruitment of mast cells to airway smooth muscles in asthma and mast cell mediators have been suggested to control this effect by differentially controlling its release from smooth muscle cells [274, 275]. Addition of tryptase was associated with a decrease in INF-γ induced IP10 probably related to it being degraded by enzymes while incubation of mast cell lysate was found to increase IP10 induction. In addition to being a chemoattractant, CXCL10 has roles in angiogenesis and T cell generation and trafficking [276].

Alterations in TGF-β mRNA levels in tryptase-treated HUVECs were not detected, but this cytokine could nonetheless participate in tryptase-induced reactions. An increase in TGF-β in supernatants from airway smooth muscle cells after addition of tryptase. Tatler et al. [99] also found that tryptase can increase active TGF-β levels by direct proteolysis of latent TGF-β without increasing production of the total cytokine pool. *In vitro*, mature TGF-β can be released from the latent TGF-β complex by thermal, acid or enzymatic treatment e.g. MMP2 or MMP9 [277-279].

Latent TGF-β can be released in substantial amounts from un-stimulated resident [280] and activated murine peritoneal macrophages [281]. Our finding that tryptase can induce MMP release from neutrophils recruited to the peritoneum of mice, thus raises the possibility that this can lead to conversion of latent to active TGF-β. Un-stimulated vascular endothelial cells including HUVECs have been reported to release the inactive form of TGF-β [282] and the potential for tryptase contributing indirectly to its activation deserves consideration.

TGF-β could contribute to inflammatory processes as a chemoattractant for monocytes and fibroblasts [277]. Many actions of TGF-β on endothelial cells have been described, including promoting neutrophil adherence to the vascular endothelium, inducing lung injury through up-regulation of ICAM-1 [283], and promoting thrombogenesis through down-regulation of thrombomodulin in HUVECs [284]. TGF-β has also been shown to have an inhibitory effect on both growth and induced apoptotic cell death in HUVECs [285, 286] and TGF-β can inhibit IL-6 and IL-8 release from HUVECs [287]. A role for TGF-β in tryptase-mediated inflammatory processes is supported by our finding of tryptase stimulated up-regulation of the SMAD2 gene which encodes one of the components of cell signalling triggered by the TGF-β receptor.

The changes induced in HUVECs by tryptase are consistent with this major mast cell product stimulating inflammatory cell recruitment at several levels. Leukocyte accumulation involves a cascade of events that starts with adhesion and activation, and finally extravasation of leukocytes to sites of inflammation. Leukocytes marginate from the central blood stream to be close to endothelial cells in peripheral blood vessels. Margination is a result of mechanical interaction between leukocytes and erythrocytes in which cell size and shape, and blood flow promote the process [288]. During inflammation, activated endothelial cells start to capture the leukocytes via their selectin family of transmembrane adhesion receptors; P-selectin and L-selectin. Once leukocytes are tethered to endothelial cells, they begin to roll in a process that relies on P-selectin, L-selectin and E-selectin. A transient stage of slow rolling follows, resulting in close contact of leukocytes and inflammatory mediators favouring their activation. Slow rolling is stimulated by surface-bound chemokines and mediated through adhesion molecule-based signalling mainly E-selectin [289] on endothelial cells. This stage plays a pivotal role in the efficiency of the recruitment process and firm adhesion and flattening of leukocytes further occurs mediated through ICAM-1 and β2 integrin binding [290]. Finally, leukocytes transmigrate to the site of inflammation in response to cytokines such as IL-8 [257] and are dependent on expression of PECAM-1, ICAM-1, VE-cadherin, CD11a, IAP (CD47) and VLA-4 (α4‹1 integrin) adhesion molecules.

Addition of tryptase to HUVECs was associated with mRNA up-regulation for adhesion molecules such as ICAM-1, VCAM-1 and E-selectin. This pattern has

been observed with HUVECs treated with TNF-α [24, 129, 261, 262] and LPS [263]. In addition, mast cell degranulation has been reported to be associated with increased ICAM-1 expression in the skin of psoriatic and atopic dermatitis patients [291]. In the present study, tryptase was found to induce expression of
ICAM-1, VCAM-1 and EpCAM by flow cytometry, and consistent with this was the observation of increased secretory ICAM-1 in HUVEC supernatants.
In a previous report, Compton et al. [128] found that human lung tryptase at a concentration similar to that employed in the present study had no effect on expression of the adhesion molecules ICAM-1, VCAM-1 and E-selectin gene expression up to 48 h following incubation with HUVECs, though increased IL-8 production was observed [128]. The discrepancy with our findings may be related to the use of serum starvation in the earlier studies. Serum-starved HUVECs have been found to undergo apoptosis within 4 h [292] and with up to 55 % of cells affected after 72 h [293]. In preliminary studies we also found that serum starvation affected gene expression and the viability of HUVECs. Endothelial cells will normally be exposed to blood containing high concentrations of growth factors which are essential for their growth. We found that medium containing 20 % FCS was optimal for maintaining the proliferation of HUVECs, but that growth was not markedly affected when the concentration was lowered to 5 % [294]. Tryptase has been reported to induce ICAM-1 gene expression in serum-starved human bronchial epithelial cells [129], but as described for fibroblasts [295], with HUVECs, tryptase is likely to act in concert with growth factors present in FCS.

In the present studies it was found that TNFRSF9 and TNFAIP3 mRNA expression was up-regulated by tryptase in HUVECs. TNFRSF9 (CD137) is a member of the TNF receptor family that is expressed by activated T cells and other various cell types including cells of blood vessel wall. Pro-inflammatory mediators such as IL-1 and TNF-α can induce expression of this cytokine receptor in HUVECs [296]. CD137 ligand (CD137L) is transmembrane protein on the surface of monocytes which transmits signalling in monocytes in the reverse direction i.e. reverse signalling. The CD137L has been found to be expressed constitutively in monocytes/macrophages and cell lines of peripheral monocytes [297]. Activation of CD137 by cross-linking with its ligand can result in activation, migration, prolonged survival and proliferation

in monocytes [296]. Moreover it can increase expression of pro-inflammatory cytokines such as TNF, IL-6, IL-8, IL-12, and enhance ICAM-1-mediated adhesion of monocytes [297, 298]. Human blood neutrophils have been reported to express CD137 constitutively [299] and CD137L when exposed to inflammatory stimuli [300]. Neutrophils derived from CD137 deficient mice have been found to be defective in their ability to generate reactive oxygen species and in phagocytic activity [301]. The TNFAIP3 gene can be induced by TNF-α and codes for a zinc finger protein which inhibits NF-kappa B activation as well as TNF-α mediated apoptosis [302, 303]. The inhibition of NF-kappa B may interfere with PAR-1 and possibly PAR-2 signalling pathways. The induction of this gene may act as a counter regulator in inflammatory responses induced by tryptase.

Tryptase can thus directly and indirectly act to induce a series of key processes that lead to inflammation. As indicated, some of the pathways are shared by other stimuli including TNF-α, IL-1β, LPS and histamine, though there were features that appear to be unique to tryptase.

4.3 Role of PAR-2 in mediating cellular responses to tryptase

The similarities in response to tryptase *in vivo* in both wild-type and PAR-2 deficient mice provided compelling evidence that many of the actions of tryptase are independent of PAR-2 activation. Detailed analysis of the findings with tryptase-treated human endothelial cells *in vitro* would tend to support this conclusion. Stimulation of PAR-2 by the peptide agonist SLIGKV-NH_2 was not associated with significant changes in IL-8 or IL-1β mRNA expression or cytokines release from HUVECs. The pattern of global gene expression in microarray studies with SLIGKV-NH_2-treated HUVECs was strikingly different from that of tryptase, and further confirmation came from qPCR and flow cytometry findings for selected genes.

Tryptase was able to stimulate a small increase in intracellular calcium in HUVECs, and this was inhibited with pertussis toxin and to a lesser extent with the peptide antagonist of PAR-2 FSLLRY-NH_2. This provide evidence in support of the idea that tryptase can stimulate PAR-2 activation. However, it has been noted previously in airway human smooth muscle cells that tryptase is not a

potent stimulus for PAR-2 activation, being about ten times less potent than trypsin in inducing calcium flux [304]. The unique structure of tryptase and the relative inaccessibility of the catalytic site are likely to be factors. PAR-2 is variably glycosylated and it has been reported that deglycosylation of PAR-2 could be necessary for tryptase to stimulate calcium flux in human embryonic kidney cells [201].

The presence of PAR-2 on HUVECs was demonstrated in the present studies by immunocytochemistry and by the responsiveness of these cells to the peptide agonist of PAR-2. Calcium flux in endothelial cells in response to PAR-2 peptide agonists [177, 184, 305], trypsin [184, 306] and to rat mast cell granules [307] has been reported previously. In agreement with the results of the current study, there is a report that tryptase (purified from HMC-1) can induce cytosolic calcium mobilization in HUVECs albeit weaker than the response to SLIKGKV [102].

It was of interest that the kinetics of calcium flux in HUVECs following addition of tryptase differed from that of SLIKGKV-NH_2 in that it failed to return to baseline. Tryptase induced calcium current was delayed and long lasting in comparison to PAR-2 peptide agonist. Activation of PAR-2 receptor with the peptide agonist requires binding of the agonist sequence to the second loop of while tryptase needs more time to process the receptor and to free the tethered ligand. Calcium entry from the extracellular space may occur through non-selective cation channels as a result of depletion of calcium stores [308], or stimulation of GPCRs or tyrosine kinase receptors [309] as has been demonstrated in HUVECs. This may result in a second rise in cytosolic calcium levels following the initial high concentrations stimulated by binding of ligands to receptors and this may account for the failure of calcium levels to return to baseline over the time period examined. Several aspects of endothelial cell function are regulated through calcium such as secretion of granular contents, permeability, adhesion, leukocyte transmigration and rearrangement of actin cytoskeleton [310-314], and the activation of PAR-2 could contribute to these.

In the current studies, the contribution of PAR-2 in mediating the actions of tryptase was found to be fairly minimal. In the absence of good PAR-2 antagonists or neutralizing antibodies other approaches that could be explored

in the future could involve blocking the signalling pathways of the receptor at certain levels e.g. blocking of IP3 mediated calcium signalling with ryanodine receptor (RyR) blockers. Techniques for reducing gene expression and post-transcriptional processing such as small interfering RNA (siRNA) methods which interfere with expression of the PAR-2 gene could also provide useful information [315-318]. Another approach that should be explored could be the application of pepducins which are novel peptides that can modulate signal transference from GPCR to G-protein by a unique intracellular allosteric mechanism [319].

Studies to date have focused on binding of the tethered ligand to PAR-2 when seeking to understand the biological actions of this receptor. However, we were concerned to investigate the potential role of the fragment of PAR-2 (PAR-2 RP) whose removal is integral to the activation process. Attempts to develop a robust assay for PAR-2 RP that could be applied to measure levels in biological fluids or cell supernatants were unsuccessful, in large part to the readiness with which PAR-2 RP as an uncoiled peptide can be degraded by proteases (including tryptase). It is possible that with antibodies directed against other epitopes of PAR-2 RP a sensitive assay can be detected in the future, and this would be a valuable tool for establishing the role of PAR-2.

Our findings have provided evidence for the first time that PAR-2 RP has biological actions of its own which are quite distinct from those mediated by peptide agonists of PAR-2. The observation that injection of PAR-2 RP into the mouse peritoneum was associated with an increase in numbers of eosinophils with a reduction in lymphocyte and mast cell numbers will require further investigation. Investigation of global gene expression in HUVECs incubated with PAR-2 RP revealed a profile quite distinct from that with tryptase or PAR-2 peptide agonist-treated cells. However, there were significant changes in HUVEC expression of such as mRNA for ITGAL in response to PAR-2 RP on microarray, and on qPCR for ITGAL, EPCAM, ICAM1, TNFAIP3 and TLL1 (all of which were upregulated by tryptase). The ability of PAR-2 RP to stimulate increased expression of ICAM-1, VCAM-1, ITGAL and EpCAM was confirmed in separate flow cytometry experiments. Thus in considering the role of PAR-2 activation, concerns should be given to the potential contribution of PAR-2 RP. The ability of tryptase and other proteases to cleave PAR-2 RP raises the

possibility that proteases can contribute to PAR-2 mediated effects, not only by activating this receptor and generating PAR-2 RP, but also by changing the actions of PAR-2 RP following its release.

4.4 Conclusions

The present studies have indicated that tryptase is a potent stimulus of inflammation *in vivo*. We found this major mast cell product at quite low concentrations can stimulate neutrophilia, microvascular leakage and the generation of MMP9 and MMP2. The studies with PAR-2 knockout mice challenge the assumption that the activation PAR-2 is the primary mechanism by which tryptase can mediate inflammatory changes. The actions of tryptase were dependent on an intact catalytic site, but in the models employed, few of the changes appeared to be mediated through PAR-2. Though agonists of PAR-2 were able to alter cell function our findings suggest that the pro-inflammatory actions of tryptase may be largely independent of PAR-2 activation.

On the basis of our findings, key events triggered by tryptase either alone or in concert with other mediators could induce the expression and release of a series of cytokines from endothelial cells including IL-2, IL-3, IL-6, IL-8 and CXCL10. Moreover, latent forms of other cytokines and growth factors such as TGF-β could be activated either directly or through other proteases released such as MMP2 and MMP9. These cytokines can trigger diverse actions including microvascular permeability and the accumulation of inflammatory cells. The latter process will be mediated also by the upregulation of adhesion molecules including ICAM-1, VCAM-1, ITGAL and EpCAM. The overall contribution of PAR-2 activation by tryptase may be a small one, but whether triggered directly by receptor activation of the actions or by PAR-2 RP, PAR-2 could play a part.

References

References

[1] Galli SJ, Nakae S, Tsai M. Mast cells in the development of adaptive immune responses. Nature Immunology 2005;6(2):135-42.

[2] Benoist C, Mathis D. Mast cells in autoimmune disease. Nature 2002;420(6917):875-8.

[3] Brown MA, Hatfield JK. Mast Cells are Important Modifiers of Autoimmune Disease: With so Much Evidence, Why is There Still Controversy? Front Immunol 2012;3:147.

[4] Metcalfe DD, Baram D, Mekori YA. Mast cells. Physiological Reviews 1997;77(4):1033-79.

[5] Weller CL, Collington SJ, Williams T, Lamb JR. Mast cells in health and disease. Clin Sci (Lond) 2011;120(11):473-84.

[6] Berger P, Compton SJ, Molimard M, Walls AF, N'Guyen C, Marthan R, et al. Mast cell tryptase as a mediator of hyperresponsiveness in human isolated bronchi. Clinical and Experimental Allergy 1999;29(6):804-12.

[7] Brightling CE, Bradding P, Symon FA, Holgate ST, Wardlaw AJ, Pavord ID. Mast-cell infiltration of airway smooth muscle in asthma. N Engl J Med 2002;346(22):1699-705.

[8] Jayapal M, Tay HK, Reghunathan R, Zhi L, Chow KK, Rauff M, et al. Genome-wide gene expression profiling of human mast cells stimulated by IgE or FcepsilonRI-aggregation reveals a complex network of genes involved in inflammatory responses. BMC Genomics 2006;7:210.

[9] Bischoff SC. Role of mast cells in allergic and non-allergic immune responses: comparison of human and murine data. Nat Rev Immunol 2007;7(2):93-104.

[10] He S, Walls AF. Human mast cell tryptase: a stimulus of microvascular leakage and mast cell activation. Eur J Pharmacol 1997;328(1):89-97.

[11] He S, Peng Q, Walls AF. Potent induction of a neutrophil and eosinophil-rich infiltrate in vivo by human mast cell tryptase: selective enhancement of eosinophil recruitment by histamine. J Immunol 1997;159(12):6216-25.

[12] Imamura T, Dubin A, Moore W, Tanaka R, Travis J. Induction of vascular permeability enhancement by human tryptase: dependence on activation of prekallikrein and direct release of bradykinin from kininogens. Lab Invest 1996;74(5):861-70.

[13] Walls AF, He S, Teran LM, Buckley MG, Jung KS, Holgate ST, et al. Granulocyte recruitment by human mast cell tryptase. Int Arch Allergy Immunol 1995;107(1-3):372-3.

[14] Galli SJ, Tsai M, Piliponsky AM. The development of allergic inflammation. Nature 2008;454(7203):445-54.

[15] Minai-Fleminger Y, Levi-Schaffer F. Mast cells and eosinophils: the two key effector cells in allergic inflammation. Inflammation Research 2009;58(10):631-8.

[16] Shakoory B, Fitzgerald SM, Lee SA, Chi DS, Krishnaswamy G. The role of human mast cell-derived cytokines in eosinophil biology. J Interferon Cytokine Res 2004;24(5):271-81.

[17] Levi-Schaffer F, Temkin V, Malamud V, Feld S, Zilberman Y. Mast cells enhance eosinophil survival in vitro: role of TNF-alpha and granulocyte-macrophage colony-stimulating factor. J Immunol 1998;160(11):5554-62.

[18] Bischoff SC, Dahinden CA. c-kit ligand: a unique potentiator of mediator release by human lung mast cells. J Exp Med 1992;175(1):237-44.

[19] Tam SY, Tsai M, Yamaguchi M, Yano K, Butterfield JH, Galli SJ. Expression of functional TrkA receptor tyrosine kinase in the HMC-1 human mast cell line and in human mast cells. Blood 1997;90(5):1807-20.

[20] O'Donnell MC, Ackerman SJ, Gleich GJ, Thomas LL. Activation of basophil and mast cell histamine release by eosinophil granule major basic protein. J Exp Med 1983;157(6):1981-91.

[21] Yang L, Froio RM, Sciuto TE, Dvorak AM, Alon R, Luscinskas FW. ICAM-1 regulates neutrophil adhesion and transcellular migration of TNF-alpha-activated vascular endothelium under flow. Blood 2005;106(2):584-92.

[22] Elices MJ, Osborn L, Takada Y, Crouse C, Luhowskyj S, Hemler ME, et al. VCAM-1 on activated endothelium interacts with the leukocyte integrin VLA-4 at a site distinct from the VLA-4/fibronectin binding site. Cell 1990;60(4):577-84.

[23] Kunkel EJ, Ley K. Distinct phenotype of E-selectin-deficient mice. E-selectin is required for slow leukocyte rolling in vivo. Circ Res 1996;79(6):1196-204.

[24] Viemann D, Goebeler M, Schmid S, Klimmek K, Sorg C, Ludwig S, et al. Transcriptional profiling of IKK2/NF-kappa B- and p38 MAP kinase-dependent gene expression in TNF-alpha-stimulated primary human endothelial cells. Blood 2004;103(9):3365-73.

[25] Hepworth MR, Danilowicz-Luebert E, Rausch S, Metz M, Klotz C, Maurer M, et al. Mast cells orchestrate type 2 immunity to helminths through regulation of tissue-derived cytokines. Proc Natl Acad Sci U S A 2012.

[26] Erb KJ. Helminths, allergic disorders and IgE-mediated immune responses: where do we stand? Eur J Immunol 2007;37(5):1170-3.

[27] Duarte J, Deshpande P, Guiyedi V, Mecheri S, Fesel C, Cazenave PA, et al. Total and functional parasite specific IgE responses in Plasmodium falciparum-infected patients exhibiting different clinical status. Malar J 2007;6:1.

[28] Theoharides TC, Alysandratos KD, Angelidou A, Delivanis DA, Sismanopoulos N, Zhang BD, et al. Mast cells and inflammation.

Biochimica et Biophysica Acta-Molecular Basis of Disease 2012;1822(1):21-33.

[29] Sayed BA, Brown MA. Mast cells as modulators of T-cell responses. Immunol Rev 2007;217:53-64.

[30] Kitamura Y, Go S, Hatanaka K. Decrease of mast cells in W/Wv mice and their increase by bone marrow transplantation. Blood 1978;52(2):447-52.

[31] Kitamura Y, Go S. Decreased production of mast cells in S1/S1d anemic mice. Blood 1979;53(3):492-7.

[32] Wershil BK. IX. Mast cell-deficient mice and intestinal biology. Am J Physiol Gastrointest Liver Physiol 2000;278(3):G343-G348.

[33] Wershil BK, Wang ZS, Gordon JR, Galli SJ. Recruitment of neutrophils during IgE-dependent cutaneous late phase reactions in the mouse is mast cell-dependent. Partial inhibition of the reaction with antiserum against tumor necrosis factor-alpha. J Clin Invest 1991;87(2):446-53.

[34] Malaviya R, Ikeda T, Ross E, Abraham SN. Mast cell modulation of neutrophil influx and bacterial clearance at sites of infection through TNF-alpha. Nature 1996;381(6577):77-80.

[35] Malaviya R, Abraham SN. Role of mast cell leukotrienes in neutrophil recruitment and bacterial clearance in infectious peritonitis. J Leukoc Biol 2000;67(6):841-6.

[36] von Recklinghausen FD. Ueber Eiter- und Bindegewebsk Φ rperchen. Virchow's Archiv fὸr pathologische Anatomie und Physiologie, und fὸr klinische Medicin.Berlin: Druck und Verlag von Georg Reimer; 1863. p. 157-97.

[37] Bloom GD. A Short History of the Mast-Cell. Acta Oto-Laryngologica 1984;87-92.

[38] Prussin C, Metcalfe DD. 4. IgE, mast cells, basophils, and eosinophils. J Allergy Clin Immunol 2003;111(2 Suppl):S486-S494.

[39] Chen CC, Grimbaldeston MA, Tsai M, Weissman IL, Galli SJ. Identification of mast cell progenitors in adult mice. Proc Natl Acad Sci U S A 2005;102(32):11408-13.

[40] Okayama Y, Kawakami T. Development, migration, and survival of mast cells. Immunol Res 2006;34(2):97-115.

[41] Hamaguchi Y, Kanakura Y, Fujita J, Takeda S, Nakano T, Tarui S, et al. Interleukin 4 as an essential factor for in vitro clonal growth of murine connective tissue-type mast cells. J Exp Med 1987;165(1):268-73.

[42] Ochi H, Hirani WM, Yuan Q, Friend DS, Austen KF, Boyce JA. T helper cell type 2 cytokine-mediated comitogenic responses and CCR3 expression during differentiation of human mast cells in vitro. J Exp Med 1999;190(2):267-80.

[43] Okayama Y, Kirshenbaum AS, Metcalfe DD. Expression of a functional high-affinity IgG receptor, Fc gamma RI, on human mast cells: Up-regulation by IFN-gamma. J Immunol 2000;164(8):4332-9.

[44] Murakumo Y, Ide H, Itoh H, Tomita M, Kobayashi T, Maruyama H, et al. Cloning of the cDNA encoding mast cell tryptase of Mongolian gerbil, Meriones unguiculatus, and its preferential expression in the intestinal mucosa. Biochem J 1995;309 (Pt 3):921-6.

[45] Blank U, Rivera J. The ins and outs of IgE-dependent mast-cell exocytosis. Trends Immunol 2004;25(5):266-73.

[46] Fukuoka Y, Xia HZ, Sanchez-Munoz LB, Dellinger AL, Escribano L, Schwartz LB. Generation of anaphylatoxins by human beta-tryptase from C3, C4, and C5. Journal of Immunology 2008;180(9):6307-16.

[47] Matsuda H, Kawakita K, Kiso Y, Nakano T, Kitamura Y. Substance P induces granulocyte infiltration through degranulation of mast cells. J Immunol 1989;142(3):927-31.

[48] Nilsson G, Johnell M, Hammer CH, Tiffany HL, Nilsson K, Metcalfe DD, et al. C3a and C5a are chemotaxins for human mast cells and act through distinct receptors via a pertussis toxin-sensitive signal transduction pathway. Journal of Immunology 1996;157(4):1693-8.

[49] Nilsson G, ForsbergNilsson K, Xiang Z, Hallbook F, Nilsson K, Metcalfe DD. Human mast cells express functional TrkA and are a source of nerve growth factor. European Journal of Immunology 1997;27(9):2295-301.

[50] Tkaczyk C, Okayama Y, Woolhiser MR, Hagaman DD, Gilfillan AM, Metcalfe DD. Activation of human mast cells through the high affinity IgG receptor. Molecular Immunology 2002;38(16-18):1289-93.

[51] Bradding P, Walk AF, Church MK. Mast cells and basophils: their role in initiating and maintaining inflammatory responses. In: Holgate ST, editor. Immunopharmacology of the Respiratory System.New York: Academic Press; 1995. p. 53-84.

[52] Schwartz LB, Lewis RA, Austen KF. Tryptase from human pulmonary mast cells. Purification and characterization. J Biol Chem 1981;256(22):11939-43.

[53] Schwartz LB, Metcalfe DD, Miller JS, Earl H, Sullivan T. Tryptase levels as an indicator of mast-cell activation in systemic anaphylaxis and mastocytosis. N Engl J Med 1987;316(26):1622-6.

[54] Kandere-Grzybowska K, Letourneau R, Kempuraj D, Donelan J, Poplawski S, Boucher W, et al. IL-1 induces vesicular secretion of IL-6 without degranulation from human mast cells. J Immunol 2003;171(9):4830-6.

[55] Cao J, Papadopoulou N, Kempuraj D, Boucher WS, Sugimoto K, Cetrulo CL, et al. Human mast cells express corticotropin-releasing hormone (CRH)

receptors and CRH leads to selective secretion of vascular endothelial growth factor. J Immunol 2005;174(12):7665-75.

[56] Cao J, Cetrulo CL, Theoharides TC. Corticotropin-releasing hormone induces vascular endothelial growth factor release from human mast cells via the cAMP/protein kinase A/p38 mitogen-activated protein kinase pathway. Mol Pharmacol 2006;69(3):998-1006.

[57] Kandere-Grzybowska K, Kempuraj D, Cao J, Cetrulo CL, Theoharides TC. Regulation of IL-1-induced selective IL-6 release from human mast cells and inhibition by quercetin. Br J Pharmacol 2006;148(2):208-15.

[58] Van LH, Kraeuter-Kops S, Askenase PW. Different mechanisms of release of vasoactive amines by mast cells occur in T cell-dependent compared to IgE-dependent cutaneous hypersensitivity responses. Eur J Immunol 1984;14(1):40-7.

[59] Mrabet-Dahbi S, Metz M, Dudeck A, Zuberbier T, Maurer M. Murine mast cells secrete a unique profile of cytokines and prostaglandins in response to distinct TLR2 ligands. Exp Dermatol 2009;18(5):437-44.

[60] Fischer M, Harvima IT, Carvalho RF, Moller C, Naukkarinen A, Enblad G, et al. Mast cell CD30 ligand is upregulated in cutaneous inflammation and mediates degranulation-independent chemokine secretion. J Clin Invest 2006;116(10):2748-56.

[61] Pallaoro M, Fejzo MS, Shayesteh L, Blount JL, Caughey GH. Characterization of genes encoding known and novel human mast cell tryptases on chromosome 16p13.3. J Biol Chem 1999;274(6):3355-62.

[62] Cromlish JA, Seidah NG, Marcinkiewicz M, Hamelin J, Johnson DA, Chretien M. Human pituitary tryptase: molecular forms, NH2-terminal sequence, immunocytochemical localization, and specificity with prohormone and fluorogenic substrates. J Biol Chem 1987;262(3):1363-73.

[63] Harvima IT, Schechter NM, Harvima RJ, Fraki JE. Human skin tryptase: purification, partial characterization and comparison with human lung tryptase. Biochim Biophys Acta 1988;957(1):71-80.

[64] McEuen AR, Walls AF. Purification and characterization of mast cell tryptase and chymase from human tissues. Methods Mol Med 2008;138:299-317.

[65] Smith TJ, Hougland MW, Johnson DA. Human lung tryptase. Purification and characterization. J Biol Chem 1984;259(17):11046-51.

[66] Schwartz LB, Sakai K, Bradford TR, Ren S, Zweiman B, Worobec AS, et al. The alpha form of human tryptase is the predominant type present in blood at baseline in normal subjects and is elevated in those with systemic mastocytosis. J Clin Invest 1995;96(6):2702-10.

[67] Hallgren J, Pejler G. Biology of mast cell tryptase - An inflammatory mediator. Febs Journal 2006;273(9):1871-95.

[68] Huang C, Li L, Krilis SA, Chanasyk K, Tang Y, Li Z, et al. Human tryptases alpha and beta/II are functionally distinct due, in part, to a single amino acid difference in one of the surface loops that forms the substrate-binding cleft. J Biol Chem 1999;274(28):19670-6.

[69] Schwartz LB, Min HK, Ren S, Xia HZ, Hu J, Zhao W, et al. Tryptase precursors are preferentially and spontaneously released, whereas mature tryptase is retained by HMC-1 cells, Mono-Mac-6 cells, and human skin-derived mast cells. J Immunol 2003;170(11):5667-73.

[70] Caughey GH, Raymond WW, Blount JL, Hau LWT, Pallaoro M, Wolters PJ, et al. Characterization of human gamma-tryptases, novel members of the chromosome 16p mast cell tryptase and prostasin gene families. Journal of Immunology 2000;164(12):6566-75.

[71] Wong UW, Tang YZ, Feyfant E, Sali A, Li LX, Li Y, et al. Identification of a new member of the tryptase family of mouse and human mast cell

proteases which possesses a novel COOH-terminal hydrophobic extension. Journal of Biological Chemistry 1999;274(43):30784-93.

[72] Yuan J, Beltman J, Gjerstad E, Nguyen MT, Sampang J, Chan H, et al. Expression and characterization of recombinant gamma-tryptase. Protein Expression and Purification 2006;49(1):47-54.

[73] Wong GW, Foster PS, Yasuda S, Qi JC, Mahalingam S, Mellor EA, et al. Biochemical and functional characterization of human transmembrane tryptase (TMT)/tryptase gamma. Journal of Biological Chemistry 2002;277(44):41906-15.

[74] Wang HW, Mcneil HP, Husain A, Liu K, Tedla N, Thomas PS, et al. delta tryptase is expressed in multiple human tissues, and a recombinant form has proteolytic activity. Journal of Immunology 2002;169(9):5145-52.

[75] Miller JS, Westin EH, Schwartz LB. Cloning and characterization of complementary DNA for human tryptase. J Clin Invest 1989;84(4):1188-95.

[76] Wong GW, Yasuda S, Madhusudhan MS, Li LX, Yang Y, Krilis SA, et al. Human tryptase epsilon (PRSS22), a new member of the chromosome 16p13.3 family of human serine proteases expressed in airway epithelial cells. Journal of Biological Chemistry 2001;276(52):49169-82.

[77] Li W, Danilenko DM, Bunting S, Ganesan R, Sa S, Ferrando R, et al. The serine protease marapsin is expressed in stratified squamous epithelia and is up-regulated in the hyperproliferative epidermis of psoriasis and regenerating wounds. J Biol Chem 2009;284(1):218-28.

[78] Sommerhoff CP. Dog mast cell proteinases in models of airway secretion, bronchoconistrction, cutaneous vascular permeability and tissue fibrosis. In: Caughey GH, editor. Mast Cell Proteases in Immunology and Biology.New York: Marcel Dekker; 1995. p. 145-67.

[79] Pereira PJ, Bergner A, Macedo-Ribeiro S, Huber R, Matschiner G, Fritz H, et al. Human beta-tryptase is a ring-like tetramer with active sites facing a central pore. Nature 1998;392(6673):306-11.

[80] Schwartz LB, Bradford TR. Regulation of tryptase from human lung mast cells by heparin. Stabilization of the active tetramer. J Biol Chem 1986;261(16):7372-9.

[81] Goldstein SM, Leong J, Schwartz LB, Cooke D. Protease composition of exocytosed human skin mast cell protease-proteoglycan complexes. Tryptase resides in a complex distinct from chymase and carboxypeptidase. J Immunol 1992;148(8):2475-82.

[82] Schwartz LB, Bradford TR, Lee DC, Chlebowski JF. Immunologic and physicochemical evidence for conformational changes occurring on conversion of human mast cell tryptase from active tetramer to inactive monomer. Production of monoclonal antibodies recognizing active tryptase. J Immunol 1990;144(6):2304-11.

[83] Ren S, Sakai K, Schwartz LB. Regulation of human mast cell beta-tryptase: conversion of inactive monomer to active tetramer at acid pH. J Immunol 1998;160(9):4561-9.

[84] Fukuoka Y, Schwartz LB. Active monomers of human beta-tryptase have expanded substrate specificities. Int Immunopharmacol 2007;7(14):1900-8.

[85] Lupas A, Flanagan JM, Tamura T, Baumeister W. Self-compartmentalizing proteases. Trends Biochem Sci 1997;22(10):399-404.

[86] Tam EK, Caughey GH. Degradation of airway neuropeptides by human lung tryptase. Am J Respir Cell Mol Biol 1990;3(1):27-32.

[87] Harvima IT, Harvima RJ, Penttila IM, Eloranta TO, Horsmanheimo M, Fraki JE. Effect of human mast cell tryptase on human plasma proenzymes. Int Arch Allergy Appl Immunol 1989;90(1):104-8.

[88] Gruber BL, Marchese MJ, Suzuki K, Schwartz LB, Okada Y, Nagase H, et al. Synovial procollagenase activation by human mast cell tryptase dependence upon matrix metalloproteinase 3 activation. J Clin Invest 1989;84(5):1657-62.

[89] Stack MS, Johnson DA. Human mast cell tryptase activates single-chain urinary-type plasminogen activator (pro-urokinase). J Biol Chem 1994;269(13):9416-9.

[90] Macfarlane SR, Seatter MJ, Kanke T, Hunter GD, Plevin R. Proteinase-activated receptors. Pharmacol Rev 2001;53(2):245-82.

[91] Hunt JF, Fang K, Malik R, Snyder A, Malhotra N, Platts-Mills TA, et al. Endogenous airway acidification. Implications for asthma pathophysiology. Am J Respir Crit Care Med 2000;161(3 Pt 1):694-9.

[92] Gillies RJ, Raghunand N, Karczmar GS, Bhujwalla ZM. MRI of the tumor microenvironment. J Magn Reson Imaging 2002;16(4):430-50.

[93] Schwartz LB, Bradford TR, Littman BH, Wintroub BU. The fibrinogenolytic activity of purified tryptase from human lung mast cells. J Immunol 1985;135(4):2762-7.

[94] Lohi J, Harvima I, Keski-Oja J. Pericellular substrates of human mast cell tryptase: 72,000 dalton gelatinase and fibronectin. J Cell Biochem 1992;50(4):337-49.

[95] Kaminska R, Helisalmi P, Harvima RJ, Naukkarinen A, Horsmanheimo M, Harvima IT. Focal dermal-epidermal separation and fibronectin cleavage in basement membrane by human mast cell tryptase. J Invest Dermatol 1999;113(4):567-73.

[96] Kielty CM, Lees M, Shuttleworth CA, Woolley D. Catabolism of intact type VI collagen microfibrils: susceptibility to degradation by serine proteinases. Biochem Biophys Res Commun 1993;191(3):1230-6.

[97] Proctor GB, Chan KM, Garrett JR, Smith RE. Proteinase activities in bovine atrium and the possible role of mast cell tryptase in the processing of atrial natriuretic factor (ANF). Comp Biochem Physiol B 1991;99(4):839-44.

[98] Spinnler K, Frohlich T, Arnold GJ, Kunz L, Mayerhofer A. Human tryptase cleaves pro-nerve growth factor (pro-NGF): hints of local, mast cell-dependent regulation of NGF/pro-NGF action. J Biol Chem 2011;286(36):31707-13.

[99] Tatler AL, Porte J, Knox A, Jenkins G, Pang L. Tryptase activates TGFbeta in human airway smooth muscle cells via direct proteolysis. Biochem Biophys Res Commun 2008;370(2):239-42.

[100] Lee M, Sommerhoff CP, von EA, Zettl F, Fritz H, Kovanen PT. Mast cell tryptase degrades HDL and blocks its function as an acceptor of cellular cholesterol. Arterioscler Thromb Vasc Biol 2002;22(12):2086-91.

[101] Corvera CU, Dery O, McConalogue K, Bohm SK, Khitin LM, Caughey GH, et al. Mast cell tryptase regulates rat colonic myocytes through proteinase-activated receptor 2. J Clin Invest 1997;100(6):1383-93.

[102] Molino M, Barnathan ES, Numerof R, Clark J, Dreyer M, Cumashi A, et al. Interactions of mast cell tryptase with thrombin receptors and PAR-2. J Biol Chem 1997;272(7):4043-9.

[103] Mirza H, Schmidt VA, Derian CK, Jesty J, Bahou WF. Mitogenic responses mediated through the proteinase-activated receptor-2 are induced by expressed forms of mast cell alpha- or beta-tryptases. Blood 1997;90(10):3914-22.

[104] Sommerhoff CP, Bode W, Matschiner G, Bergner A, Fritz H. The human mast cell tryptase tetramer: a fascinating riddle solved by structure. Biochimica et Biophysica Acta-Protein Structure and Molecular Enzymology 2000;1477(1-2):75-89.

[105] Strik MCM, Wolbink A, Wouters D, Bladergroen BA, Verlaan AR, van Houdt IS, et al. Intracellular serpin SERPINB6 (PI6) is abundantly expressed by

human mast cells and forms complexes with beta-tryptase monomers. Blood 2004;103(7):2710-7.

[106] Alter SC, Kramps JA, Janoff A, Schwartz LB. Interactions of Human Mast-Cell Tryptase with Biological Protease Inhibitors. Archives of Biochemistry and Biophysics 1990;276(1):26-31.

[107] Sommerhoff CP, Sollner C, Mentele R, Piechottka GP, Auerswald EA, Fritz H. A Kazal-Type Inhibitor of Human Mast-Cell Tryptase - Isolation from the Medical Leech Hirudo-Medicinalis, Characterization, and Sequence-Analysis. Biological Chemistry Hoppe-Seyler 1994;375(10):685-94.

[108] Paesen GC, Siebold C, Harlos K, Peacey MF, Nuttall PA, Stuart DI. A tick protein with a modified Kunitz fold inhibits human tryptase. J Mol Biol 2007;368(4):1172-86.

[109] Cairns JA. Inhibitors of mast cell tryptase beta as therapeutics for the treatment of asthma and inflammatory disorders. Pulm Pharmacol Ther 2005;18(1):55-66.

[110] Rice KD, Tanaka RD, Katz BA, Numerof RP, Moore WR. Inhibitors of tryptase for the treatment of mast cell-mediated diseases. Current Pharmaceutical Design 1998;4(5):381-96.

[111] Krishna MT, Chauhan A, Little L, Sampson K, Hawksworth R, Mant T, et al. Inhibition of mast cell tryptase by inhaled APC 366 attenuates allergen-induced late-phase airway obstruction in asthma. J Allergy Clin Immunol 2001;107(6):1039-45.

[112] Numerof RP, Simpson PJ, Tanaka R. Tryptase inhibitors: a novel class of anti-inflammatory drugs. Expert Opin Investig Drugs 1997;6(7):811-7.

[113] Clark JM, Abraham WM, Fishman CE, Forteza R, Ahmed A, Cortes A, et al. Tryptase Inhibitors Block Allergen-Induced Airway and Inflammatory Responses in Allergic Sheep. American Journal of Respiratory and Critical Care Medicine 1995;152(6):2076-83.

[114] Costanzo MJ, Yabut SC, Almond HR, Andrade-Gordon P, Corcoran TW, de Garavilla L, et al. Potent, small-molecule inhibitors of human mast cell tryptase. Antiasthmatic action of a dipeptide-based transition-state analogue containing a benzothiazole ketone. Journal of Medicinal Chemistry 2003;46(18):3865-76.

[115] Mori S, Itoh Y, Shinohata R, Sendo T, Oishi R, Nishibori M. Nafamostat mesilate is an extremely potent inhibitor of human tryptase. J Pharmacol Sci 2003;92(4):420-3.

[116] Isozaki Y, Yoshida N, Kuroda M, Handa O, Takagi T, Kokura S, et al. Anti-tryptase treatment using nafamostat mesilate has a therapeutic effect on experimental colitis. Scand J Gastroenterol 2006;41(8):944-53.

[117] Burgess LE, Newhouse BJ, Ibrahim P, Rizzi J, Kashem MA, Hartman A, et al. Potent selective nonpeptidic inhibitors of human lung tryptase. Proceedings of the National Academy of Sciences of the United States of America 1999;96(15):8348-52.

[118] Wright CD, Havill AM, Middleton SC, Kashem MA, Dripps DJ, Abraham WM, et al. Inhibition of allergen-induced pulmonary responses by the selective tryptase inhibitor 1,5-bis-{4-[(3-carbamimidoyl-benzenesulfonylamino)-methyl]phenoxy}-pentane (AMG-126737). Biochemical Pharmacology 1999;58(12):1989-96.

[119] Oh SW, Pae CI, Lee DK, Jones F, Chiang GKS, Kim HO, et al. Tryptase inhibition blocks airway inflammation in a mouse asthma model. Journal of Immunology 2002;168(4):1992-2000.

[120] Brown JK, Tyler CL, Jones CA, Ruoss SJ, Hartmann T, Caughey GH. Tryptase, the Dominant Secretory Granular Protein in Human Mast-Cells, Is A Potent Mitogen for Cultured Dog Tracheal Smooth-Muscle Cells. American Journal of Respiratory Cell and Molecular Biology 1995;13(2):227-36.

[121] Tremaine WJ, Brzezinski A, Katz JA, Wolf DC, Fleming TJ, Mordenti J, et al. Treatment of mildly to moderately active ulcerative colitis with a tryptase

inhibitor (APC 2059): an open-label pilot study. Alimentary Pharmacology & Therapeutics 2002;16(3):407-13.

[122] CHOI-SLEDESKI YM, FITCH N, MINNICH A, inventors; TREATMENT OF DERMATOLOGICAL ALLERGIC CONDITIONS.WO/2011/106334. 2011 Jan 9.

[123] Vliagoftis H, Lacy P, Luy B, Adamko D, Hollenberg M, Befus D, et al. Mast cell tryptase activates peripheral blood eosinophils to release granule-associated enzymes. International Archives of Allergy and Immunology 2004;135(3):196-204.

[124] Walls AF, Bennett AR, Sueiras-Diaz J, Olsson H. The kininogenase activity of human mast cell tryptase. Biochem Soc Trans 1992;20(3):260S.

[125] Huang C, De Sanctis GT, O'Brien PJ, Mizgerd JP, Friend DS, Drazen JM, et al. Evaluation of the substrate specificity of human mast cell tryptase beta I and demonstration of its importance in bacterial infections of the lung. J Biol Chem 2001;276(28):26276-84.

[126] Huang C, Sali A, Stevens RL. Regulation and function of mast cell proteases in inflammation. J Clin Immunol 1998;18(3):169-83.

[127] Molinari JF, Moore WR, Clark J, Tanaka R, Butterfield JH, Abraham WM. Role of tryptase in immediate cutaneous responses in allergic sheep. J Appl Physiol 1995;79(6):1966-70.

[128] Compton SJ, Cairns JA, Holgate ST, Walls AF. The role of mast cell tryptase in regulating endothelial cell proliferation, cytokine release, and adhesion molecule expression: tryptase induces expression of mRNA for IL-1 beta and IL-8 and stimulates the selective release of IL-8 from human umbilical vein endothelial cells. J Immunol 1998;161(4):1939-46.

[129] Cairns JA, Walls AF. Mast cell tryptase is a mitogen for epithelial cells. Stimulation of IL-8 production and intercellular adhesion molecule-1 expression. J Immunol 1996;156(1):275-83.

[130] Cairns JA, Walls AF. Mast cell tryptase stimulates the synthesis of type I collagen in human lung fibroblasts. J Clin Invest 1997;99(6):1313-21.

[131] Levi-Schaffer F, Piliponsky AM. Tryptase, a novel link between allergic inflammation and fibrosis. Trends in Immunology 2003;24(4):158-61.

[132] Molinari JF, Scuri M, Moore WR, Clark J, Tanaka R, Abraham WM. Inhaled tryptase causes bronchoconstriction in sheep via histamine release. American Journal of Respiratory and Critical Care Medicine 1996;154(3):649-53.

[133] Sylvin H, Dahlback M, Van Der Ploeg I, Alving K. The tryptase inhibitor APC-366 reduces the acute airway response to allergen in pigs sensitized to Ascaris suum. Clinical and Experimental Allergy 2002;32(6):967-71.

[134] Caughey GH. Mast cell tryptases and chymases in inflammation and host defense. Immunol Rev 2007;217:141-54.

[135] Sekizawa K, Caughey GH, Lazarus SC, Gold WM, Nadel JA. Mast cell tryptase causes airway smooth muscle hyperresponsiveness in dogs. J Clin Invest 1989;83(1):175-9.

[136] Johnson PR, Ammit AJ, Carlin SM, Armour CL, Caughey GH, Black JL. Mast cell tryptase potentiates histamine-induced contraction in human sensitized bronchus. Eur Respir J 1997;10(1):38-43.

[137] Berger P, Girodet PO, Begueret H, Ousova O, Perng DW, Marthan R, et al. Tryptase-stimulated human airway smooth muscle cells induce cytokine synthesis and mast cell chemotaxis. FASEB J 2003;17(14):2139-41.

[138] Blair RJ, Meng H, Marchese MJ, Ren SL, Schwartz LB, Tonnesen MG, et al. Human mast cells stimulate vascular tribe formation - Tryptase is a novel, potent angiogenic factor. Journal of Clinical Investigation 1997;99(11):2691-700.

[139] Pang L, Nie M, Corbett L, Sutcliffe A, Knox AJ. Mast cell beta-tryptase selectively cleaves eotaxin and RANTES and abrogates their eosinophil chemotactic activities. J Immunol 2006;176(6):3788-95.

[140] Mellon MB, Frank BT, Fang KC. Mast cell alpha-chymase reduces IgE recognition of birch pollen profilin by cleaving antibody-binding epitopes. J Immunol 2002;168(1):290-7.

[141] Ossovskaya VS, Bunnett NW. Protease-activated receptors: contribution to physiology and disease. Physiol Rev 2004;84(2):579-621.

[142] Nystedt S, Larsson AK, Aberg H, Sundelin J. The mouse proteinase-activated receptor-2 cDNA and gene. Molecular cloning and functional expression. J Biol Chem 1995;270(11):5950-5.

[143] Nystedt S, Emilsson K, Larsson AK, Strombeck B, Sundelin J. Molecular cloning and functional expression of the gene encoding the human proteinase-activated receptor 2. Eur J Biochem 1995;232(1):84-9.

[144] Bohm SK, Kong W, Bromme D, Smeekens SP, Anderson DC, Connolly A, et al. Molecular cloning, expression and potential functions of the human proteinase-activated receptor-2. Biochem J 1996;314 (Pt 3):1009-16.

[145] Claytor RB, Michelson AD, Li JM, Frelinger AL, Rohrer MJ, Garnette CSC, et al. The cleaved peptide of PARI is a more potent stimulant of platelet-endothelial cell adhesion than is thrombin. Journal of Vascular Surgery 2003;37(2):440-5.

[146] Hong JH, Hong JY, Park B, Lee SI, Seo JT, Kim KE, et al. Chitinase activates protease-activated receptor-2 in human airway epithelial cells. Am J Respir Cell Mol Biol 2008;39(5):530-5.

[147] Stefansson K, Brattsand M, Roosterman D, Kempkes C, Bocheva G, Steinhoff M, et al. Activation of proteinase-activated receptor-2 by human kallikrein-related peptidases. J Invest Dermatol 2008;128(1):18-25.

[148] Schmidlin F, Bunnett NW. Protease-activated receptors: how proteases signal to cells. Curr Opin Pharmacol 2001;1(6):575-82.

[149] Wakita H, Furukawa F, Takigawa M. Thrombin and trypsin induce granulocyte-macrophage colony-stimulating factor and interleukin-6 gene expression in cultured normal human keratinocytes. Proc Assoc Am Physicians 1997;109(2):190-207.

[150] Vliagoftis H, Befus AD, Hollenberg MD, Moqbel R. Airway epithelial cells release eosinophil survival-promoting factors (GM-CSF) after stimulation of proteinase-activated receptor 2. J Allergy Clin Immunol 2001;107(4):679-85.

[151] Ostrowska E, Reiser G. Protease-activated receptor (PAR)-induced interleukin-8 production in airway epithelial cells requires activation of MAP kinases p44/42 and JNK. Biochem Biophys Res Commun 2008;366(4):1030-5.

[152] Goh FG, Ng PY, Nilsson M, Kanke T, Plevin R. Dual effect of the novel peptide antagonist K-14585 on proteinase-activated receptor-2-mediated signalling. Br J Pharmacol 2009;158(7):1695-704.

[153] Schultheiss M, Neumcke B, Richter HP. Endogenous trypsin receptors in Xenopus oocytes: linkage to internal calcium stores. Cell Mol Life Sci 1997;53(10):842-9.

[154] Defea KA, Zalevsky J, Thoma MS, Dery O, Mullins RD, Bunnett NW. beta-arrestin-dependent endocytosis of proteinase-activated receptor 2 is required for intracellular targeting of activated ERK1/2. J Cell Biol 2000;148(6):1267-81.

[155] Kanke T, Takizawa T, Kabeya M, Kawabata A. Physiology and pathophysiology of proteinase-activated receptors (PARs): PAR-2 as a potential therapeutic target. J Pharmacol Sci 2005;97(1):38-42.

[156] Kanke T, Macfarlane SR, Seatter MJ, Davenport E, Paul A, McKenzie RC, et al. Proteinase-activated receptor-2-mediated activation of stress-

activated protein kinases and inhibitory kappa B kinases in NCTC 2544 keratinocytes. J Biol Chem 2001;276(34):31657-66.

[157] Kong W, McConalogue K, Khitin LM, Hollenberg MD, Payan DG, Bohm SK, et al. Luminal trypsin may regulate enterocytes through proteinase-activated receptor 2. Proc Natl Acad Sci U S A 1997;94(16):8884-9.

[158] Luo W, Wang Y, Hanck T, Stricker R, Reiser G. Jab1, a novel protease-activated receptor-2 (PAR-2)-interacting protein, is involved in PAR-2-induced activation of activator protein-1. J Biol Chem 2006;281(12):7927-36.

[159] Dery O, Thoma MS, Wong H, Grady EF, Bunnett NW. Trafficking of proteinase-activated receptor-2 and beta-arrestin-1 tagged with green fluorescent protein. beta-Arrestin-dependent endocytosis of a proteinase receptor. J Biol Chem 1999;274(26):18524-35.

[160] Trejo J, Altschuler Y, Fu HW, Mostov KE, Coughlin SR. Protease-activated receptor-1 down-regulation: a mutant HeLa cell line suggests novel requirements for PAR1 phosphorylation and recruitment to clathrin-coated pits. J Biol Chem 2000;275(40):31255-65.

[161] Ramachandran R, Hollenberg MD. Proteinases and signalling: pathophysiological and therapeutic implications via PARs and more. Br J Pharmacol 2008;153 Suppl 1:S263-S282.

[162] Cocks TM, Moffatt JD. Protease-activated receptor-2 (PAR2) in the airways. Pulm Pharmacol Ther 2001;14(3):183-91.

[163] Cocks TM, Fong B, Chow JM, Anderson GP, Frauman AG, Goldie RG, et al. A protective role for protease-activated receptors in the airways. Nature 1999;398(6723):156-60.

[164] Cocks TM, Moffatt JD. Protease-activated receptors: sentries for inflammation? Trends Pharmacol Sci 2000;21(3):103-8.

[165] Perretti M. Endogenous mediators that inhibit the leukocyte-endothelium interaction. Trends Pharmacol Sci 1997;18(11):418-25.

[166] Magazine HI, King JM, Srivastava KD. Protease activated receptors modulate aortic vascular tone. Int J Cardiol 1996;53 Suppl:S75-S80.

[167] Langer F, Morys-Wortmann C, Kusters B, Storck J. Endothelial protease-activated receptor-2 induces tissue factor expression and von Willebrand factor release. Br J Haematol 1999;105(2):542-50.

[168] Cottrell GS, Amadesi S, Schmidlin F, Bunnett N. Protease-activated receptor 2: activation, signalling and function. Biochem Soc Trans 2003;31(Pt 6):1191-7.

[169] Robin J, Kharbanda R, Mclean P, Campbell R, Vallance P. Protease-activated receptor 2-mediated vasodilatation in humans in vivo: role of nitric oxide and prostanoids. Circulation 2003;107(7):954-9.

[170] Gui Y, Loutzenhiser R, Hollenberg MD. Bidirectional regulation of renal hemodynamics by activation of PAR1 and PAR2 in isolated perfused rat kidney. Am J Physiol Renal Physiol 2003;285(1):F95-104.

[171] Roy SS, Saifeddine M, Loutzenhiser R, Triggle CR, Hollenberg MD. Dual endothelium-dependent vascular activities of proteinase-activated receptor-2-activating peptides: evidence for receptor heterogeneity. Br J Pharmacol 1998;123(7):1434-40.

[172] Saifeddine M, Roy SS, Al-Ani B, Triggle CR, Hollenberg MD. Endothelium-dependent contractile actions of proteinase-activated receptor-2-activating peptides in human umbilical vein: release of a contracting factor via a novel receptor. Br J Pharmacol 1998;125(7):1445-54.

[173] Namkung W, Yoon JS, Kim KH, Lee MG. PAR2 exerts local protection against acute pancreatitis via modulation of MAP kinase and MAP kinase phosphatase signaling. Am J Physiol Gastrointest Liver Physiol 2008;295(5):G886-G894.

[174] Laukkarinen JM, Weiss ER, van Acker GJ, Steer ML, Perides G. Protease-activated receptor-2 exerts contrasting model-specific effects on acute experimental pancreatitis. J Biol Chem 2008;283(30):20703-12.

[175] Liu Y, Mueller BM. Protease-activated receptor-2 regulates vascular endothelial growth factor expression in MDA-MB-231 cells via MAPK pathways. Biochem Biophys Res Commun 2006;344(4):1263-70.

[176] Feistritzer C, Lenta R, Riewald M. Protease-activated receptors-1 and -2 can mediate endothelial barrier protection: role in factor Xa signaling. J Thromb Haemost 2005;3(12):2798-805.

[177] Cairns JA, Webber SE, Williams J. The PAR-2 derived peptide SLIGKV stimulates calcium mobilisation and proliferation in H292 and normal bronchial epithelial (NHBE) cells. American Journal of Respiratory and Critical Care Medicine [161], A438. 2000.

[178] Feld M, Shpacovitch VM, Ehrhardt C, Kerkhoff C, Hollenberg MD, Vergnolle N, et al. Agonists of proteinase-activated receptor-2 enhance IFN-gamma-inducible effects on human monocytes: role in influenza A infection. J Immunol 2008;180(10):6903-10.

[179] Moraes TJ, Martin R, Plumb JD, Vachon E, Cameron CM, Danesh A, et al. Role of PAR2 in murine pulmonary pseudomonal infection. Am J Physiol Lung Cell Mol Physiol 2008;294(2):L368-L377.

[180] Miike S, McWilliam AS, Kita H. Trypsin induces activation and inflammatory mediator release from human eosinophils through protease-activated receptor-2. J Immunol 2001;167(11):6615-22.

[181] Temkin V, Kantor B, Weg V, Hartman ML, Levi-Schaffer F. Tryptase activates the mitogen-activated protein kinase/activator protein-1 pathway in human peripheral blood eosinophils, causing cytokine production and release. J Immunol 2002;169(5):2662-9.

[182] Howells GL, Macey MG, Chinni C, Hou L, Fox MT, Harriott P, et al. Proteinase-activated receptor-2: expression by human neutrophils. J Cell Sci 1997;110 (Pt 7):881-7.

[183] Kajikawa H, Yoshida N, Katada K, Hirayama F, Handa O, Kokura S, et al. Helicobacter pylori activates gastric epithelial cells to produce interleukin-8 via protease-activated receptor 2. Digestion 2007;76(3-4):248-55.

[184] Shpacovitch VM, Brzoska T, Buddenkotte J, Stroh C, Sommerhoff CP, Ansel JC, et al. Agonists of proteinase-activated receptor 2 induce cytokine release and activation of nuclear transcription factor kappaB in human dermal microvascular endothelial cells. J Invest Dermatol 2002;118(2):380-5.

[185] Scott G, Leopardi S, Printup S, Malhi N, Seiberg M, Lapoint R. Proteinase-activated receptor-2 stimulates prostaglandin production in keratinocytes: analysis of prostaglandin receptors on human melanocytes and effects of PGE2 and PGF2alpha on melanocyte dendricity. J Invest Dermatol 2004;122(5):1214-24.

[186] Yoshida N, Katada K, Handa O, Takagi T, Kokura S, Naito Y, et al. Interleukin-8 production via protease-activated receptor 2 in human esophageal epithelial cells. Int J Mol Med 2007;19(2):335-40.

[187] Vergnolle N. Proteinase-activated receptor-2-activating peptides induce leukocyte rolling, adhesion, and extravasation in vivo. J Immunol 1999;163(9):5064-9.

[188] Knight DA, Lim S, Scaffidi AK, Roche N, Chung KF, Stewart GA, et al. Protease-activated receptors in human airways: upregulation of PAR-2 in respiratory epithelium from patients with asthma. J Allergy Clin Immunol 2001;108(5):797-803.

[189] Roche N, Stirling RG, Lim S, Oliver BG, Oates T, Jazrawi E, et al. Effect of acute and chronic inflammatory stimuli on expression of protease-activated receptors 1 and 2 in alveolar macrophages. J Allergy Clin Immunol 2003;111(2):367-73.

[190] Bolton SJ, McNulty CA, Thomas RJ, Hewitt CR, Wardlaw AJ. Expression of and functional responses to protease-activated receptors on human eosinophils. J Leukoc Biol 2003;74(1):60-8.

[191] Takizawa T, Tamiya M, Hara T, Matsumoto J, Saito N, Kanke T, et al. Abrogation of bronchial eosinophilic inflammation and attenuated eotaxin content in protease-activated receptor 2-deficient mice. J Pharmacol Sci 2005;98(1):99-102.

[192] Lindner JR, Kahn ML, Coughlin SR, Sambrano GR, Schauble E, Bernstein D, et al. Delayed onset of inflammation in protease-activated receptor-2-deficient mice. J Immunol 2000;165(11):6504-10.

[193] Lin KW, Park J, Crews AL, Li Y, Adler KB. Protease-activated receptor-2 (PAR-2) is a weak enhancer of mucin secretion by human bronchial epithelial cells in vitro. Int J Biochem Cell Biol 2008;40(6-7):1379-88.

[194] Schmidlin F, Amadesi S, Dabbagh K, Lewis DE, Knott P, Bunnett NW, et al. Protease-activated receptor 2 mediates eosinophil infiltration and hyperreactivity in allergic inflammation of the airway. J Immunol 2002;169(9):5315-21.

[195] Derian CK, Eckardt AJ, Andrade-Gordon P. Differential regulation of human keratinocyte growth and differentiation by a novel family of protease-activated receptors. Cell Growth Differ 1997;8(7):743-9.

[196] Bueno L, Fioramonti J. Protease-activated receptor 2 and gut permeability: a review. Neurogastroenterol Motil 2008;20(6):580-7.

[197] Cenac N, Andrews CN, Holzhausen M, Chapman K, Cottrell G, Andrade-Gordon P, et al. Role for protease activity in visceral pain in irritable bowel syndrome. J Clin Invest 2007;117(3):636-47.

[198] Hyun E, Andrade-Gordon P, Steinhoff M, Vergnolle N. Protease-activated receptor-2 activation: a major actor in intestinal inflammation. Gut 2008;57(9):1222-9.

[199] Ferrell WR, Kelso EB, Lockhart JC, Plevin R, McInnes IB. Protease-activated receptor 2: a novel pathogenic pathway in a murine model of osteoarthritis. Ann Rheum Dis 2010;69(11):2051-4.

[200] Ferrell WR, Lockhart JC, Kelso EB, Dunning L, Plevin R, Meek SE, et al. Essential role for proteinase-activated receptor-2 in arthritis. J Clin Invest 2003;111(1):35-41.

[201] Compton SJ, Renaux B, Wijesuriya SJ, Hollenberg MD. Glycosylation and the activation of proteinase-activated receptor 2 (PAR(2)) by human mast cell tryptase. Br J Pharmacol 2001;134(4):705-18.

[202] Berger P, Tunon-De-Lara JM, Savineau JP, Marthan R. Selected contribution: tryptase-induced PAR-2-mediated Ca(2+) signaling in human airway smooth muscle cells. J Appl Physiol 2001;91(2):995-1003.

[203] Berger P, Perng DW, Thabrew H, Compton SJ, Cairns JA, McEuen AR, et al. Tryptase and agonists of PAR-2 induce the proliferation of human airway smooth muscle cells. J Appl Physiol 2001;91(3):1372-9.

[204] Asano-Kato N, Fukagawa K, Okada N, Dogru M, Tsubota K, Fujishima H. Tryptase increases proliferative activity of human conjunctival fibroblasts through protease-activated receptor-2. Invest Ophthalmol Vis Sci 2005;46(12):4622-6.

[205] Duchesne E, Tremblay MH, Cote CH. Mast cell tryptase stimulates myoblast proliferation; a mechanism relying on protease-activated receptor-2 and cyclooxygenase-2. BMC Musculoskelet Disord 2011;12:235.

[206] Frungieri MB, Weidinger S, Meineke V, Kohn FM, Mayerhofer A. Proliferative action of mast-cell tryptase is mediated by PAR2, COX2, prostaglandins, and PPARgamma : Possible relevance to human fibrotic disorders. Proc Natl Acad Sci U S A 2002;99(23):15072-7.

[207] Wang H, He S. Induction of lactoferrin and IL-8 release from human neutrophils by tryptic enzymes via proteinase activated receptor-2. Cell Biol Int 2006;30(9):688-97.

[208] He S, Aslam A, Gaca MD, He Y, Buckley MG, Hollenberg MD, et al. Inhibitors of tryptase as mast cell-stabilizing agents in the human airways: effects of tryptase and other agonists of proteinase-activated receptor 2 on histamine release. J Pharmacol Exp Ther 2004;309(1):119-26.

[209] Vergnolle N, Macnaughton WK, Al-Ani B, Saifeddine M, Wallace JL, Hollenberg MD. Proteinase-activated receptor 2 (PAR2)-activating peptides: identification of a receptor distinct from PAR2 that regulates intestinal transport. Proc Natl Acad Sci U S A 1998;95(13):7766-71.

[210] Mullan CS, Riley M, Clarke D, Tatler A, Sutcliffe A, Knox AJ, et al. Beta-tryptase regulates IL-8 expression in airway smooth muscle cells by a PAR-2-independent mechanism. Am J Respir Cell Mol Biol 2008;38(5):600-8.

[211] Buddenkotte J, Stroh C, Engels IH, Moormann C, Shpacovitch VM, Seeliger S, et al. Agonists of proteinase-activated receptor-2 stimulate upregulation of intercellular cell adhesion molecule-1 in primary human keratinocytes via activation of NF-kappa B. J Invest Dermatol 2005;124(1):38-45.

[212] Ramachandran R, Morice AH, Compton SJ. Proteinase-activated receptor2 agonists upregulate granulocyte colony-stimulating factor, IL-8, and VCAM-1 expression in human bronchial fibroblasts. Am J Respir Cell Mol Biol 2006;35(1):133-41.

[213] Hartwig W, Werner J, Warshaw AL, Antoniu B, Castillo CF, Gebhard MM, et al. Membrane-bound ICAM-1 is upregulated by trypsin and contributes to leukocyte migration in acute pancreatitis. Am J Physiol Gastrointest Liver Physiol 2004;287(6):G1194-G1199.

[214] Al-Ani B, Saifeddine M, Kawabata A, Renaux B, Mokashi S, Hollenberg MD. Proteinase-activated receptor 2 (PAR(2)): development of a ligand-binding

assay correlating with activation of PAR(2) by PAR(1)- and PAR(2)-derived peptide ligands. J Pharmacol Exp Ther 1999;290(2):753-60.

[215] Al-Ani B, Saifeddine M, Wijesuriya SJ, Hollenberg MD. Modified proteinase-activated receptor-1 and -2 derived peptides inhibit proteinase-activated receptor-2 activation by trypsin. J Pharmacol Exp Ther 2002;300(2):702-8.

[216] Murray DB, McLarty-Williams J, Nagalla KT, Janicki JS. Tryptase activates isolated adult cardiac fibroblasts via protease activated receptor-2 (PAR-2). J Cell Commun Signal 2012;6(1):45-51.

[217] McLarty JL, Melendez GC, Brower GL, Janicki JS, Levick SP. Tryptase/Protease-activated receptor 2 interactions induce selective mitogen-activated protein kinase signaling and collagen synthesis by cardiac fibroblasts. Hypertension 2011;58(2):264-70.

[218] Yang XP, Li Y, Wang Y, Wang Y, Wang P. beta-Tryptase up-regulates vascular endothelial growth factor expression via proteinase-activated receptor-2 and mitogen-activated protein kinase pathways in bone marrow stromal cells in acute myeloid leukemia. Leuk Lymphoma 2010;51(8):1550-8.

[219] Kelso EB, Dunning L, Lockhart JC, Ferrell WR, Plevin R, Sommerhoff CP. Tryptase as a PAR-2 activator in joint inflammation. Arthritis Research & Therapy 2005;7:S38.

[220] Niles AL, Maffitt M, Haak-Frendscho M, Wheeless CJ, Johnson DA. Recombinant human mast cell tryptase beta: stable expression in Pichia pastoris and purification of fully active enzyme. Biotechnol Appl Biochem 1998;28 (Pt 2):125-31.

[221] Togawa D, Koshino T, Saito T, Takagi T, Machida J. Highly activated matrix metalloproteinase-2 secreted from clones of metastatic lung nodules of nude mice injected with human fibrosarcoma HT1080. Cancer Letters 1999;146(1):25-33.

[222] Watt SM, Burgess AW, Metcalf D. Isolation and Surface Labeling of Murine Polymorphonuclear Neutrophils. Journal of Cellular Physiology 1979;100(1):1-21.

[223] Moczar M, Moczar E, Robert L. Peptides on partial hydrolysis of elastin with aqueous ethanolic potassium hyroxide. In: Robert A.M, Robert L, editors. Biology and Pathology of Elastic Tissues.Basel: S.Karger AG; 1980. p. 174.

[224] Forough R, Lea H, Starcher B, Allaire E, Clowes M, Hasenstab D, et al. Metalloproteinase blockade by local overexpression of TIMP-1 increases elastin accumulation in rat carotid artery intima. Arteriosclerosis Thrombosis and Vascular Biology 1998;18(5):803-7.

[225] Roberts RW. 6M Urea SDS-Tricine Gel. The Roberts Laboratory Group. http://mrnadisplay.usc.edu/lab/protocols/tricine-gel/small-peptide-separatory-gel. 2-14-2007.

[226] Baker D. Tris-Tricine Protein/Peptide Separation Gels. Baker Laboratory. http://depts.washington.edu/bakerpg/protocols/tris_tricine_gels.html. 2-22-1999.

[227] Trah TJ, Schleyer M. Formaldehyde fixation of proteins and small polypeptides after isoelectric focusing in polyacrylamide gels. Anal Biochem 1982;127(2):326-9.

[228] Aslam A. The role of tryptase and activation of protease activated receptor-2 (PAR-2) in human airways disease School of Medicine, University of Southampton; 2003.

[229] Assay Design Center. Universal ProbeLibrary System. Roche Applied Science https://www.roche-applied-science.com/sis/rtpcr/upl/index.jsp?id=UP030000. 2012.

[230] Viemann D, Goebeler M, Schmid S, Nordhues U, Klimmek K, Sorg C, et al. TNF induces distinct gene expression programs in microvascular and macrovascular human endothelial cells. J Leukoc Biol 2006;80(1):174-85.

[231] Sjostrom M, Johansson AS, Schroder O, Qiu H, Palmblad J, Haeggstrom JZ. Dominant expression of the CysLT2 receptor accounts for calcium signaling by cysteinyl leukotrienes in human umbilical vein endothelial cells. Arterioscler Thromb Vasc Biol 2003;23(8):e37-e41.

[232] Dale DC, Liles WC, Garwicz D, Aprikyan AG. Clinical implications of mutations of neutrophil elastase in congenital and cyclic neutropenia. J Pediatr Hematol Oncol 2001;23(4):208-10.

[233] Aviv H, Leder P. Purification of biologically active globin messenger RNA by chromatography on oligothymidylic acid-cellulose. Proc Natl Acad Sci U S A 1972;69(6):1408-12.

[234] Bautista AC, Yue E, Chirmule N, Swanson S, Jawa V. Elimination of rheumatoid factor interference in immunoassays using the electrochemiluminescence (ECL) based Meso Scale Discovery (MSD) platform. FASEB J 22 [Meeting Abstract Supplement]. 2008.

[235] Gasteiger E, Gattiker A, Hoogland C, Ivanyi I, Appel RD, Bairoch A. ExPASy: The proteomics server for in-depth protein knowledge and analysis. Nucleic Acids Res 2003;31(13):3784-8.

[236] Heinzel FP, Sadick MD, Holaday BJ, Coffman RL, Locksley RM. Reciprocal expression of interferon gamma or interleukin 4 during the resolution or progression of murine leishmaniasis. Evidence for expansion of distinct helper T cell subsets. J Exp Med 1989;169(1):59-72.

[237] Berger A. Th1 and Th2 responses: what are they? BMJ 2000;321(7258):424.

[238] Corrigan CJ, Kay AB. T cells and eosinophils in the pathogenesis of asthma. Immunol Today 1992;13(12):501-7.

[239] Mori A, Ogawa K, Someya K, Kunori Y, Nagakubo D, Yoshie O, et al. Selective suppression of Th2-mediated airway eosinophil infiltration by low-molecular weight CCR3 antagonists. Int Immunol 2007;19(8):913-21.

[240] HayGlass KT, Nashed B, Haile S, Marshall AJ, Thomas W. C57Bl/6 and BALB/c mice do not represent default Th1 and Th2 strains in allergen-driven immune responses. Journal of Allergy and Clinical Immunology 115[2], S258. 2005.

[241] Stockinger B, Veldhoen M, Martin B. Th17 T cells: linking innate and adaptive immunity. Semin Immunol 2007;19(6):353-61.

[242] Veldhoen M, Hirota K, Westendorf AM, Buer J, Dumoutier L, Renauld JC, et al. The aryl hydrocarbon receptor links TH17-cell-mediated autoimmunity to environmental toxins. Nature 2008;453(7191):106-9.

[243] Peterson MW, Walter ME, Nygaard SD. Effect of Neutrophil Mediators on Epithelial Permeability. American Journal of Respiratory Cell and Molecular Biology 1995;13(6):719-27.

[244] Takeda Y, Tamaoki J, Yamawaki I, Kondo M, Nagai A. [Role of neutrophil elastase in allergen-induced airway microvascular leakage in sensitized guinea pigs]. Arerugi 1997;46(6):496-501.

[245] Tanita T, Song C, Kubo H, Ono S, Sagawa M, Sato M, et al. Stimulated neutrophils evoke signal transduction to increase vascular permeability in rat lungs. Tohoku Journal of Experimental Medicine 1999;189(3):213-25.

[246] Faurschou M, Borregaard N. Neutrophil granules and secretory vesicles in inflammation. Microbes Infect 2003;5(14):1317-27.

[247] Pham CT. Neutrophil serine proteases: specific regulators of inflammation. Nat Rev Immunol 2006;6(7):541-50.

[248] Zaoui P, Barro C, Morel F. Differential expression and secretion of gelatinases and tissue inhibitor of metalloproteinase-1 during neutrophil adhesion. Biochim Biophys Acta 1996;1290(1):101-12.

[249] Okada Y, Nakanishi I. Activation of matrix metalloproteinase 3 (stromelysin) and matrix metalloproteinase 2 ('gelatinase') by human neutrophil elastase and cathepsin G. FEBS Lett 1989;249(2):353-6.

[250] Shoelson SE, White MF, Kahn CR. Tryptic activation of the insulin receptor. Proteolytic truncation of the alpha-subunit releases the beta-subunit from inhibitory control. J Biol Chem 1988;263(10):4852-60.

[251] Prenzel N, Zwick E, Daub H, Leserer M, Abraham R, Wallasch C, et al. EGF receptor transactivation by G-protein-coupled receptors requires metalloproteinase cleavage of proHB-EGF. Nature 1999;402(6764):884-8.

[252] Lu C, Zhao FD, Li XB, Yin LH. Up regulation of interleukin-8 expressions induced by mast cell tryptase via protease activated receptor-2 in endothelial cell line. Chin Med J (Engl) 2005;118(22):1900-6.

[253] Wolff B, Burns AR, Middleton J, Rot A. Endothelial cell "memory" of inflammatory stimulation: human venular endothelial cells store interleukin 8 in Weibel-Palade bodies. J Exp Med 1998;188(9):1757-62.

[254] Utgaard JO, Jahnsen FL, Bakka A, Brandtzaeg P, Haraldsen G. Rapid secretion of prestored interleukin 8 from Weibel-Palade bodies of microvascular endothelial cells. J Exp Med 1998;188(9):1751-6.

[255] Compton SJ, Cairns JA, Holgate ST, Walls AF. Human mast cell tryptase stimulates the release of an IL-8-dependent neutrophil chemotactic activity from human umbilical vein endothelial cells (HUVEC). Clin Exp Immunol 2000;121(1):31-6.

[256] Erger RA, Casale TB. Interleukin-8 is a potent mediator of eosinophil chemotaxis through endothelium and epithelium. Am J Physiol 1995;268(1 Pt 1):L117-L122.

[257] Smith WB, Gamble JR, Clark-Lewis I, Vadas MA. Interleukin-8 induces neutrophil transendothelial migration. Immunology 1991;72(1):65-72.

[258] Wang H, Zheng Y, He S. Induction of release and up-regulated gene expression of interleukin (IL)-8 in A549 cells by serine proteinases. BMC Cell Biol 2006;7:22.

[259] Wilson HL, Varcoe RW, Stokes L, Holland KL, Francis SE, Dower SK, et al. P2X receptor characterization and IL-1/IL-1Ra release from human endothelial cells. Br J Pharmacol 2007;151(1):115-27.

[260] Elias JA, Trinchieri G, Beck JM, Simon PL, Sehgal PB, May LT, et al. A synergistic interaction of IL-6 and IL-1 mediates the thymocyte-stimulating activity produced by recombinant IL-1-stimulated fibroblasts. J Immunol 1989;142(2):509-14.

[261] Murakami T, Mataki C, Nagao C, Umetani M, Wada Y, Ishii M, et al. The gene expression profile of human umbilical vein endothelial cells stimulated by tumor necrosis factor alpha using DNA microarray analysis. J Atheroscler Thromb 2000;7(1):39-44.

[262] Natarajan S. Defining the Human Endothelial Transcriptome. Massachusetts Institute of Technology: Harvard University--MIT Division of Health Sciences and Technology; 2005.

[263] Magder S, Neculcea J, Neculcea V, Sladek R. Lipopolysaccharide and TNF-alpha produce very similar changes in gene expression in human endothelial cells. J Vasc Res 2006;43(5):447-61.

[264] Unger RE, Krump-Konvalinkova V, Peters K, Kirkpatrick CJ. In vitro expression of the endothelial phenotype: comparative study of primary isolated cells and cell lines, including the novel cell line HPMEC-ST1.6R. Microvasc Res 2002;64(3):384-97.

[265] Cantrell DA, Smith KA. The interleukin-2 T-cell system: a new cell growth model. Science 1984;224(4655):1312-6.

[266] Nelson BH. IL-2, regulatory T cells, and tolerance. J Immunol 2004;172(7):3983-8.

[267] Miller JD, Clabaugh SE, Smith DR, Stevens RB, Wrenshall LE. Interleukin-2 is present in human blood vessels and released in biologically active form by heparanase. Immunol Cell Biol 2012;90(2):159-67.

[268] Nilsen EM, Johansen FE, Jahnsen FL, Lundin KE, Scholz T, Brandtzaeg P, et al. Cytokine profiles of cultured microvascular endothelial cells from the human intestine. Gut 1998;42(5):635-42.

[269] Ikebuchi K, Ihle JN, Hirai Y, Wong GG, Clark SC, Ogawa M. Synergistic factors for stem cell proliferation: further studies of the target stem cells and the mechanism of stimulation by interleukin-1, interleukin-6, and granulocyte colony-stimulating factor. Blood 1988;72(6):2007-14.

[270] Nickel TJ, Kabir MH, Talreja J, Dileepan K, Stechschulte DJ. Stimulation of interleukin-6 production by human conjunctival epithelial cells (HCEC) with thrombin and tryptase. Journal of Allergy and Clinical Immunology 2004;113(2, Supplement):S177.

[271] Li T, He S. Induction of IL-6 release from human T cells by PAR-1 and PAR-2 agonists. Immunol Cell Biol 2006;84(5):461-6.

[272] Geiger T, Andus T, Klapproth J, Hirano T, Kishimoto T, Heinrich PC. Induction of rat acute-phase proteins by interleukin 6 in vivo. Eur J Immunol 1988;18(5):717-21.

[273] Loetscher M, Gerber B, Loetscher P, Jones SA, Piali L, Clark-Lewis I, et al. Chemokine receptor specific for IP10 and mig: structure, function, and expression in activated T-lymphocytes. J Exp Med 1996;184(3):963-9.

[274] Brightling CE, Ammit AJ, Kaur D, Black JL, Wardlaw AJ, Hughes JM, et al. The CXCL10/CXCR3 axis mediates human lung mast cell migration to asthmatic airway smooth muscle. Am J Respir Crit Care Med 2005;171(10):1103-8.

[275] Alkhouri H, Tong K, Cha V, Moir LM, Armour CL, Hughes JM. Asthmatic Airway Smooth Muscle CXCL10 Release Is Modulated by Mast Cell Products. American Journal of Respiratory and Critical Care Medicine 179. 2009.

[276] Dufour JH, Dziejman M, Liu MT, Leung JH, Lane TE, Luster AD. IFN-gamma-inducible protein 10 (IP-10; CXCL10)-deficient mice reveal a role

for IP-10 in effector T cell generation and trafficking. J Immunol 2002;168(7):3195-204.

[277] Massague J. The transforming growth factor-beta family. Annu Rev Cell Biol 1990;6:597-641.

[278] Ge G, Greenspan DS. BMP1 controls TGFbeta1 activation via cleavage of latent TGFbeta-binding protein. J Cell Biol 2006;175(1):111-20.

[279] Yu Q, Stamenkovic I. Cell surface-localized matrix metalloproteinase-9 proteolytically activates TGF-beta and promotes tumor invasion and angiogenesis. Genes Dev 2000;14(2):163-76.

[280] Schindler H, Diefenbach A, Rollinghoff M, Bogdan C. IFN-gamma inhibits the production of latent transforming growth factor-beta1 by mouse inflammatory macrophages. Eur J Immunol 1998;28(4):1181-8.

[281] Nunes I, Shapiro RL, Rifkin DB. Characterization of latent TGF-beta activation by murine peritoneal macrophages. J Immunol 1995;155(3):1450-9.

[282] Hannan RL, Kourembanas S, Flanders KC, Rogelj SJ, Roberts AB, Faller DV, et al. Endothelial cells synthesize basic fibroblast growth factor and transforming growth factor beta. Growth Factors 1988;1(1):7-17.

[283] Suzuki Y, Tanigaki T, Heimer D, Wang W, Ross WG, Murphy GA, et al. TGF-beta 1 causes increased endothelial ICAM-1 expression and lung injury. J Appl Physiol 1994;77(3):1281-7.

[284] Ohji T, Urano H, Shirahata A, Yamagishi M, Higashi K, Gotoh S, et al. Transforming growth factor beta 1 and beta 2 induce down-modulation of thrombomodulin in human umbilical vein endothelial cells. Thromb Haemost 1995;73(5):812-8.

[285] Hirai R, Kaji K. Transforming growth factor beta 1-specific binding proteins on human vascular endothelial cells. Exp Cell Res 1992;201(1):119-25.

[286] Tsukada T, Eguchi K, Migita K, Kawabe Y, Kawakami A, Matsuoka N, et al. Transforming growth factor beta 1 induces apoptotic cell death in cultured human umbilical vein endothelial cells with down-regulated expression of bcl-2. Biochem Biophys Res Commun 1995;210(3):1076-82.

[287] Chen CC, Manning AM. TGF-beta 1, IL-10 and IL-4 differentially modulate the cytokine-induced expression of IL-6 and IL-8 in human endothelial cells. Cytokine 1996;8(1):58-65.

[288] Goldsmith HL, Spain S. Margination of leukocytes in blood flow through small tubes. Microvasc Res 1984;27(2):204-22.

[289] Jung U, Ley K. Mice lacking two or all three selectins demonstrate overlapping and distinct functions for each selectin. J Immunol 1999;162(11):6755-62.

[290] Jung U, Norman KE, Scharffetter-Kochanek K, Beaudet AL, Ley K. Transit time of leukocytes rolling through venules controls cytokine-induced inflammatory cell recruitment in vivo. J Clin Invest 1998;102(8):1526-33.

[291] Ackermann L, Harvima IT. Mast cells of psoriatic and atopic dermatitis skin are positive for TNF-alpha and their degranulation is associated with expression of ICAM-1 in the epidermis. Arch Dermatol Res 1998;290(7):353-9.

[292] Raymond MA, Desormeaux A, Laplante P, Vigneault N, Filep JG, Landry K, et al. Apoptosis of endothelial cells triggers a caspase-dependent anti-apoptotic paracrine loop active on VSMC. FASEB J 2004;18(6):705-7.

[293] Hasanbasic I, Cuerquis J, Varnum B, Blostein MD. Intracellular signaling pathways involved in Gas6-Axl-mediated survival of endothelial cells. Am J Physiol Heart Circ Physiol 2004;287(3):H1207-H1213.

[294] Marin V, Kaplanski G, Gres S, Farnarier C, Bongrand P. Endothelial cell culture: protocol to obtain and cultivate human umbilical endothelial cells. J Immunol Methods 2001;254(1-2):183-90.

[295] Ruoss SJ, Hartmann T, Caughey GH. Mast cell tryptase is a mitogen for cultured fibroblasts. J Clin Invest 1991;88(2):493-9.

[296] Drenkard D, Becke FM, Langstein J, Spruss T, Kunz-Schughart LA, Tan TE, et al. CD137 is expressed on blood vessel walls at sites of inflammation and enhances monocyte migratory activity. FASEB J 2007;21(2):456-63.

[297] Schwarz H. Biological activities of reverse signal transduction through CD137 ligand. J Leukoc Biol 2005;77(3):281-6.

[298] Quek BZ, Lim YC, Lin JH, Tan TE, Chan J, Biswas A, et al. CD137 enhances monocyte-ICAM-1 interactions in an E-selectin-dependent manner under flow conditions. Mol Immunol 2010;47(9):1839-47.

[299] Heinisch IV, Daigle I, Knopfli B, Simon HU. CD137 activation abrogates granulocyte-macrophage colony-stimulating factor-mediated anti-apoptosis in neutrophils. Eur J Immunol 2000;30(12):3441-6.

[300] Kwon B. CD137-CD137 Ligand Interactions in Inflammation. Immune Netw 2009;9(3):84-9.

[301] Lee SC, Ju SA, Pack HN, Heo SK, Suh JH, Park SM, et al. 4-1BB (CD137) is required for rapid clearance of Listeria monocytogenes infection. Infect Immun 2005;73(8):5144-51.

[302] Cooper JT, Stroka DM, Brostjan C, Palmetshofer A, Bach FH, Ferran C. A20 blocks endothelial cell activation through a NF-kappaB-dependent mechanism. J Biol Chem 1996;271(30):18068-73.

[303] Thippegowda PB, Singh V, Sundivakkam PC, Xue J, Malik AB, Tiruppathi C. Ca2+ influx via TRPC channels induces NF-kappaB-dependent A20 expression to prevent thrombin-induced apoptosis in endothelial cells. Am J Physiol Cell Physiol 2010;298(3):C656-C664.

[304] Schmidlin F, Amadesi S, Vidil R, Trevisani M, Martinet N, Caughey G, et al. Expression and function of proteinase-activated receptor 2 in human

bronchial smooth muscle. Am J Respir Crit Care Med 2001;164(7):1276-81.

[305] Cleator JH, Zhu WQ, Vaughan DE, Hamm HE. Differential regulation of endothelial exocytosis of P-selectin and von Willebrand factor by protease-activated receptors and cAMP. Blood 2006;107(7):2736-44.

[306] Santulli RJ, Derian CK, Darrow AL, Tomko KA, Eckardt AJ, Seiberg M, et al. Evidence for the presence of a protease-activated receptor distinct from the thrombin receptor in human keratinocytes. Proc Natl Acad Sci U S A 1995;92(20):9151-5.

[307] Chi L, Stehno-Bittel L, Smirnova I, Stechschulte DJ, Dileepan KN. Signal transduction pathways in mast cell granule-mediated endothelial cell activation. Mediators Inflamm 2003;12(2):79-87.

[308] Oike M, Gericke M, Droogmans G, Nilius B. Calcium entry activated by store depletion in human umbilical vein endothelial cells. Cell Calcium 1994;16(5):367-76.

[309] Nilius B, Droogmans G. Ion channels and their functional role in vascular endothelium. Physiol Rev 2001;81(4):1415-59.

[310] Huang AJ, Manning JE, Bandak TM, Ratau MC, Hanser KR, Silverstein SC. Endothelial cell cytosolic free calcium regulates neutrophil migration across monolayers of endothelial cells. J Cell Biol 1993;120(6):1371-80.

[311] Pfau S, Leitenberg D, Rinder H, Smith BR, Pardi R, Bender JR. Lymphocyte adhesion-dependent calcium signaling in human endothelial cells. J Cell Biol 1995;128(5):969-78.

[312] Kohn EC, Alessandro R, Spoonster J, Wersto RP, Liotta LA. Angiogenesis: role of calcium-mediated signal transduction. Proc Natl Acad Sci U S A 1995;92(5):1307-11.

[313] Bennett J, Weeds A. Calcium and the cytoskeleton. Br Med Bull 1986;42(4):385-90.

[314] Gurubhagavatula I, Amrani Y, Pratico D, Ruberg FL, Albelda SM, Panettieri RA, Jr. Engagement of human PECAM-1 (CD31) on human endothelial cells increases intracellular calcium ion concentration and stimulates prostacyclin release. J Clin Invest 1998;101(1):212-22.

[315] Borensztajn K, Stiekema J, Nijmeijer S, Reitsma PH, Peppelenbosch MP, Spek CA. Factor Xa stimulates proinflammatory and profibrotic responses in fibroblasts via protease-activated receptor-2 activation. Am J Pathol 2008;172(2):309-20.

[316] Lin KW, Park J, Crews AL, Li Y, Adler KB. Protease-activated receptor-2 (PAR-2) is a weak enhancer of mucin secretion by human bronchial epithelial cells in vitro. Int J Biochem Cell Biol 2008;40(6-7):1379-88.

[317] Morris DR, Ding Y, Ricks TK, Gullapalli A, Wolfe BL, Trejo J. Protease-activated receptor-2 is essential for factor VIIa and Xa-induced signaling, migration, and invasion of breast cancer cells. Cancer Res 2006;66(1):307-14.

[318] Trian T, Girodet PO, Ousova O, Marthan R, Tunon-De-Lara JM, Berger P. RNA interference decreases PAR-2 expression and function in human airway smooth muscle cells. Am J Respir Cell Mol Biol 2006;34(1):49-55.

[319] Covic L, Gresser AL, Talavera J, Swift S, Kuliopulos A. Activation and inhibition of G protein-coupled receptors by cell-penetrating membrane-tethered peptides. Proc Natl Acad Sci U S A 2002;99(2):643-8.